

Applications of a Concise and General Strategy for the Syntheses of Transtaganolide and Basiliolide

Natural Products

Thesis by

Jonny Robert Gordon

In Partial Fulfillment of the Requirements

for the Degree of

Doctor of Philosophy

CALIFORNIA INSTITUTE OF TECHNOLOGY

Pasadena, California

2015

(Defended November 10, 2014)

© 2015

Jonny Robert Gordon

All Rights Reserved

To my Grandfather, Jerome Schwarzbach

ACKNOWLEDGEMENTS

First, I must thank my parents David Gordon and Donna Schwarzbach, my sister Courtney, and my girlfriend/unofficial life partner Lily for their continued support and belief in me as I pursued a PhD in organic chemistry. This has been the most challenging experience of my life and without these people in my corner I wouldn't have come this far.

However, without the unending support from Professor Brian Stoltz I wouldn't have survived. Brian has inspired, supported, and challenged me in ways I never thought possible. He has always encouraged me to pursue my intellectual interests and has tackled my adversities with openness and support. Under his guidance, I have managed to achieve academic success with my syntheses of the transtaganolide and basiliolide natural products. Brian has taught me that a strong chemist is both a scientist within and outside lab walls, providing reassurance that my never-sleeping brain is above all a gift.

I also praise my thesis committee members, Professors Bob Grubbs, Peter Dervan, Sarah Reisman, and Scott Virgil. During our meetings and throughout my graduate education they have been an invaluable resource guiding me and encouraging my success.

I thank my undergraduate academic supervisor, Professor Jason Sello. I was his first student as he began his academic career at Brown University. In our first meeting, I, a wide-eyed student of chemistry, and him, a seasoned scientist itching to educate, had realized we had been discussing chemistry for close to four hours, resulting in a missed evening class and a missed dinner with his wife. This passion for chemistry we both shared only grew and I hold Jason solely responsible for my deep love of experimental chemistry and the reason why I chose to pursue a PhD in chemistry.

As for my co-workers, I must first and foremost thank Hosea Nelson. He has been my primary collaborator on the transtaganolide and basiliolide research project as well as a dear friend. He is an excellent scientist and a person I hope to have the pleasure of working closely with once again.

I would also like to thank Chris Henry, a former post doc in the laboratory. He began his post doc around the time I joined Brian's group and was a treasured mentor, and I believe made me a better bench chemist.

I thank Alex (Rookie) Goldberg for the hours we have spent together discussing our chemistry and challenging one another to become better scientists. I must also acknowledge the rest of the Stoltz and Reisman group past and present. I have had the pleasure to work alongside a group of talented comrades who have contributed to my success and I couldn't have achieved this degree without them. In particular, I must thank Robert Craig and Beau Pritchett for taking the time to proofread my thesis.

Lastly, I must thank the technical and support staff of the chemistry department, including Dr. Scott Virgil, Dr. Dave VanderVelde, Lynne Martinez, Rick Gerhart, Joe Drew, Agnes Tong, and Anne Penney. Without them none of this could be possible.

Jonny

ABSTRACT

Herein are described the total syntheses of all members of the transtaganolide and basiliolide natural product family. Utilization of an Ireland–Claisen rearrangement/Diels–Alder cycloaddition cascade (ICR/DA) allowed for rapid assembly of the transtaganolide and basiliolide oxabicyclo[2.2.2]octane core. This methodology is general and was applicable to all members of the natural product family.

A brief introduction outlines all the synthetic progress previously disclosed by Lee, Dudley, and Johansson. This also includes the initial syntheses of transtaganolides C and D, as well as basiliolide B and epi-basiliolide B accomplished by Stoltz in 2011. Lastly, we discuss our racemic synthesis of basiliolide C and epi-basiliolide C, which utilized an ICR/DA cascade to construct the oxabicyclo[2.2.2]octane core and formal [5+2] annulation to form the ketene-acetal containing 7-membered C-ring.

Next, we describe a strategy for an asymmetric ICR/DA cascade, by incorporation of a chiral silane directing group. This allowed for enantioselective construction of the C8 all-carbon quaternary center formed in the Ireland–Claisen rearrangement. Furthermore, a single hydride reduction and subsequent transactonization of a C4 methylester bearing oxabicyclo[2.2.2]octane core demonstrated a viable strategy for the desired skeletal rearrangement to obtain pentacyclic transtaganolides A and B. Application of the asymmetric strategy culminated in the total syntheses of (–)-transtaganolide A, (+)-transtaganolide B, (+)-transtaganolide C, and (–)-transtaganolide D. Comparison of the optical rotation data of the synthetically derived transtaganolides to that from the isolated counterparts has overarching biosynthetic implications which are discussed.

Lastly, improvement to the formal [5+2] annulation strategy is described. Negishi cross-coupling of methoxyethynyl zinc chloride using a palladium Xantphos catalyst is optimized for iodo-cyclohexene. Application of this technology to an iodo-pyrone geranyl ester allowed for formation and isolation of the eneyne product. Hydration of the eneyne product forms natural metabolite basiliopyrone. Furthermore, the eneyne product can undergo an ICR/DA cascade and form transtaganolides C and D in a single step from an achiral monocyclic precursor.

TABLE OF CONTENTS

Acknowledgements	iv
Abstract	vi
Table of Contents	vii
List of Figures.....	xi
List of Schemes.....	xvii
List of Tables.....	xx
List of Abbreviations	xxii
CHAPTER 1	1
<i>Transtaganolide and Basiliolide Natural Products and Early Efforts Toward their Total Synthesis</i>	
1.1 Introduction	1
1.1.1 Isolation and Biological Activity.....	1
1.1.2 Biosynthetic Proposals	3
1.2 Synthetic Strategies for the Transtaganolide and Basiliolide ABD Tricyclic Core.....	6
1.3 Progress Toward the Synthesis of Transtaganolides C and D and Basiliolides B and C.....	9
1.3.1 Retrosynthetic Analysis	9
1.3.2 Progress for the Forward Synthesis	11
1.4 Total Syntheses of Transtaganolides C and D	12
1.5 Total Syntheses of Basiliolide B and epi-Basiliolide B.....	14
1.5.1 Stoltz and Coworkers' Approach.....	14
1.5.2 Lee and Coworkers' Approach.....	15
1.6 Total Syntheses of Basiliolide C and epi-Basiliolide C	18
1.7 Conclusion.....	20
1.8 Experimental Section.....	22
1.8.1 Materials and Methods.....	22
1.8.2 Preparative Procedures	23
1.9 Notes and References.....	33
APPENDIX 1	37
<i>Synthetic Summary for Basiliolide C and epi-Basiliolide C: Relevant to Chapter 1</i>	
A1.1 Synthetic Summary for Basiliolide C and epi-Basiliolide C	38

APPENDIX 2	40
<i>Comparison of Spectral Data for Synthetic and Reported Basiliolide C, as well as Biological Assays for Synthetic Transtaganolide C: Relevant to Chapter 1</i>	
A2.1 Comparison of ¹ H NMR and ¹³ C NMR for Synthetic and Reported Basiliolide C.....	41
A2.2 Bioactivity of Synthetic Transtaganolide C.....	43
A2.3 Notes and References.....	46
APPENDIX 3	47
<i>Spectra Relevant to Chapter 1</i>	
CHAPTER 2.....	66
<i>Total Syntheses of (–)-Transtaganolide A, (+)-Transtaganolide B, (+)-Transtaganolide C, and (–)-Transtaganolide D and Biosynthetic Implications</i>	
2.1 Introduction	66
2.2 Retrosynthetic Analysis	68
2.3 Enantioselective Total Syntheses of Transtaganolides C and D	69
2.4 Synthetic Strategies for the Total Syntheses of Transtaganolides A and B	71
2.5 Enantioselective Total Syntheses of Transtaganolides A and B	76
2.6 Biosynthetic Implications and Stereochemical Analysis of the Enantioselective Total Syntheses of Transtaganolides C and D.....	80
2.7 Conclusion.....	85
2.8 Experimental Section.....	86
2.8.1 Materials and Methods.....	86
2.8.2 Preparative Procedures	88
2.9 Notes and References.....	131
APPENDIX 4	134
<i>Synthetic Summary for (–)-Transtaganolide A, (+)-Transtaganolide B, (+)-Transtaganolide C, and (–)-Transtaganolide D: Relevant to Chapter 2</i>	
A4.1 Synthetic Summary for (+)-Transtaganolide C and (–)-Transtaganolide D.....	135
A4.2 Synthetic Summary for (–)-Transtaganolide A and (+)-Transtaganolide B	137
APPENDIX 5	143
<i>Comparison of Spectral Data for Synthetic and Reported Transtaganolides A–D, as well as CD Spectra: Relevant to Chapter 2</i>	
A5.1 Comparison of ¹ H NMR and ¹³ C NMR for Synthetic and Reported Transtaganolide A ..	144
A5.2 Comparison of ¹ H NMR and ¹³ C NMR for Synthetic and Reported Transtaganolide B ..	146

A5.3 Comparison of ^1H NMR and ^{13}C NMR for Synthetic and Reported Transtaganolide C ..	148
A5.4 Comparison of ^1H NMR and ^{13}C NMR for Synthetic and Reported Transtaganolide D..	150
A5.5 CD Spectra of Diffracted Crystal 133.....	152
A5.6 Notes and References.....	153
APPENDIX 6	154
<i>Spectra Relevant to Chapter 2</i>	
APPENDIX 7	216
<i>X-ray Crystallography Reports: Relevant to Chapter 2</i>	
A7.1 Crystal Structure Analysis for Compound 133	216
CHAPTER 3.....	235
<i>Negishi Cross-Coupling of Zinc Methoxyacetylides and Protecting-Group-Free Total Syntheses of Basiliopyrone and Transtaganolides C and D</i>	
3.1 Introduction	235
3.2 Model Cross-Coupling Reactions of Zinc Methoxyacetylides	238
3.3 Ligand Bite Angles and the Relationship to Organozinc Cross-Coupling of Methoxyethynyl Zinc Chloride	240
3.4 Applications of Organozinc Cross-Couplings to the Syntheses of Transtaganolide Natural Products	242
3.5 Protecting-Group-Free Syntheses of Basiliopyrone and Transtaganolides C and D.....	247
3.6 Conclusion.....	249
3.7 Experimental Section.....	250
3.7.1 Materials and Methods.....	250
3.7.2 Preparative Procedures	252
3.8 Notes and References.....	258
APPENDIX 8	260
<i>Synthetic Summary for Protecting-Group-Free Total Syntheses of Basiliopyrone and Transtaganolides C and D: Relevant to Chapter 3</i>	
A8.1 Synthetic Summary for Basiliopyrone and Transtaganolides C and D	261
APPENDIX 9	263
<i>Gas Chromatography and Supercritical Fluid Chromatography Data: Relevant to Chapter 3</i>	
A9.1 Gas Chromatography Data for Organozinc Cross-Coupling Optimization.....	264

A9.2 Supercritical Fluid Chromatography Data for Organozinc Cross-Coupling Optimization	265
A9.3 Notes and References	267
APPENDIX 10	268
<i>Spectra Relevant to Chapter 3</i>	
<i>Comprehensive Bibliography</i>	273
<i>Index</i>	278
<i>About the Author</i>	285

LIST OF FIGURES

CHAPTER 1*Transtaganolide and Basiliolide Natural Products and Early Efforts Toward their Total Synthesis*

Figure 1.1.1. A) Thapsigargin (1). B) Crystal structure of thapsigargin (1) bound SERCA-ATPase.....	2
Figure 1.1.2. Natural products isolated from <i>Thapsia</i>	3
Figure 1.2.1. The transtaganolide and basiliolide structural features.....	7

APPENDIX 2*Comparison of Spectral Data for Synthetic and Reported Basiliolide C, as well as Biological Assays for Synthetic Transtaganolide C: Relevant to Chapter 1*

Figure A2.2.1. A) Thapsigargin (1) and transtaganolide C (9). B) The effect of synthetic transtaganolide C (9) or naturally isolated thapsigargin (1) on calcium mobilization as a function of time (arrows indicate the time at which a reagent was added). ³	43
Figure A2.2.2. Percentage of cells still viable after 24 hours of exposure to either synthetic transtaganolide C (9) or thapsigargin (1). ³	44

APPENDIX 3*Spectra Relevant to Chapter 1*

Figure A3.1.1 ¹ H NMR (300 MHz, CDCl ₃) of compound 84	48
Figure A3.1.2 Infrared spectrum (thin film/NaCl) of compound 84	49
Figure A3.1.3 ¹³ C NMR (75 MHz, CDCl ₃) of compound 84	49
Figure A3.2.1 ¹ H NMR (300 MHz, CDCl ₃) of compound 85	50
Figure A3.2.2 Infrared spectrum (thin film/NaCl) of compound 85	51
Figure A3.2.3 ¹³ C NMR (75 MHz, CDCl ₃) of compound 85	51
Figure A3.3.1 ¹ H NMR (300 MHz, CDCl ₃) of compound 85.5	52
Figure A3.3.2 Infrared spectrum (thin film/NaCl) of compound 85.5	53
Figure A3.3.3 ¹³ C NMR (75 MHz, CDCl ₃) of compound 85.5	53
Figure A3.4.1 ¹ H NMR (300 MHz, CDCl ₃) of compound 86	54
Figure A3.4.2 Infrared spectrum (thin film/NaCl) of compound 86	55
Figure A3.4.3 ¹³ C NMR (75 MHz, CDCl ₃) of compound 86	55
Figure A3.5.1 ¹ H NMR (300 MHz, CDCl ₃) of compound 87	56
Figure A3.5.2 Infrared spectrum (thin film/NaCl) of compound 87	57
Figure A3.5.3 ¹³ C NMR (75 MHz, CDCl ₃) of compound 87	57
Figure A3.6.1 ¹ H NMR (300 MHz, CDCl ₃) of compounds 88a and 88b	58

Figure A3.6.2 Infrared spectrum (thin film/NaCl) of compounds 88a and 88b	59
Figure A3.6.3 ¹³ C NMR (75 MHz, CDCl ₃) of compounds 88a and 88b	59
Figure A3.7.1 ¹ H NMR (300 MHz, CDCl ₃) of compounds 89a and 89b	60
Figure A3.7.2 Infrared spectrum (thin film/NaCl) of compounds 89a and 89b	61
Figure A3.7.3 ¹³ C NMR (75 MHz, CDCl ₃) of compounds 89a and 89b	61
Figure A3.8.1 ¹ H NMR (500 MHz, CDCl ₃) of basiliolide C (12).....	62
Figure A3.8.2 Infrared spectrum (thin film/NaCl) of basiliolide C (12).....	63
Figure A3.8.3 ¹³ C NMR (125 MHz, CDCl ₃) of basiliolide C (12).....	63
Figure A3.9.1 ¹ H NMR (500 MHz, CDCl ₃) of epi-basiliolide C (43).....	64
Figure A3.9.2 Infrared spectrum (thin film/NaCl) of epi-basiliolide C (43).....	65
Figure A3.9.3 ¹³ C NMR (125 MHz, CDCl ₃) of epi-basiliolide C (43).....	65

CHAPTER 2

Total Syntheses of (–)-Transtaganolide A, (+)-Transtaganolide B, (+)-Transtaganolide C, and (–)-Transtaganolide D and Biosynthetic Implications

Figure 2.1.1. Transtaganolide and basiliolide natural products (7–11 and 42).....	67
Figure 2.8.1. Racemic SFC trace of compound 97	90
Figure 2.8.2. Enantioenriched SFC trace of compound 97	90
Figure 2.8.3. Racemic SFC trace of compounds 100a and 100b	92
Figure 2.8.4. Enantioenriched SFC trace of compounds 100a and 100b	93
Figure 2.8.5. Racemic SFC trace of transtaganolide C (9).....	96
Figure 2.8.6. Enantioenriched SFC trace of transtaganolide C (9).....	96
Figure 2.8.7. Racemic SFC trace of transtaganolide D (10).....	97
Figure 2.8.8. Enantioenriched SFC trace of transtaganolide D (10).....	97
Figure 2.8.9. Reaction schematic for the single hydride reduction of tricyclic acids 120a and 120b using a glass cannula.	113
Figure 2.8.10. Racemic SFC trace of transtaganolide B (8).....	127
Figure 2.8.11. Enantioenriched SFC trace of transtaganolide B (8).....	127
Figure 2.8.12. Racemic SFC trace of transtaganolide A (7).....	128
Figure 2.8.13. Enantioenriched SFC trace of transtaganolide A (7).....	128

APPENDIX 5

Comparison of Spectral Data for Synthetic and Reported Transtaganolides A–D, as well as CD Spectra: Relevant to Chapter 2

Figure A5.5.1. CD spectral comparison of diffracted crystal 133 to 90% enantioenriched bulk sample of 133 and 135	152
--	-----

APPENDIX 6*Spectra Relevant to Chapter 2*

Figure A6.1.1 ^1H NMR (500 MHz, CDCl_3) of compound 97	155
Figure A6.1.2 Infrared spectrum (thin film/ NaCl) of compound 97	156
Figure A6.1.3 ^{13}C NMR (125 MHz, CDCl_3) of compound 97	156
Figure A6.2.1 ^1H NMR (500 MHz, CDCl_3) of compounds 100a and 100b	157
Figure A6.2.2 Infrared spectrum (thin film/ NaCl) of compounds 100a and 100b	158
Figure A6.2.3 ^{13}C NMR (125 MHz, CDCl_3) of compounds 100a and 100b	158
Figure A6.3.1 ^1H NMR (500 MHz, CDCl_3) of transtaganolide C (9).....	159
Figure A6.3.2 Infrared spectrum (thin film/ NaCl) of transtaganolide C (9).....	160
Figure A6.3.3 ^{13}C NMR (125 MHz, CDCl_3) of transtaganolide C (9).....	160
Figure A6.4.1 ^1H NMR (500 MHz, CDCl_3) of transtaganolide D (10).....	161
Figure A6.4.2 Infrared spectrum (thin film/ NaCl) of transtaganolide D (10).....	162
Figure A6.4.3 ^{13}C NMR (125 MHz, CDCl_3) of transtaganolide D (10).....	162
Figure A6.5.1 ^1H NMR (500 MHz, CDCl_3) of compound 105	163
Figure A6.5.2 Infrared spectrum (thin film/ NaCl) of compound 105	164
Figure A6.5.3 ^{13}C NMR (125 MHz, CDCl_3) of compound 105	164
Figure A6.6.1 ^1H NMR (300 MHz, CDCl_3) of compound 106	165
Figure A6.6.2 Infrared spectrum (thin film/ NaCl) of compound 106	166
Figure A6.6.3 ^{13}C NMR (75 MHz, CDCl_3) of compound 106	166
Figure A6.7.1 ^1H NMR (300 MHz, CDCl_3) of compound 107	167
Figure A6.7.2 Infrared spectrum (thin film/ NaCl) of compound 107	168
Figure A6.7.3 ^{13}C NMR (125 MHz, CDCl_3) of compound 107	168
Figure A6.8.1 ^1H NMR (300 MHz, CDCl_3) of compound 108	169
Figure A6.8.2 Infrared spectrum (thin film/ NaCl) of compound 108	170
Figure A6.8.3 ^{13}C NMR (75 MHz, CDCl_3) of compound 108	170
Figure A6.9.1 ^1H NMR (300 MHz, CDCl_3) of compound 109	171
Figure A6.9.2 Infrared spectrum (thin film/ NaCl) of compound 109	172
Figure A6.9.3 ^{13}C NMR (75 MHz, CDCl_3) of compound 109	172
Figure A6.10.1 ^1H NMR (300 MHz, CDCl_3) of compounds 110a and 110b	173
Figure A6.10.2 Infrared spectrum (thin film/ NaCl) of compounds 110a and 110b	174
Figure A6.10.3 ^{13}C NMR (125 MHz, CDCl_3) of compounds 110a and 110b	174
Figure A6.11.1 ^1H NMR (300 MHz, CDCl_3) of compounds 112a and 112b	175
Figure A6.11.2 Infrared spectrum (thin film/ NaCl) of compounds 112a and 112b	176

Figure A6.11.3 ^{13}C NMR (125 MHz, CDCl_3) of compounds 112a and 112b	176
Figure A6.12.1 ^1H NMR (500 MHz, CDCl_3) of compound 113	177
Figure A6.12.2 Infrared spectrum (thin film/ NaCl) of compound 113	178
Figure A6.12.3 ^{13}C NMR (125 MHz, CDCl_3) of compound 113	178
Figure A6.13.1 ^1H NMR (300 MHz, CDCl_3) of compound 114	179
Figure A6.13.2 Infrared spectrum (thin film/ NaCl) of compound 114	180
Figure A6.13.3 ^{13}C NMR (125 MHz, CDCl_3) of compound 114	180
Figure A6.14.1 ^1H NMR (300 MHz, CDCl_3) of compound 115	181
Figure A6.14.2 Infrared spectrum (thin film/ NaCl) of compound 115	182
Figure A6.14.3 ^{13}C NMR (125 MHz, CDCl_3) of compound 115	182
Figure A6.15.1 ^1H NMR (500 MHz, CDCl_3) of a crude mixture of compounds 116a and 116b	183
Figure A6.16.1 ^1H NMR (300 MHz, CDCl_3) of compound 118	184
Figure A6.16.2 Infrared spectrum (thin film/ NaCl) of compound 118	185
Figure A6.16.3 ^{13}C NMR (125 MHz, CDCl_3) of compound 118	185
Figure A6.17.1 ^1H NMR (300 MHz, CDCl_3) of compound 119	186
Figure A6.17.2 Infrared spectrum (thin film/ NaCl) of compound 119	187
Figure A6.17.3 ^{13}C NMR (75 MHz, CDCl_3) of compound 119	187
Figure A6.18.1 ^1H NMR (500 MHz, CDCl_3) of compounds 120a and 120b	188
Figure A6.18.2 Infrared spectrum (thin film/ NaCl) of compounds 120a and 120b	189
Figure A6.18.3 ^{13}C NMR (125 MHz, CDCl_3) of compounds 120a and 120b	189
Figure A6.19.1 ^1H NMR (300 MHz, CDCl_3) of compound 122	190
Figure A6.19.2 Infrared spectrum (thin film/ NaCl) of compound 122	191
Figure A6.19.3 ^{13}C NMR (75 MHz, CDCl_3) of compound 122	191
Figure A6.20.1 ^1H NMR (500 MHz, CDCl_3) of compound 123	192
Figure A6.20.2 Infrared spectrum (thin film/ NaCl) of compound 123	193
Figure A6.20.3 ^{13}C NMR (125 MHz, CDCl_3) of compound 123	193
Figure A6.21.1 ^1H NMR (300 MHz, CDCl_3) of compound 124	194
Figure A6.21.2 Infrared spectrum (thin film/ NaCl) of compound 124	195
Figure A6.21.3 ^{13}C NMR (75 MHz, CDCl_3) of compound 124	195
Figure A6.22.1 ^1H NMR (300 MHz, CDCl_3) of compound 125	196
Figure A6.22.2 Infrared spectrum (thin film/ NaCl) of compound 125	197
Figure A6.22.3 ^{13}C NMR (75 MHz, CDCl_3) of compound 125	197
Figure A6.23.1 ^1H NMR (300 MHz, CDCl_3) of compound 126	198
Figure A6.23.2 Infrared spectrum (thin film/ NaCl) of compound 126	199
Figure A6.23.3 ^{13}C NMR (75 MHz, CDCl_3) of compound 126	199

Figure A6.24.1 ¹ H NMR (300 MHz, CDCl ₃) of compound 127	200
Figure A6.24.2 Infrared spectrum (thin film/NaCl) of compound 127	201
Figure A6.24.3 ¹³ C NMR (125 MHz, CDCl ₃) of compound 127	201
Figure A6.25.1 ¹ H NMR (500 MHz, CDCl ₃) of compounds 128a and 128b	202
Figure A6.25.2 Infrared spectrum (thin film/NaCl) of compounds 128a and 128b	203
Figure A6.25.3 ¹³ C NMR (125 MHz, CDCl ₃) of compounds 128a and 128b	203
Figure A6.26.1 ¹ H NMR (500 MHz, CDCl ₃) of compounds 121a and 121b	204
Figure A6.26.2 Infrared spectrum (thin film/NaCl) of compounds 121a and 121b	205
Figure A6.26.3 ¹³ C NMR (125 MHz, CDCl ₃) of compounds 121a and 121b	205
Figure A6.27.1 ¹ H NMR (500 MHz, CDCl ₃) of compounds 130a and 130b	206
Figure A6.27.2 Infrared spectrum (thin film/NaCl) of compounds 130a and 130b	207
Figure A6.27.3 ¹³ C NMR (125 MHz, CDCl ₃) of compounds 130a and 130b	207
Figure A6.28.1 ¹ H NMR (500 MHz, CDCl ₃) of transtaganolide B (8).....	208
Figure A6.28.2 Infrared spectrum (thin film/NaCl) of transtaganolide B (8).....	209
Figure A6.28.3 ¹³ C NMR (125 MHz, CDCl ₃) of transtaganolide B (8).....	209
Figure A6.29.1 ¹ H NMR (500 MHz, CDCl ₃) of transtaganolide A (7).....	210
Figure A6.29.2 Infrared spectrum (thin film/NaCl) of transtaganolide A (7).....	211
Figure A6.29.3 ¹³ C NMR (125 MHz, CDCl ₃) of transtaganolide A (7).....	211
Figure A6.30.1 ¹ H NMR (500 MHz, CDCl ₃) of compound 133	212
Figure A6.30.2 Infrared spectrum (thin film/NaCl) of compound 133	213
Figure A6.30.3 ¹³ C NMR (125 MHz, CDCl ₃) of compound 133	213
Figure A6.31.1 ¹ H NMR (500 MHz, CDCl ₃) of compound 135	214
Figure A6.31.2 Infrared spectrum (thin film/NaCl) of compound 135	215
Figure A6.31.3 ¹³ C NMR (125 MHz, CDCl ₃) of compound 135	215

APPENDIX 7

X-ray Crystallography Reports: Relevant to Chapter 2

Figure A7.1.1. Ortep diagram of **133**. The crystallographic data have been deposited in the Cambridge Database (CCDC) and has been placed on hold pending further instructions. . 217

CHAPTER 3

Negishi Cross-Coupling of Zinc Methoxyacetylides and Protecting-Group-Free Total Syntheses of Basiliopyrone and Transtaganolides C and D

Figure 3.1.1. Transtaganolides and basiliolides (**7–12**, **42**, and **43**)..... 236

APPENDIX 9*Gas Chromatography and Supercritical Fluid Chromatography Data: Relevant to Chapter 3*

Figure A9.1.1. A) Calibration curve used to determine cross-coupling yields comparing methyl ester 139 and tridecane internal standard. B) Calibration curve used to determine cross-coupling substrate consumption by comparing vinyl iodide 137 and tridecane internal standard.....	264
Figure A9.2.1. Calibration curve used to determine cross-coupling yields comparing eneyne 141 and diphenylether internal standard.	266

APPENDIX 10*Spectra Relevant to Chapter 3*

Figure A10.1.1 ¹ H NMR (500 MHz, CDCl ₃) of compound 141	269
Figure A10.1.2 Infrared spectrum (thin film/NaCl) of compound 141	270
Figure A10.1.3 ¹³ C NMR (125 MHz, CDCl ₃) of compound 141	270
Figure A10.2.1 ¹ H NMR (300 MHz, CDCl ₃) of basiliopyrone (3)	271
Figure A10.2.2 Infrared spectrum (thin film/NaCl) of basiliopyrone C (3)	272
Figure A10.2.3 ¹³ C NMR (125 MHz, CDCl ₃) of basiliopyrone (3)	272

LIST OF SCHEMES

CHAPTER 1*Transtaganolide and Basiliolide Natural Products and Early Efforts Toward their Total Synthesis*

<i>Scheme 1.1.1. Appendino's biosynthetic proposal</i>	4
<i>Scheme 1.1.2. Massanet's biosynthetic proposal</i>	5
<i>Scheme 1.1.3. Johansson's biosynthetic proposal</i>	6
<i>Scheme 1.2.1. Stoltz's synthesis of ABD tricyclic core of the transtaganolides and basiliolides</i>	8
<i>Scheme 1.2.2. A) Dudley's synthesis of ABD tricyclic core of the transtaganolides and basiliolides. B) Lee's synthesis of ABD tricyclic core of the transtaganolides and basiliolides</i>	9
<i>Scheme 1.3.1. Retrosynthetic analysis of transtaganolides C and D (9 and 10) and basiliolides B and C (11 and 12)</i>	10
<i>Scheme 1.3.2. Stoltz's progress toward the synthesis of transtaganolides C and D (9 and 10)</i>	11
<i>Scheme 1.3.3. Johansson's progress toward the synthesis of transtaganolides C and D (9 and 10)</i> ...	12
<i>Scheme 1.4.1. Ireland–Claisen/Diels–Alder cycloaddition cascade (ICR/DA)</i>	13
<i>Scheme 1.4.2. Synthesis of stannyl methoxyacetylde 62</i>	13
<i>Scheme 1.4.3. Total syntheses of transtaganolides C and D (9 and 10)</i>	14
<i>Scheme 1.5.1. Stoltz's total syntheses of basiliolide B and epi-basiliolide B (11 and 42)</i>	15
<i>Scheme 1.5.2. Lee's synthesis of basiliolide B (11)</i>	16
<i>Scheme 1.5.3. Lee's continued synthesis of basiliolide B (11)</i>	18
<i>Scheme 1.6.1. Total syntheses of basiliolide C (12) and epi-basiliolide C (43)</i>	20

APPENDIX 1*Synthetic Summary for Basiliolide C and epi-Basiliolide C: Relevant to Chapter 1*

<i>Scheme A1.1.1. Retrosynthetic analysis for basiliolide C (12) and epi-basiliolide C (43)</i>	38
<i>Scheme A1.1.2. Syntheses of basiliolide C (12) and epi-basiliolide C (43)</i>	39

CHAPTER 2*Total Syntheses of (–)-Transtaganolide A, (+)-Transtaganolide B, (+)-Transtaganolide C, and (–)-Transtaganolide D and Biosynthetic Implications*

<i>Scheme 2.1.1. General synthetic strategy</i>	67
<i>Scheme 2.2.1. Retrosynthetic analysis for the asymmetric construction of transtaganolides A (7) and B (8)</i>	68
<i>Scheme 2.2.2. Retrosynthetic analysis for the asymmetric construction of transtaganolides C (9) and D (10)</i>	69

Scheme 2.3.1. <i>Enantioselective total syntheses of transtaganolides C and D (9 and 10)</i>	70
Scheme 2.4.1. <i>Initial attempts at preparing the tricyclic cores of transtaganolides A and B (103a and 103b)</i>	71
Scheme 2.4.2. <i>Studies for the transtaganolide A and B (7 and 8) tetracyclic core via protected alcohol 109</i>	73
Scheme 2.4.3. <i>Studies for the transtaganolide A and B (7 and 8) tetracyclic core via Weinreb amide 115</i>	74
Scheme 2.4.4. <i>Studies for the transtaganolide A and B (7 and 8) tetracyclic core via methylester 119</i>	76
Scheme 2.5.1. <i>Syntheses of enantioenriched tricyclic cores of transtaganolides A and B (128a and 128b)</i>	77
Scheme 2.5.2. <i>Enantioselective total syntheses of transtaganolides A and B (7 and 8)</i>	79
Scheme 2.6.1. <i>Johansson's biosynthetic proposal</i>	81
Scheme 2.6.2. <i>Analysis of chiral silane directed ICR/DA cascade (where pyr = iodo pyrone)</i>	82
Scheme 2.6.3. <i>Determination of the absolute stereochemistry of intermediate 100a</i>	83
Scheme 2.6.4. <i>Proposed biosynthesis of basiliopyrone (3)</i>	85

APPENDIX 4

Synthetic Summary for (-)-Transtaganolide A, (+)-Transtaganolide B, (+)-Transtaganolide C, and (-)-Transtaganolide D: Relevant to Chapter 2

Scheme A4.1.1. <i>Retrosynthetic analysis for (+)-transtaganolide C (9) and (-)-transtaganolide D (10)</i>	135
Scheme A4.1.2. <i>Syntheses of (+)-transtaganolide C (9) and (-)-transtaganolide D (10)</i>	136
Scheme A4.2.1. <i>Retrosynthetic analysis for (-)-transtaganolide A (7) and (+)-transtaganolide B (8)</i>	137
Scheme A4.2.2. <i>First attempt to synthesize (\pm)-transtaganolide A and B (7-8) tetracyclic core via protected alcohol 109</i>	138
Scheme A4.2.3. <i>Second attempt to synthesize (\pm)-transtaganolide A and B (7-8) tetracyclic core via Weinreb amide 115</i>	139
Scheme A4.2.4. <i>Third attempt to synthesize (\pm)-transtaganolide A and B (7-8) tetracyclic core via methylester 119</i>	140
Scheme A4.2.5. <i>Forward syntheses of (-)-transtaganolide A (7) and (+)-transtaganolide B (8)</i>	141
Scheme A4.2.6. <i>Continued forward syntheses of (-)-transtaganolide A (7) and (+)-transtaganolide B (8)</i>	142

CHAPTER 3*Negishi Cross-Coupling of Zinc Methoxyacetylides and Protecting-Group-Free Total Syntheses of Basiliopyrone and Transtaganolides C and D*

- Scheme 3.1.1. A) Cross-coupling to form transtaganolides A and B (**7** and **8**). B) Cross-coupling to form transtaganolides C and D (**9** and **10**). C) Cross-coupling to form basiliolide B (**11**) and epi-basiliolide B (**42**). D) Cross-coupling to form basiliolide C (**12**) and epi-basiliolide C (**43**). 237
- Scheme 3.2.1. Synthesis of methoxyethynyl zinc chloride (**136**)..... 238
- Scheme 3.4.1. A) Cross-coupling of tricycles **63a** and **63b** using the palladium Xantphos catalytic conditions developed on model cross-couplings to iodo-cyclohexene (**137**). B) Cross-coupling of tricycles **63a** and **63b** facilitated by microwave irradiation..... 243
- Scheme 3.4.2. Retrosynthetic Analysis illuminates a viable cross-coupling substrate pyrone ester **57**. 244
- Scheme 3.4.3. Cross-coupling of pyrone **57** and methoxyethynyl zinc chloride (**136**) using our optimized reaction conditions. 247
- Scheme 3.5.1. Acid catalyzed hydration of **141** allows for the formation of basiliopyrone (**3**)..... 248
- Scheme 3.5.2. A one-pot synthesis of transtaganolides C and D (**9** and **10**) from alkynyl pyrone **141**. 249

APPENDIX 8*Synthetic Summary for Protecting-Group-Free Total Syntheses of Basiliopyrone and Transtaganolides C and D: Relevant to Chapter 3*

- Scheme A8.1.1. Protecting-group-free synthesis of basiliopyrone (**3**)..... 261
- Scheme A8.1.2. Protecting-group-free syntheses of transtaganolides C and D (**9–10**). 262

LIST OF TABLES

APPENDIX 2

Comparison of Spectral Data for Synthetic and Reported Basiliolide C, as well as Biological Assays for Synthetic Transtaganolide C: Relevant to Chapter 1

Table A2.1.1. Comparison of ^1H NMR data for synthetic and reported natural basiliolide C (**12**)..... 41

Table A2.1.2. Comparison of ^{13}C NMR data for synthetic and reported natural¹ basiliolide C (**12**)..... 42

CHAPTER 2

Total Syntheses of (–)-Transtaganolide A, (+)-Transtaganolide B, (+)-Transtaganolide C, and (–)-Transtaganolide D and Biosynthetic Implications

Table 2.6.1. Comparison of the optical rotations of synthetic and natural transtaganolides A–D (**7–10**).83

APPENDIX 5

Comparison of Spectral Data for Synthetic and Reported Transtaganolides A–D, as well as CD Spectra: Relevant to Chapter 2

Table A5.1.1. Comparison of ^1H NMR data for synthetic and reported natural transtaganolide A (**7**).144

Table A5.1.2. Comparison of ^{13}C NMR data for synthetic and reported natural¹ transtaganolide A (**7**).145

Table A5.2.1. Comparison of ^1H NMR data for synthetic and reported natural¹ transtaganolide B (**8**).146

Table A5.2.2. Comparison of ^{13}C NMR data for synthetic and reported natural¹ transtaganolide B (**8**).147

Table A5.3.1. Comparison of ^1H NMR data for synthetic and reported natural¹ transtaganolide C (**9**).148

Table A5.3.2. Comparison of ^{13}C NMR data for synthetic and reported natural¹ transtaganolide C (**9**).149

Table A5.4.1. Comparison of ^1H NMR data for synthetic and reported natural¹ transtaganolide D (**10**).150

Table A5.4.2. Comparison of ^{13}C NMR data for synthetic and reported natural¹ transtaganolide D (**10**).151

APPENDIX 7

X-ray Crystallography Reports: Relevant to Chapter 2

Table A7.1.1. Crystal data and structure analysis details for **133**. 218

Table A7.1.2. Atomic coordinates ($\times 10^4$) and equivalent isotropic displacement parameter ($\text{\AA}^2 \times 10^3$) for **133**. $U(\text{eq})$ is defined as one third of the trace of the orthogonalized U^{ij} tensor 221

Table A7.1.3. Bond lengths [\AA] and angles [$^\circ$] for **133**. 223

Table A7.1.4. Anisotropic displacement parameters ($\text{\AA}^2 \times 10^4$) for **133**. The anisotropic displacement factor exponent takes the form: $-2\pi^2 [h^2 a^{*2} U^{11} + \dots + 2 h k a^* b^* U^{12}]$ 231

Table A7.1.5. Hydrogen coordinates ($\times 10^3$) and isotropic displacement parameters ($\text{\AA}^2 \times 10^3$) for **133**. 233

CHAPTER 3*Negishi Cross-Coupling of Zinc Methoxyacetylides and Protecting-Group-Free Total Syntheses of Basiliopyrone and Transtaganolides C and D*

<i>Table 3.2.1. Ligand screen for the cross-coupling of methoxyethynyl zinc chloride (136) and iodo-cyclohexene (137).</i>	240
<i>Table 3.3.1. Comparing dppb, dppf, and Xantphos as ligands for catalyzing the cross-coupling of methoxyethynyl zinc chloride (136) and iodo-cyclohexene (137) as a function of time.</i>	242
<i>Table 3.4.1. Comparing methoxyethynyl zinc chloride (136) equivalents, catalyst loading, and concentration as they effect the cross-coupling reaction at 50 °C of organozinc 136 and pyrone 57 as a function of time.</i>	245
<i>Table 3.4.2. Comparing methoxyethynyl zinc chloride (136) equivalents and catalyst loading as they effect the cross-coupling reaction at 40 °C of organozinc 136 and pyrone 57 as a function of time.</i>	246

APPENDIX 9*Gas Chromatography and Supercritical Fluid Chromatography Data: Relevant to Chapter 3*

<i>Table A9.1.1. A) The molar ratio of product 139 and tridecane with the associated peak area ratio obtained from GC analysis. B) The molar ratio of substrate 137 and tridecane with the associated peak area ratio obtained from GC analysis.</i>	265
<i>Table A9.2.1. The molar ratio of product 141 and diphenylether internal standard with the associated peak area ratio obtained from SFC analysis.</i>	266

LIST OF ABBREVIATIONS

Å	Ångstrom
$[\alpha]_D$	specific rotation at wavelength of sodium D line
Ac	acetyl
Anal.	Combustion elemental analysis
APCI	atmospheric pressure chemical ionization
app	apparent
aq	aqueous
AIBN	2,2'-azobisisobutyronitrile
Ar	aryl
atm	atmosphere
BBN	borabicyclononane
Bn	benzyl
Boc	<i>tert</i> -butyloxycarbonyl
bp	boiling point
br	broad
Bu	butyl
<i>i</i> -Bu	<i>iso</i> -butyl
<i>n</i> -Bu	butyl
<i>t</i> -Bu	<i>tert</i> -Butyl
Bz	benzoyl
<i>c</i>	concentration for specific rotation measurements
°C	degrees Celsius
ca.	about (Latin circa)
calc'd	calculated
CAN	ceric ammonium nitrate
cat	catalytic
Cbz	carbobenzyloxy
CCDC	Cambridge Crystallographic Data Centre
CDI	1,1'-carbonyldiimidazole

cf.	compare (Latin confer)
CI	chemical ionization
CID	collision-induced dissociation
cm ⁻¹	wavenumber(s)
comp	complex
Cy	cyclohexyl
d	doublet
D	deuterium
dba	dibenzylideneacetone
DBU	1,8-diazabicyclo[5.4.0]undec-7-ene
DCE	dichloroethane
dec	decomposition
DIAD	diisopropyl azodicarboxylate
DMA	<i>N,N</i> -dimethylacetamide
DMAP	4-dimethylaminopyridine
dmdba	bis(3,5-dimethoxybenzylidene)acetone
DMF	<i>N,N</i> -dimethylformamide
DMSO	dimethyl sulfoxide
DNA	(deoxy)ribonucleic acid
dppb	1,4-bis(diphenylphosphino)butane
dppf	1,1'-bis(diphenylphosphino)ferrocene
dr	diastereomeric ratio
<i>E</i> _A	activation energy
EC ₅₀	median effective concentration (50%)
EDC	<i>N</i> -(3-dimethylaminopropyl)- <i>N</i> '-ethylcarbodiimide
ee	enantiomeric excess
EI	electron impact
e.g.	for example (Latin exempli gratia)
equiv	equivalent
ESI	electrospray ionization
Et	ethyl
FAB	fast atom bombardment

FID	flame ionization detector
g	gram(s)
GC	gas chromatography
gCOSY	gradient-selected correlation spectroscopy
GlyPHOX	2-(2-(diphenylphosphino)phenyl)oxazoline
h	hour(s)
HMDS	1,1,1,3,3,3-hexamethyldisilazane
HMPA	hexamethylphosphoramide
HOBt	1-hydroxybenzotriazole
HPLC	high-performance liquid chromatography
HRMS	high-resolution mass spectroscopy
HSV	herpes simplex virus
$h\nu$	light
Hz	hertz
IC ₅₀	median inhibition concentration (50%)
ICR/DA	Ireland–Claisen rearrangement/Diels–Alder cycloaddition cascade
i.e.	that is (Latin id est)
IR	infrared (spectroscopy)
J	coupling constant
kcal	kilocalorie
KDA	potassium diisopropylamide
KHMDS	potassium hexamethyldisilazide
λ	wavelength
L	liter
LDA	lithium diisopropylamide
lit.	literature value
LTQ	linear trap quadrupole
m	multiplet; milli
m	meta
m/z	mass to charge ratio
M	metal; molar; molecular ion
Me	methyl

MHz	megahertz
μ	micro
μwaves	microwave irradiation
min	minute(s)
MM	mixed method
mol	mole(s)
MOM	methoxymethyl
mp	melting point
Ms	methanesulfonyl (mesyl)
MS	molecular sieves
n	nano
N	normal
nbd	norbornadiene
NBS	<i>N</i> -bromosuccinimide
NIST	National Institute of Standards and Technology
NMO	<i>N</i> -methylmorpholine <i>N</i> -oxide
NMR	nuclear magnetic resonance
NOE	nuclear Overhauser effect
NOESY	nuclear Overhauser enhancement spectroscopy
Nu	nucleophile
[O]	oxidation
<i>o</i>	ortho
<i>p</i>	para
PA	proton affinity
PCC	pyridinium chlorochromate
PDC	pyridinium dichromate
Ph	phenyl
pH	hydrogen ion concentration in aqueous solution
PhH	benzene
PhMe	toluene
PHOX	phosphinooxazoline
Piv	pivaloyl

pK_a	pK for association of an acid
PMB	<i>p</i> -methoxybenzyl
pmdba	bis(4-methoxybenzylidene)acetone
ppm	parts per million
PPTS	pyridinium <i>p</i> -toluenesulfonate
Pr	propyl
<i>i</i> -Pr	isopropyl
Py	pyridine
q	quartet
ref	reference
R	generic for any atom or functional group
R_f	retention factor
rt	room temperature
s	singlet or strong or selectivity factor
sat.	saturated
SET	single electron transfer
S_N2	second-order nucleophilic substitution
sp.	species
t	triplet
TBAF	tetrabutylammonium fluoride
TBHP	<i>tert</i> -butyl hydroperoxide
TBS	<i>tert</i> -butyldimethylsilyl
TCDI	1,1'-thiocarbonyldiimidazole
TCNE	tetracyanoethylene
Tf	trifluoromethanesulfonyl (trifyl)
TFA	trifluoroacetic acid
TFE	2,2,2-trifluoroethanol
THF	tetrahydrofuran
TIPS	triisopropylsilyl
TLC	thin-layer chromatography
TMEDA	<i>N,N,N',N'</i> -tetramethylethylenediamine
TMS	trimethylsilyl

TOF	time-of-flight
Tol	tolyl
TON	turnover number
t_R	retention time
Ts	<i>p</i> -toluenesulfonyl (tosyl)
UV	ultraviolet
v/v	volume to volume
w	weak
w/v	weight to volume
X	anionic ligand or halide

CHAPTER 1

Transtaganolide and Basiliolide Natural Products and Early Efforts

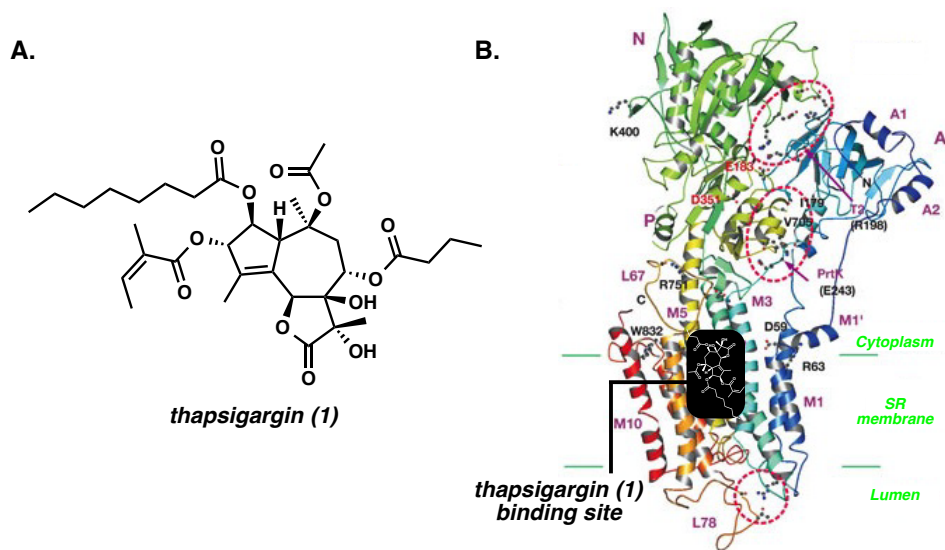
Toward their Total Synthesis

1.1 INTRODUCTION

1.1.1 ISOLATION AND BIOLOGICAL ACTIVITY

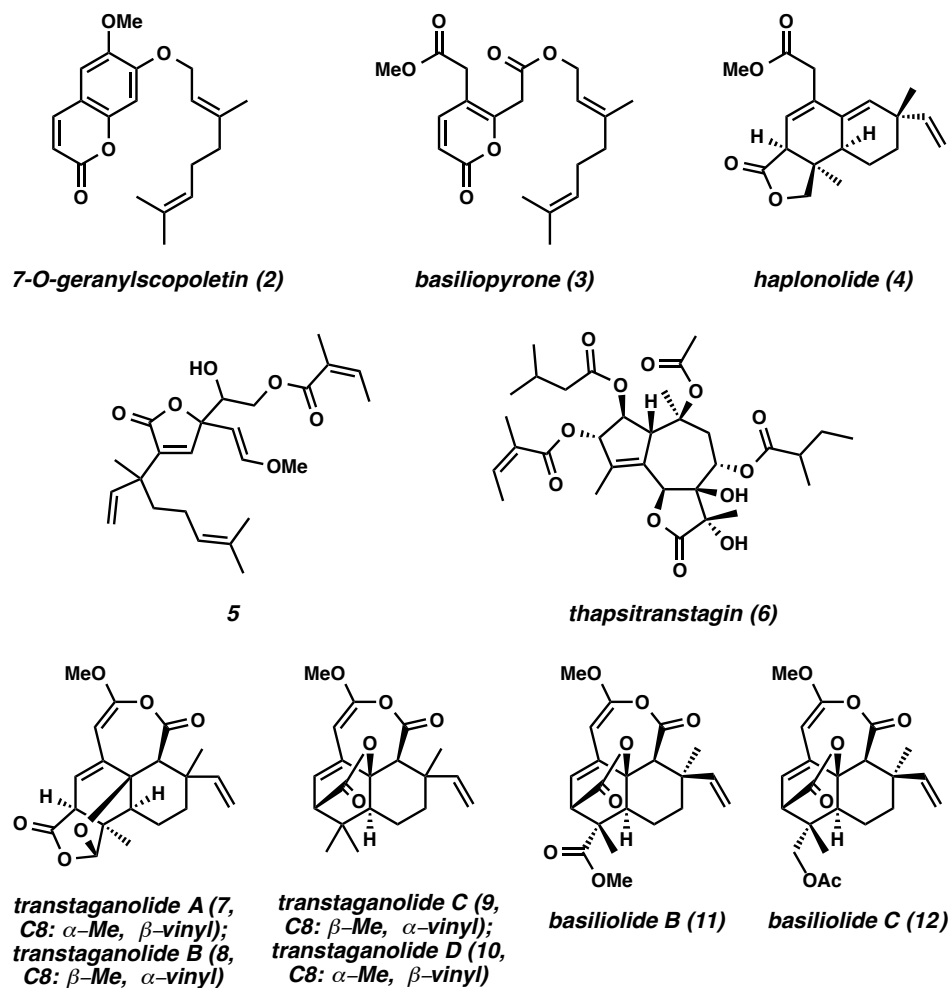
Indigenous to the Mediterranean, plants of the genus *Thapsia* have been recognized to possess valuable therapeutic properties since the birth of western medicine.¹ In modern times, their bioactivity has been attributed to major metabolite thapsigargin (**1**), a potent histamine releaser² and non-tetradecanoylphorbol acetate (TPA) type tumor promoter³ (Figure 1.1.1A). More importantly, thapsigargin (**1**) is a powerful, irreversible, sacroplasmatic-endoplasmatic reticulum Ca²⁺-ATPase (SERCA-ATPase) inhibitor, which allows for the net transfer of endoplasmic reticular Ca²⁺ to the cytosol and eventual apoptosis resulting from the endoplasmic reticular stress.⁴ Furthermore, thapsigargin's (**1**) potent SERCA-ATPases inhibitory activity has been exploited and widely utilized as an invaluable biochemical tool⁵ (Figure 1.1.1B)⁶.

Figure 1.1.1. A) Thapsigargin (**1**). B) Crystal structure of thapsigargin (**1**) bound SERCA-ATPase.



Further investigations of the chemical components of *Thapsia* have elucidated the existence of several additional novel metabolites (Figure 1.1.2). These include 7-*O*-geranylscopoletin (**2**),⁷ basiliopyrone (**3**),⁸ haplolonide (**4**),⁹ lactonic meroterpenoid **5**,^{8a} thapsitranstaganin (**6**),¹⁰ transtaganolides A–D (**7–10**),¹¹ and basiliolides B and C (**11** and **12**).¹² In particular, the transtaganolides and basiliolides (**7–12**), like thapsigargin (**1**), demonstrated SERCA-ATPase inhibitory activity, despite bearing characteristically different structural cores than that of thapsigargin (**1**), suggesting a mechanistically different mode of action. Appendino, Muñoz, and coworkers found that unlike thapsigargin (**1**), Ca²⁺ mobilization resulting from transtaganolide C (**9**) and basiliolides B and C (**11** and **12**) was reversible and did not induce apoptosis.¹³ Furthermore, the possibility of trace thapsigargin (**1**) contamination of the transtaganolide and basiliolide (**9**, **11**, and **12**) samples was later ruled out when synthetically derived transtaganolide C was assayed and gave similar results to those of the original study.¹⁴

Figure 1.1.2. Natural products isolated from *Thapsia*.

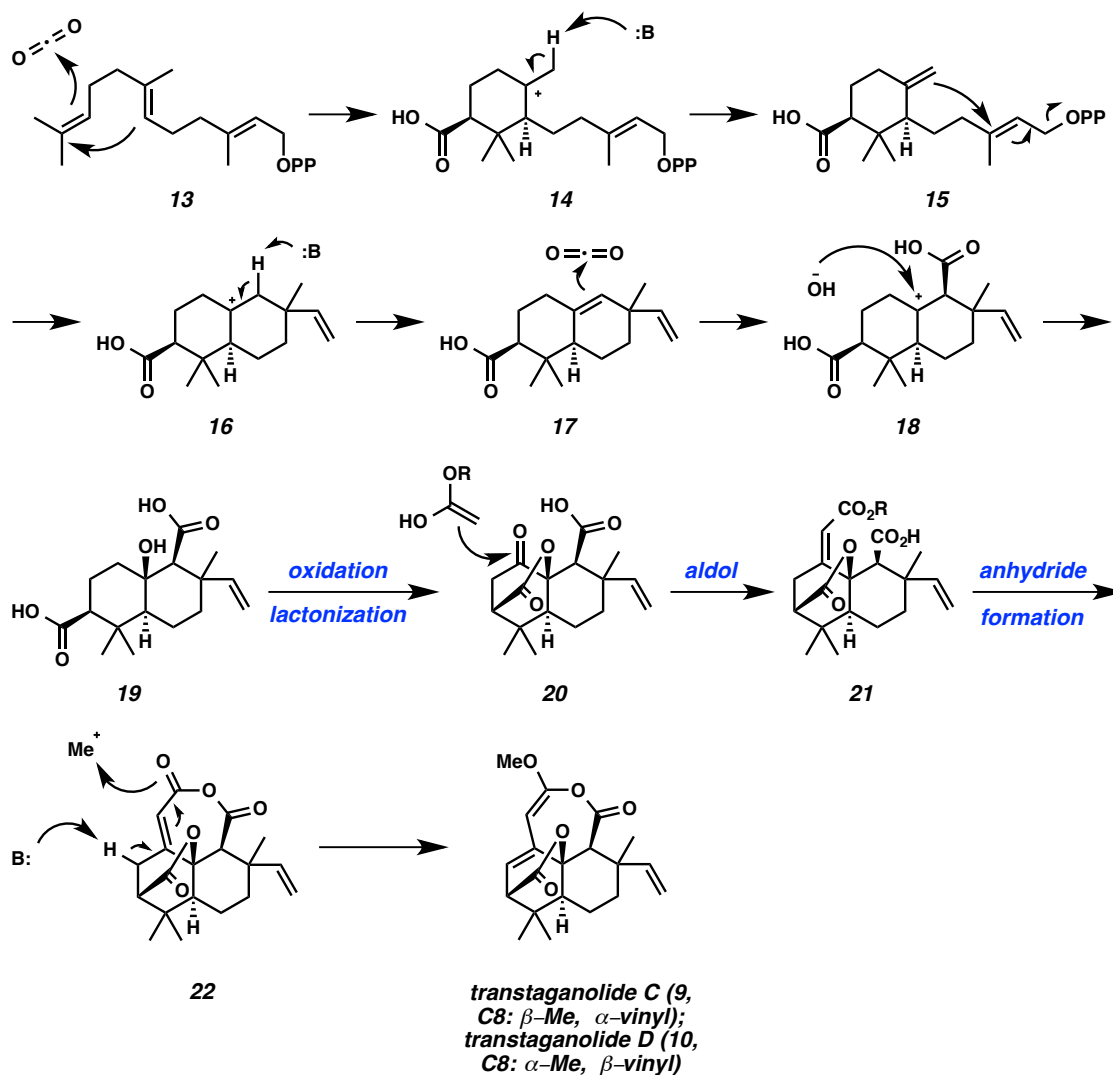


1.1.2 BIOSYNTHETIC PROPOSALS

Following the initial isolation of transtaganolides A–D and basiliolides B and C (7–12), Appendino and coworkers proposed a possible biosynthetic route to the tetracyclic framework of transtaganolides C and D (9 and 10, Scheme 1.1.1).¹² Starting with farnesyl pyrophosphate (13), olefin cyclization triggered by carbon dioxide incorporation and subsequent cation quenching gives monocyclic pyrophosphate 15. Another round of olefin cyclization and cation quenching forms bicycle 17, which upon addition of carbon dioxide and water gives bicycle 19. Oxidation and lactonization forms tricycle 20, and

subsequent aldol condensation forms the tricycle **21** to give the necessary 2-carbon homologation observed in the carbon skeleton. Lastly, anhydride formation and methylation yield the desired natural products **9** and **10**.

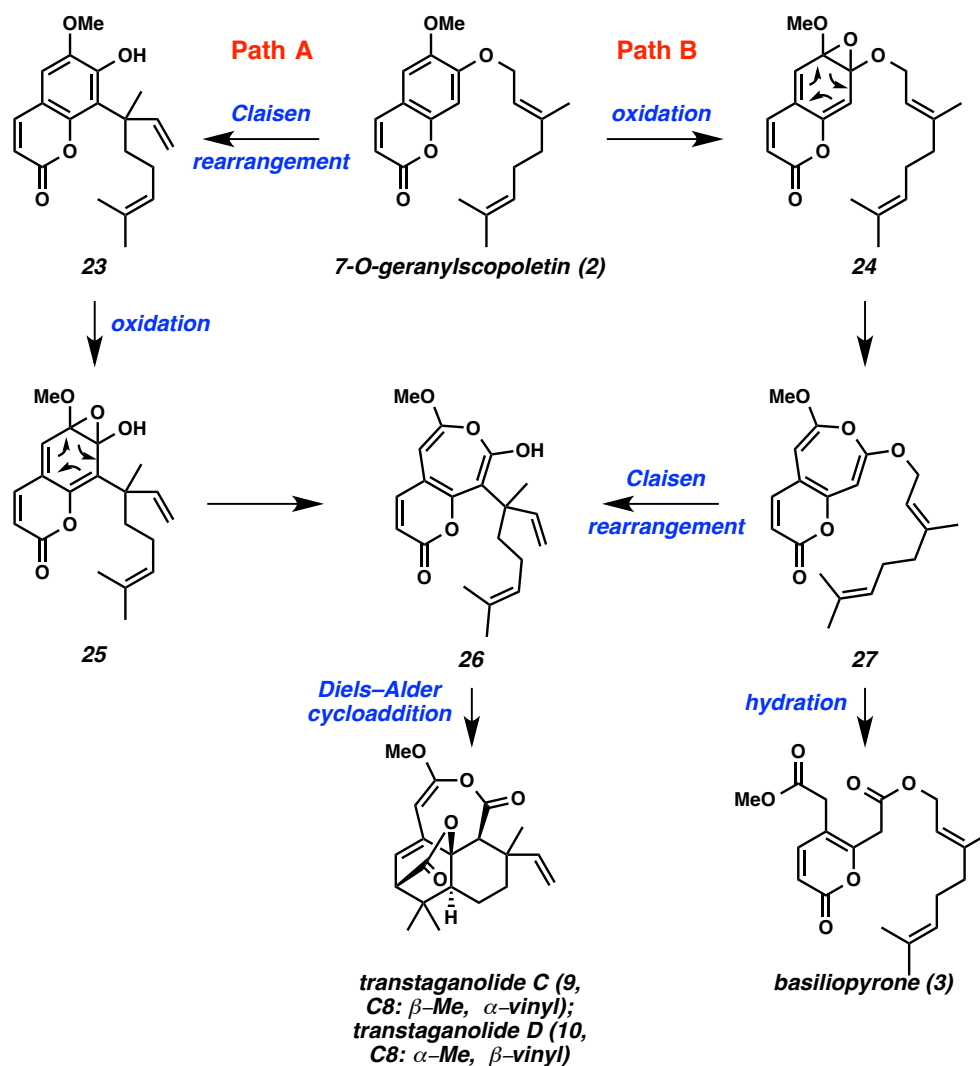
Scheme 1.1.1. Appendino's biosynthetic proposal.



Two years after Appendino's initial proposal,¹² Massanet and coworkers proposed a different biosynthetic hypothesis for the transtaganolides C and D (**9** and **10**), which better explained the existence of many of the other co-isolated secondary metabolites (Scheme 1.1.2).⁸ From co-isolated 7-*O*-geranylscopoletin (**2**), they propose two possible

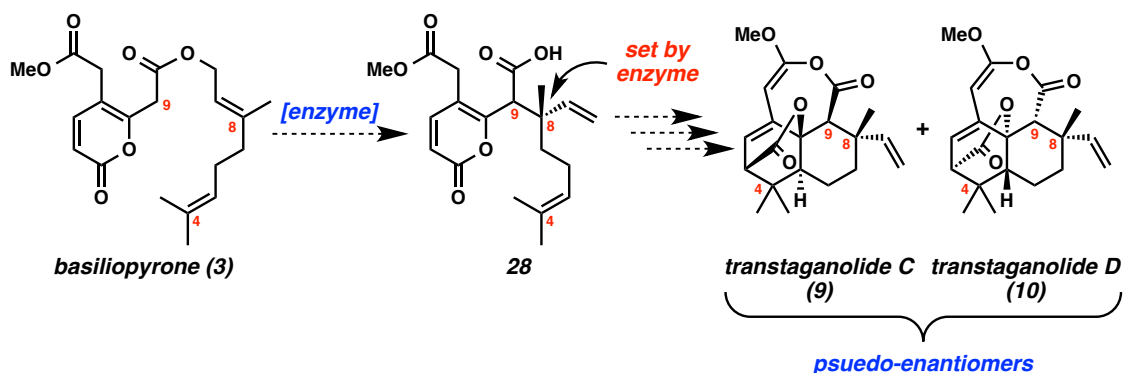
paths toward the biosynthesis of the transtaganolides. Both path A (Claisen rearrangement, oxidation, then 6π electrocyclic rearrangement) and path B (oxidation, 6π electrocyclic rearrangement, followed lastly by Claisen rearrangement) form bicycle **26**, which upon undergoing an intramolecular Diels–Alder cycloaddition gives transtaganolides C and D (**9** and **10**). Furthermore, co-isolated basiliopyrone (**3**) could be the hydration product of biosynthetic precursor **27**, giving further credence to this biosynthetic hypothesis.

Scheme 1.1.2. Massanet's biosynthetic proposal.



Lastly, Johansson and coworkers, proposed a variation to Massanet’s biomimetic hypothesis (Scheme 1.1.2), suggesting basiliopyrone (**3**) was not a byproduct of the biosynthesis but rather a biosynthetic precursor to transtaganolides C and D (**9** and **10**, Scheme 1.1.3).¹⁵ Biosynthesis would commence with an initial Ireland–Claisen rearrangement of basiliopyrone (**3**) to form pyrone **28** with all-carbon quaternary center at C8. Diels–Alder cycloaddition of **28** followed by C-ring closure could then form the natural products **9** and **10**. Additionally, they hypothesized that the stereochemistry at the C8 all-carbon quaternary center could be set by a rare and unprecedented “Ireland–Claisenase” enzyme.

Scheme 1.1.3. Johansson’s biosynthetic proposal.

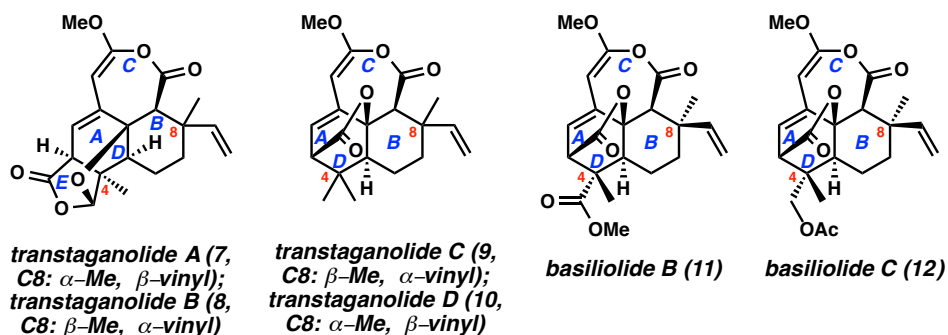


1.2 SYNTHETIC STRATEGIES FOR THE TRANSTAGANOLIDE AND BASILIOLIDE ABD TRICYCLIC CORE

Owing to the novel structures and bioactivity of the transtaganolides and basiliolides (**7–12**, Figure 1.2.1), several research groups have undertaken programs targeting the syntheses of these metabolites. Moreover, the oxabicyclo[2.2.2]octene core (ABD tricycle) of **9–12** and the caged ABDE tetracycle of **7** and **8** with two all-carbon quaternary centers at C4 and C8 comprise novel frameworks which present a

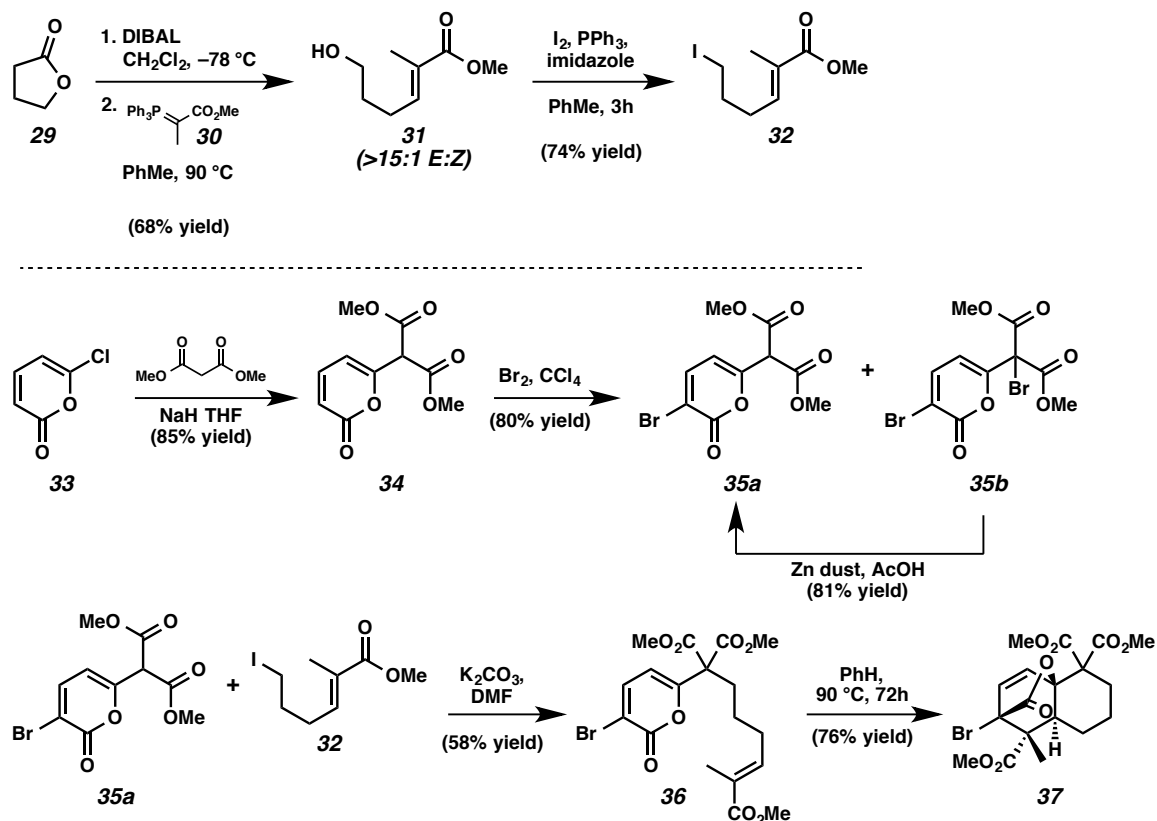
considerable challenge for total synthesis. Using Massanet's biomimetic proposal (Scheme 1.1.2) as a guide, initial efforts to form the ABD rings of transtaganolides C and D and basiliolides B and C utilized intramolecular pyrone Diels–Alder cycloadditions.

Figure 1.2.1. The transtaganolide and basiliolide structural features.



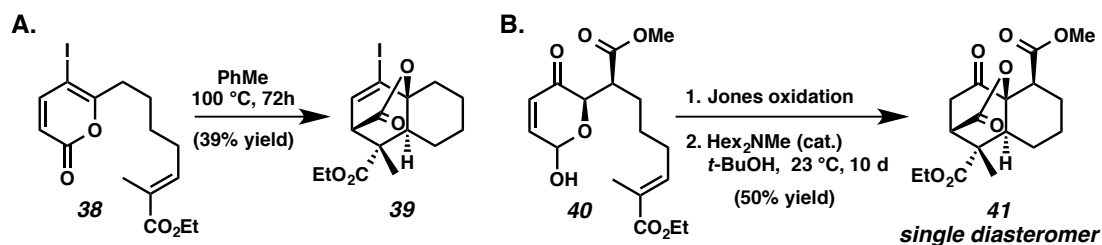
Stoltz and coworkers were the first to report the successful construction of the ABD tricyclic core via an intramolecular pyrone Diels–Alder cycloaddition reaction (Scheme 1.2.1).¹⁶ Synthesis began with the one hydride reduction of γ -butyrolactone (**29**) and subsequent Wittig olefination to form alcohol-bearing enoate **31**. Iodine displacement of the primary alcohol of enoate **31** with I_2 formed alkylating agent **32**, to be used later for elaboration of pyrone **35a**. Pyrone **35a** was made concurrently by dimethyl malonate substitution of chloro pyrone **33** followed by bromination. Alkylation of pyrone **35a** with iodo-enoate **32**, was accomplished using standard conditions, and the subsequent product, pyrone **36**, underwent the desired intramolecular pyrone Diels–Alder cycloaddition in 76% yield to form tricycle **37**, containing the transtaganolide and basiliolide ABD tricyclic core and C4 all-carbon quaternary center. Furthermore, it was shown that intramolecular pyrone Diels–Alder cycloaddition could not be accomplished without prior bromination of the pyrone ring to avoid decarboxylation during the reaction.¹⁷

Scheme 1.2.1. Stoltz's synthesis of ABD tricyclic core of the transtaganolides and basiliolides.



Subsequent studies published by both Dudley¹⁸ and Lee¹⁹ further demonstrated the efficacy of an intramolecular pyrone Diels–Alder cycloaddition to construct the transtaganolide and basiliolide (**9–12**) ABD tricyclic core (Scheme 1.2.2A and B). Using iodo pyrone **38**, Dudley and coworkers could effect the desired Diels–Alder cycloaddition in 39% yield (Scheme 1.2.2A). On the other hand, Lee and coworkers, following oxidation of **40**, were able to effect a base catalyzed Diels–Alder cycloaddition at ambient temperature in 50% yield over the two reactions (Scheme 1.2.2B).

Scheme 1.2.2. A) Dudley's synthesis of ABD tricyclic core of the transtaganolides and basiliolides.
B). Lee's synthesis of ABD tricyclic core of the transtaganolides and basiliolides.



1.3 PROGRESS TOWARD THE SYNTHESIS OF TRANSTAGANOLIDES C AND D AND BASILIOLIDES B AND C

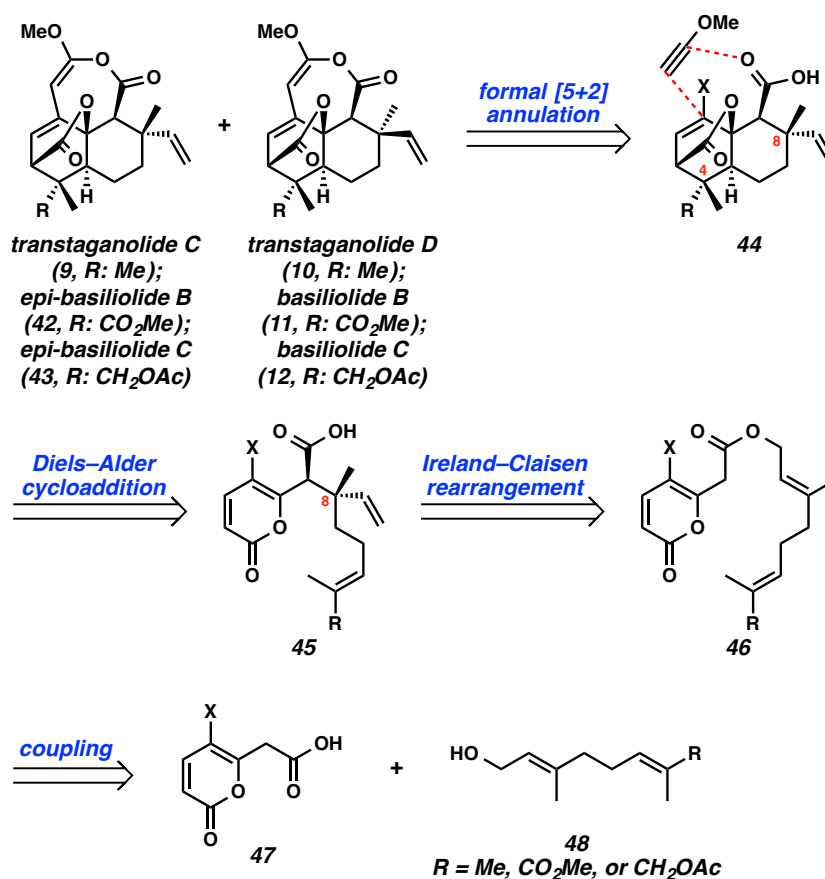
1.3.1 RETROSYNTHETIC ANALYSIS

Despite having successfully constructed the transtaganolide and basiliolide (9–12, Figure 1.2.1) ABD tricyclic core, none of the previously discussed methods^{16,18,19} had addressed construction of the C8 all-carbon quaternary stereocenter characteristic of this family of natural products. In 2009, both Stoltz²⁰ and Johansson¹⁵ simultaneously divulged similar strategies toward the synthesis of transtaganolides C and D as well as basiliolides B and C that included successful construction of the C8 all-carbon quaternary stereocenter. Though neither group at the time could successfully construct the final cycloheptene C-ring, Stoltz and coworkers would eventually accomplish this feat and publish the first total syntheses of transtaganolides C and D (9 and 10) as well as basiliolide B (11) in 2011.²¹

Consider the retrosynthetic analysis outlined by Stoltz and coworkers (Scheme 1.3.1).²¹ The first disconnection breaks apart the 7-membered ketene-acetal containing C-ring, allowing natural products 9–12, 42, and 43 to form by a formal [5+2] annulation of a methoxy acetylene species and tricycle 43. Tricycle 43 arises from an intramolecular

pyrone Diels–Alder cycloaddition of acid **45**, which builds the ABD tricyclic core. The next disconnection is formation of the C8 all carbon quaternary center of acid **45**, which we envision to arise from an Ireland–Claisen rearrangement of pyrone **46**, the coupling product of acid **47** and geraniol derivative **48**. Furthermore the sequential Ireland–Claisen, Diels–Alder cycloaddition reactions (**46**⇒**48**), could be accomplished in a single operation, allowing the simultaneous construction of the ABD tricyclic core as well as C4 and C8 all-carbon quaternary stereocenters.

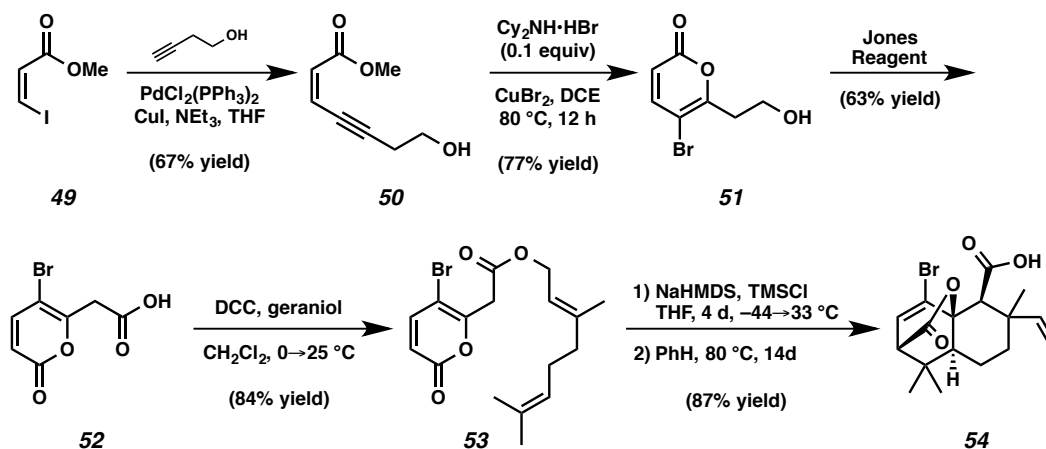
Scheme 1.3.1. Retrosynthetic analysis of transtaganolides C and D (**9** and **10**) and basiliolides B and C (**11** and **12**).



1.3.2 PROGRESS FOR THE FORWARD SYNTHESIS

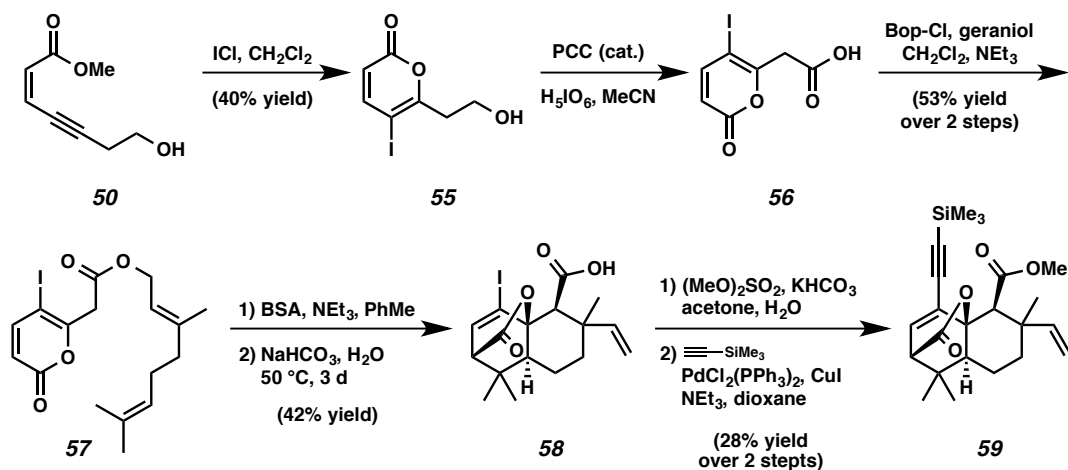
Stoltz and coworkers' original synthetic approach began with the synthesis of homoallylic alcohol **50** via Sonagashira cross-coupling (Scheme 1.3.2).²⁰ Bromo lactonization of ester **50** followed by subsequent oxidation provided the bromo acid **52** in good yield. DCC coupling of acid **52** to geraniol formed the bromo pyrone **53**, which successfully underwent the sequential Ireland–Claisen and Diels–Alder cyclization in good yield over the two steps.

Scheme 1.3.2. Stoltz's progress toward the synthesis of transtaganolides C and D (**9** and **10**).



Johansson¹⁵ and coworkers' synthetic strategy was nearly identical to that of Stoltz¹⁹ and coworkers (Scheme 1.3.3),¹⁵ the major difference being the synthesis and use of iodo pyrone **57**, rather than bromo pyrone **53**, for use in the sequential Ireland–Claisen and Diels–Alder cyclizations, to form tricycle **58**. Furthermore, Johansson and coworkers were able to demonstrate a successful cross-coupling, forming eneyne **59**, and providing a possible strategy for the eventual formation of the elusive transtaganolide and basiliolide C-ring (**7–12**, Figure 1.2.1).

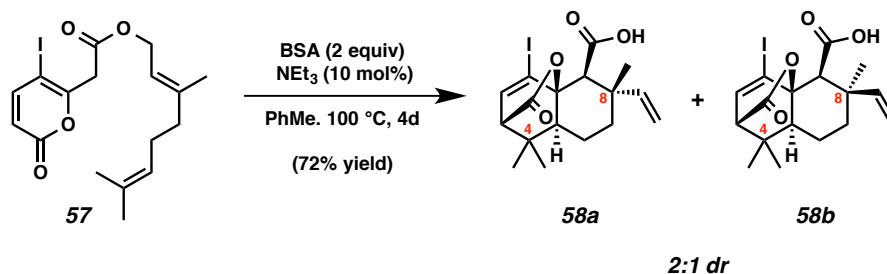
Scheme 1.3.3. Johansson's progress toward the synthesis of transtaganolides C and D (**9** and **10**).



1.4 TOTAL SYNTHESIS OF TRANSTAGANOLIDES C AND D

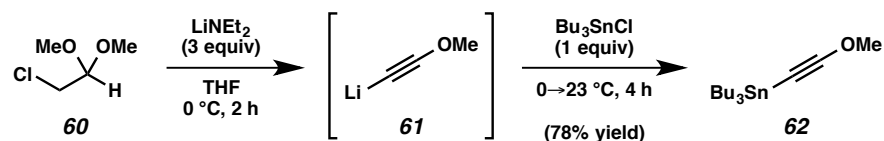
Following initial progress reports by Stoltz²⁰ and Johansson¹⁵, Stoltz and coworkers published the first successful total synthesis of (\pm)-transtaganolides C and D (**9** and **10**) in 2011.²¹ By using the information learned from their own work²⁰ and that published by Johansson¹⁵, Stoltz and coworkers were able to develop an Ireland–Claisen rearrangement/Diels–Alder cycloaddition cascade reaction (ICR/DA), which has become their general synthetic strategy for all members of the natural product family (Scheme 1.4.1).²² Treatment of iodo pyrone **57** with an excess of bistrimethyl acetamide (BSA) and catalytic triethylamine in a sealed tube of toluene at $100\text{ }^\circ\text{C}$ for 4 days gave tricycles **58a** and **58b** in 72% yield as a 2:1 mixture of diastereomers, respectively. This method allowed for the simultaneous construction of the ABD tricyclic core as well as C4 and C8 all-carbon quaternary centers in a single step.

Scheme 1.4.1. Ireland–Claisen/Diels–Alder cycloaddition cascade (ICR/DA).



Having developed a successful strategy for the formation of tricycles **58a** and **58b**, it then became a question of forming the elusive C-ring to finish the synthesis of transtaganolides C and D (**9** and **10**). Using the formal [5+2] annulation strategy outlined in the retrosynthetic analysis (Scheme 1.3.1), it became instantly clear that a direct coupling of methoxy acetylene to iodides **58a** and **58b** followed by an *in situ* cyclization was unachievable. Drawing from the few reported successful cross-couplings of zinc and tin ethoxyacetylide,²³ Stoltz and coworkers began synthesis of a suitable stannyl methoxyacetylide derivative **62** (Scheme 1.4.2).²¹ Treatment of known 1,1-dimethoxy-2-chloro-acetaldehyde (**60**) with 3 equivalents of lithium diethyl amide formed the putative lithium acetylide **61**, which was then trapped as the stannyl acetylide **62** by the addition of tributyl tin chloride in 78% yield.

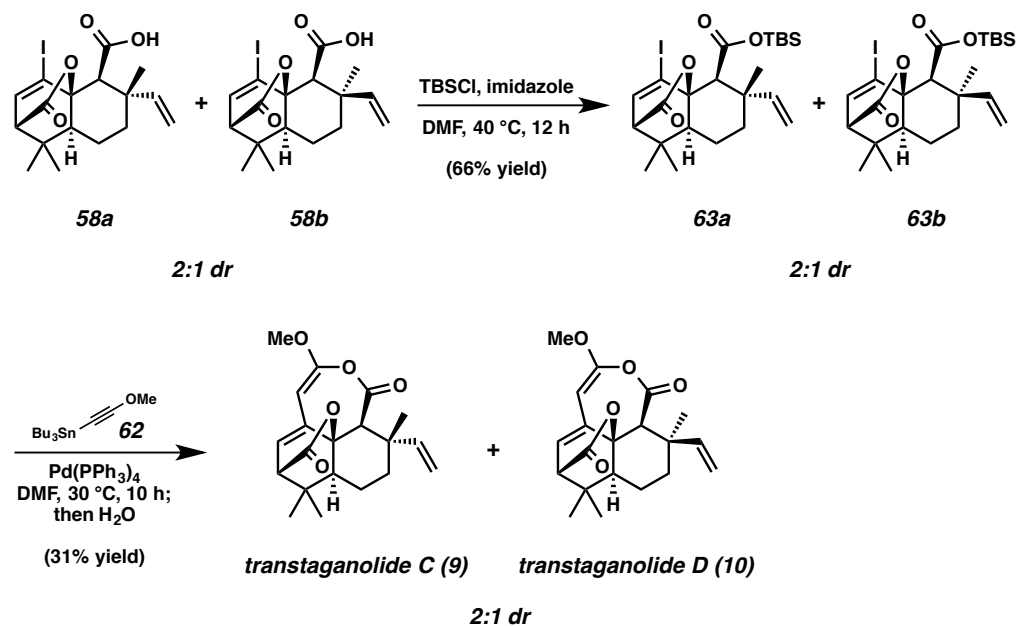
Scheme 1.4.2. Synthesis of stannyl methoxyacetylide **62**.



With suitable cross-coupling partner stannane **62** in hand, formation of the C-ring could commence with protection of the free acid of tricycles **58a** and **58b** in 66% yield (Scheme 1.4.3).²³ Finally, palladium cross-coupling of stannyl methoxyacetylide **62** with

silyl esters **63a** and **63b** followed by the *in situ* cyclization upon the addition of water gave the natural products, transtaganolides C and D (**9** and **10**), in 31% yield.

Scheme 1.4.3. Total syntheses of transtaganolides C and D (**9** and **10**).



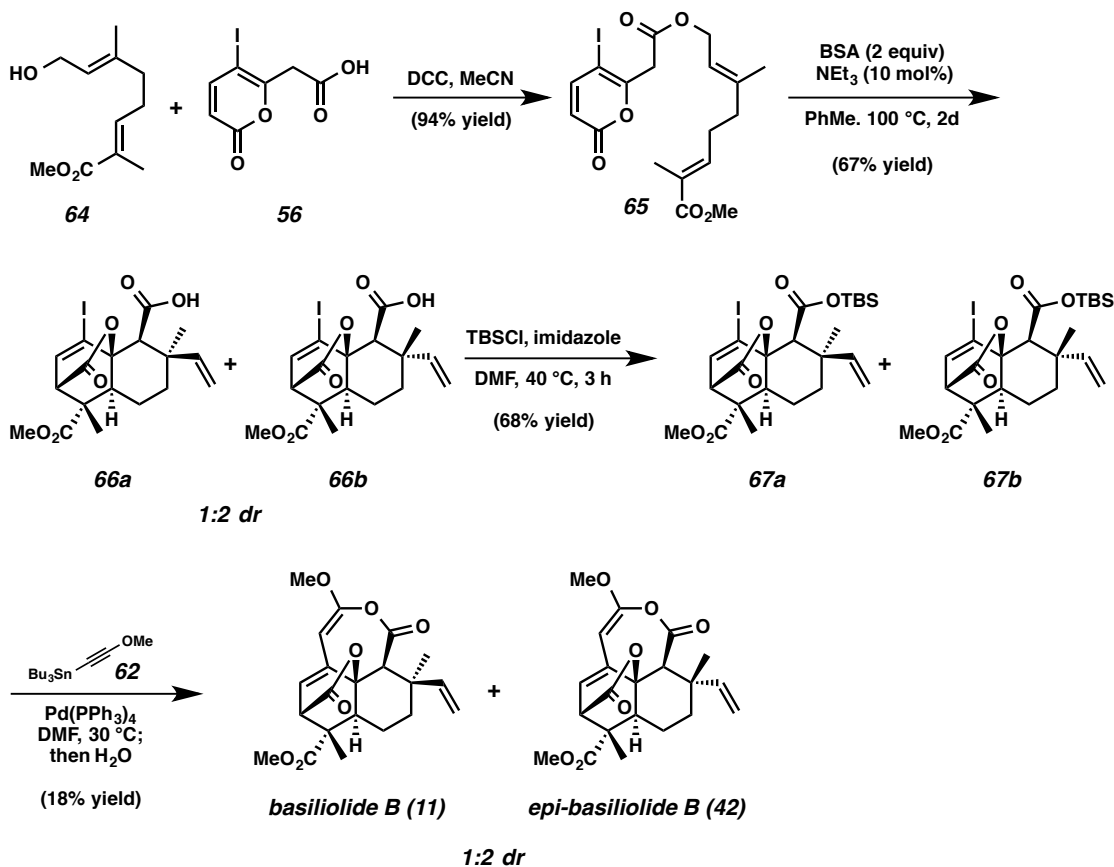
1.5 TOTAL SYNTHESIS OF BASILIOLOIDE B AND EPI-BASILIOLOIDE B

1.5.1 STOLTZ AND COWORKERS' APPROACH

Having established a general ICR/DA strategy for the synthesis of transtaganolides C and D (**9** and **10**), Stoltz and coworkers then applied this approach to the synthesis of basiliolide B and epi-basiliolide B (**11** and **42**, Scheme 1.5.1).²¹ DCC coupling of known geraniol derivative **64** (available in four steps from commercial starting materials)²⁴ and iodo-acid **56** formed pyrone **65** in 94% yield. Treatment of pyrone **65**, with the standard ICR/DA cascade conditions, gave tricycles **66a** and **66b** in 67% yield as a 1:2 mixture of diastereomers, respectively. Protection as the silyl esters **67a** and **67b** proceeded under standard conditions. Finally, palladium cross-coupling of stannyl methoxyacetylide **62**

followed by the *in situ* cyclization formed natural product, basiliolide B (**11**), and previously unreported epi-basiliolide B (**42**) in 6% and 12% yield, respectively.

Scheme 1.5.1. Stoltz's total syntheses of basiliolide B and epi-basiliolide B (**11** and **42**).



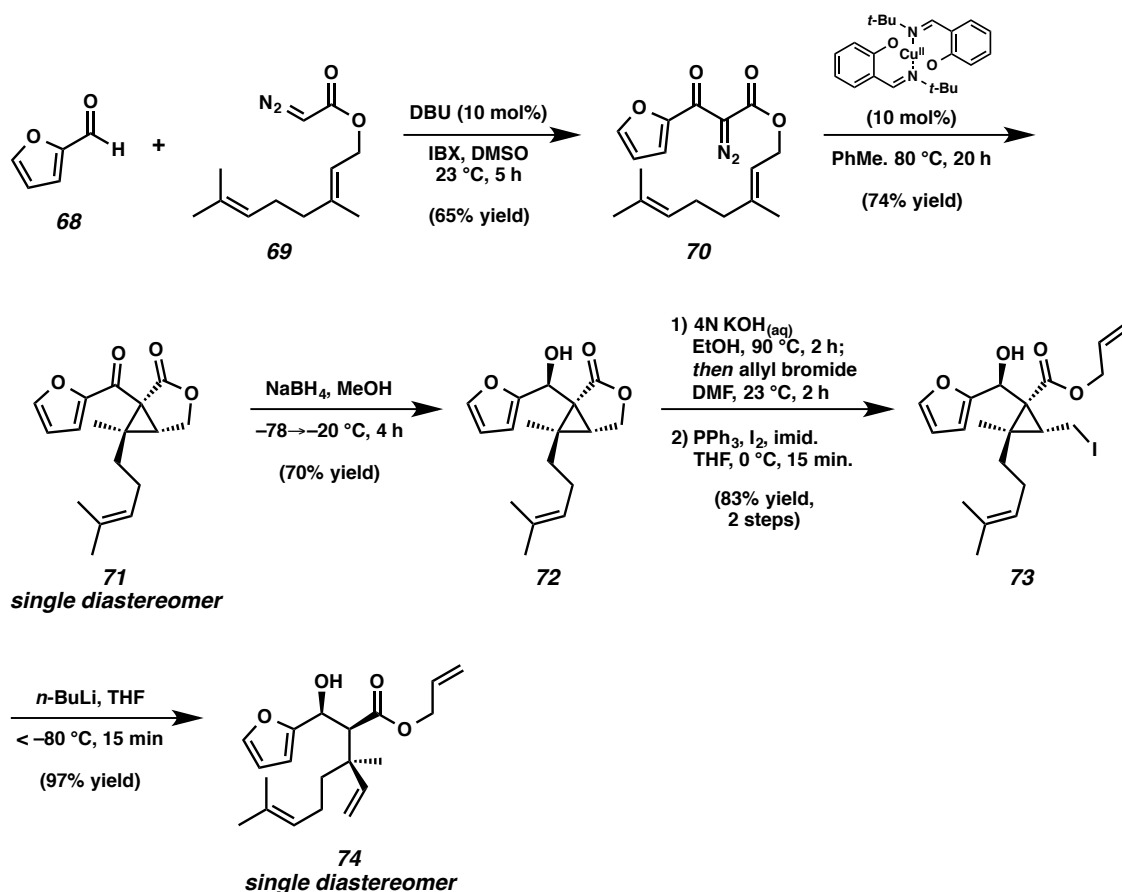
1.5.2 LEE AND COWORKERS' APPROACH

Lee and coworkers' approach²⁵ to basiliolide B (**11**) took advantage of their previously disclosed methodology (Scheme 1.2.2B)¹⁹ which allowed for diastereoselective formation of basiliolide B (**11**), rather than both basiliolide B (**11**) and epi-basiliolide B (**42**). Furthermore, unlike Stoltz and coworkers, who were able to set the C8 all-carbon quaternary center by means of an Ireland–Claisen rearrangement, Lee and coworkers employed a cyclopropanation followed by ring opening strategy, which

allowed for diastereoselective C8 all-carbon quaternary center formation and access to basiliolide B (**11**).

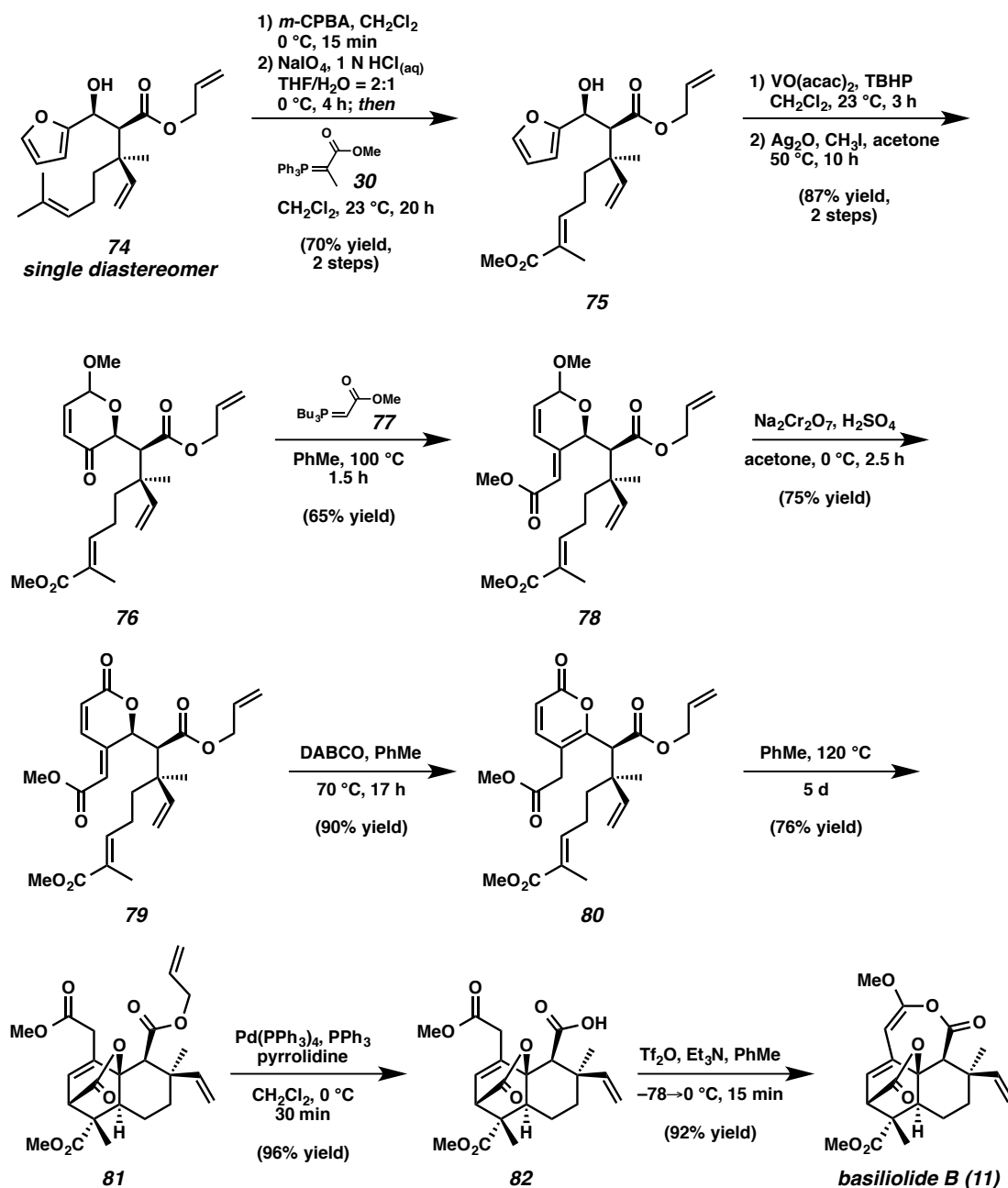
Lee's synthesis began with the coupling of furfural (**68**) and geranyl diazoacetate (**69**) to form diazo ester **70** (Scheme 1.5.2). Treatment of diazo **70** with copper (II) allowed for a diastereoselective intramolecular cyclopropanation, forming cyclopropane **71** in good yield. Reduction followed by saponification and iodine displacement formed cyclopropane **73**. Finally, treatment of cyclopropane **73** with *n*-BuLi effected the desired ring opening reaction, giving a single diastereomer **74** that contained the required C8 all-carbon quaternary center indicative of basiliolide B (**11**).

Scheme 1.5.2. Lee's synthesis of basiliolide B (**11**)



Having formed ester **74** with C8 all-carbon quaternary center, Lee and coworkers sought to finish their synthesis of basiliolide B (**11**, Scheme 1.5.3). Oxidative cleavage of **74** followed by Wittig olefination furnished enone **75** in 70% yield over the two steps. Achmatowicz reaction of furan **75** followed by methylation and Wittig olefination afforded lactal **78**. Jones oxidation of lactal **78** and subsequent olefin isomerization formed Diels–Alder substrate **80** in good yield. Finally, intramolecular Diels–Alder cycloaddition of pyrone **80** gave tricycle **81**, which following palladium assisted allyl ester cleavage, and intramolecular O-acylation produced basiliolide B (**11**) as a single diastereomer.

Scheme 1.5.3. Lee's continued synthesis of basiliolide B (**11**).

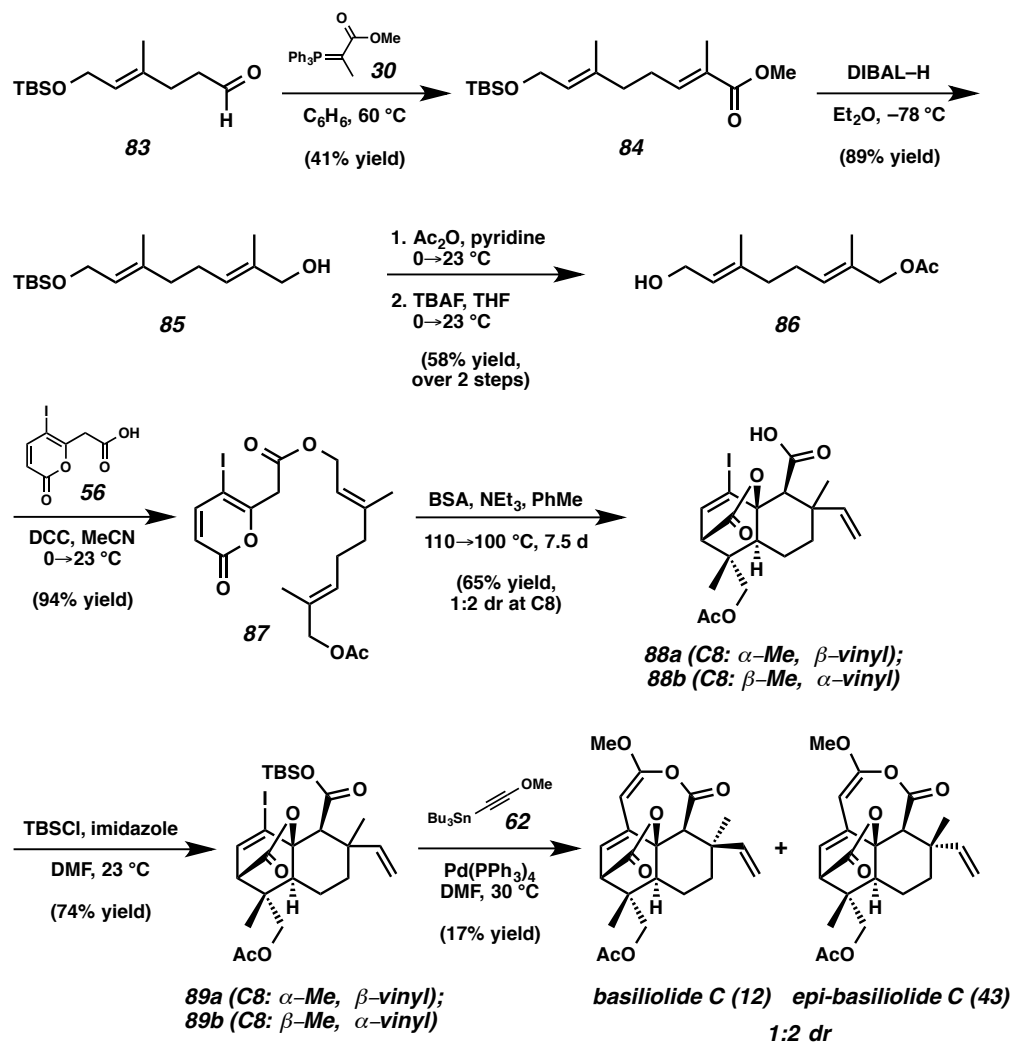


1.6 TOTAL SYNTHESIS OF BASILIOLOIDE C AND EPI-BASILIOLOIDE C

Stoltz and coworkers' envisioned that basiliolide C (**12**) and epi-basiliolide C (**43**) could also be synthesized using their ICR/DA cascade and formal [5+2] annulation sequence.²⁶ The total synthesis commenced with the treatment of known γ,δ -unsaturated

aldehyde **83**,²⁷ with triphenylphosphonium ylide **30**, to give the enoate **84** (Scheme 1.6.1). Subsequent reduction of α,β -unsaturated ester **84** with DIBAL-H afforded allylic alcohol **85** in 89% yield. Following protecting group manipulations (**85**→**86**), DCC coupling of alcohol **86** with pyrone acid **56** efficiently generated the ICR/DA cascade substrate **87**. Submission of pyrone ester **87** to our ICR/DA protocol proved successful, affording tricycles **88a** and **88b** in 65% combined yield and as a 1:2 mixture of C8 diastereomers, respectively. Only two diastereomers, **88a** and **88b**, are formed in the reaction resulting from the diastereoselective Diels–Alder cycloaddition, where diastereoselectivity is dictated by the C7 ester formed in the Ireland–Claisen rearrangement. Protection of tricycles **88a** and **88b** gave silyl esters **89a** and **89b** in 74% yield. Completion of the synthesis was achieved via a palladium promoted formal [5+2] annulation of tricycles **89a** and **89b** with stannyl methoxyacetylide **62** to form basiliolide C (**12**) and previously unreported epi-basiliolide C (**43**), respectively, albeit in low yield (17% yield).

Scheme 1.6.1. Total syntheses of basiliolide C (**12**) and epi-basiliolide C (**43**).



1.7 CONCLUSION

In conclusion, we have discussed all previous progress toward the synthesis of (\pm) transtaganolides C and D (**9** and **10**). We have summarized the ICR/DA cascade technology disclosed by Stoltz and coworkers allowing for the simultaneous construction of the ABD tricyclic core as well as formation of C4 and C8 all-carbon quaternary centers. Using this approach, Stoltz and coworkers have developed concise total

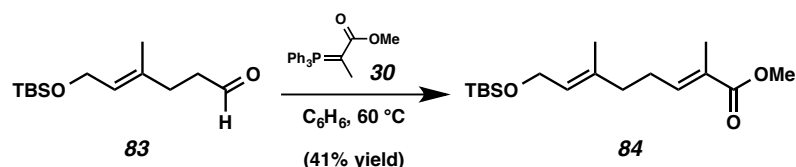
syntheses of (±)-transtaganolides C and D (**9** and **10**), (±)-basiliolide B (**11**), (±)-epi-basiliolide B (**42**), (±)-basiliolide C (**12**), and (±)-epi-basiliolide C (**43**).

1.8 EXPERIMENTAL SECTION

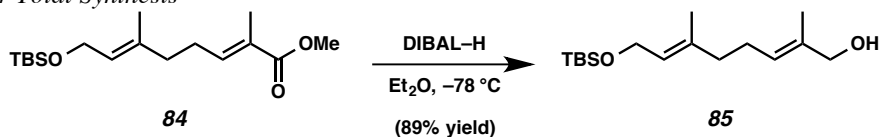
1.8.1 MATERIALS AND METHODS

Unless otherwise stated, reactions were performed in flame-dried glassware under an argon or nitrogen atmosphere using dry deoxygenated solvents. Solvents were dried by passage through an activated alumina column under argon. Chemicals were purchased from Sigma-Aldrich Chemical Company and used as received. Pd(PPh₃)₄ was prepared using known methods. Thin layer chromatography (TLC), both preparatory and analytical, was performed using E. Merck silica gel 60 F254 precoated plates (0.25 mm) and visualized by UV fluorescence quenching, *p*-anisaldehyde, I₂, or KMnO₄ staining. ICN Silica gel (particle size 0.032-0.063 mm) was used for flash chromatography. ¹H NMR and ¹³C NMR spectra were recorded on a Varian Mercury 300 (at 300 MHz) or on a Varian Unity Inova 500 (at 500 MHz) spectrometer. ¹H NMR spectra are reported relative to CDCl₃ (7.26 ppm). Data for ¹H NMR spectra are reported as follows: chemical shift (ppm), multiplicity, coupling constant (Hz), and integration. Multiplicities are reported as follows: s = singlet, d = doublet, t = triplet, q = quartet, sept. = septet, m = multiplet, bs = broad singlet. ¹³C NMR spectra are reported relative to CDCl₃ (77.16 ppm). FTIR spectra were recorded on a Perkin Elmer SpectrumBX spectrometer and are reported in frequency of absorption (cm⁻¹). HRMS were acquired using an Agilent 6200 Series TOF with an Agilent G1978A Multimode source in electrospray ionization (ESI), atmospheric pressure chemical ionization (APCI), or multimode-ESI/APCI.

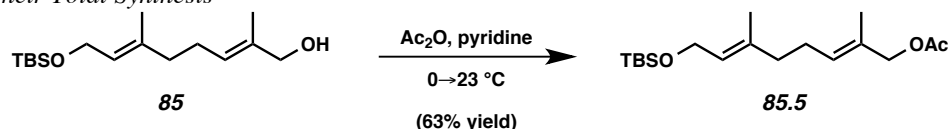
1.8.2 PREPARATIVE PROCEDURES



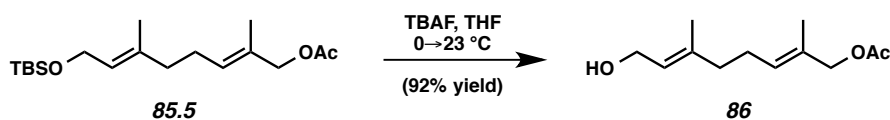
Enoate 84. To a 23 °C solution of aldehyde **83** (1.39 g, 5.74 mmol) in benzene (57 mL, 0.1 M) was added ylide **30** (2.92 g, 8.38 mmol). The reaction was stirred at 60 °C for 6 h. The reaction flask was then cooled to ambient temperature. The crude mixture was poured directly onto a short pad of silica and subsequently flushed with Et₂O (150 mL). Solvent was removed by rotary evaporation. The crude oil was redissolved in CH₂Cl₂ (50 mL) and then dry loaded onto silica (5 g). Purification by column chromatography (EtOAc in hexanes 1%→1.5% on silica) yielded 722 mg (41% yield) of enoate **84** as clear oil and a single diastereomer; ¹H NMR (300 MHz, CDCl₃) δ 6.72 (tq, *J* = 7.3, 1.5 Hz, 1H), 5.31 (tq, *J* = 6.3, 1.3 Hz, 1H), 4.18 (dd, *J* = 6.3, 0.8 Hz, 2H), 3.71 (s, 3H), 2.34–2.23 (m, 2H), 2.16–2.06 (m, 2H), 1.82 (s, 3H), 1.62 (s, 3H), 0.88 (s, 9H), 0.05 (s, 6H); ¹³C NMR (75 MHz, CDCl₃) δ 168.7, 142.0, 135.8, 127.8, 125.3, 60.3, 51.8, 38.1, 27.0, 26.1, 18.5, 16.5, 12.5, -5.0; FTIR (Neat Film NaCl) 2952, 2930, 2896, 2857, 1717, 1672, 1651, 1472, 1463, 1436, 1387, 1361, 1259, 1218, 1193, 1124, 1107, 1065, 1006, 939, 837, 814, 776, 744 cm⁻¹; HRMS (ESI) *m/z* calc'd for C₁₇H₃₂O₃SiNH₄ [M+NH₄]⁺: 330.2459, found 330.2468.



Allyl alcohol 85. To a $-78\text{ }^\circ\text{C}$ solution of enoate **84** (722 mg, 2.31 mmol) in Et_2O (23 mL, 0.1 M) was added neat DIBAL-H (1.03 mL, 5.78 mmol) in a dropwise fashion. The reaction mixture was then stirred for 45 min at $-78\text{ }^\circ\text{C}$ before being carefully quenched by the dropwise addition of a saturated solution of Rochelle's salt (6 mL over 5 min). The reaction mixture was then removed from the cold bath and allowed to warm to ambient temperature while being vigorously stirred for another 2 h. The aqueous phase was extracted with Et_2O (4 x 10 mL), and the organics were combined, washed with saturated brine (40 mL), and then dried over MgSO_4 . Solvent was removed by rotary evaporation and purification by column chromatography (EtOAc in hexanes 3.5% \rightarrow 15% on silica) resulted in the isolation of 587 mg (89% yield) of allyl alcohol **85** as a clear oil; ^1H NMR (300 MHz, CDCl_3) δ 5.37 (tq, $J = 7.0, 1.3$ Hz, 1H), 5.29 (tq, $J = 6.3, 1.3$ Hz, 1H), 4.18 (dd, $J = 6.4, 0.8$ Hz, 2H), 3.97 (s, 2H), 2.22–2.08 (m, 2H), 2.09–1.98 (m, 2H), 1.65 (s, 3H), 1.61 (s, 3H), 0.89 (s, 9H), 0.06 (s, 6H); ^{13}C NMR (75 MHz, CDCl_3) δ 136.6, 135.1, 125.8, 124.7, 69.0, 60.4, 39.2, 26.1, 25.9, 18.6, 16.4, 13.8, -4.9; FTIR (Neat Film NaCl) 3346, 2955, 2929, 2857, 1671, 1472, 1463, 1407, 1385, 1361, 1255, 1111, 1094, 1066, 1006, 939, 836, 814, 776 cm^{-1} ; HRMS (ESI) m/z calc'd for $\text{C}_{16}\text{H}_{32}\text{O}_2\text{SiNa}$ $[\text{M}+\text{Na}]^+$: 307.2064, found 307.2052.

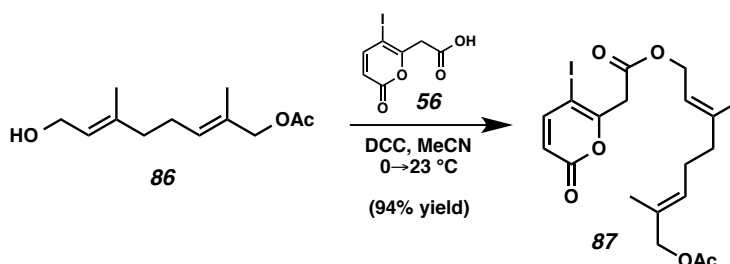


Allyl acetate 85.5. To a 0°C solution of allyl alcohol **85** (585 mg, 2.06 mmol) in pyridine (2 mL, 1 M) was added acetic anhydride (390 μL , 4.11 mmol). The reaction was allowed to warm to 23°C and stirred for 3.5 h. At this time the reaction mixture was diluted with Et_2O (15 mL) and washed with saturated NaHCO_3 solution (3 x 10 mL), saturated CuSO_4 solution (3 x 10 mL), and brine (10 mL). The organic fraction was dried with MgSO_4 and the solvent was removed by rotary evaporation. Purification by column chromatography (2.5% EtOAc in hexanes on silica) yielded 423 mg (63% yield) of the acetate protected product **85.5** as a clear oil; $^1\text{H NMR}$ (300 MHz, CDCl_3) δ 5.43 (tq, $J = 7.0, 1.3$ Hz, 1H), 5.30 (tq, $J = 6.3, 1.3$ Hz, 1H), 4.43 (s, 2H), 4.18 (dq, $J = 6.3, 0.9$ Hz, 2H), 2.23–2.09 (m, 2H), 2.06–1.99 (m, 5H), 1.64 (s, 3H), 1.61 (s, 3H), 0.89 (s, 9H), 0.06 (s, 6H); $^{13}\text{C NMR}$ (75 MHz, CDCl_3) δ 171.1, 136.4, 130.3, 129.4, 124.9, 70.4, 60.4, 39.0, 26.1, 21.1, 18.6, 16.5, 14.1, -4.9; FTIR (Neat Film NaCl) 2954, 2930, 2886, 2857, 1744, 1671, 1472, 1462, 1445, 1377, 1360, 1249, 1230, 1111, 1065, 1024, 836, 776 cm^{-1} ; HRMS (APCI) m/z calc'd for $\text{C}_{18}\text{H}_{34}\text{O}_3\text{SiNa}$ $[\text{M}+\text{Na}]^+$: 349.2169, found 349.2180.



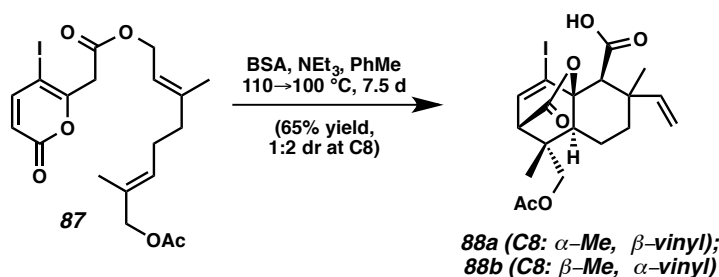
Allyl acetate 86. Cleavage of the silyl protecting group could be accomplished by the addition of 1M TBAF solution in THF (1.95 mL, 1.94 mmol) to a 0°C solution of the previously isolated acetate protected product **85.5** (423 mg, 1.30 mmol) in THF (6.5 mL, 0.2 M). The reaction was allowed to warm to 23°C and then was stirred for an

additional hour, prior to quenching with saturated NH_4Cl (5 mL). The aqueous phase was extracted with Et_2O (3 x 5 mL), and the organics were combined, washed with brine (15 mL), and dried over MgSO_4 . Solvent was removed by rotary evaporation and purification by column chromatography (EtOAc in hexanes 10%→20% on silica) resulted in the isolation of 253 mg (92% yield) of allyl acetate **86** as a clear oil; ^1H NMR (300 MHz, CDCl_3) δ 5.44–5.30 (m, 2H), 4.39 (s, 2H), 4.08 (d, $J = 6.8$ Hz, 2H), 2.19–1.97 (m, 7H), 1.61 (s, 3H), 1.60 (s, 3H); ^{13}C NMR (75 MHz, CDCl_3) δ 171.1, 138.5, 130.2, 129.1, 124.0, 70.2, 59.2, 38.8, 25.9, 21.0, 16.8, 14.0; FTIR (Neat Film NaCl) 3423, 2975, 2923, 2879, 1738, 1671, 1442, 1378, 1232, 1090, 1022, 844 cm^{-1} ; HRMS (ESI) m/z calc'd for $\text{C}_{12}\text{H}_{20}\text{O}_3\text{Na}$ $[\text{M}+\text{Na}]^+$: 235.1305, found 235.1300.



Iodo pyrone ester 87. To a 0 °C solution of allyl acetate **86** (254 mg, 1.20 mmol) and pyrone acid **56** (403 mg, 1.44 mmol) in MeCN (12 mL, 0.1 M) was added DCC (297 mg, 1.44 mmol). The reaction was allowed to warm to 23 °C and stirred for 1 h. The crude reaction mixture was then flushed through a short pad of celite with additional MeCN (15 mL) to remove the insoluble urea byproduct. Solvent was removed by rotary evaporation and purification by column chromatography (EtOAc in hexanes 5%→15% on silica) resulted in the isolation of 531 mg (94% yield) of iodo pyrone ester **87** as a yellow oil; ^1H NMR (300 MHz, CDCl_3) δ 7.45 (d, $J = 9.7$ Hz, 1H), 6.06 (d, $J = 9.7$ Hz,

1H), 5.45–5.38 (m, 1H), 5.33 (tq, $J = 7.1, 1.3$ Hz, 1H), 4.66 (d, $J = 7.2$ Hz, 2H), 4.43 (s, 2H), 3.77 (s, 2H), 2.24–2.02 (m, 7H), 1.70 (s, 3H), 1.64 (s, 3H); ^{13}C NMR (75 MHz, CDCl_3) δ 171.1, 166.8, 160.5, 158.0, 151.3, 142.8, 130.6, 128.8, 118.0, 116.3, 70.8, 70.3, 62.7, 42.7, 38.9, 26.0, 21.2, 16.7, 14.1; FTIR (Neat Film NaCl) 2973, 2933, 2854, 1732, 1607, 1546, 1443, 1376, 1357, 1345, 1230, 1167, 1133, 1063, 1016, 959, 865, 821 cm^{-1} ; HRMS (ESI) m/z calc'd for $\text{C}_{19}\text{H}_{23}\text{IO}_6\text{Na}$ $[\text{M}+\text{Na}]^+$: 497.0432, found 497.0428.



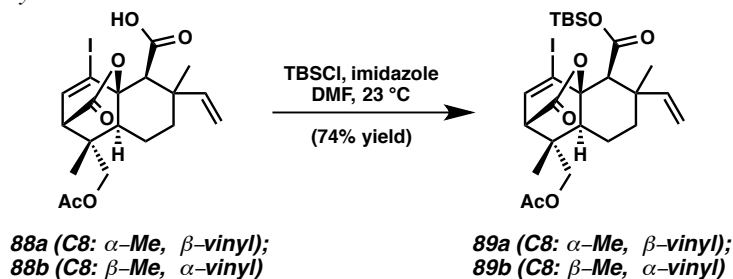
Tricyclic acids 88a and 88b. To a 23 °C solution of iodo pyrone ester **87** (385 mg, 0.812 mmol) in toluene (4 mL, 0.2 M) in a 250 mL sealed tube was added *N,O*-bis(trimethylsilyl)acetamide (BSA) (397 μL , 1.62 mmol) and triethylamine (11.3 μL , 0.0812 mmol). The reaction was heated to 110 °C and stirred for 20 min. The solution was then cooled to 23 °C and diluted with toluene (200 mL, 0.004 M), leaving ample headspace in the sealed tube to allow for solvent expansion. The reaction mixture was then heated to 100 °C for 7.5 d or until complete as determined by ^1H NMR. The reaction mixture was then cooled to 23 °C, a 1% aqueous solution of AcOH was added (10 mL), and the reaction was stirred for an additional 2 min. The reaction was washed with an additional 1% aqueous solution of AcOH (3 x 10 mL), and the aqueous phases were combined and back extracted with EtOAc (3 x 30 mL), while making sure the pH of the aqueous phase remained acidic. The organics were combined and dried over Na_2SO_4 ,

and solvent was removed by rotary evaporation. Purification by column chromatography (EtOAc in hexanes with 0.1% AcOH, 17%→25% on silica) gave desired tricycles **88a** and **88b** with a co-eluding impurity (<5% by ¹H NMR). Subsequent recrystallization from heptane and EtOAc gave 249 mg (65% yield) of pure tricyclic acids **88a** and **88b** as white solids and a 1:2 mixture of the respective diastereomers (**88a** and **88b**).

Minor diastereomer **88a**: ¹H NMR (300 MHz, CDCl₃) δ 6.91 (d, *J* = 6.7 Hz, 1H), 6.34 (dd, *J* = 17.4, 11.0 Hz, 1H), 5.17–4.96 (m, 2H), 3.86–3.61 (m, 2H), 3.20 (d, *J* = 6.8 Hz, 1H), 2.95 (s, 1H), 2.09 (s, 3H), 2.00–1.37 (m, 5H), 1.37 (s, 3H), 1.11 (s, 3H); ¹³C NMR (75 MHz, CDCl₃) δ 174.2, 170.9, 169.7, 140.5, 139.2, 113.5, 98.5, 84.2, 70.0, 60.6, 52.6, 44.1, 40.3, 40.1, 38.6, 29.9, 20.9, 19.5, 18.3.

Major diastereomer **88b**: ¹H NMR (300 MHz, CDCl₃) δ 6.91 (d, *J* = 6.7 Hz, 1H), 6.01 (dd, *J* = 17.4, 10.7 Hz, 1H), 5.17–4.96 (m, 2H), 3.86–3.61 (m, 2H), 3.21 (d, *J* = 6.7 Hz, 1H), 3.01 (s, 1H), 2.09 (s, 3H), 2.00–1.37 (m, 5H), 1.30 (s, 3H), 1.13 (s, 3H); ¹³C NMR (75 MHz, CDCl₃) δ 174.1, 170.9, 169.8, 148.0, 138.9, 111.5, 98.9, 84.1, 70.0, 59.2, 52.5, 44.0, 40.1, 39.9, 39.5, 38.1, 20.9, 19.5, 18.3.

FTIR (Neat Film NaCl) 3084, 2977, 2665, 2253, 1733, 1638, 1465, 1438, 1414, 1394, 1379, 1337, 1315, 1229, 1172, 1120, 1041, 967, 913, 876, 839, 795, 735 cm⁻¹; HRMS (Multimode-ESI/APCI) *m/z* calc'd for C₁₉H₂₄IO₆ [M+H]⁺: 475.0612, found 475.0608.



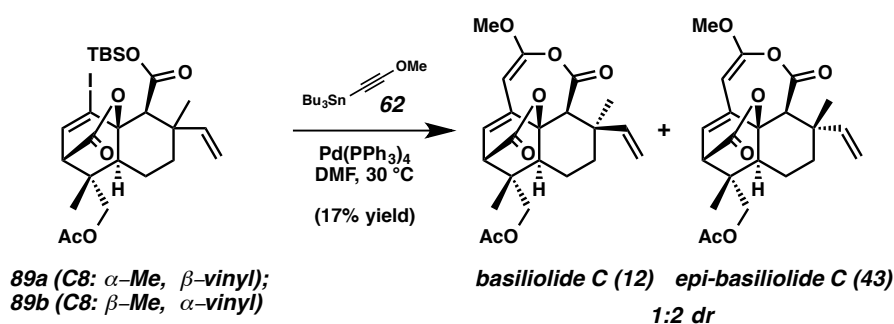
Silyl esters 89a and 89b. To a 23 °C solution of iodo acids **88a** and **88b** (115 mg, 0.243 mmol) in DMF (1.2 mL, 0.2 M) were added sequentially imidazole (99.4 mg, 1.46 mmol) and TBSCl (147 mg, 0.973 mmol). The reaction was stirred for 1 h at 23 °C and then quenched by the addition of saturated brine (4 mL). The resulting aqueous phase was extracted with a 50% solution of EtOAc in hexanes (3 x 4 mL), after which the organics were combined, washed with brine (6 mL), and dried with Na₂SO₄. Solvent was removed by rotary evaporation and purification by column chromatography (EtOAc in hexanes 10%⇒20% on silica) gave 106 mg (74% yield) of silyl esters **89a** and **89b** as white solids and a 1:2 mixture of the respected diastereomers (**89a** and **89b**).

Minor diastereomer **89a**: ¹H NMR (300 MHz, CDCl₃) δ 6.87 (d, J = 6.7 Hz, 1H), 6.36 (dd, J = 17.4, 11.0 Hz, 1H), 5.19–4.88 (m, 2H), 3.80–3.63 (m, 2H), 3.14 (d, J = 6.8 Hz, 1H), 2.85 (s, 1H), 2.07 (s, 3H), 1.91–1.19 (m, 8H), 1.10 (s, 3H), 0.88 (s, 9H), 0.27 (s, 3H), 0.26 (s, 3H); ¹³C NMR (75 MHz, CDCl₃) δ 170.7, 169.7, 169.1, 141.0, 138.9, 113.2, 99.2, 84.3, 70.0, 61.8, 52.8, 44.4, 40.5, 39.6, 39.2, 29.8, 25.5, 21.1, 20.91, 19.5, 17.6, -4.8, -4.8.

Major diastereomer **89b**: ¹H NMR (300 MHz, CDCl₃) δ 6.87 (d, J = 6.7 Hz, 1H), 6.01 (dd, J = 17.4, 10.6 Hz, 1H), 5.19–4.88 (m, 2H), 3.80–3.63 (m, 2H), 3.16 (d, J = 6.8 Hz, 1H), 2.94 (s, 1H), 2.07 (s, 3H), 1.91–1.19 (m, 8H), 1.10 (s, 3H), 0.88 (s, 9H), 0.27 (s, 3H), 0.24 (s, 3H); ¹³C NMR (75 MHz, CDCl₃) δ 170.7, 169.7, 168.9, 149.0, 138.7, 110.8,

99.6, 84.2, 70.0, 60.4, 52.6, 44.3, 40.3, 40.2, 38.5, 25.6, 21.1, 20.9, 19.52, 18.1, 17.6, -
4.7, -4.8.

FTIR (Neat Film NaCl) 2951, 2930, 2896, 2858, 1760, 1745, 1716, 1472, 1464, 1413,
1393, 1378, 1364, 1341, 1283, 1250, 1229, 1194, 1173, 1042, 1021, 1007, 984, 968, 939,
930, 915, 885, 843, 828, 790, 733 cm^{-1} ; HRMS (Multimode-ESI/APCI) m/z calc'd for
 $\text{C}_{25}\text{H}_{38}\text{IO}_6\text{Si}$ $[\text{M}+\text{H}]^+$: 589.1477, found 589.1496.



Basiliolide C (12) and epi-basiliolide C (43). In a nitrogen filled glovebox, to a solution of silyl esters **89a** and **89b** (13 mg, 0.022 mmol) and $\text{Pd}(\text{PPh}_3)_4$ (28 mg, 0.0242 mmol) in DMF (220 μL , 0.1 M) was added tributyl(2-methoxyethynyl)stannane (**62**) (29 mg, 0.088 mmol). The reaction was stirred at 30 $^\circ\text{C}$ for 15 h at which point another equivalent of stannane **62** was added (7.5 mg, 0.022 mmol). The reaction was stirred for an addition 5 h and then additional stannane **62** was added (7.5 mg, 0.022 mmol). After another 4 h of stirring at 30 $^\circ\text{C}$ (a total reaction time of 24 h) the reaction was filtered through cotton washing with MeCN in order to remove $\text{Pd}(\text{PPh}_3)_4$. The filtrate was further diluted with MeCN (making a total reaction volume of 8 mL) and the reaction solution was removed from the glovebox. pH 7 phosphate buffer (150 μL) was added to the crude reaction solution and then stirred at 23 $^\circ\text{C}$ for 6 h. MeCN was then removed by

passing a stream of air over the reaction vessel (rotary evaporation could not be accomplished without bumping the liquid). The remaining liquid was diluted with 25% saturated brine solution in water (350 μ L) and the aqueous phase extracted with EtOAc (4 x 750 μ L). The organics were pooled, dried over Na₂SO₄, and concentrated by rotary evaporation. The crude oil was purified by normal phase HPLC (33% EtOAc in hexanes) to yield 0.51 mg (6% yield) of basiliolide C (**12**) and 0.97 mg (11% yield) of epi-basiliolide C (**43**). The spectroscopic data obtained from synthetic **12** match those published from natural sources.

Basiliolide C (**12**): ¹H NMR (500 MHz, CDCl₃) δ 7.00 (dd, J = 17.7, 11.1 Hz, 1H), 6.05 (dd, J = 6.5, 1.2 Hz, 1H), 5.16 (dd, J = 11.1, 1.4 Hz, 1H), 5.06 (dd, J = 17.7, 1.2 Hz, 1H), 5.00 (d, J = 1.4 Hz, 1H), 3.73 (s, 3H), 3.73 (d, J = 10.8 Hz, 1H), 3.69 (d, J = 10.8 Hz, 1H), 3.29 (d, J = 6.5 Hz, 1H), 3.14 (s, 1H), 2.08 (s, 3H), 1.93 (dt, J = 13.5, 3.4 Hz, 1H), 1.75 (qd, J = 13.5, 3.0 Hz, 1H), 1.64–1.50 (m, 1H), 1.41 (td, J = 13.5, 3.0 Hz, 1H), 1.32–1.24 (m, 1H), 1.23 (s, 3H), 1.12 (s, 3H); ¹³C NMR (125 MHz, CDCl₃) δ 171.0, 170.7, 162.4, 157.0, 142.7, 138.6, 123.0, 112.5, 87.0, 79.2, 70.6, 56.6, 53.4, 49.8, 44.8, 40.3, 38.6, 37.1, 28.7, 21.2, 20.9, 19.8; FTIR (Neat Film NaCl) 3083, 2942, 2873, 2851, 1766, 1745, 1620, 1464, 1444, 1378, 1334, 1262, 1233, 1199, 1178, 1108, 1038, 1010, 994, 955, 914, 831, 733 cm⁻¹; HRMS (Multimode-ESI/APCI) m/z calc'd for C₂₂H₂₇O₇ [M+H]⁺: 403.1751, found 403.1736.

Epi-basiliolide C (**43**): ¹H NMR (500 MHz, CDCl₃) δ 6.04 (dd, J = 6.5, 1.3 Hz, 1H), 5.80 (dd, J = 17.4, 10.8 Hz, 1H), 5.11–5.03 (m, 2H), 4.98 (d, J = 1.3 Hz, 1H), 3.72 (q, J = 10.8 Hz, 2H), 3.72 (s, 3H), 3.29 (d, J = 6.5 Hz, 1H), 3.23 (s, 1H), 2.09 (s, 3H), 1.84–1.72 (m, 1H), 1.70–1.62 (m, 2H), 1.61 (s, 3H), 1.50–1.41 (m, 1H), 1.26 (dd, J = 13.1, 4.9 Hz,

1H), 1.16 (s, 3H); ¹³C NMR (125 MHz, CDCl₃) δ 171.0, 170.8, 162.1, 157.0, 146.3, 138.9, 122.7, 113.2, 87.0, 79.0, 70.6, 56.5, 50.7, 49.7, 44.5, 38.6, 38.3, 37.0, 20.9, 20.7, 19.9, 19.3; FTIR (Neat Film NaCl) 2931, 1763, 1742, 1666, 1619, 1442, 1377, 1335, 1228, 1195, 1178, 1113, 1038, 1021, 999, 970, 952, 914, 830, 732 cm⁻¹; HRMS (Multimode-ESI/APCI) m/z calc'd for C₂₂H₂₇O₇ [M+H]⁺: 403.1751, found 403.1744.

1.9 NOTES AND REFERENCES

Note: Portions of this chapter have been published, see: Gordon, J. R.; Nelson, H. M.; Virgil, S. C.; Stoltz, B. M. *J. Org. Chem.* **2014**, Article ASAP. doi: 10.1021/jo501924u.

- (1) (a) Christensen, S. B.; Rasmussen, U. *Tetrahedron Lett.* **1980**, *21*, 3829–3830; (b) Christensen, S. B.; Andersen, A.; Smitt, U. W. *Prog. Chem. Org. Nat. Prod.* **1997**, *71*, 130–167.
- (2) Christensen, S. B.; Larsen, I. K.; Rasmussen, U.; Christophersen, C. *J. Org. Chem.* **1982**, *47*, 649–652.
- (3) Perchellet, E. M.; Gali, H. U.; Gao, X. M.; Perchellet, J. *Int. J. Cancer* **2006**, *55*, 1036–1043.
- (4) (a) Thastrup, O.; Cullen, P. J.; Droback, B. K.; Hanley, M. R.; Dawson, A. P. *Proc. Natl. Acad. Sci. USA* **1990**, *87*, 2466–2470; (b) Lytton, J.; Westlin, M.; Hanley, M. R. *J. Biol. Chem.* **1991**, *266*, 17067–17071; (c) Rooney, E.; Meldolesi, J. *J. Biol. Chem.* **1996**, *271*, 29304–29311.
- (5) Treiman, T.; Caspersen, C.; Christensen, S. B. *Trends Pharma. Sciences* **1998**, *19*, 131–135.
- (6) Toyoshima, C.; Nomura, H. *Nature* **2002**, *418*, 605–611.
- (7) Larsen, P. K.; Sandberg, F. *Acta Chem. Scand.* **1970**, *24*, 1113–1114.
- (8) (a) Rubal, J. J.; Moreno-Dorado, F. J.; Guerra, F. M.; Jorge, Z. D.; Saouf, A.; Akssira, M.; Mellouki, F.; Romero-Garrido, R.; Massanet, G. M. *Phytochemistry* **2007**, *68*, 2480–2486; (b) To enable convenient discussion of the previously unnamed natural metabolite **3**, Stoltz and coworkers have given the name

“basiliopyrone” to metabolite **3** as it is believed to be a biosynthetically related to the basiliolide and transtaganolide (**7–12**) family of natural products.

- (9) Gunes, H. S. *J. Fac. Pharm. Gazi*. **2001**, *18*, 35–41.
- (10) Rasmussen, U.; Christensen, S. B.; Sandberg, F. *Planta Med.* **1981**, *43*, 336–341.
- (11) Saouf, A.; Guerra, F. M.; Rubal, J. J.; Moreno-Dorado, F. J.; Akssira, M.; Mellouki, F.; López, M.; Pujadas, A. J.; Jorge, Z. D.; Massanet, G. M. *Org. Lett.* **2005**, *7*, 881–884.
- (12) Appendino, G.; Prosperini, S.; Valdivia, C.; Ballero, M.; Colombano, G.; Billington, R. A.; Genazzani, A. A.; Sterner, O. *J. Nat. Prod.* **2005**, *68*, 1213–1217.
- (13) Navarrete, C.; Sancho, R.; Caballero, F. J.; Pollastro, F.; Fiebich, B. L.; Sterner, O.; Appendino, G.; Muñoz, E. *J. Pharmacol. Exp. Ther.* **2006**, *319*, 422–430.
- (14) Through close correspondence with Appendino¹² and Muñoz,¹³ it had come to our attention that even though the assayed transtaganolide and basiliolides (**9**, **11**, and **12**) were by all observable methods pure, trace thapsigargin (**1**) contamination was still a looming possibility. As a control, synthetically derived racemic transtaganolide C (**9**) was sent for testing and results were consistent with those observed from the isolated natural products, removing any possibility that the previously observed activity had resulted from trace thapsigargin (**1**) contamination.
- (15) Larsson, R.; Sterner, O.; Johansson, M. *Org. Lett.* **2009**, *11*, 657–660.

- (16) Nelson, H. M.; Stoltz, B. M. *Org. Lett.* **2008**, *10*, 25–28.
- (17) (a) Posner, G. H.; Nelson, T. D.; Kinter, C. M.; Afarinkia, K. *Tetrahedron Lett.* **1991**, *32*, 5295–5298; (b) Posner, G. H.; Dai, H.; Afarinkia, K.; Murthy, N. N.; Guyton, K. Z.; Kensler, T. W. *J. Org. Chem.* **1993**, *58*, 7209–7215; (c) for a theoretical discussion and computational models, see: Afarinkia, K.; Bearpark, M. J.; Ndibwami, A. *J. Org. Chem.* **2005**, *70*, 1122–1133.
- (18) Kozytska, M. V.; Dudley, G. B. *Tetrahedron Lett.* **2008**, *49*, 2899–2901.
- (19) Zhou, X.; Wu, W.; Liu, X.; Lee, C.-S. *Org. Lett.* **2008**, *10*, 5525–5528.
- (20) Nelson, H. M.; Stoltz, B. M. *Tetrahedron Lett.* **2009**, *50*, 1699–1701.
- (21) Nelson, H. M.; Murakami, K.; Virgil, S. C.; Stoltz, B. M. *Angew. Chem. Int. Ed.* **2011**, *50*, 3688–3691.
- (22) Nelson, H. M. A Unified Synthetic Approach to the Transtaganolide and Basiliolide Natural Products. Ph.D. Dissertation, California Institute of Technology, Pasadena, CA, 2013.
- (23) (a) Marshall, J. A. in *Organometallics in Synthesis: A Manual* (Ed.: M. Schlosser) Wiley, Chichester, **2002**, 457; (b) Sakamoto, T.; Yasuhara, A.; Kondo, Y.; Yamanaka, H. *Synlett* **1992**, 502; (c) Sakamoto, T.; Yasuhara, A.; Kondo, Y.; Yamanaka, H. *Chem. Pharm. Bull.* **1994**, *42*, 2032–2035; (d) Löffler, A.; Himbert, G. *Synthesis* **1992**, 495–498.
- (24) Shibuya, H.; Ohashi, K.; Narita, N.; Ishida, T.; Kitagawa, I. *Chem. Pharm. Bull.* **1994**, *42*, 293–299.

- (25) Min, L.; Zhang, Y.; Liang, X.; Huang, J.; Bao, W.; Lee, C.-S. *Angew. Chem. Int. Ed.* **2014**, Article ASAP. doi: 10.1002/anie.201405770.
- (26) Gordon, J. R.; Nelson, H. M.; Virgil, S. C.; Stoltz, B. M. *J. Org. Chem.* **2014**, Article ASAP. doi: 10.1021/jo501924u.
- (27) (a) Gordon, J.; Hamilton, C.; Hooper, A. M.; Ibbotson, H. C.; Kurosawa, S.; Mori, K.; Muto, S.; Pickett, J. A. *Chem. Comm.* **1999**, 2335–2336; (b) Imamura, Y.; Takikawa, H.; Mori, K. *Tetrahedron Lett.* **2002**, 43, 5743–5746.

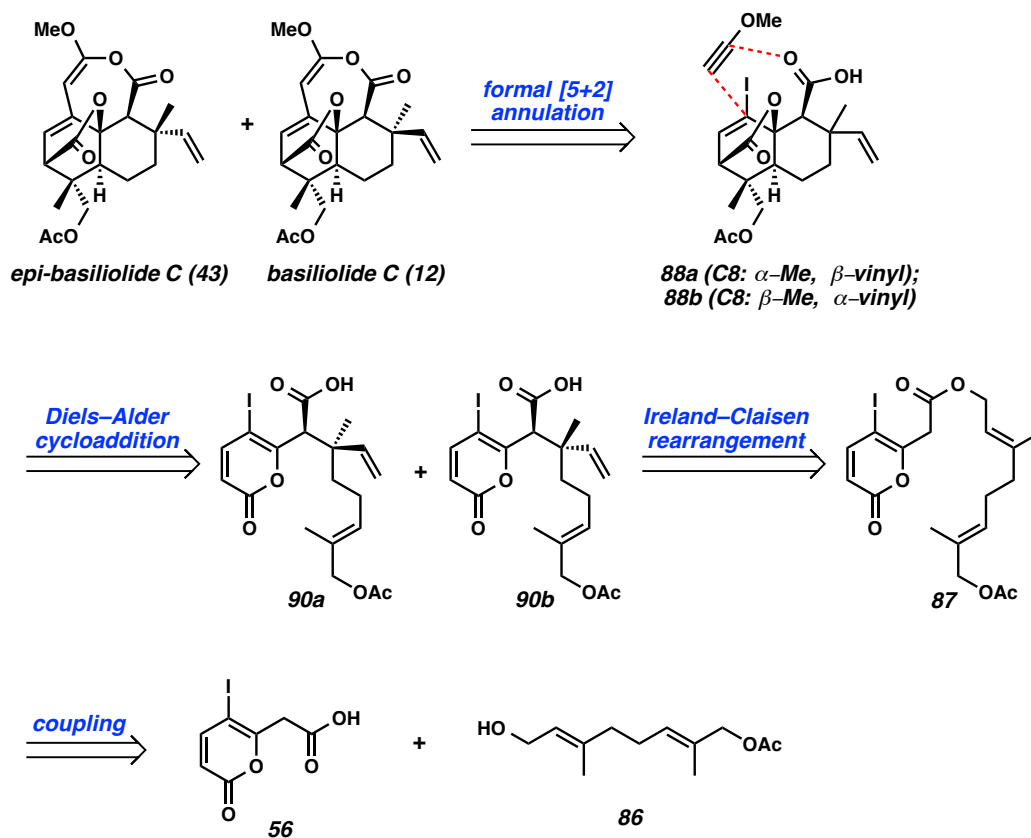
APPENDIX 1

Synthetic Summary for Basiliolide C and epi-Basiliolide C:

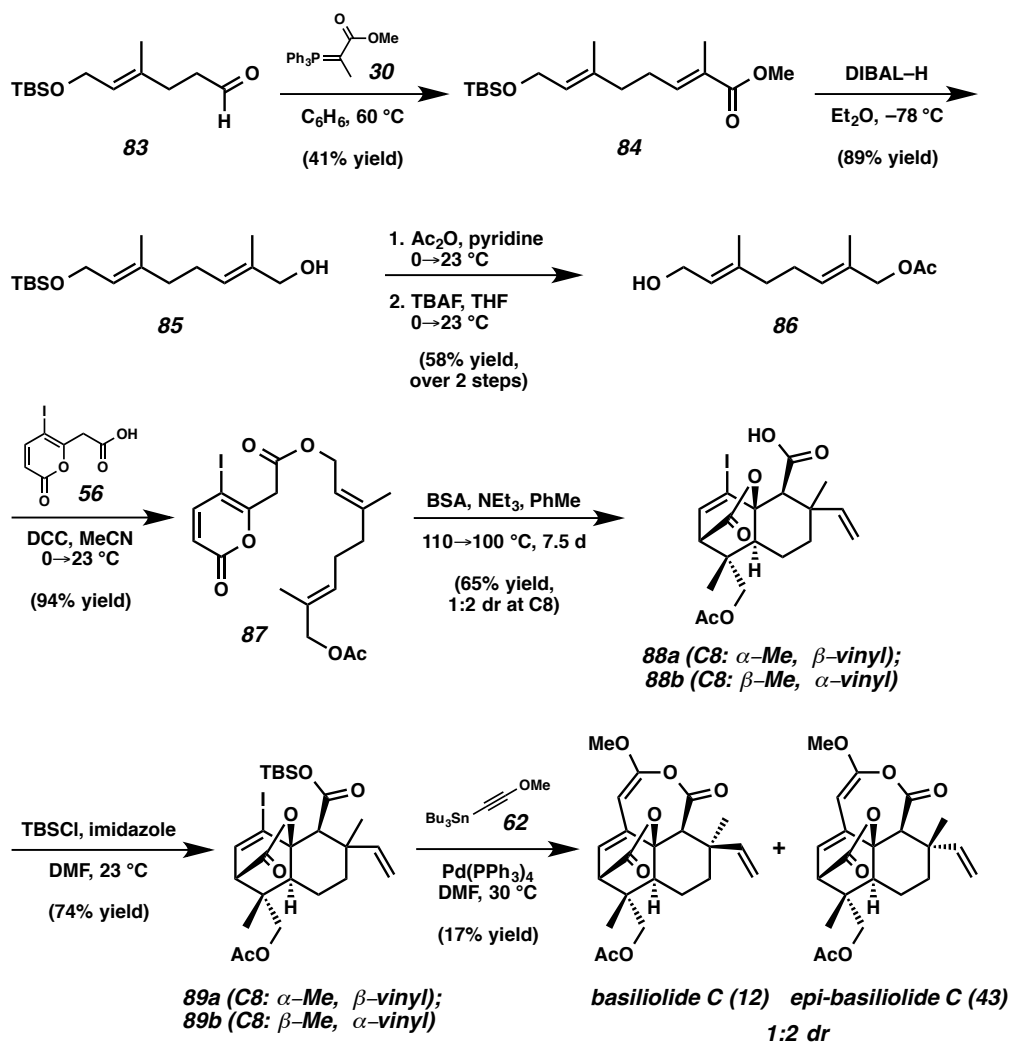
Relevant to Chapter 1

A1.1 SYNTHETIC SUMMARY FOR BASIOLIDE C AND EPI-BASIOLIDE C

Scheme A1.1.1. Retrosynthetic analysis for basilolide C (**12**) and epi-basilolide C (**43**).



Scheme A1.1.2. Syntheses of basilolide C (**12**) and epi-basilolide C (**43**).



APPENDIX 2

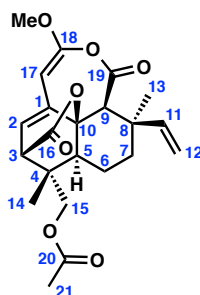
Comparison of Spectral Data for Synthetic and Reported Basiliolide C,

As well as Biological Assays for Synthetic Transtaganolide C:

Relevant to Chapter 1

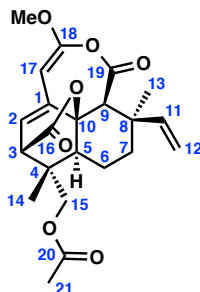
A2.1 COMPARISON OF ¹H NMR AND ¹³C NMR FOR SYNTHETIC AND REPORTED BASILIOLOIDE C

Table A2.1.1. Comparison of ¹H NMR data for synthetic and reported natural¹ basiliolide C (**12**).



Assignment	Synthetic ¹² (ppm)	Multiplicity, <i>J</i> (Hz)	Natural ¹² (ppm)	Multiplicity, <i>J</i> (Hz)
C1	—	—	—	—
C2	6.05	dd, 6.5, 1.2	6.06	dd, 6.4, 1.1
C3	3.29	d, 6.5	3.29	d, 6.4
C4	—	—	—	—
C5	1.32–1.24	m	1.29	dd, 12.9, 4.6
C6	1.75	qd, 13.5, 3.0	1.76	dddd, 13.8, 13.0, 12.9, 2.8
	1.64–1.50	m	1.54	dddd, 13.8, 4.6, 3.9, 2.8
C7	1.93	dt, 13.5, 3.4	1.94	ddd, 13.7, 3.9, 2.8
	1.41	td, 13.5, 3.0	1.42	ddd, 13.7, 13.0, 2.8
C8	—	—	—	—
C9	3.14	s	3.15	s
C10	—	—	—	—
C11	7.00	dd, 17.7, 11.1	7.00	dd, 17.7, 11.1
C12	5.16	dd, 11.1, 1.4	5.17	dd, 11.0, 1.0
	5.06	dd, 17.7, 1.2	5.06	dd, 17.7, 1.0
C13	1.23	s	1.24	s
C14	1.12	s	1.12	s
C15	3.73	d, 10.8	3.74	d, 10.8
	3.69	d, 10.8	3.70	d, 10.8
C16	—	—	—	—
C17	5.00	d, 1.4	5.01	d, 1.1
C18	—	—	—	—
C19	—	—	—	—
C20	—	—	—	—
C21	2.08	s	2.09	s
OMe	3.73	s	3.74	s

Table A2.1.2. Comparison of ^{13}C NMR data for synthetic and reported natural¹ basiliolide C (**12**).

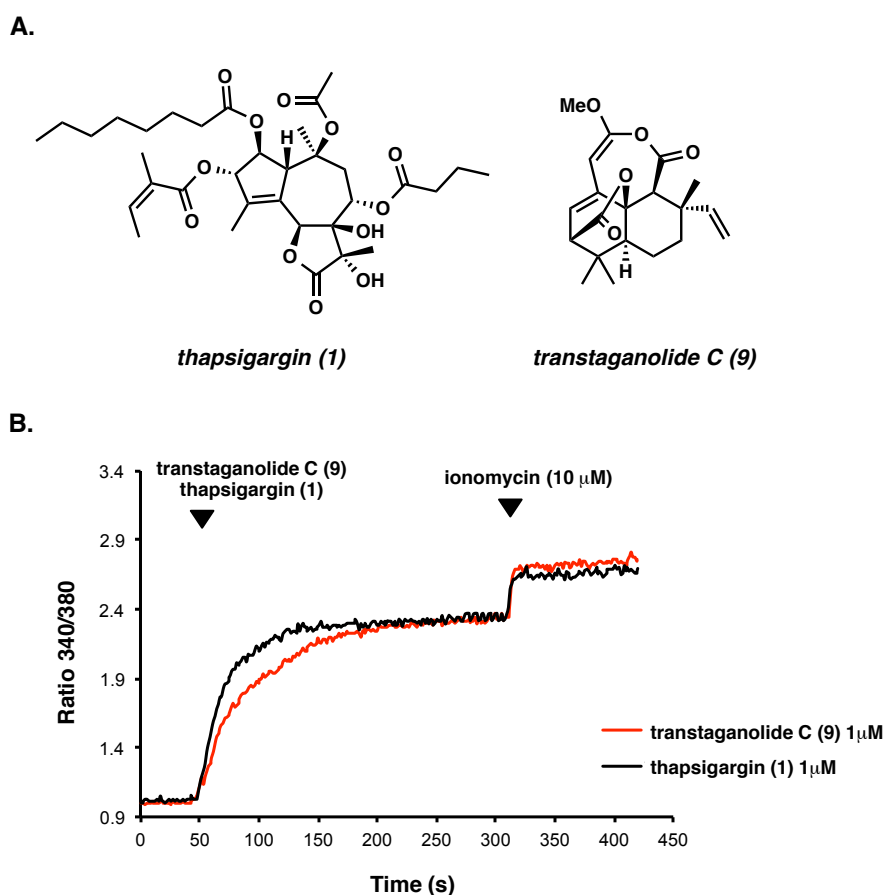


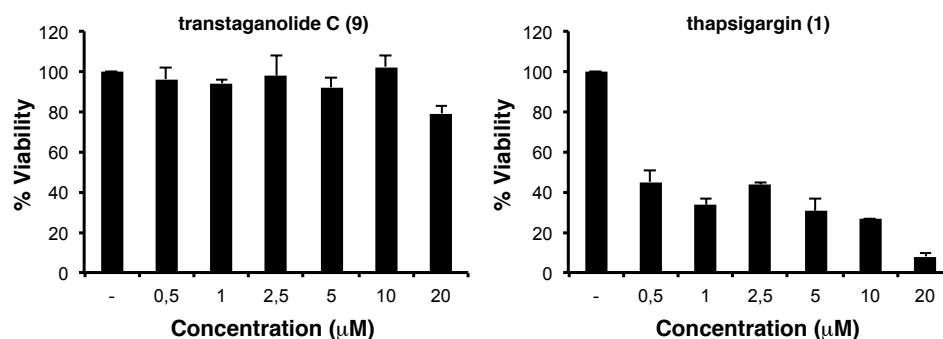
Assignment	Synthetic 12 (ppm)	Natural 12 (ppm)
C1	138.6	138.6
C2	123.0	122.8
C3	49.8	49.7
C4	37.1	37.0
C5	44.8	44.7
C6	21.2	21.1
C7	40.3	40.2
C8	38.6	38.4
C9	53.4	53.3
C10	87.0	86.9
C11	142.7	142.6
C12	112.5	112.3
C13	28.7	28.6
C14	19.8	19.6
C15	70.6	70.4
C16	170.7	170.7
C17	79.2	79.0
C18	157.0	156.9
C19	162.4	162.3
C20	171.0	170.8
C21	20.9	20.7
OMe	56.6	56.4

A2.2 BIOACTIVITY OF SYNTHETIC TRANSTAGANOLIDE C

Appendino, Muñoz, and coworkers assayed naturally isolated transtaganolide C (**9**) for its effect on calcium mobilization as well as cell viability following exposure to the natural product **9**.² To ensure the data obtained was not the result of trace thapsigargin (**1**) contamination in the isolation sample, we sent synthetic transtaganolide C (**9**) to be tested as a control. Both calcium mobilization (Figure A2.2.1)³ and cell viability (Figure A2.2.2)³ assays were consistent with those observed with naturally isolated transtaganolide C (**9**).

Figure A2.2.1. A) Thapsigargin (**1**) and transtaganolide C (**9**). B) The effect of synthetic transtaganolide C (**9**) or naturally isolated thapsigargin (**1**) on calcium mobilization as a function of time (arrows indicate the time at which a reagent was added).³





General procedure for calcium mobilization. Jurkat cells were incubated for 1 h at 37 °C in Tyrode's salt solution (137 mM NaCl, 2.7 mM KCl, 1.8 mM CaCl₂, 1.0 mM MgCl₂, 0.4 mM NaH₂PO₄, 12.0 mM NaHCO₃, 5.6 mM D-glucose) containing 5 µM Indo-1-AM (Invitrogen) for 30 min at 37 °C in the dark. Cells were then harvested, washed three times with buffer to remove extracellular Indo-1 dye, readjusted to 10⁶ cells/mL in the appropriate buffer, and analyzed in a spectrofluorimeter operated in the ratio mode (Hitachi F-2500 model, Hitachi Ltd.) under continuous stirring and at a constant temperature of 37 °C using a water-jacketed device. After 5 min for accommodation to equilibrate temperatures, samples were excited at 338 nm and emission was collected at 405 and 485 nm, corresponding to the fluorescence emitted by Ca²⁺-bound and free Indo-1, respectively. [Ca²⁺]_i was calculated using the ratio values between bound- and free-Indo-1 fluorescence, and assuming an Indo-1 K_d for Ca²⁺ of 0.23 µM. Maximum and minimum ratio values for calculations were determined by the addition at the end of the measurements of 10 µM ionomycin. [Ca²⁺]_i changes are presented as changes in the ratio of bound-to-free calcium (340 nm/380 nm).³

General procedure for cell viability. For cytotoxicity analysis, Jurkat cells were seeded in 96-well plates in complete medium and treated with increasing doses of

transtaganolide C (**9**) or thapsigargin (**1**) at the indicated concentrations (μM) for 24 hours. Samples were then diluted with 300 μL of PBS and incubated for 1 min at 23 °C in the presence of propidium iodine (10 $\mu\text{g}/\text{ml}$). After incubation, cells were immediately analyzed by flow cytometry. The results are represented as the percentage of viability considering 100% viability for the untreated cells.³

A2.3 NOTES AND REFERENCES

- (1) Appendino, G.; Prosperini, S.; Valdivia, C.; Ballero, M.; Colombano, G.; Billington, R. A.; Genazzani, A. A.; Sterner, O. *J. Nat. Prod.* **2005**, *68*, 1213–1217.
- (2) Navarrete, C.; Sancho, R.; Caballero, F. J.; Pollastro, F.; Fiebich, B. L.; Sterner, O.; Appendino, G.; Muñoz, E. *J. Pharmacol. Exp. Ther.* **2006**, *319*, 422–430.
- (3) Muñoz, E. Departamento de Biología Celular, Fisiología e Inmunología, Facultad de Medicina, Universidad de Córdoba, Córdoba, Spain. Personal communication, July 2013.

APPENDIX 3

Spectra Relevant to Chapter 1:

Transtaganolide and Basiliolide Natural Products and Early Efforts

Toward their Total Synthesis

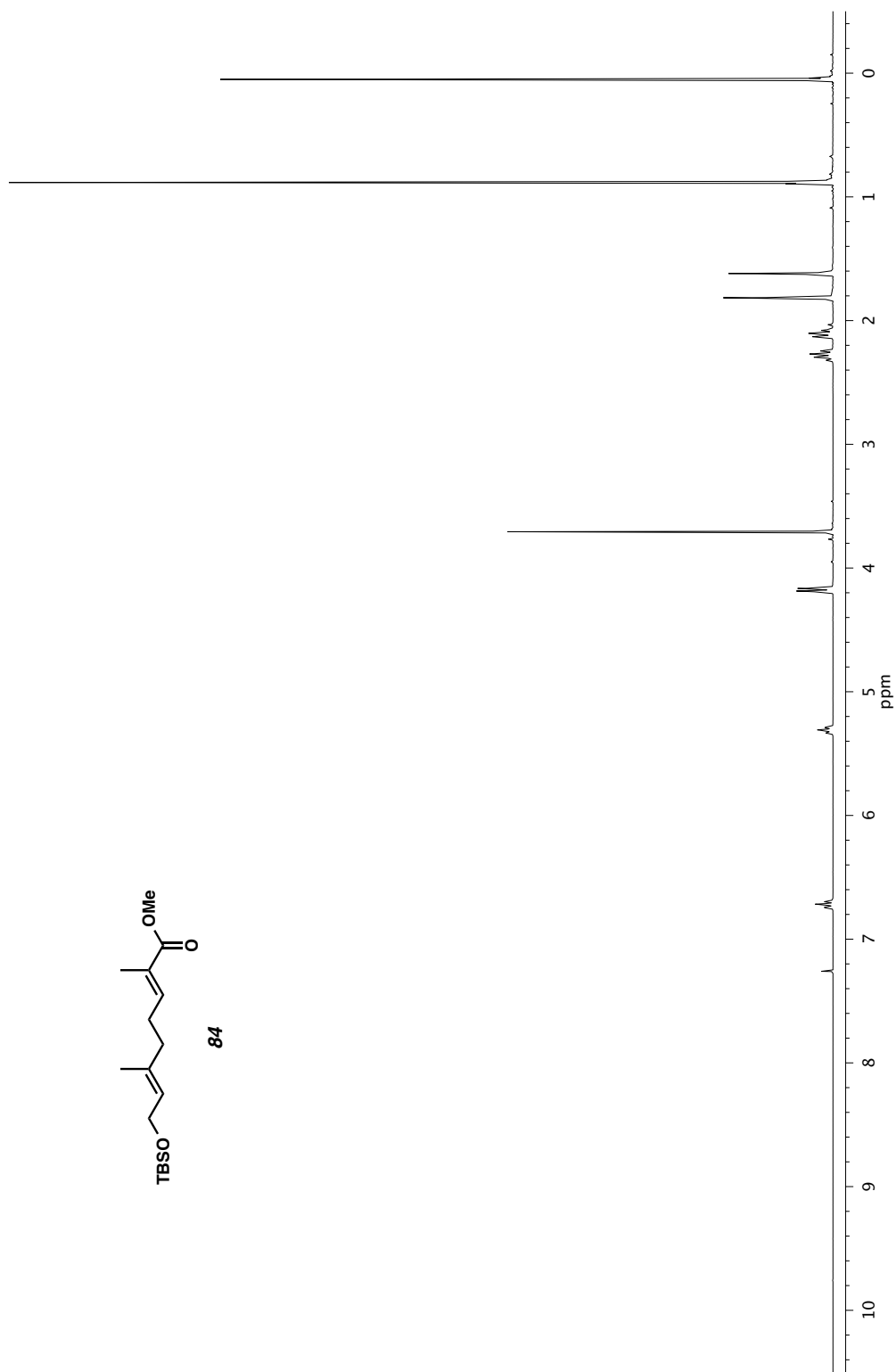


Figure A3.1.1 ¹H NMR 300 MHz, CDCl₃) of compound **84**.

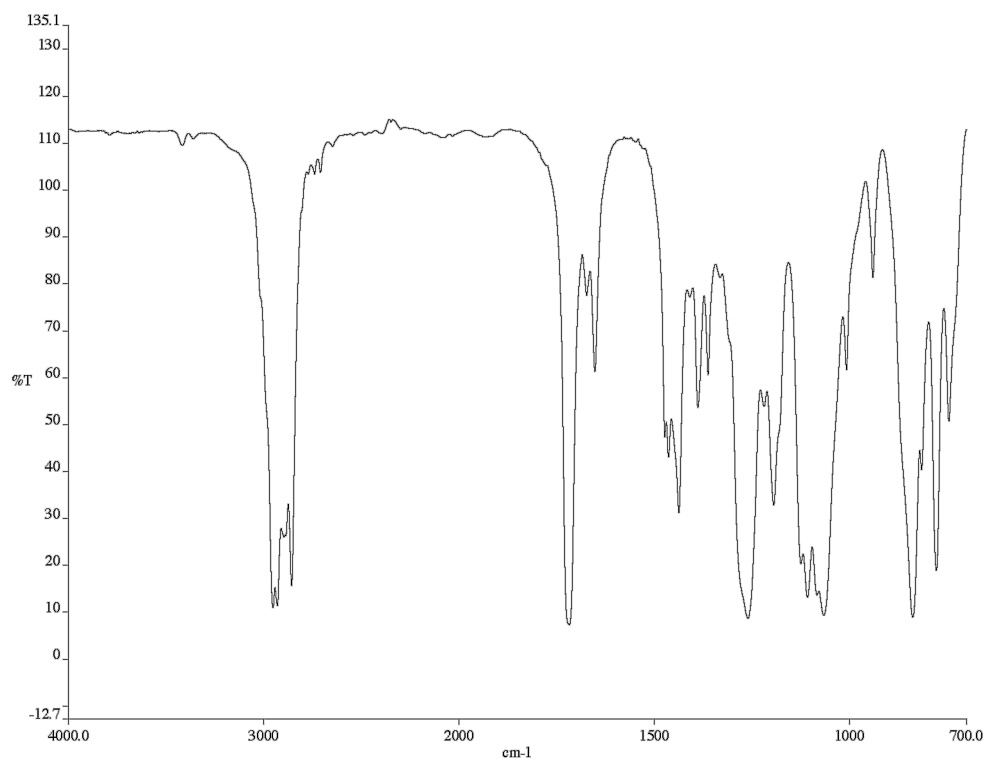


Figure A3.1.2 infrared spectrum (Thin Film, NaCl) of compound **84**.

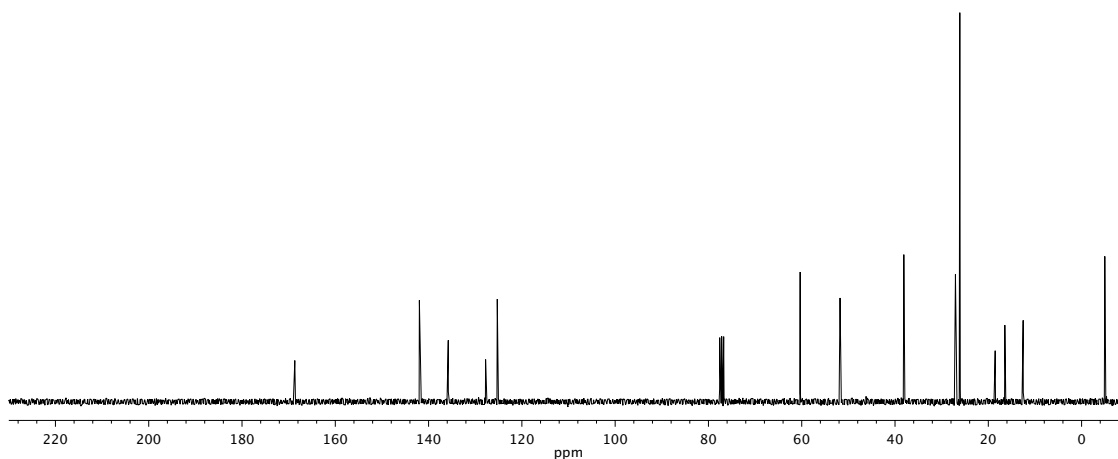


Figure A3.1.3 ¹³C NMR (75 MHz, CDCl₃) of compound **84**.

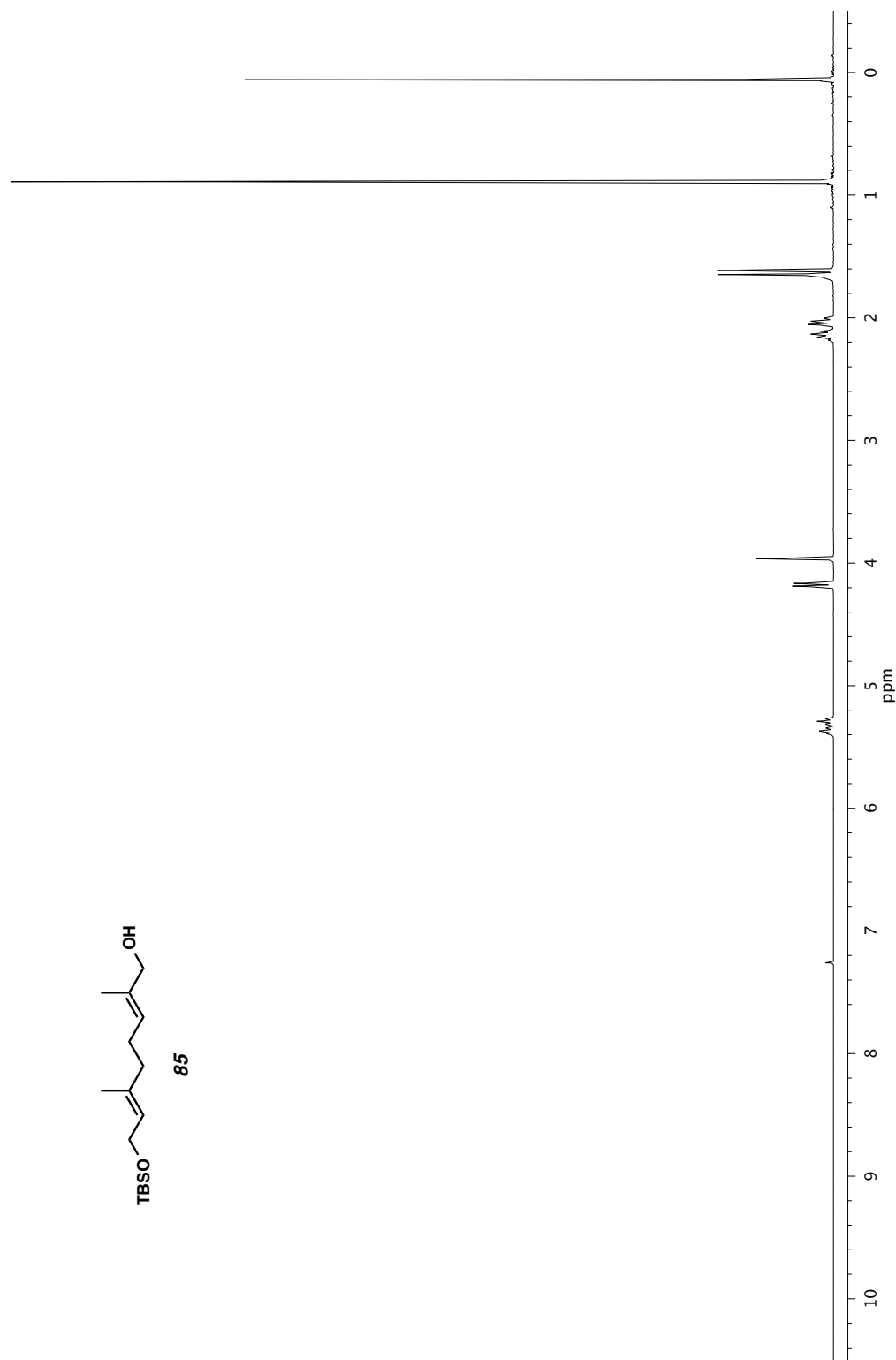


Figure A3.2.1 ¹H NMR 300 MHz, CDCl₃) of compound **85**.

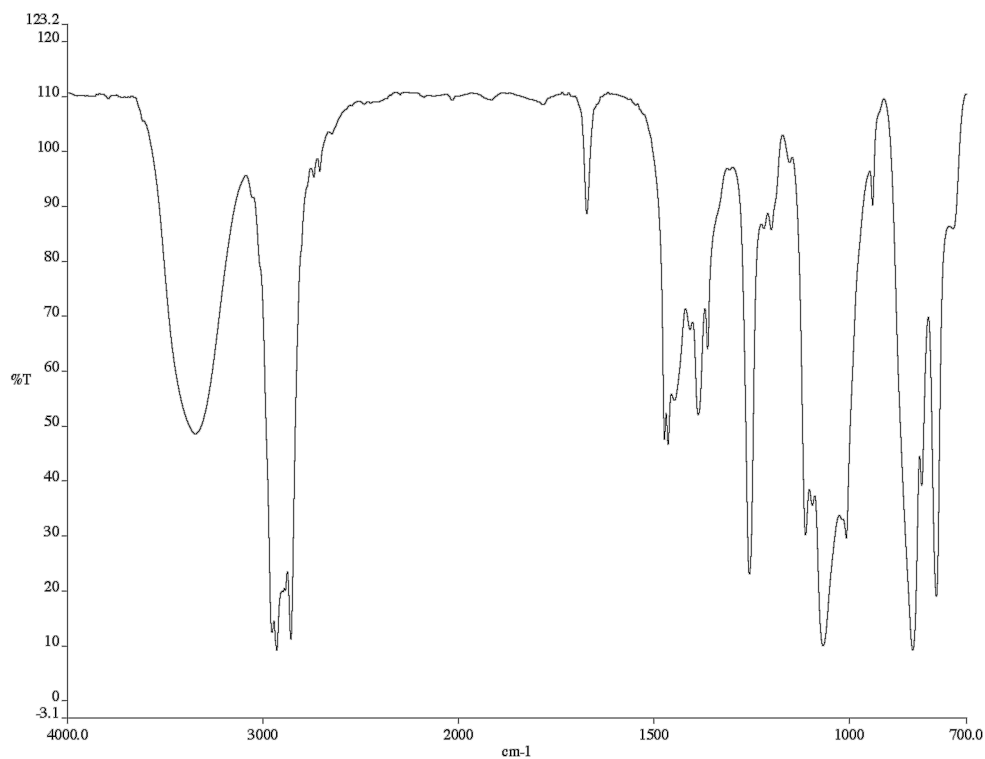


Figure A3.2.2 infrared spectrum (Thin Film, NaCl) of compound **85**.

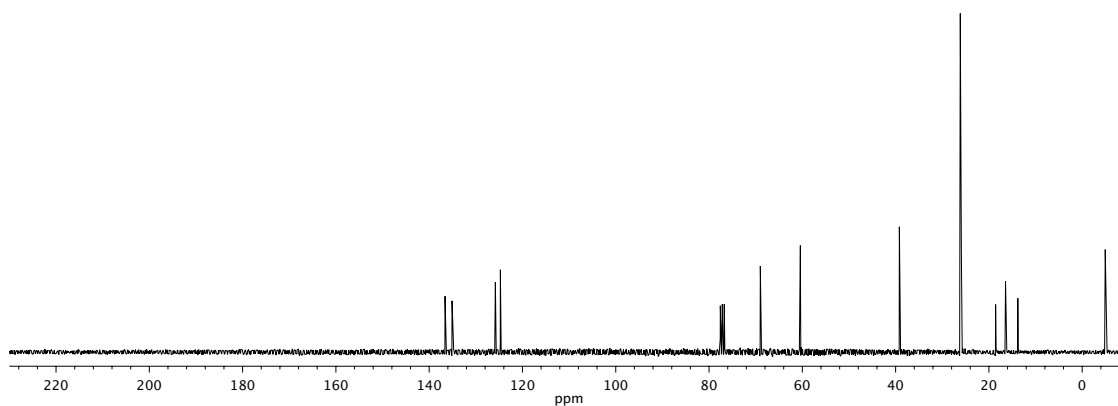


Figure A3.2.3 ^{13}C NMR (75 MHz, CDCl_3) of compound **85**.

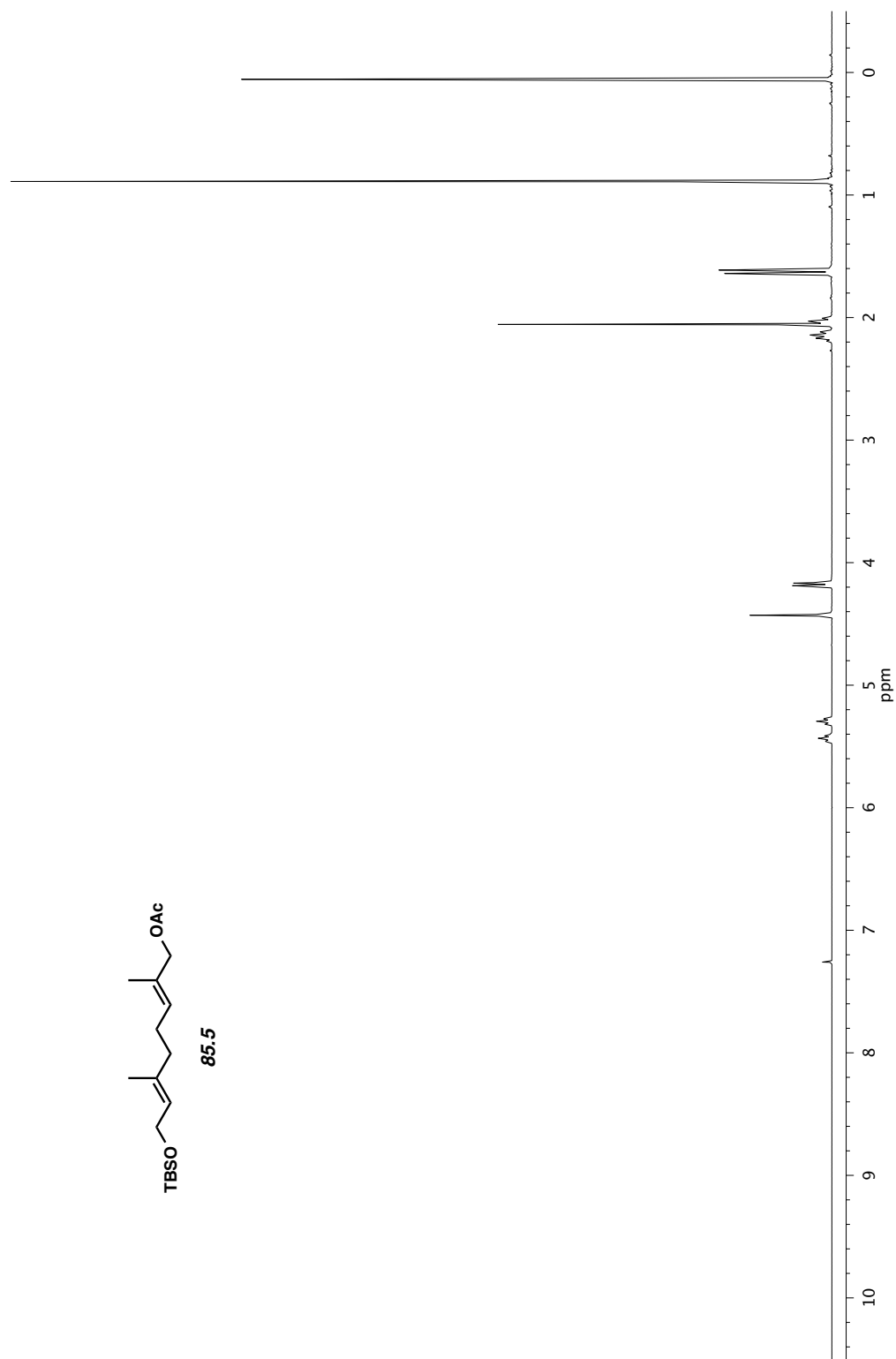


Figure A3.3.1 $^1\text{H NMR}$ 300 MHz, CDCl_3) of compound **85.5**.

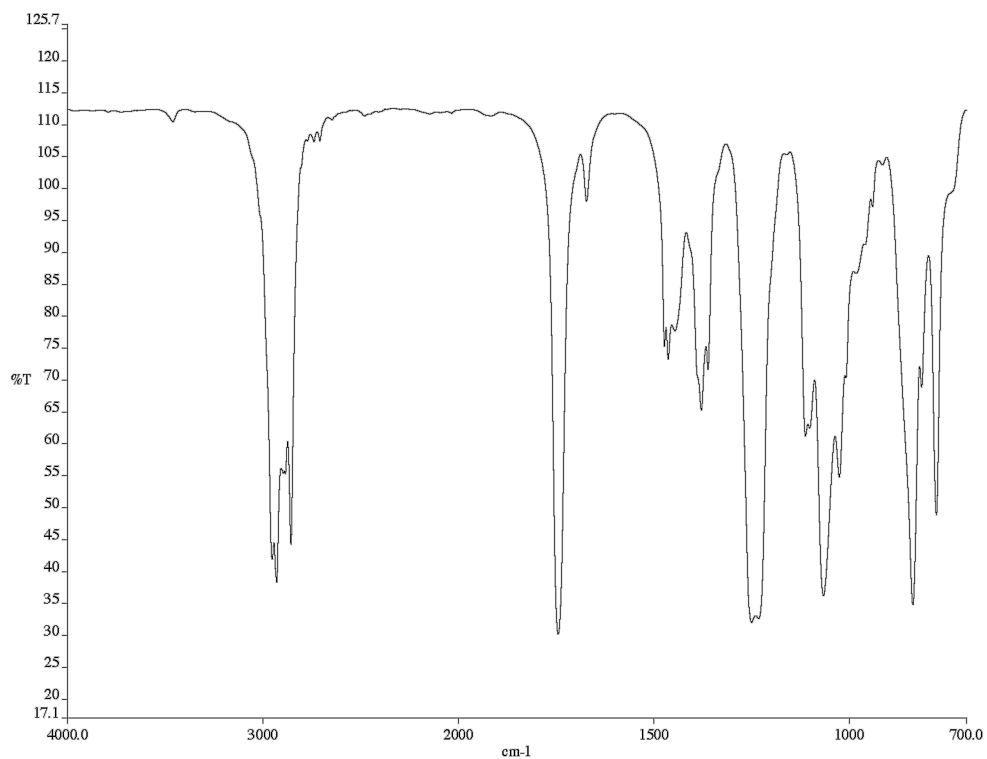


Figure A3.3.2 infrared spectrum (Thin Film, NaCl) of compound **85.5**.

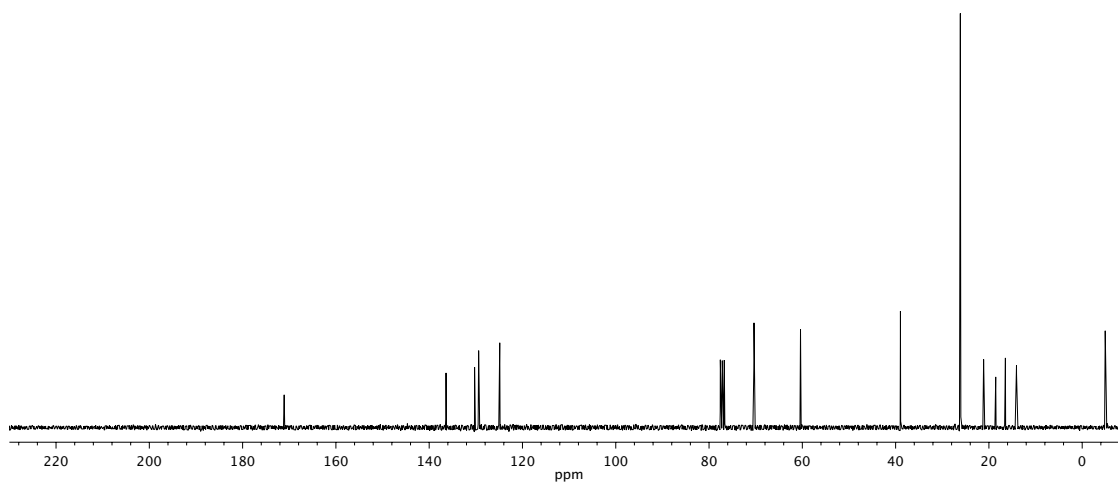


Figure A3.3.3 ^{13}C NMR (75 MHz, CDCl_3) of compound **85.5**.

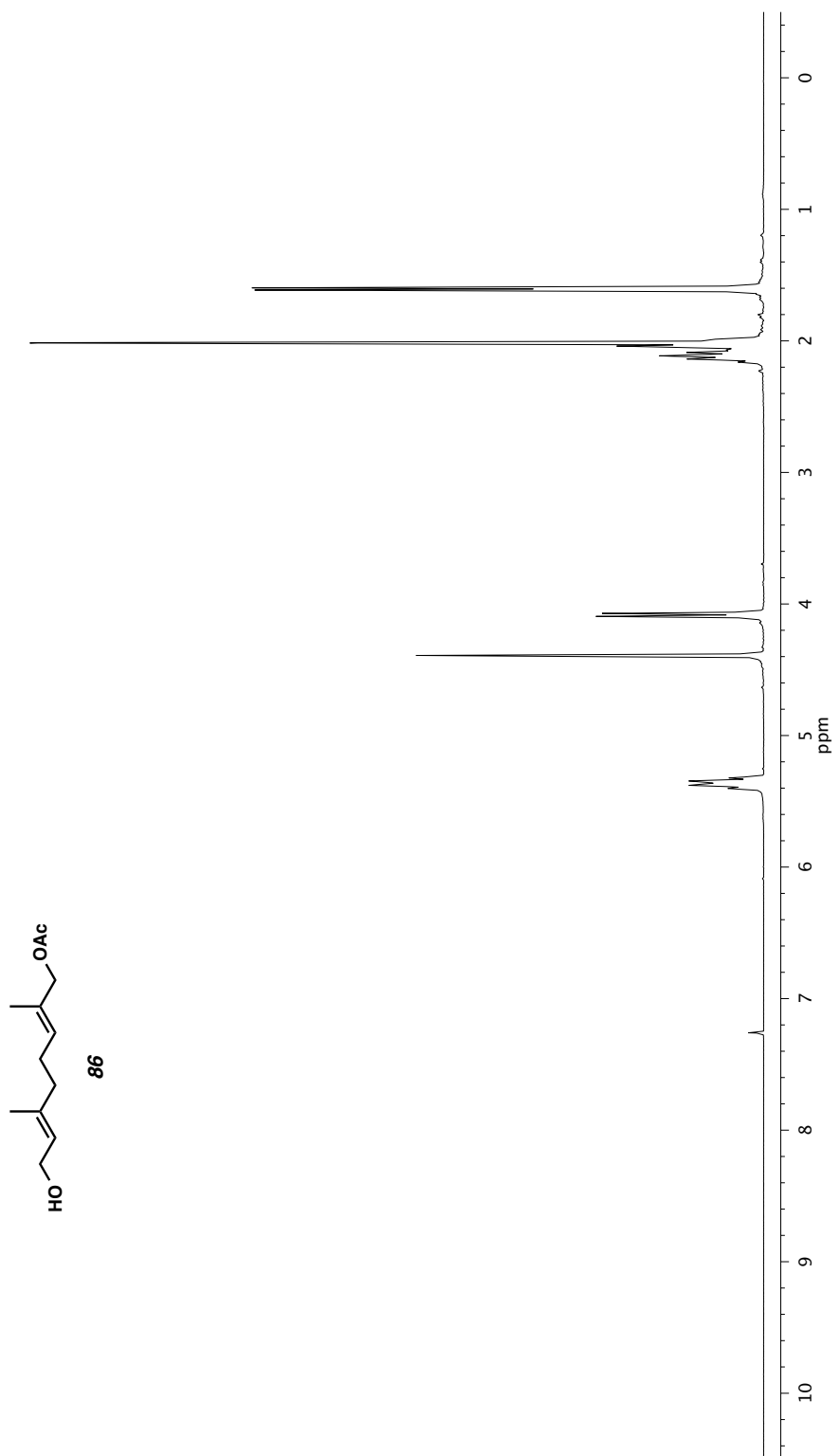


Figure A3.4.1 ^1H NMR 300 MHz, CDCl_3) of compound **86**.

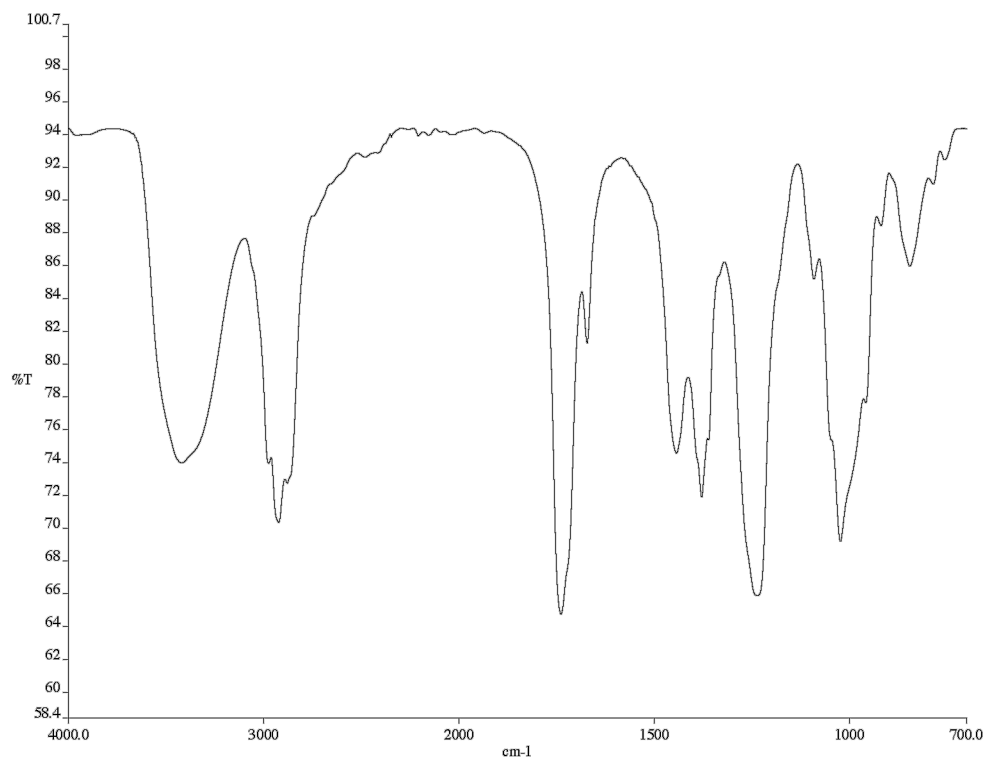


Figure A3.4.2 infrared spectrum (Thin Film, NaCl) of compound **86**.

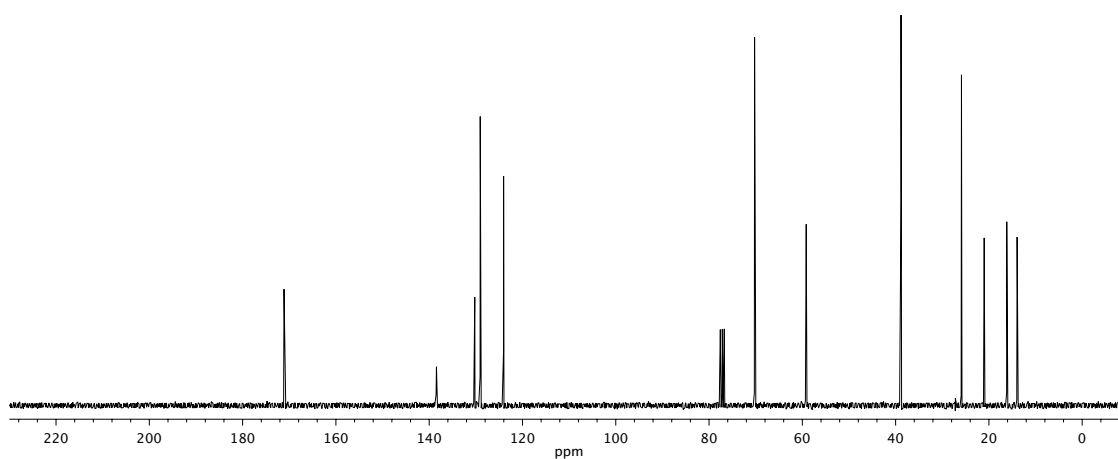
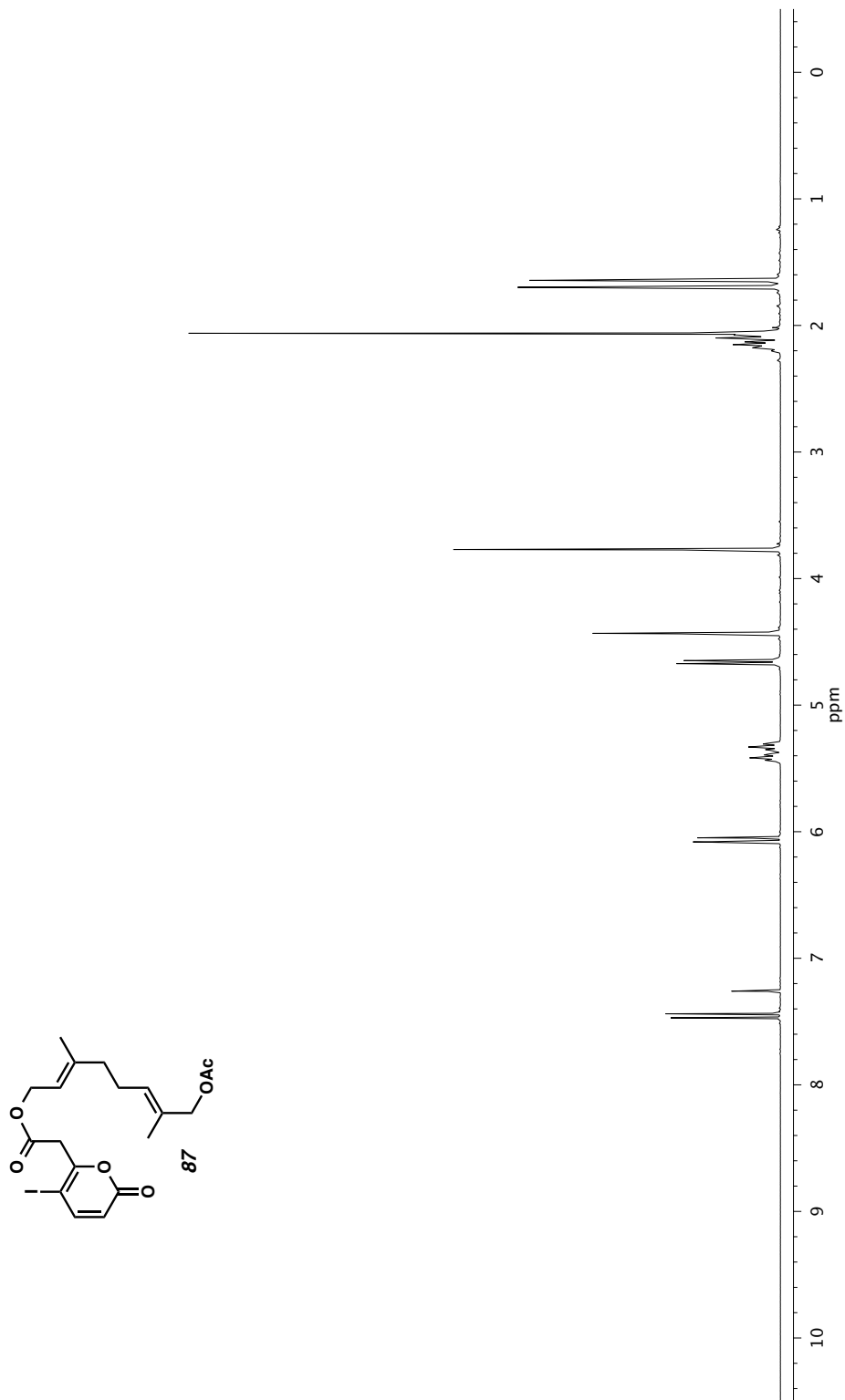


Figure A3.4.3 ^{13}C NMR (75 MHz, CDCl_3) of compound **86**.



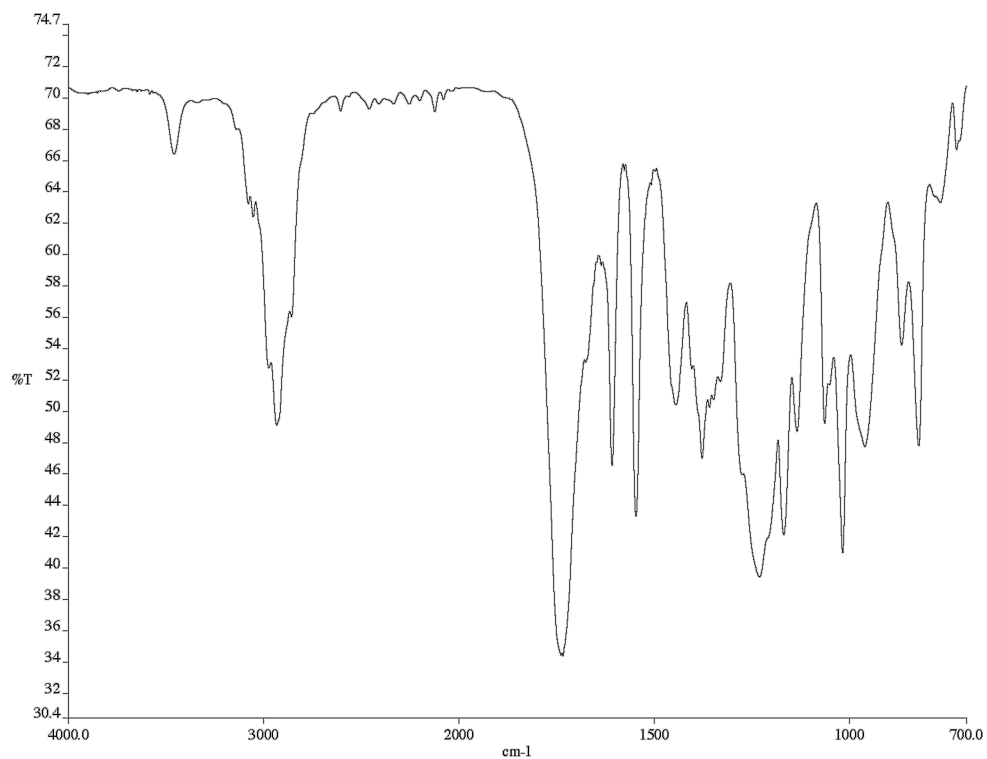


Figure A3.5.2 infrared spectrum (Thin Film, NaCl) of compound **87**.

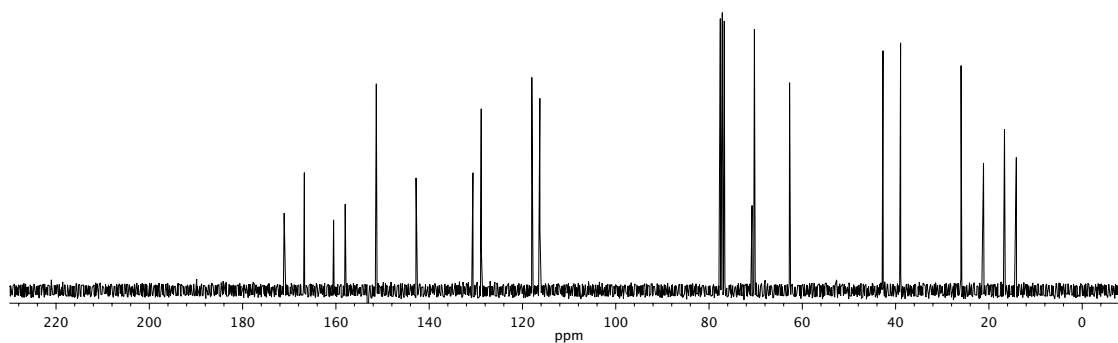


Figure A3.5.3 ^{13}C NMR (75 MHz, CDCl_3) of compound **87**.

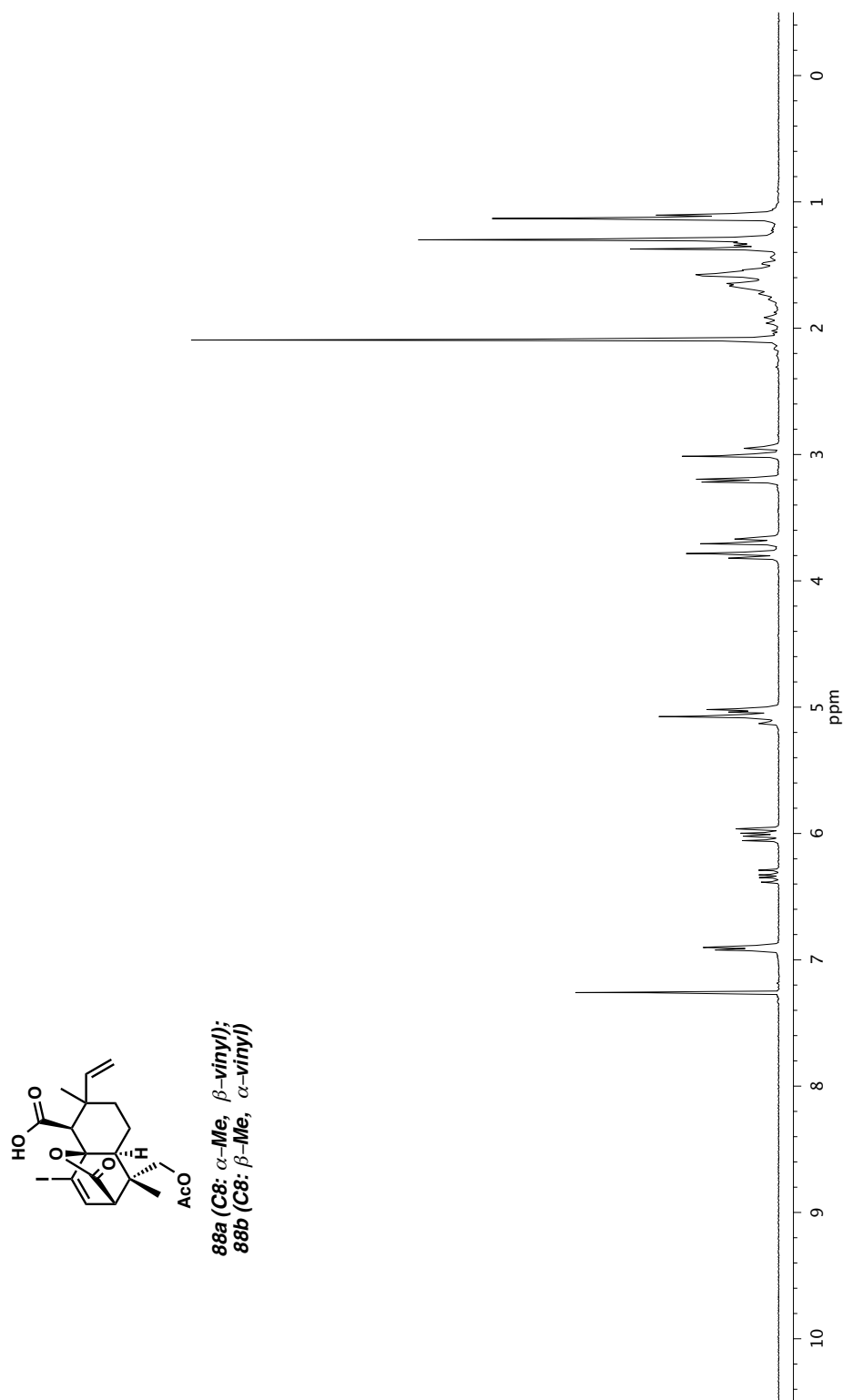


Figure A3.6.1 ¹H NMR 300 MHz, CDCl₃) of compound **88a** and **88b**.

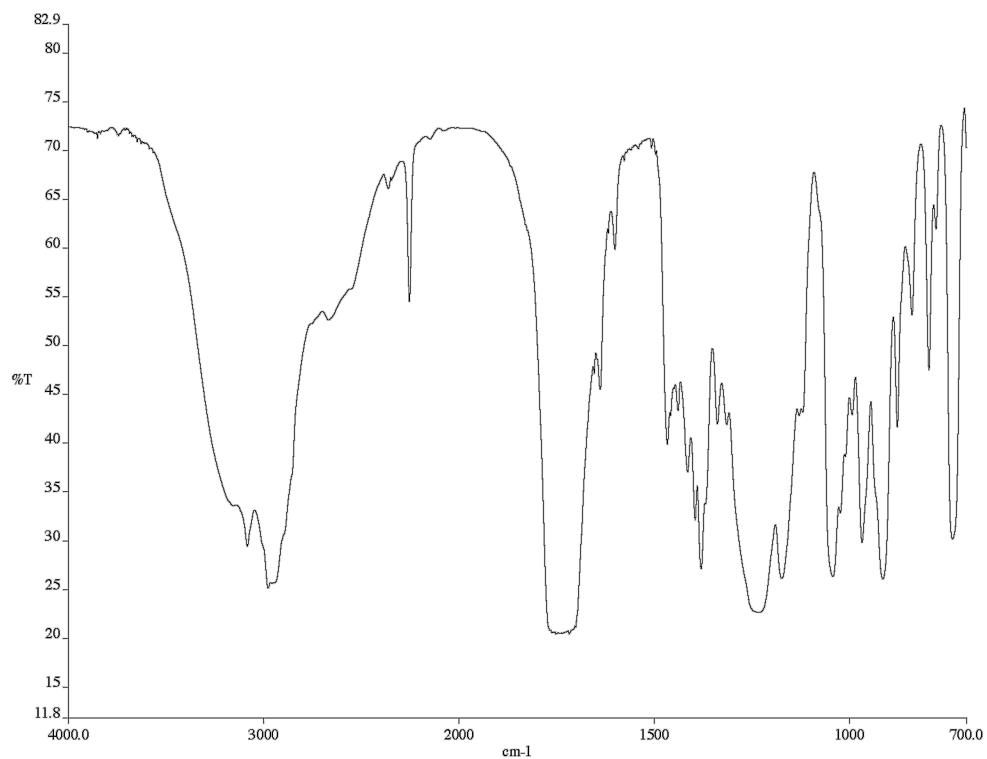


Figure A3.6.2 infrared spectrum (Thin Film, NaCl) of compound **88a** and **88b**.

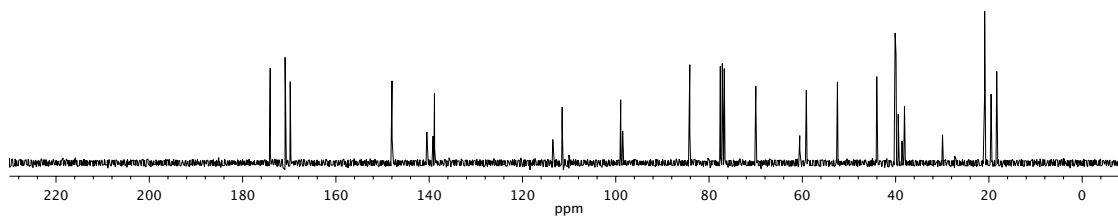


Figure A3.6.3 ¹³C NMR (75 MHz, CDCl₃) of compound **88a** and **88b**.

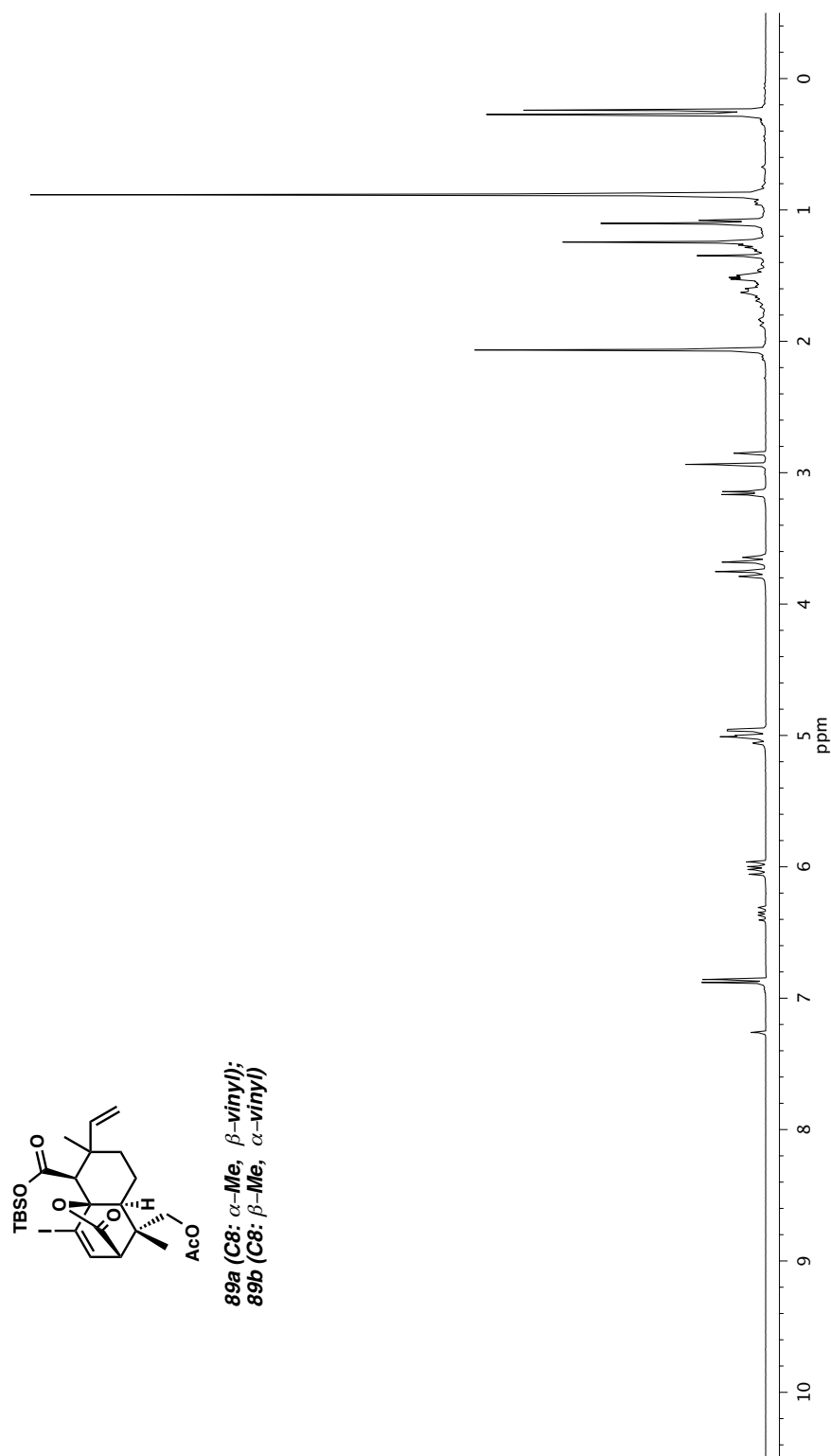


Figure A3.7.1 ¹H NMR 300 MHz, CDCl₃) of compound **89a** and **89b**.

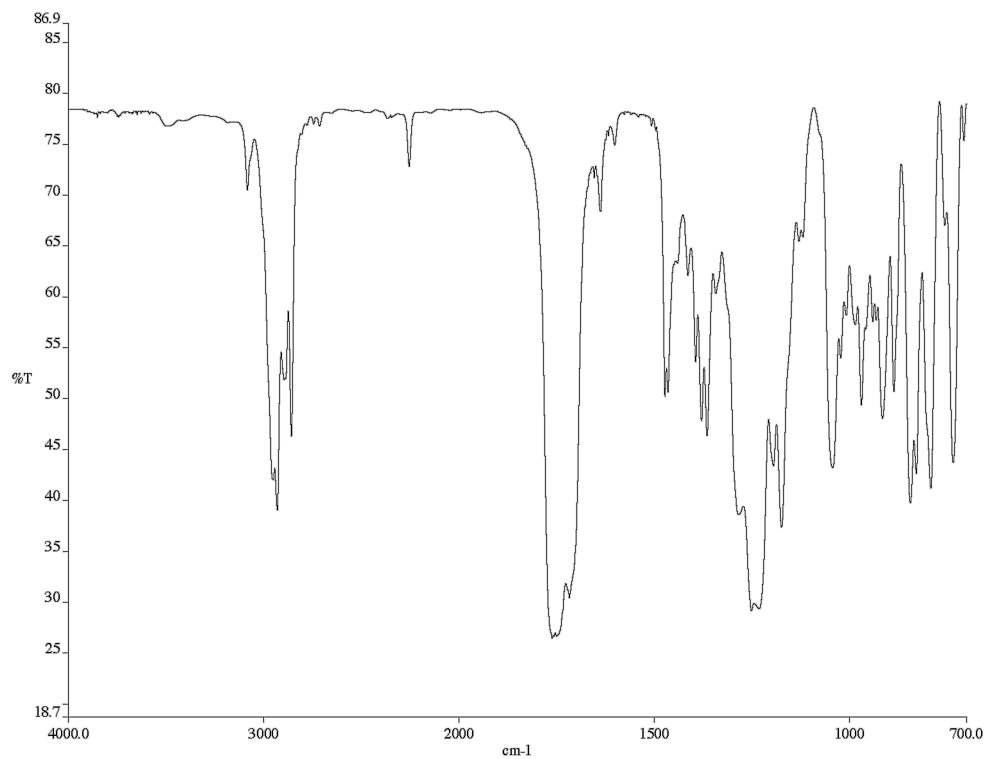


Figure A3.7.2 infrared spectrum (Thin Film, NaCl) of compound **89a** and **89b**.

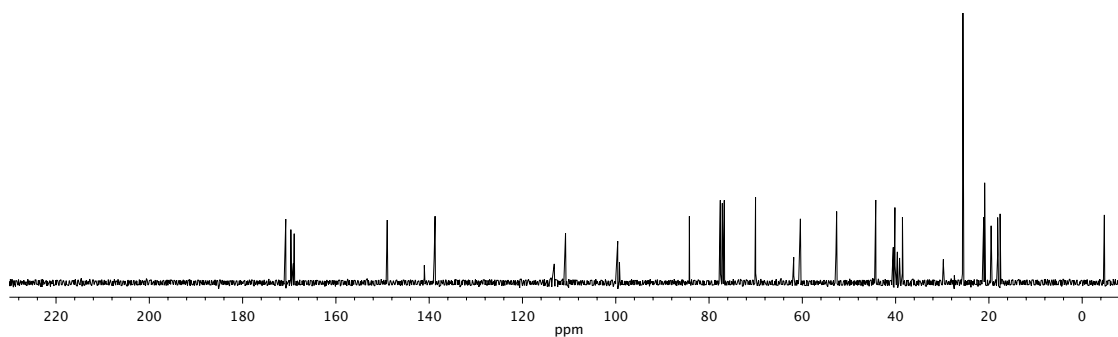
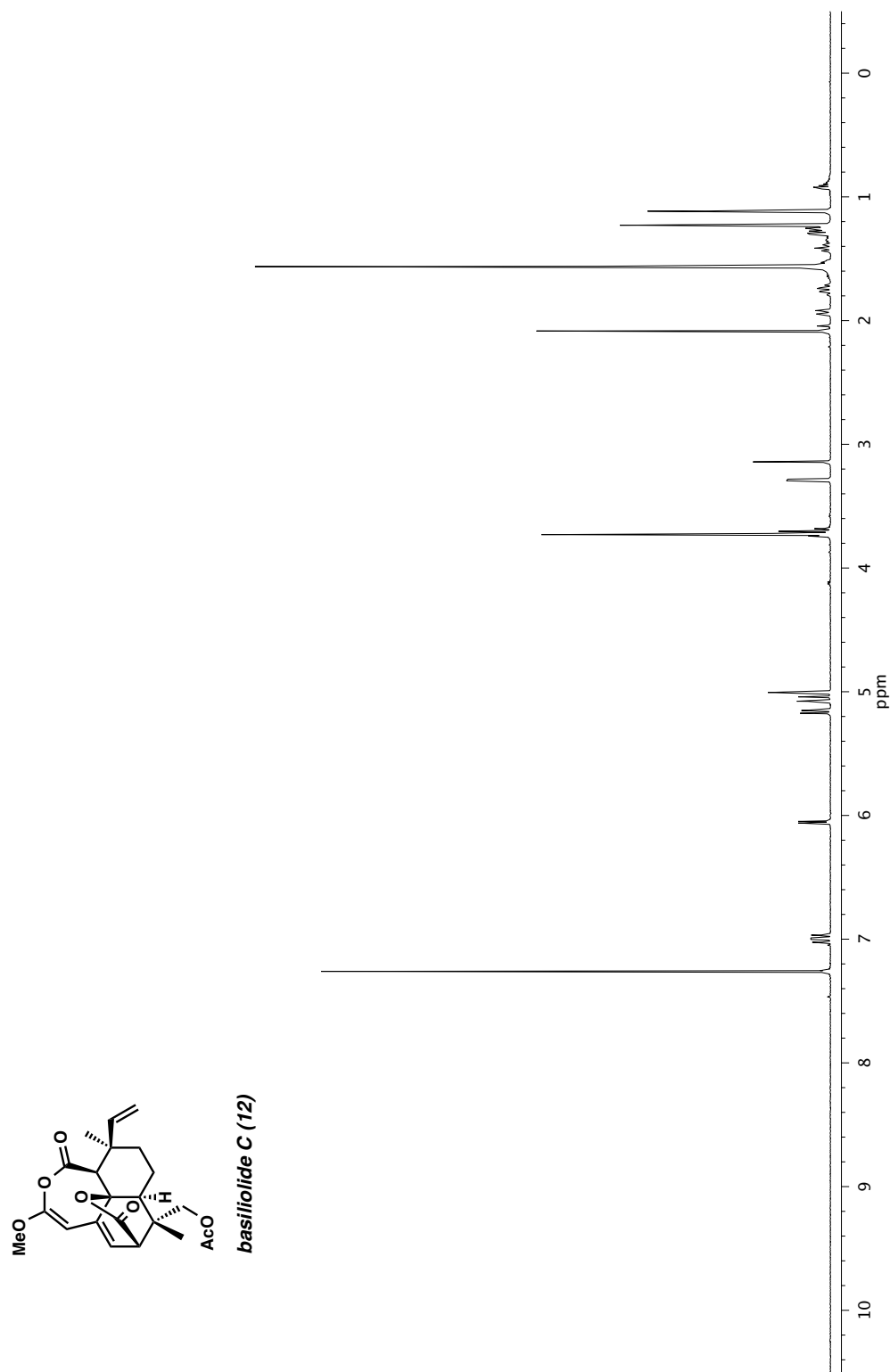


Figure A3.7.3 ¹³C NMR (75 MHz, CDCl₃) of compound **89a** and **89b**.



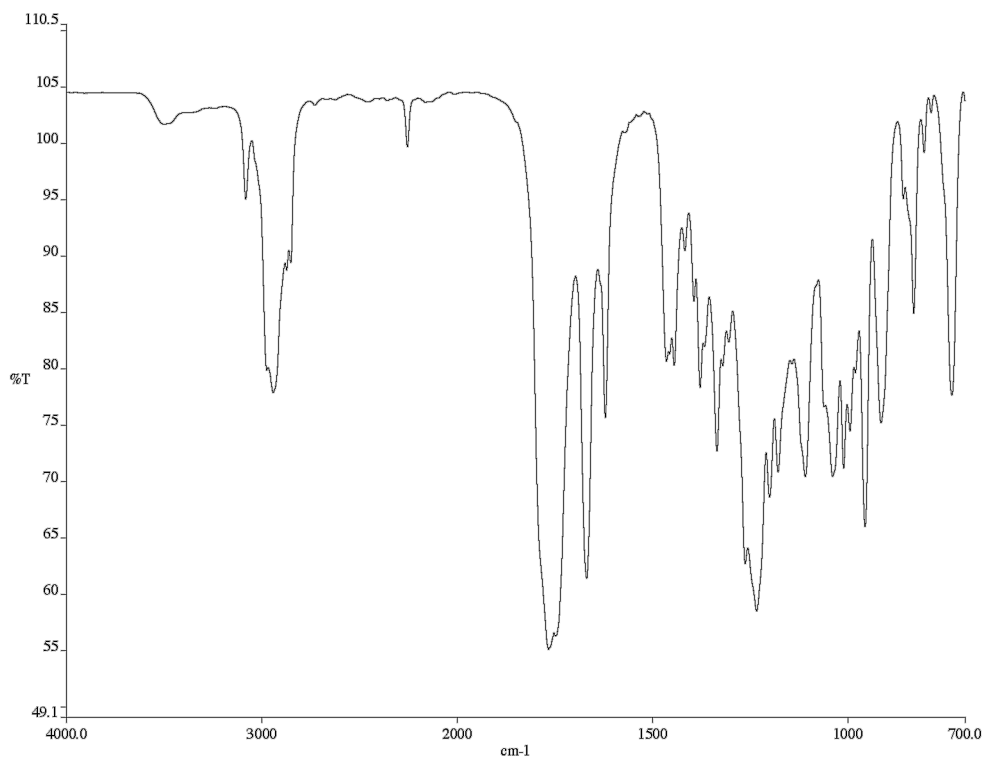


Figure A3.8.2 infrared spectrum (Thin Film, NaCl) of basiliolide C (**12**).

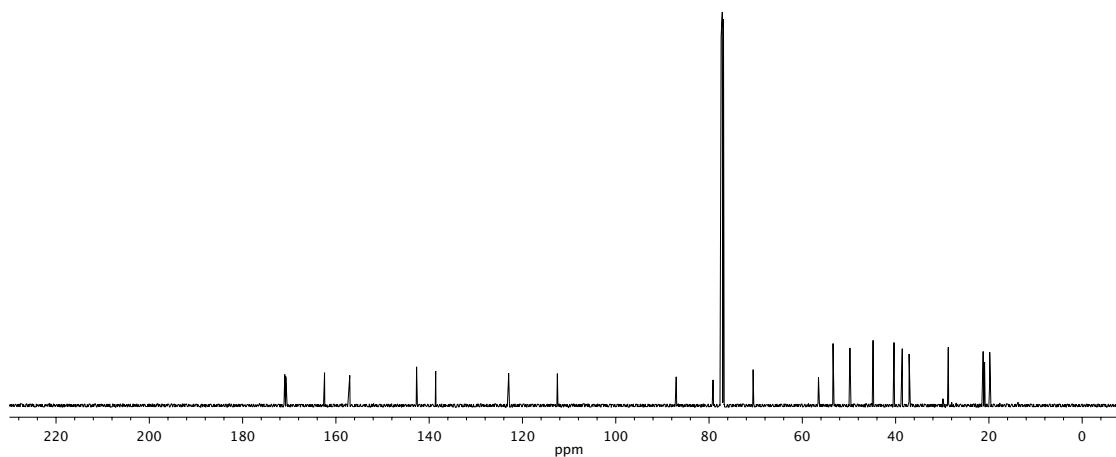


Figure A3.8.3 ^{13}C NMR (125 MHz, CDCl_3) of basiliolide C (**12**).

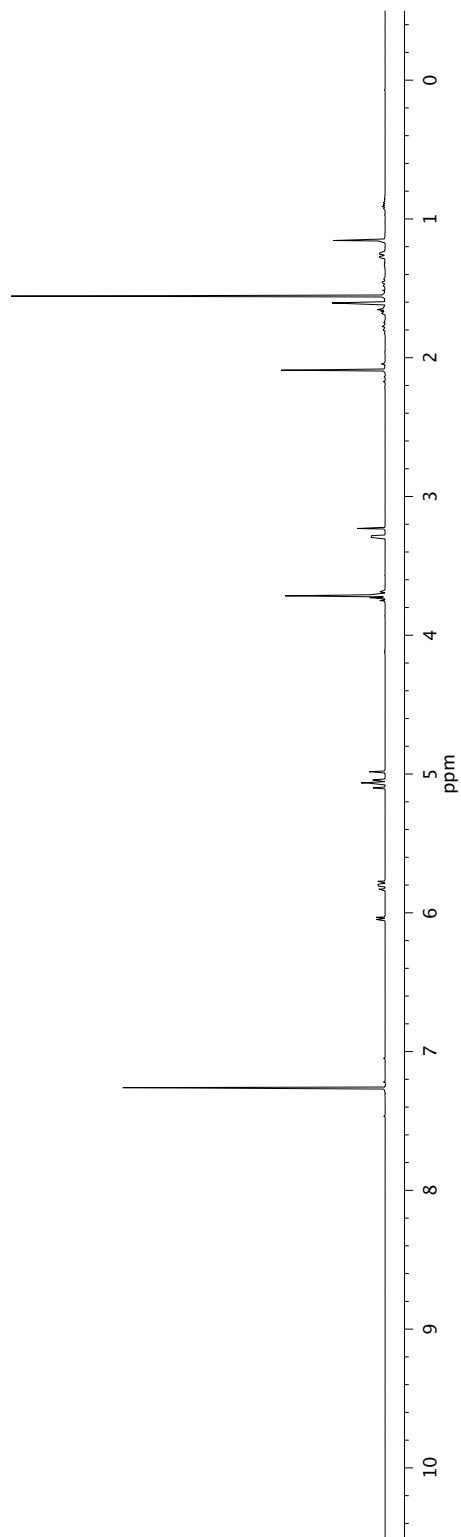
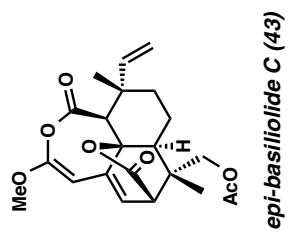


Figure A3.9.1 ¹H NMR 500 MHz, CDCl₃ of epi-basiliolide C (43).

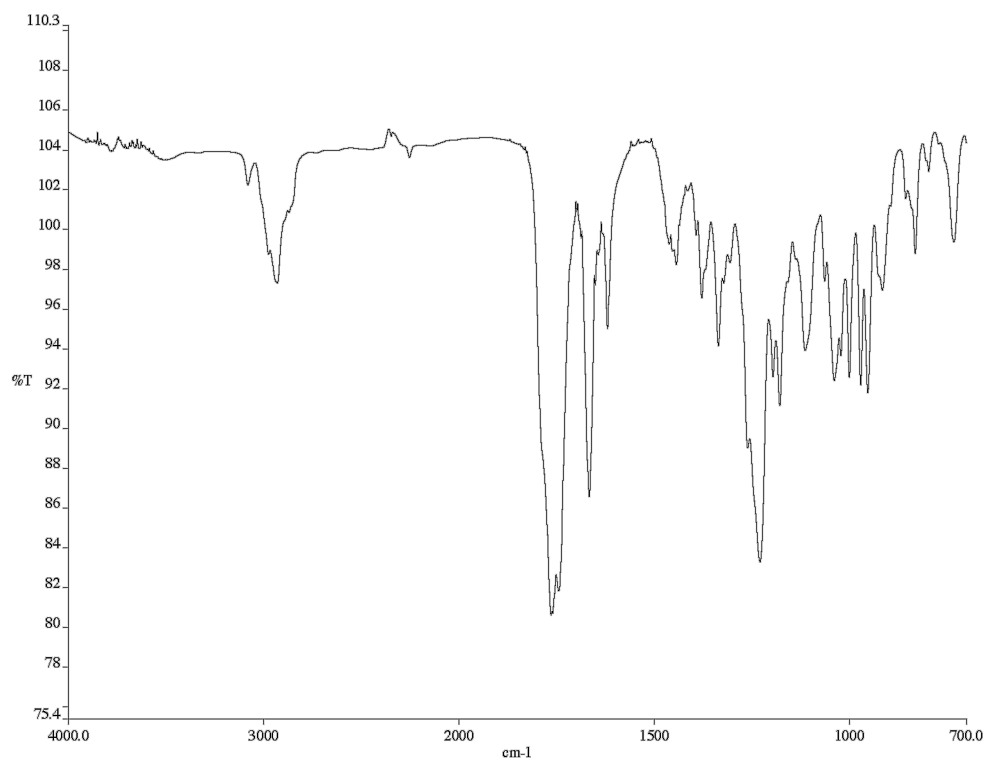


Figure A3.9.2 infrared spectrum (Thin Film, NaCl) of epi-basiliolide C (**43**).

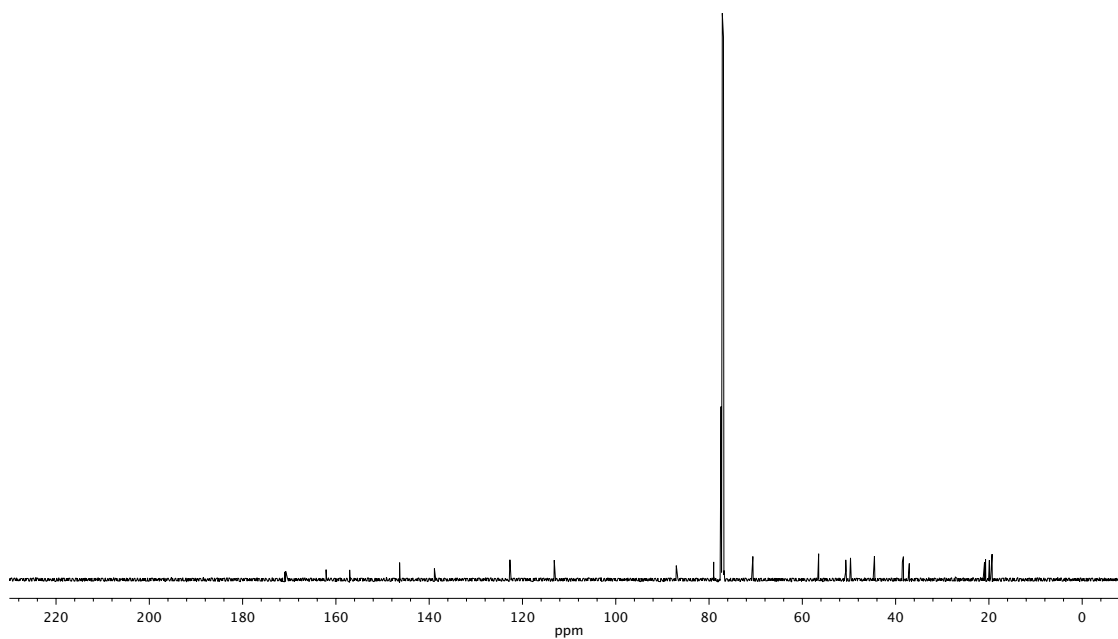


Figure A3.9.3 ¹³C NMR (125 MHz, CDCl₃) of epi-basiliolide C (**43**).

CHAPTER 2

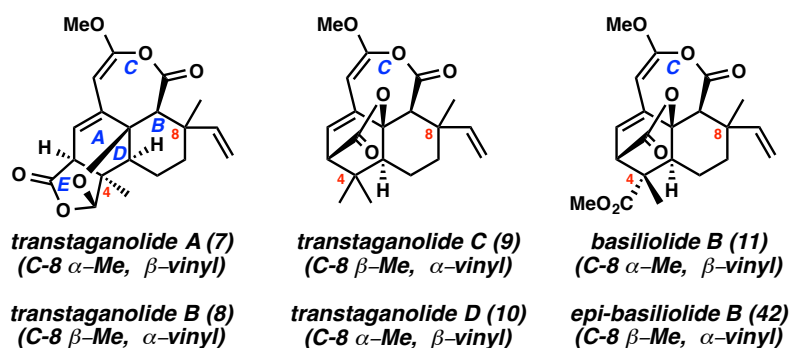
Total Syntheses of (–)-Transtaganolide A, (+)-Transtaganolide B, (+)-Transtaganolide C, and (–)-Transtaganolide D and Biosynthetic Implications

2.1 INTRODUCTION

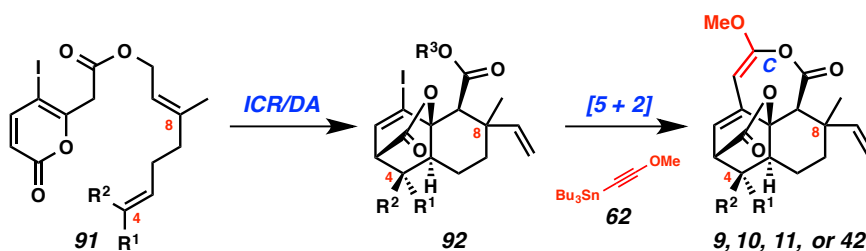
Enticed by the opportunity to prepare structurally novel and biologically relevant molecules, our group undertook extensive synthetic efforts that resulted in the development of a general strategy for the total syntheses of several transtaganolide¹ natural products (Figure 2.1.1, **9–11** and **42**).² Integral to this approach was an Ireland–Claisen rearrangement/intramolecular pyrone Diels–Alder cyclization (ICR/DA) cascade³ that furnished the stereochemically complex, tricyclic cores (**92**) in a single step from monocyclic, achiral precursors (**91**). Additionally, a formal [5+2] annulation process forged the formidable C-ring (Scheme 2.1.1).² While concise and modular, our initial approach fell short of achieving two key goals: 1) the preparation of enantioenriched products and 2) the synthesis of transtaganolides A (**7**) and B (**8**), the most complex

members of the natural product family. Transtaganolides A (**7**) and B (**8**) are unique within their class due to their lack of an oxabicyclo[2.2.2]octene structural motif (Figure 2.1.1, **7** and **8** vs. **9–11** and **42**). In its place is a fused γ -lactone (E ring, **7** and **8**), bridged by an ether linkage (D-ring) that contorts the pentacyclic core into a compact, caged structure (Figure 2.1.1 and Scheme 2.2.1, see boxed insert). Strategies to overcome these synthetic challenges are presented herein, culminating in the enantioselective total syntheses of (–)-transtaganolide A (**7**) and (+)-transtaganolide B (**8**), which previously had eluded total synthesis. Furthermore, (–)-transtaganolide C (**9**) and (+)-transtaganolide D (**10**), which were previously prepared as racemates, have now been synthesized asymmetrically. The absolute configurations of these compounds are also disclosed and discussed within the context of existing biosynthetic hypotheses.^{3b,4}

Figure 2.1.1. Transtaganolide and basiliolide natural products (**7–11** and **42**).



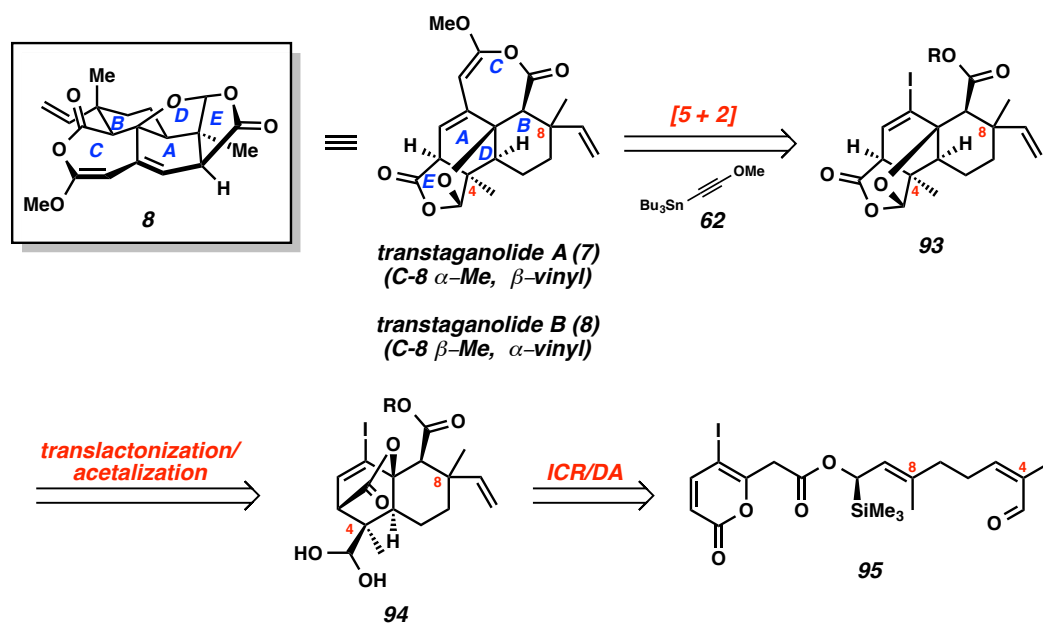
Scheme 2.1.1. General synthetic strategy.



2.2 RETROSYNTHETIC ANALYSIS

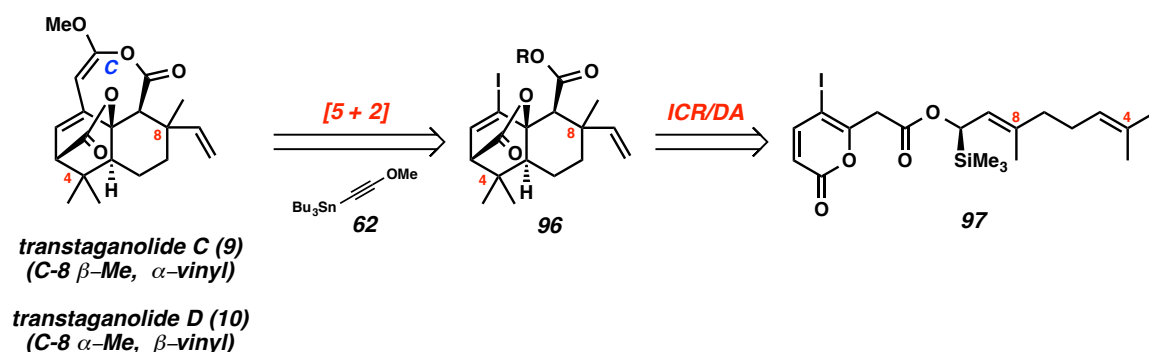
Retrosynthetically, transtaganolides A (**7**) and B (**8**) could derive from iodo tetracycle **93** by application of our [5+2] annulation strategy (Scheme 2.2.1).² We envisioned that the tetracyclic core (**93**) could in turn arise from a translactonization/acetalization reaction of aldehyde-hydrate **94**. Tricycle **94** could be derived from an enantiospecific ICR/DA cascade of monocyclic precursor **95** with the requisite aldehyde oxidation state.

Scheme 2.2.1. Retrosynthetic analysis for the asymmetric construction of transtaganolides A (**7**) and B (**8**).



In a similar fashion to that of transtaganolides A and B (**7** and **8**), enantioenriched transtaganolides C and D (**9** and **10**) could be prepared from tricycle **96**, which could derive from a pyrone ester **97** by a stereocontrolled ICR/DA cascade reaction (Scheme 2.2.2).

Scheme 2.2.2. Retrosynthetic analysis for the asymmetric construction of transtaganolides C (**9**) and D (**10**).

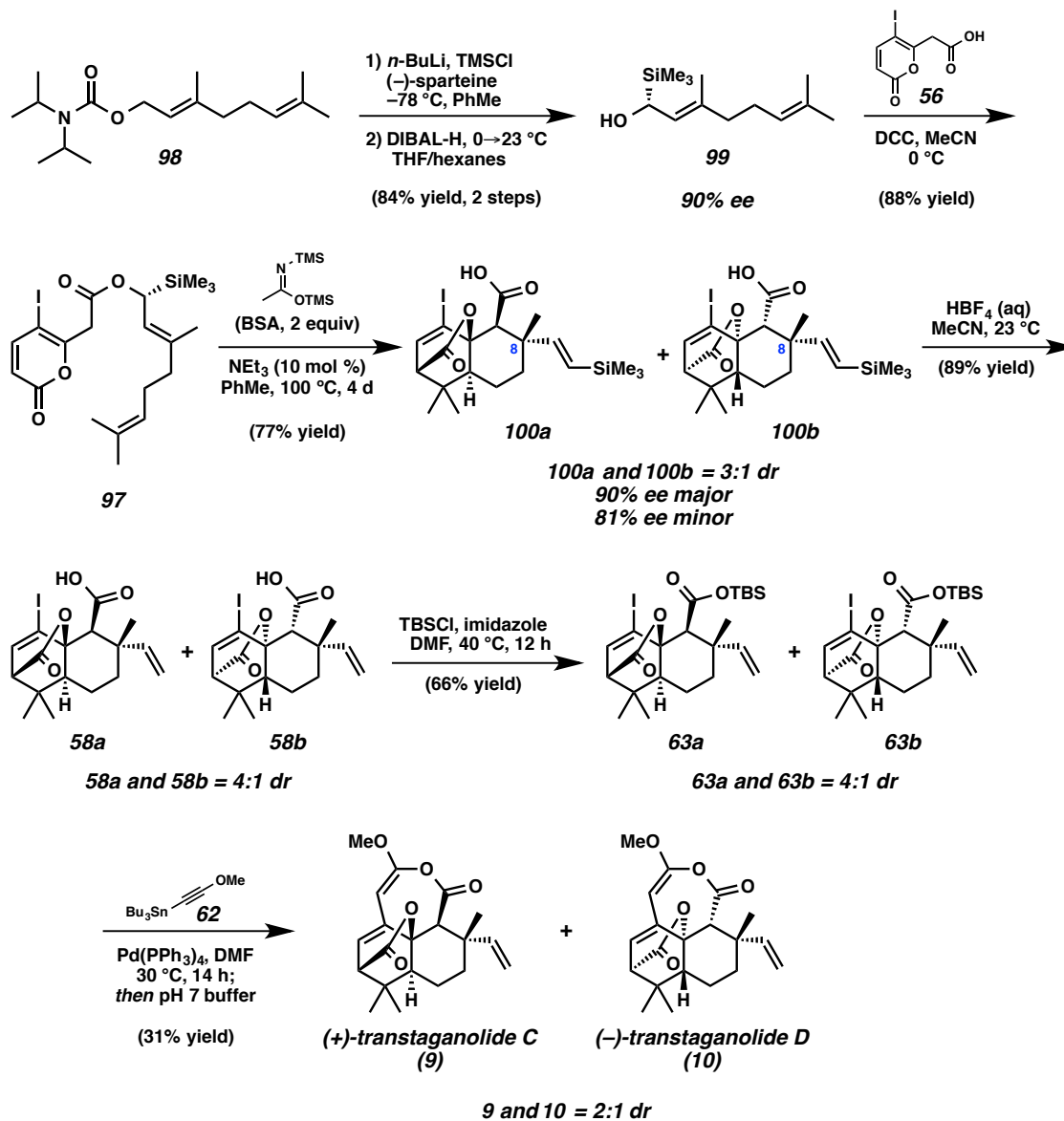


2.3 ENANTIOSELECTIVE TOTAL SYNTHESIS OF TRANSTAGANOLIDES C AND D

Our studies began with the application of this retrosynthetic analysis to transtaganolides C (**9**) and D (**10**) (Scheme 2.2.2).⁵ To impart asymmetry we turned to the early work of Ireland and co-workers.⁶ They demonstrated the efficient employment of α-acyloxy allylsilanes (e.g., **97** in Scheme 2.2.2) as chiral, primary alcohol equivalents in Ireland–Claisen rearrangements. Hoppe’s enantioenriched geraniol derivative **99** was prepared by treatment of carbamate **98** with *n*-BuLi, freshly distilled (–)-sparteine, and trimethylsilyl chloride.⁷ Subsequent reduction of the intermediate carbamate furnished enantioenriched geraniol equivalent **99** in 90% ee and 84% yield over the two steps. Coupling of alcohol **99** to pyrone acid **56** provided the desired cascade substrate **97** in 88% yield. Gratifyingly, exposure of pyrone ester **97** to our ICR/DA cascade conditions afforded diastereomeric vinyl silanes **100a** and **100b** in 77% overall yield and 90% ee and 81% ee, respectively. We were pleased to find that subsequent exposure of the vinyl silanes **100a** and **100b** to aqueous HBF₄ yielded a mixture of tricycles **58a** and **58b**. Protection of the free acids (**58a** and **58b**) as the silyl esters **63a** and **63b** followed by

treatment with stannane **62** and Pd(PPh₃)₄ yielded (+)-transtaganolide C (**9**) and (–)-transtaganolide D (**10**).

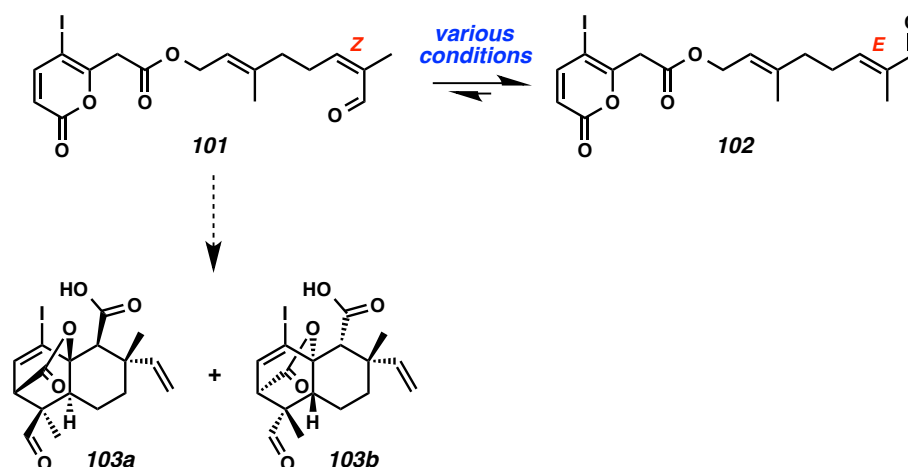
Scheme 2.3.1. Enantioselective total syntheses of transtaganolides C and D (**9** and **10**).



2.4 SYNTHETIC STRATEGIES FOR THE TOTAL SYNTHESSES OF TRANSTAGANOLIDES A AND B

Having established the feasibility of the chiral geraniol derivative approach to setting the critical absolute stereochemistry in this series of natural products, we sought to prepare the transtaganolide A (**7**) and B (**8**) novel frameworks. The most apparent path to this goal relies on the utilization of a chiral (*Z*)-enal such as **101** in our ICR/DA cyclization cascade to produce aldehydes **103a** and **103b**, which are predisposed by proximity to undergo the desired ring-chain tautomerism upon hydration (Scheme 2.4.1). However, we found that (*Z*)-enal **101** was challenging to prepare and configurationally unstable under myriad reaction conditions.⁸

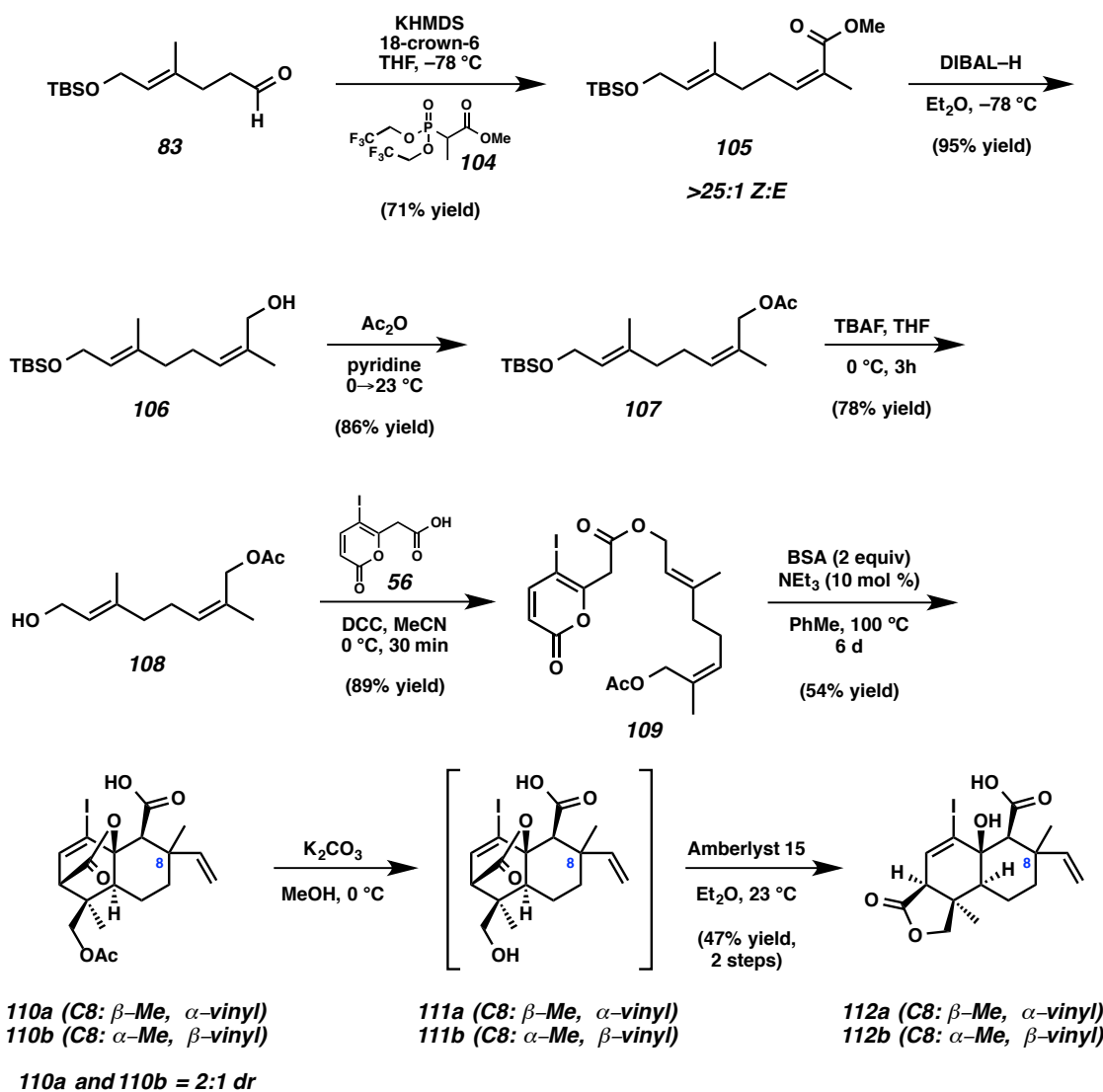
Scheme 2.4.1. Initial attempts at preparing the tricyclic cores of transtaganolides A and B (**103a** and **103b**).



Prompted by these experimental cues, our efforts were refocused on preparing a more stable aldehyde surrogate. Initial studies focused on preparing protected alcohol **109**, which could be oxidized to the aldehyde following the ICR/DA cascade (Scheme 2.4.2). The forward synthesis began with the Still–Gennari modification of the Horner–

Wadsworth–Emmons reaction of known γ,δ -unsaturated aldehyde **83**⁹ to form (Z)-methyleneate **105** in 71% yield and excellent diastereoselectivity.¹⁰ DIBAL reduction of methyleneate **105** proceeded at –78 °C in 95% yield. Acetate protection of alcohol **106** followed by TBS deprotection furnished alcohol **108** in 67% yield over the two steps. Finally, coupling of alcohol **108** to iodo-acid **56** gave ICR/DA cascade substrate **109** in 89% yield. Upon submitting pyrone **109** to our standard ICR/DA cascade conditions formed tricycles **110a** and **110b** in a combined 54% yield and 2:1 dr, respectively. Cleavage of the acetate protecting group gave a mixture of alcohols **111a** and **111b** along with the translactonized products **112a** and **112b**. For the purposes of characterization, the crude mixture could be stirred with Amberlyst 15 in Et₂O to give solely the translactonized products **112a** and **112b** in 47% yield over the two steps. Unfortunately all attempts to oxidize either alcohols **111a** and **111b** or the translactonized products **112a** and **112b** proved fruitless and therefore we required a different approach to the transtaganolide A and B (**7** and **8**) natural product syntheses.

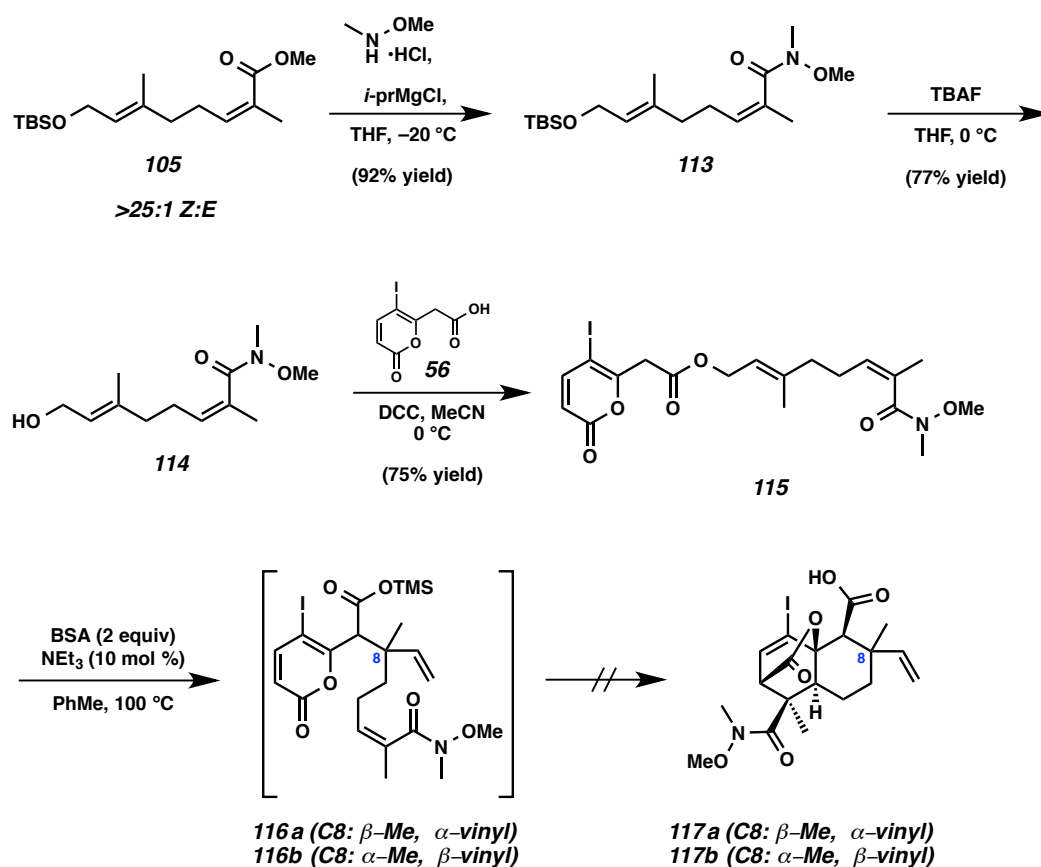
Scheme 2.4.2. Studies for the transtaganolide A and B (**7** and **8**) tetracyclic core via protected alcohol **109**.



As we were not able to oxidize the alcohol to the appropriate aldehyde, we decided it better to attempt the ICR/DA on a more highly oxidized substrate, which would require a reduction to achieve the desired aldehyde oxidation state. Therefore we targeted the synthesis of pyrone **115** with Weinreb amide functionality for the ICR/DA cascade and subsequent single hydride reduction (Scheme 2.4.3). The synthesis began with (Z)-methyleneoate **105**, which was readily converted to Weinreb amide **113** in 92% yield and

with no loss of diastereoselectivity. Subsequent TBAF deprotection of the TBS protecting group formed alcohol **114** in 77% yield. Lastly, coupling to iodo-acid **56** formed the desired ICR/DA substrate **115** in 75% yield. Unfortunately, pyrone **115** did not successfully undergo the ICR/DA cascade. For pyrone **115**, the Ireland–Claisen rearrangement proceeded smoothly, forming silylesters **116a** and **116b**, but under the reaction conditions, even after one month of heating, no appreciable Diels–Alder product **117a** and **117b** could be observed.

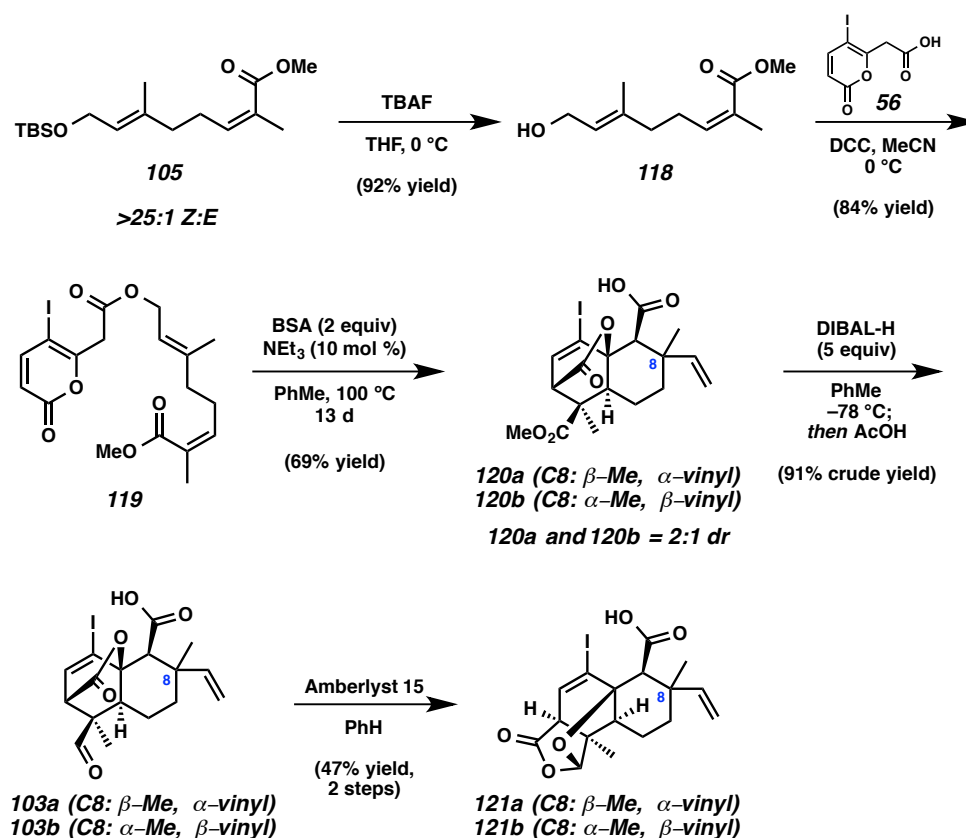
Scheme 2.4.3. Studies for the transtaganolide A and B (**7** and **8**) tetracyclic core via Weinreb amide **115**.



Since the Weinreb amide bearing pyrone **117** was not a viable substrate for our ICR/DA cascade, we decided to attempt the ICR/DA with ester **119** and envisioned a

single hydride reduction to the aldehyde (Scheme 2.4.4). Once again, the forward synthesis began with (*Z*)-methyl enoate **105**. Deprotection to form alcohol **118** proceeded in 92% yield and subsequent coupling to iodo-acid **56** furnished the ICR/DA substrate **119** in 84% yield. Submission of pyrone **119** to our standard ICR/DA cascade conditions for 13 days furnished tricycles **120a** and **120b** in a combined 69% yield and a 2:1 mixture of diastereomers, respectively. To our delight, single hydride reduction of tricycles **120a** and **120b** was accomplished at low temperature with DIBAL. The crude aldehyde products **103a** and **103b** then underwent the desired translactonization event with an appropriate acid catalyst (i.e., Amberlyst 15) to form the transtaganolide A and B tetracyclic cores **121a** and **121b** in 47% yield over the two steps. Having been able to successfully synthesize the transtaganolide A and B tetracyclic cores **121a** and **121b**, we turned our attentions toward accomplishing this feat asymmetrically.

Scheme 2.4.4. Studies for the transtaganolide A and B (**7** and **8**) tetracyclic core via methylester **119**.

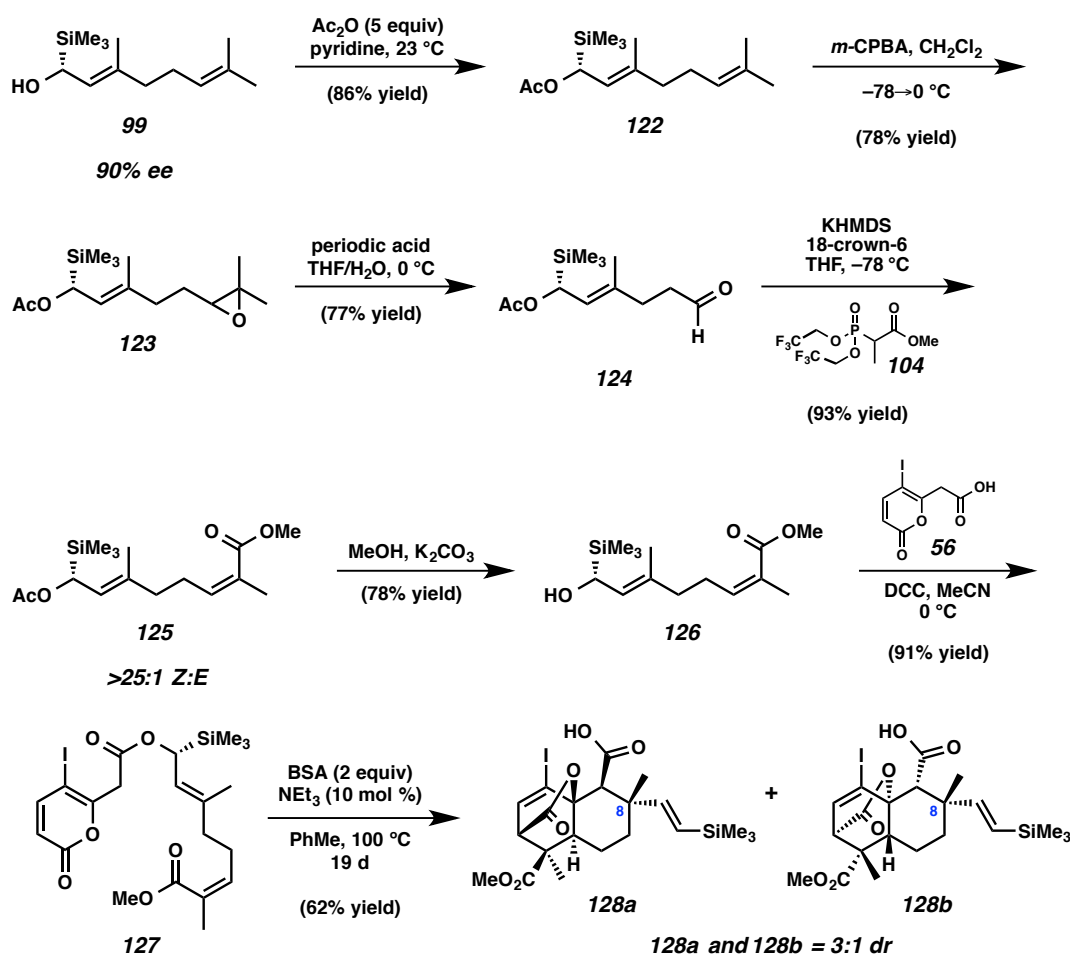


2.5 ENANTIOSELECTIVE TOTAL SYNTHESIS OF TRANSTAGANOLIDES A AND B

Enantioselective synthesis of transtaganolides A and B (**7** and **8**) could be accomplished utilizing enantioenriched geraniol derivative **99**, as was done for enantioselective total synthesis of transtaganolides C and D (**9** and **10**). To this end, enantioenriched geraniol derivative **99** was protected as the acetate ester **122** in 86% yield (Scheme 2.5.1).¹¹ Selective epoxidation with *m*-CPBA afforded epoxide **123** in 78% yield. Subsequent oxidative cleavage of epoxide **123** with aqueous periodic acid provided aldehyde **124** in good yield.¹² Utilization of the Still–Gennari modification of

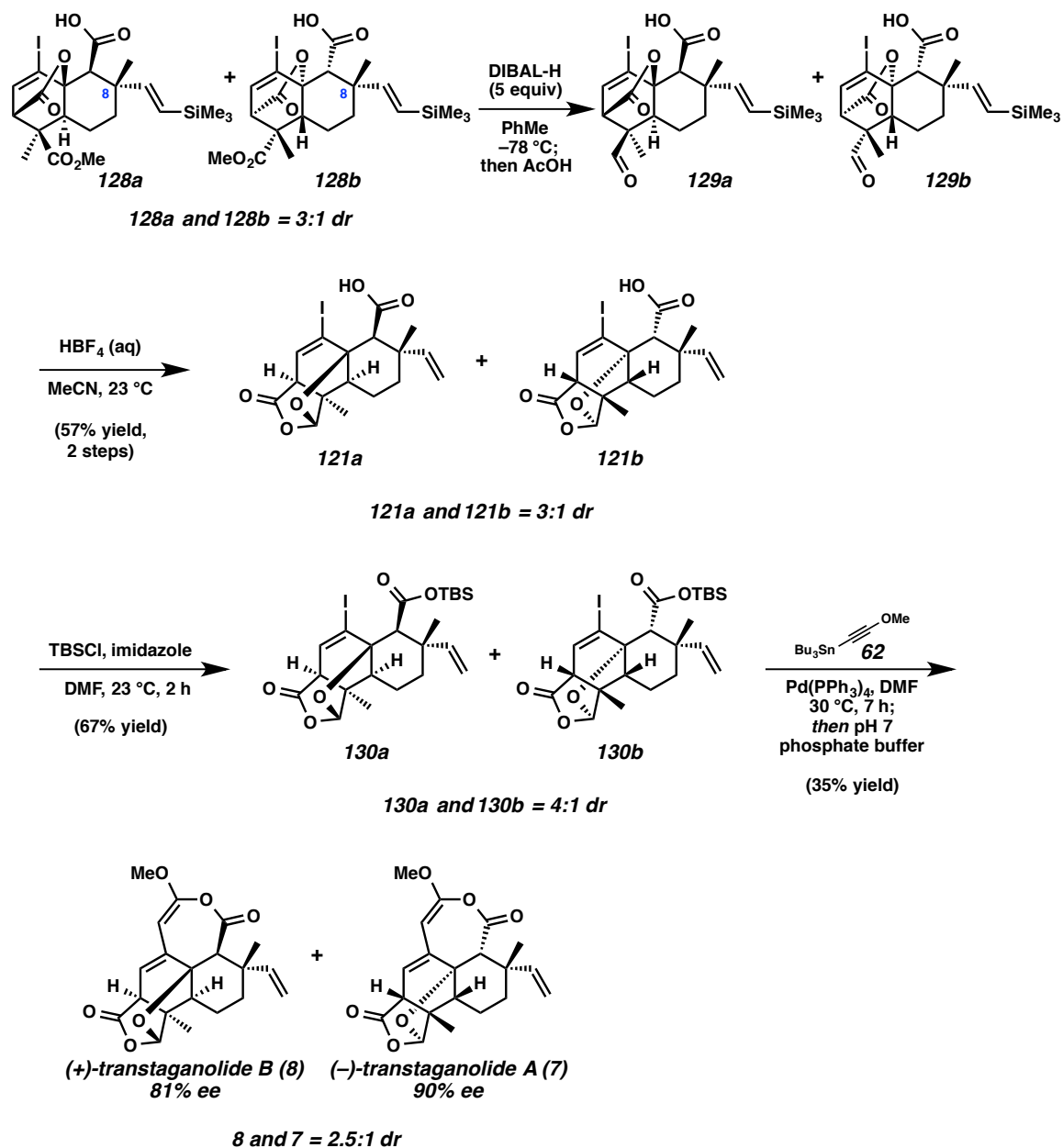
the Horner–Wadsworth–Emmons reaction allowed for formation of (*Z*)-methyleneate **125** in 93% yield and excellent *Z*:*E* selectivity.¹⁰ Acetate deprotection of (*Z*)-methyleneate **125** afforded alcohol **126** in 78% yield. Efficient coupling of alcohol **126** to acid **56** yielded the ICR/DA cascade substrate, pyrone ester **127**. Gratifyingly, prolonged heating of ester **127** in toluene with *N,O*-bis(trimethylsilyl)acetamide (BSA) in the presence of a catalytic amount of triethylamine afforded diastereomeric tricycles **128a** and **128b** in a combined 62% yield and as a 3:1 mixture of C8 diastereomers, respectively.

Scheme 2.5.1. Syntheses of enantioenriched tricyclic cores of transtaganolides A and B (**128a** and **128b**).



Remarkably, brief exposure of acids **128a** and **128b** to an excess of DIBAL-H at low temperature followed by careful quenching with acetic acid resulted in smooth, chemoselective ester reduction to furnish corresponding aldehydes **129a** and **129b** (Scheme 2.5.2). Upon exposure of the crude aldehydes **129a** and **129b** to aqueous HBF_4 , the desired translactonization/acetalization proceeded and proteodesilylation occurred in one pot to yield caged tetracycles **121a** and **121b**. Transient protection of the free acids (**121a** and **121b**) as the TBS-esters (**130a** and **130b**) in 67% yield, followed by application of our [5+2] annulation technology, allowed for the enantioselective syntheses of (+)-transtaganolide B (**8**) and (–)-transtaganolide A (**7**) in 35% combined yield and good optical purity.

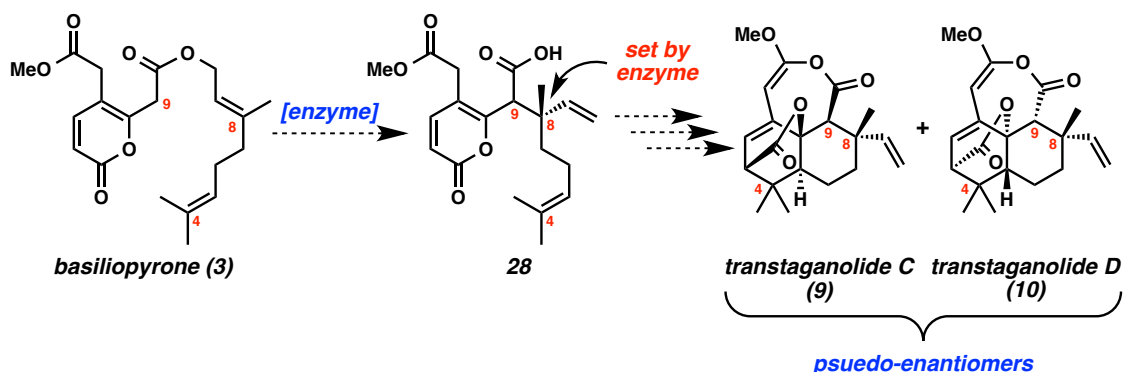
Scheme 2.5.2. Enantioselective total syntheses of transtaganolides A and B (7 and 8).



2.6 BIOSYNTHETIC IMPLICATIONS AND STEREOCHEMICAL ANALYSIS OF THE ENANTIOSELECTIVE TOTAL SYNTHESIS OF TRANSTAGANOLIDES C AND D

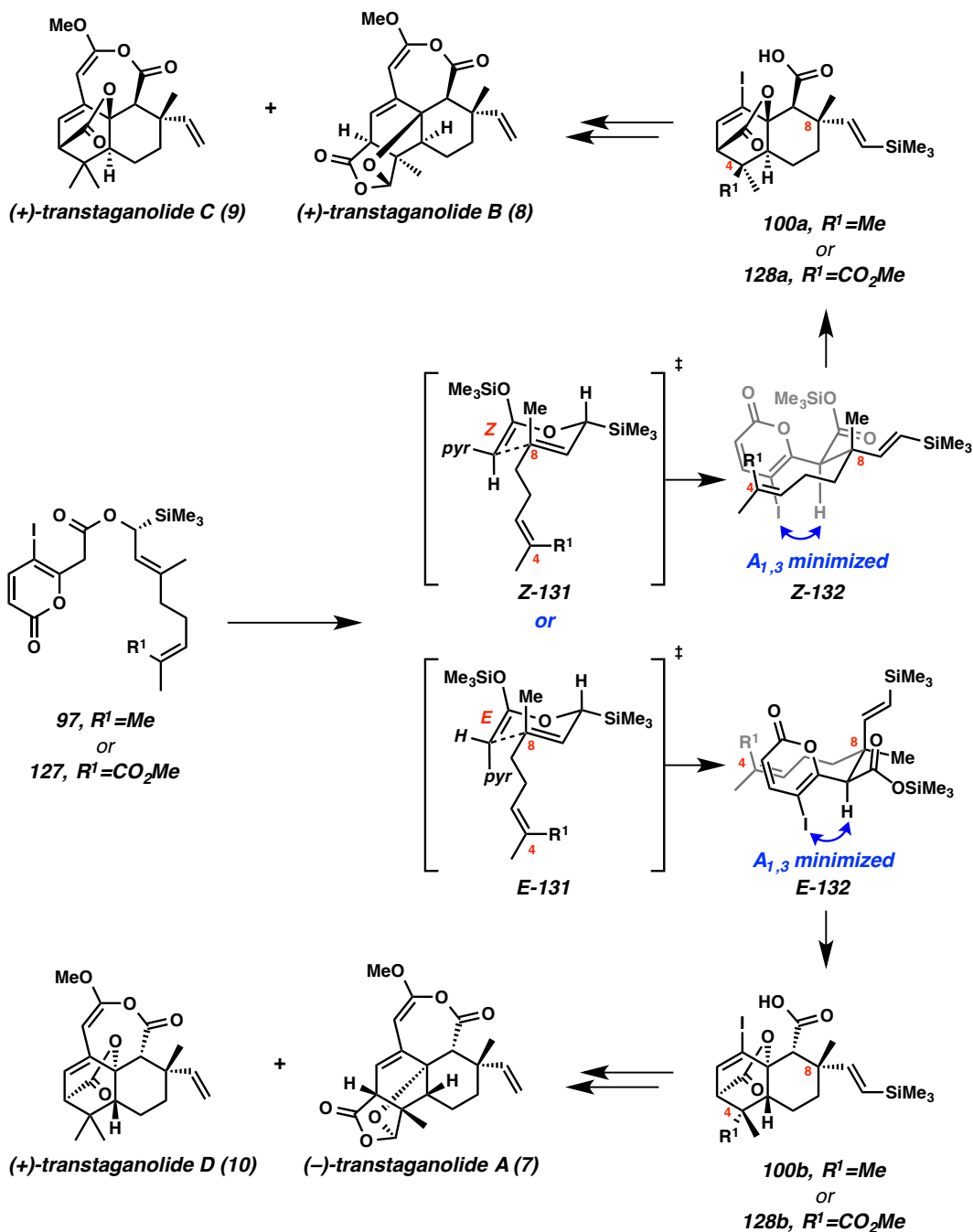
Recently, Johansson and co-workers have proposed that co-isolated basiliopyrone **3** is the direct biosynthetic precursor of transtaganolides C (**9**) and D (**10**) (Scheme 2.6.1).^{3b, 4} They suggest that a rare naturally-occurring ester-enolate-Claisen rearrangement is responsible for the production of optically-pure transtaganolides. Enzymatically controlled Claisen processes are particularly uncommon, but are known, as in Chorismate mutase.¹³ Under this scenario, and assuming that the C9 proton is relatively acidic due to the withdrawing nature of the pyrone, it could be anticipated that an enzymatic and presumably enantioselective¹⁴ rearrangement would produce optically pure C9 diastereomers **28** (with absolute stereocontrol at C8), while a non-enzymatically governed process would likely result in a racemic mixture of C9 diastereomers. The demonstrated propensity of these systems to undergo diastereoselective Diels–Alder rearrangements under allylic strain control¹⁵ would lead to pseudo-enantiomeric transtaganolides C (**9**) and D (**10**). Having prepared enantioenriched transtaganolides A–D (**7–10**) via an analogous, synthetic enantioselective Ireland–Claisen rearrangement, we believe that determination of the absolute stereochemistries of the synthetic transtaganolides could provide insight into this biosynthetic hypothesis.

Scheme 2.6.1. Johansson's biosynthetic proposal.



Hoppe has previously established the absolute stereochemistry of geraniol derivatives such as **99** prepared by (–)-sparteine mediated deprotonation as the (*R*)-enantiomer (Scheme 2.6.2).⁷ As acyclic Ireland-Claisen rearrangements prefer chair transition states, we postulated that the Ireland–Claisen rearrangement of esters **97** and **127** could proceed through two ketene-acetal geometry dependent pathways (Scheme 2.6.2, *Z*-**131** and *E*-**131**).¹⁶ Furthermore, transformations analogous to the ensuing Diels–Alder cyclization are known to proceed through allylic ($A_{1,3}$) strain minimized geometries such as *Z*-**132** and *E*-**132**.¹⁴ These proposed reaction pathways result in the formation of diastereomeric intermediates **100a/128a** and **100b/128b**.

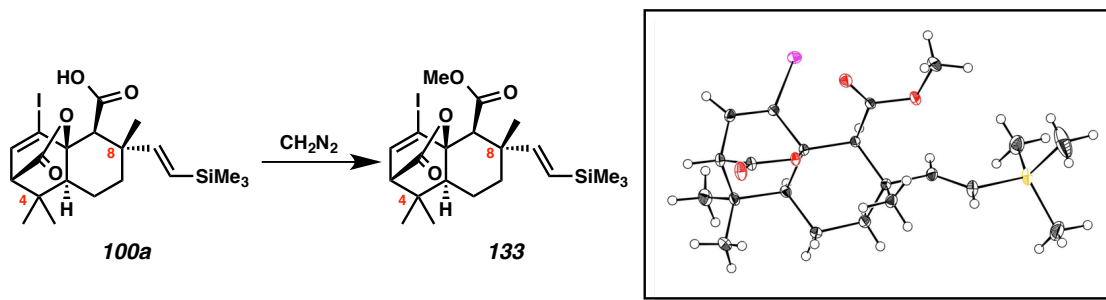
Scheme 2.6.2. Analysis of chiral silane directed ICR/DA cascade (where pyr = iodo pyrone).



Acid **100a** was converted to the corresponding methyl ester (**133**) by treatment with diazomethane, and anomalous dispersion analysis of a single crystal confirmed the hypothesized stereochemistry of **133** (Scheme 2.6.3).¹⁷ As **100a** was advanced to (+)-

transtaganolide C, we unambiguously assign its absolute structure as **9** (Scheme 2.3.1). Furthermore, by analogy we assigned (–)-transtaganolide D as **10** (Scheme 2.3.1), (–)-transtaganolide A as **7**, and (+)-transtaganolide B as **8** (Scheme 2.5.2).

Scheme 2.6.3. Determination of the absolute stereochemistry of intermediate **100a**.



The optical rotations obtained from synthetic and natural transtaganolides A–D (**7–10**) are depicted in Table 2.6.1.^{1, 18} Interestingly, the synthetic transtaganolides uniformly rotate plane polarized light to a much greater extent than their naturally occurring counterparts.¹⁹ As demonstrated by our synthetic efforts, the Ireland–Claisen/Diels–Alder cascade of prenylated pyrones similar to basiliopyrone (**3**) is a facile process: the metabolites may be biosynthetically derived from basiliopyrone (**3**), but without action of an enzymatic Claisen rearrangement.

Table 2.6.1. Comparison of the optical rotations of synthetic and natural transtaganolides A–D (**7–10**).

	transtaganolide A (7)	transtaganolide B (8)	transtaganolide C (9)	transtaganolide D (10)
synthetic	–98.8 (90% ee)	+207.9 (81% ee)	+120.7 (96% ee) ^[a]	–51.6 (92% ee) ^[a]
natural	–44.8	–25.8	–10.0	–14.2

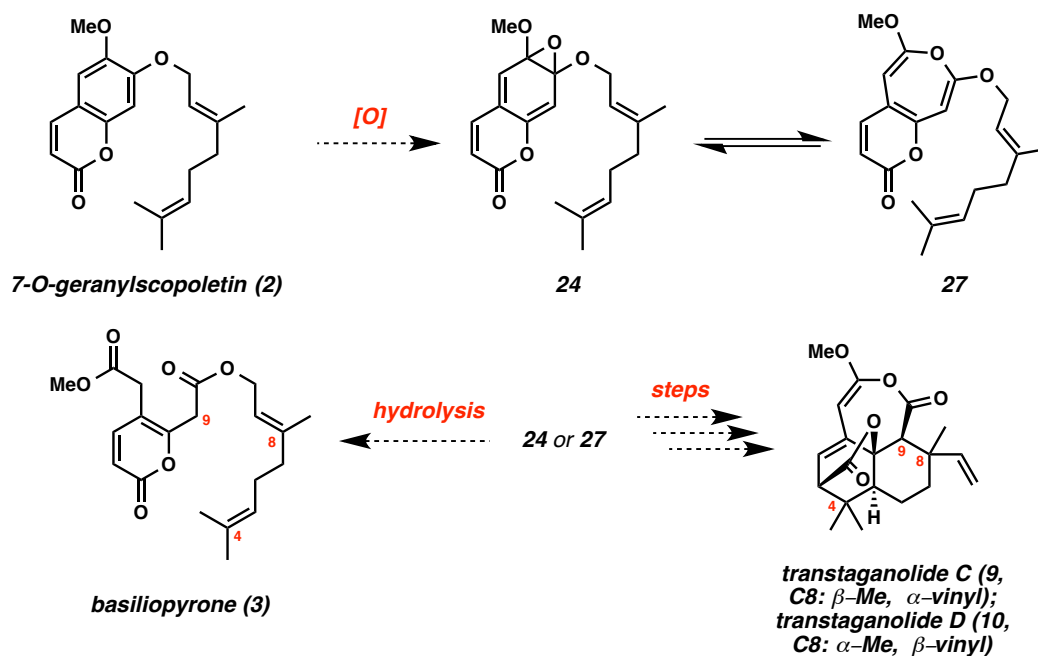
[a] For the purposes polarimetric analysis intermediate **97** was enriched to enantiopurity by chiral phase chromatography.

Furthermore, while the naturally occurring C8 diastereomeric pairs (e.g., transtaganolides C (**9**) and D (**10**)) rotate plane-polarized light with the same sign, the

samples derived from a synthetic, enantioselective Ireland–Claisen rearrangement rotate light with opposite sign (Table 2.6.1). This data does not support the action of an enzymatic enolate-Claisen rearrangement, as metabolites resulting from this pathway would likely have analogous rotations to the synthetic transtaganolides (Scheme 2.6.1).

Comparison of the natural compounds to the synthetic counterparts by chiral phase chromatography is needed before conclusions about the stereochemistry and enantiopurity of this series of natural products can be drawn.²⁰ Unfortunately, it appears that there are no available samples of natural **7–10** for thorough comparison. At this juncture, however, our optical data strongly suggest that basiliopyrone (**3**) is not a Claisenase substrate in the biosynthesis of transtaganolides C and D (**9** and **10**). As previously proposed by Massanet and co-workers, basiliopyrone (**3**) can instead be viewed as a decomposition product of epoxide **24** or oxepine **27**, which can be derived from co-isolated 7-*O*-geranylscopoletin (**2**) by oxidation (Scheme 2.6.4).⁴ Furthermore, these high energy intermediates (**24** and **27**) could undergo a series of non-enzymatic, pericyclic transformations to produce the natural products.

Scheme 2.6.4. Proposed biosynthesis of basiliopyrone (**3**).



2.7 CONCLUSION

In conclusion, enantioenriched transtaganolides A–D (**7–10**) have been prepared by Ireland–Claisen/Diels–Alder cascade of chiral pyrone esters **97** or **127** that proceed with excellent stereofidelity. Remarkably, all of the titled natural products were prepared in ten steps or less from a simple chiral geraniol derivative **99**. Single crystal X-ray diffraction studies of a synthetic intermediate have unambiguously determined the absolute stereochemistry of (+)-transtaganolide C (**9**). By inference, the absolute stereochemistries of (–)-transtaganolide D (**10**), (–)-transtaganolide A (**7**), and (+)-transtaganolide B (**8**) have been proposed. Finally, analysis of optical rotation data does not support the role of a putative Claisenase in the biosynthesis of the transtaganolides.

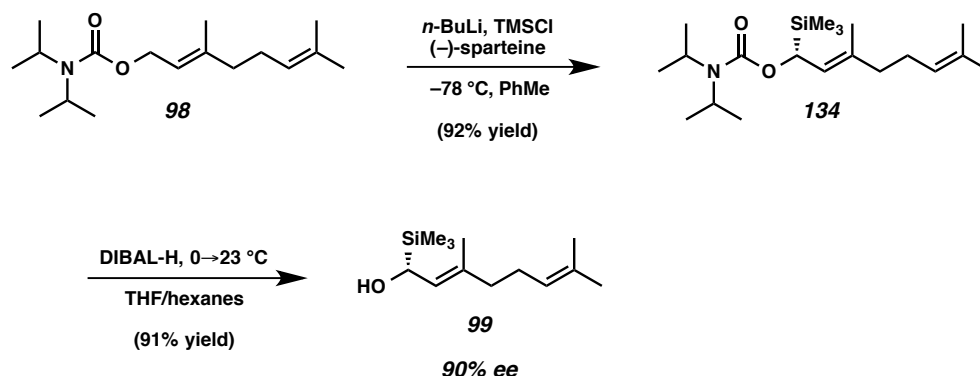
2.8 EXPERIMENTAL SECTION

2.8.1 MATERIALS AND METHODS

Unless otherwise stated, reactions were performed in flame-dried glassware under an argon or nitrogen atmosphere using dry deoxygenated solvents. Solvents were dried by passage through an activated alumina column under argon. Chemicals were purchased from Sigma-Aldrich Chemical Company and used as received. Pd(PPh₃)₄ was prepared using known methods. Thin layer chromatography (TLC), both preparatory and analytical, was performed using E. Merck silica gel 60 F254 precoated plates (0.25 mm) and visualized by UV fluorescence quenching, *p*-anisaldehyde, I₂, or KMnO₄ staining. Analytical super critical fluid (SFC) chromatography was performed using a Thar SFC and either Chiralpak IA or AD-H columns. Preparatory SFC was performed with a Jasco SFC and a prep AD-H column (21 x 250 mm, 5mic part# 19445). ICN Silica gel (particle size 0.032–0.063 mm) was used for flash chromatography. ¹H NMR and ¹³C NMR spectra were recorded on a Varian Mercury 300 (at 300 MHz) or on a Varian Unity Inova 500 (at 500 MHz). ¹H NMR spectra are reported relative to CDCl₃ (7.26 ppm). Data for ¹H NMR spectra are reported as follows: chemical shift (ppm), multiplicity, coupling constant (Hz), and integration. Multiplicities are reported as follows: s = singlet, d = doublet, t = triplet, q = quartet, sept. = septet, m = multiplet, bs = broad singlet, bm = broad multiplet. ¹³C NMR spectra are reported relative to CDCl₃ (77.16 ppm). FTIR spectra were recorded on a Perkin Elmer SpectrumBX spectrometer and are reported in frequency of absorption (cm⁻¹). HRMS were acquired using an Agilent 6200 Series TOF with an Agilent G1978A Multimode source in electrospray ionization (ESI),

Crystallographic data were obtained from the Caltech X-Ray Diffraction Facility.

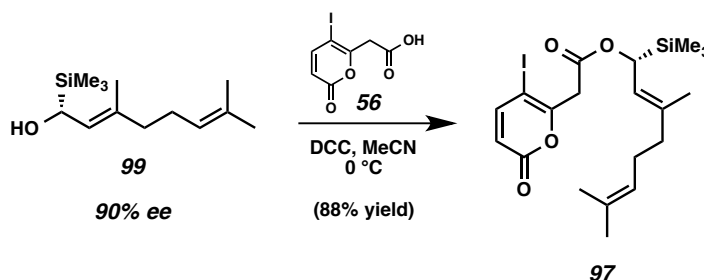
2.8.2 PREPARATIVE PROCEDURES



Enantioenriched allyl silane 99. To a $23\text{ }^\circ\text{C}$ solution of known diisopropyl geraniol carbamate^{6a} (**98**, 519 mg, 1.84 mmol) in toluene (9.2 mL, 0.2M) was added freshly distilled $(-)\text{-sparteine}$ (635 μL , 2.76 mmol) and TMSCl (352 μL , 2.76 mmol). The solution was then cooled to $-78\text{ }^\circ\text{C}$ and a solution of 2.5M $n\text{-BuLi}$ in hexanes (1.1 mL, 2.76 mmol) was added dropwise. The reaction was allowed to stir at $-78\text{ }^\circ\text{C}$ for 3 h. The reaction was then quenched at $-78\text{ }^\circ\text{C}$ by slow addition of MeOH (250 μL) and allowed to warm to $23\text{ }^\circ\text{C}$. The reaction was washed with saturated NH_4Cl (2 x 10 mL). Aqueous layers were combined and back extracted with Et_2O (3 x 20 mL). The combined organics were then washed with saturated brine (20 mL), dried over MgSO_4 , and concentrated by rotary evaporation. This crude oil could be taken on without further purification. Purification, if desired, was done via column chromatography (EtOAc in hexanes 2% \rightarrow 10% on silica) to yield 602 mg (92% yield) of allyl silane **134** as a colorless oil.

Allyl silane **134** (2.36 g, 6.7 mmol) was dissolved in THF (67 mL, 0.1M with respect to substrate) and hexanes (40 mL, 1.0 M with respect to DIBAL-H) and cooled to $0\text{ }^\circ\text{C}$. To this $0\text{ }^\circ\text{C}$ solution was slowly added neat DIBAL-H (7.1 mL, 40.2 mmol) dropwise. After the addition, the reaction was warmed to $23\text{ }^\circ\text{C}$ and stirred for 6 h. The reaction

was then cooled to 0 °C and slowly quenched with saturated aqueous Rochelle's salt (35 mL) with vigorous stirring. After addition of Rochelle's salt, the reaction was allowed to warm to 23 °C and celite (10 g) was added. The suspension was vigorously stirred for another 5 min and then filtered through a small pad of celite. The organic layer was collected, washed with saturated brine (35 mL), dried over MgSO₄, and concentrated by rotary evaporation. The crude oil could be taken on without further purification. If desired, purification was accomplished by column chromatography (EtOAc in hexanes 2%→20% on silica) to yield 1.38 g (91% yield) of colorless oil **99**. $[\alpha]_D^{20} = +69.71$ (*c* 1.00 in CHCl₃). Enantiomeric excess (*ee*) was determined for **97** inferred for **99**. All other spectral data matches the literature.^{7a}



Pyrone ester 97. To a solution of enantioenriched geraniol derivative **99** (202 mg, 0.89 mmol) in MeCN (9 mL, 0.1 M) at 0 °C was added sequentially pyrone acid **56** (300 mg, 1.07 mmol) and DCC (221 mg, 1.07 mmol). After 20 min at 0 °C, the reaction was filtered through a small pad of celite washing with MeCN. The filtrate was collected and concentrated by rotary evaporation and the crude oil was purified by column chromatography (EtOAc in hexanes 2%→10% on silica) to yield 384 mg (88% yield) of ICR/DA precursor **97** as a colorless oil; ¹H NMR (500 MHz, CDCl₃) δ 7.46 (d, *J* = 9.7 Hz, 1H), 6.06 (d, *J* = 9.7 Hz, 1H), 5.42 (d, *J* = 10.4 Hz, 1H), 5.14 (dq, *J* = 10.4, 1.2 Hz,

1H), 5.04 (tm, $J = 6.2$, 1H), 3.76 (s, 2H), 2.16 – 2.00 (m, 4H), 1.66 (d, $J = 1.4$ Hz, 6H), 1.59 (d, $J = 1.2$ Hz, 3H), 0.01 (s, 9H); ^{13}C NMR (125 MHz, CDCl_3) δ 166.6, 160.6, 158.6, 151.4, 138.0, 131.8, 124.1, 120.9, 116.1, 70.5, 69.7, 43.1, 40.0, 26.6, 25.9, 17.9, 17.0, –3.7; FTIR (Neat Film NaCl) 2959, 2923, 2854, 1741, 1607, 1546, 1445, 1404, 1382, 1336, 1293, 1273, 1249, 1206, 1170, 1134, 1062, 1016, 960, 908, 842, 819, 750 cm^{-1} ; HRMS (Multimode-ESI/APCI) m/z calc'd for $\text{C}_{20}\text{H}_{28}\text{IO}_4\text{Si}$ $[\text{M}-\text{H}]^-$: 487.0807, found 487.0821.

90% ee; SFC conditions: 3.0% IPA, 2.5mL/min, AD-H column, t_{R} (min): major = 7.02, minor = 7.79. A portion of this material was then separated by preparatory chiral SFC to obtain >99% ee material; $[\alpha]_{\text{D}}^{20} = +69.71$ (c 1.00, CHCl_3 , >99% ee).

Figure 2.8.1. Racemic SFC trace of compound **97**.

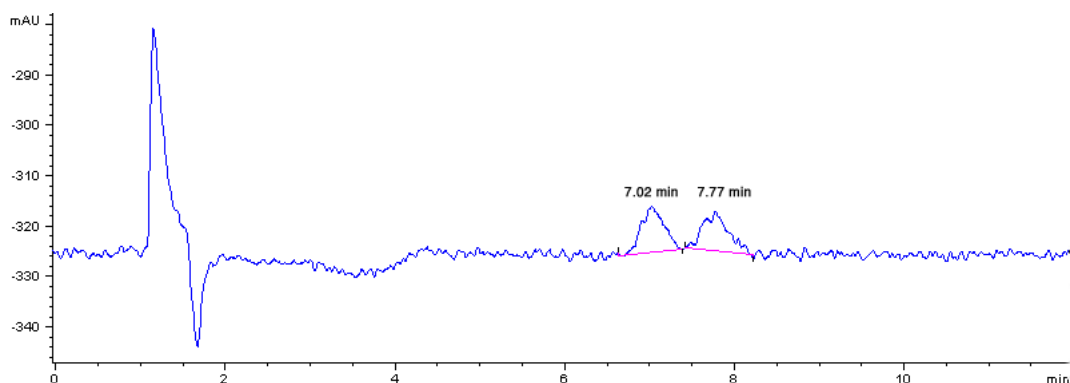
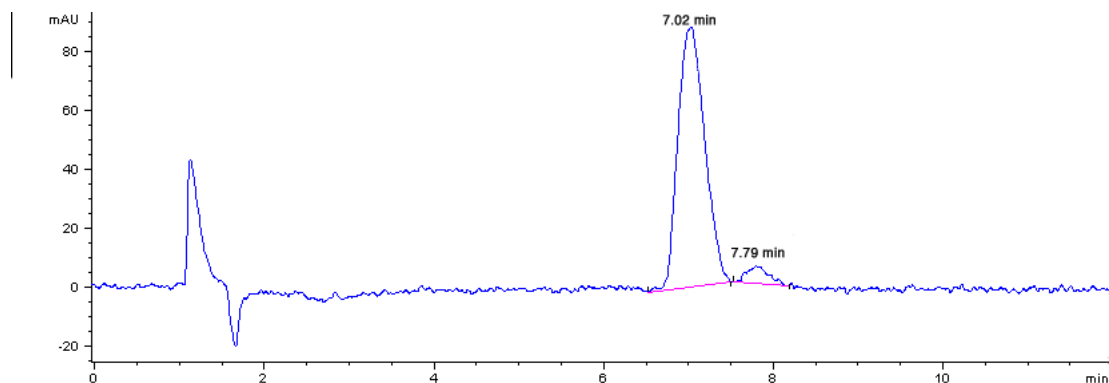
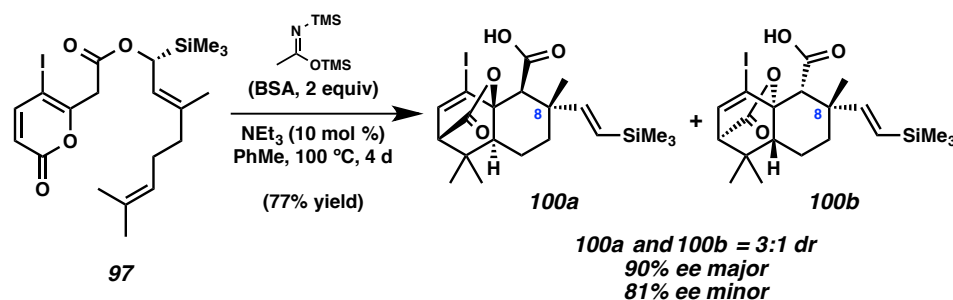


Figure 2.8.2. Enantioenriched SFC trace of compound **97**.





Vinyl silanes 100a and 100b. To a 23 °C solution of pyrone ester **97** (384 mg, 0.79 mmol) in toluene (4 mL, 0.2M) in a 500 mL sealed tube was added *N,O*-bis(trimethylsilyl)acetamide (BSA) (384 μL , 1.58 mmol) and NEt_3 (11 μL , 0.08 mmol). The reaction mixture was heated to 110 °C and stirred for 20 min. The solution was then cooled to 23 °C and diluted with toluene (450 mL), leaving ample headspace in the sealed tube to allow for solvent expansion. The reaction mixture was then re-heated to 100 °C and stirred for 4 d until complete as determined by NMR analysis. The reaction mixture was then cooled to 23 °C and 0.02% $\text{HCl}_{(\text{aq})}$ (20 mL) was added, after which the reaction mixture was stirred vigorously for 1 min. The organic phase was then separated and washed with 0.02% $\text{HCl}_{(\text{aq})}$ (3 x 25 mL), making sure the aqueous phase remained acidic. The aqueous phases were then combined and back extracted with ethyl acetate (3 x 30 mL) and all organic phases were combined, dried with Na_2SO_4 , and concentrated by rotary evaporation. The crude oil was purified by column chromatography (Et_2O in hexanes with 0.1% AcOH, 10% \rightarrow 20% on silica) to yield 294 mg (77% yield) of a 3:1 diastereomeric mixture of ICR/DA products **100a** and **100b** as white solids.

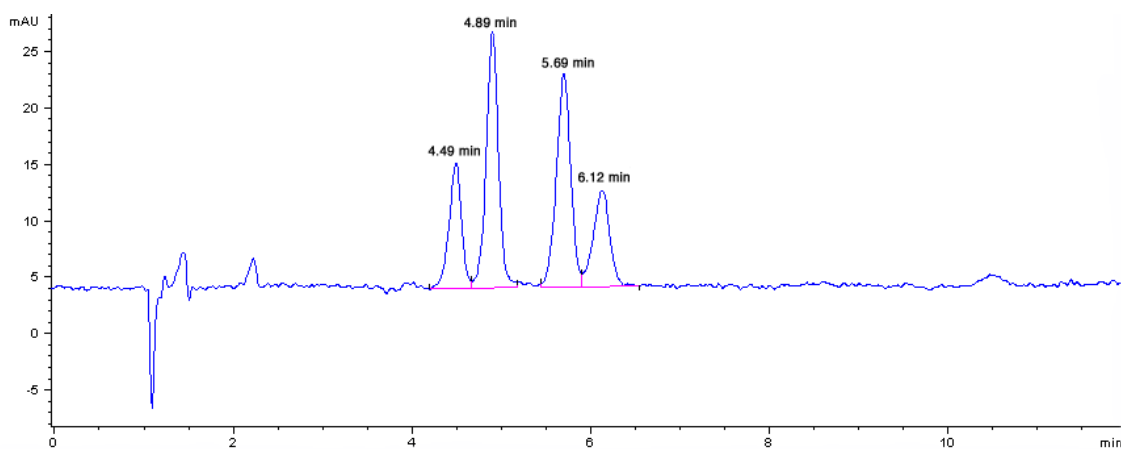
Major (100a): ^1H NMR (300 MHz, CDCl_3) δ 6.94 (d, J = 6.9 Hz, 1H), 6.12 (d, J = 18.9 Hz, 1H), 5.64 (d, J = 18.9 Hz, 1H), 3.01 (s, 1H), 2.97 (d, J = 6.9 Hz, 1H), 1.72–1.21 (m, 5H), 1.28 (s, 3H), 1.08 (s, 3H), 1.00 (s, 3H), 0.07 (s, 9H); ^{13}C NMR (125 MHz,

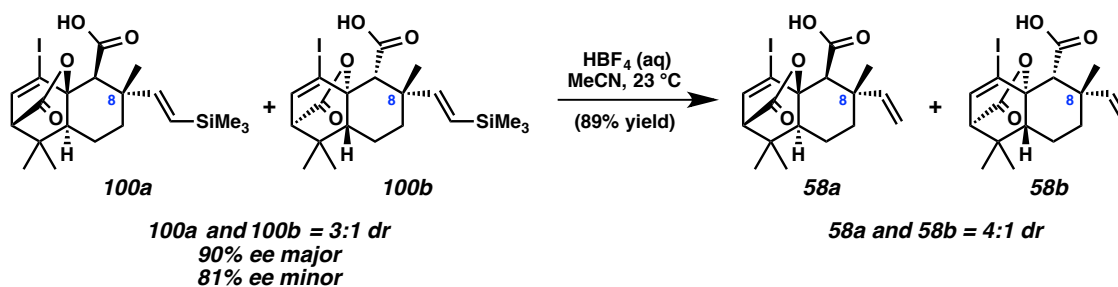
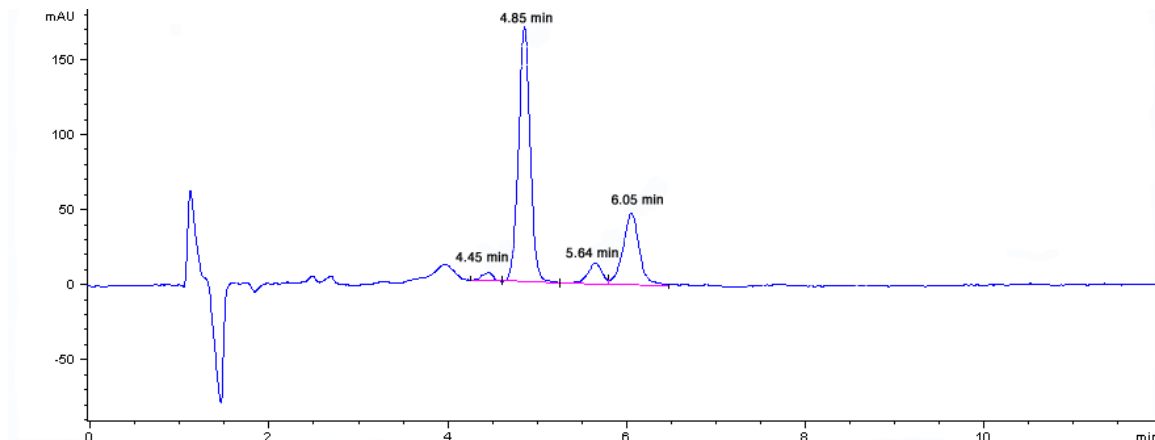
CDCl₃) δ 173.6, 170.8, 155.4, 140.2, 125.3, 98.0, 84.7, 59.3, 56.7, 48.1, 41.3, 38.2, 36.9, 29.9, 24.6, 20.8, 18.5, –1.0.

Minor (100b): ¹H NMR (300 MHz, CDCl₃) δ 6.94 (d, *J* = 6.8 Hz, 1H), 6.44 (d, *J* = 19.2 Hz, 1H), 5.68 (d, *J* = 19.2 Hz, 1H), 2.95 (d, *J* = 6.8 Hz, 1H), 2.95 (s, 1H) 1.96 (dt, *J* = 13.5, 3.1 Hz, 2H), 1.72–1.21 (m, 3H), 1.31 (s, 3H), 1.04 (s, 3H), 0.99 (s, 3H), 0.06 (s, 9H); ¹³C NMR (125 MHz, CDCl₃) δ 173.4, 169.9, 148.0, 140.5, 127.8, 97.5, 84.8, 61.2, 56.8, 47.9, 40.5, 38.1, 37.0, 29.7, 24.6, 20.7, 18.5, –1.1.

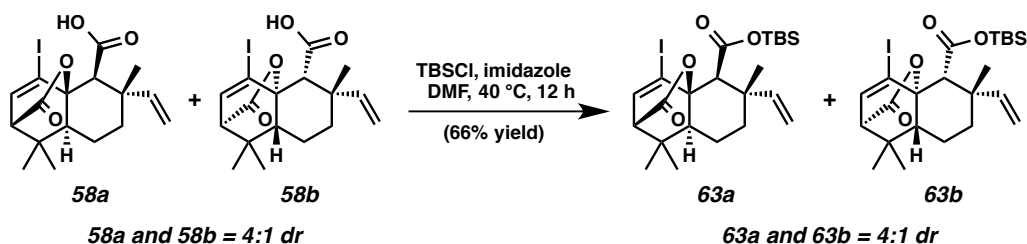
FTIR (Neat Film NaCl) 3075, 3014, 2955, 2671, 2545, 1755, 1713, 1612, 1464, 1455, 1415, 1397, 1386, 1373, 1338, 1286, 1246, 1218, 1174, 1133, 1103, 1048, 1016, 990, 967, 932, 903, 867, 838, 796, 757 cm⁻¹; HRMS (Multimode-ESI/APCI) *m/z* calc'd for C₂₀H₃₀IO₄Si [M+H]⁺: 489.0953, found 489.0952; [α]_D²⁰ = +13.28 (*c* 2.00, CHCl₃, 90% ee of **100a**, 81% ee of **100b**); SFC conditions: 15.0% IPA, 2.5 mL/min, IA column, *t*_R(min): **100a**) major = 4.85, minor = 5.64; **100b**) minor = 4.05, major = 6.05.

Figure 2.8.3. Racemic SFC trace of compounds **100a** and **100b**.

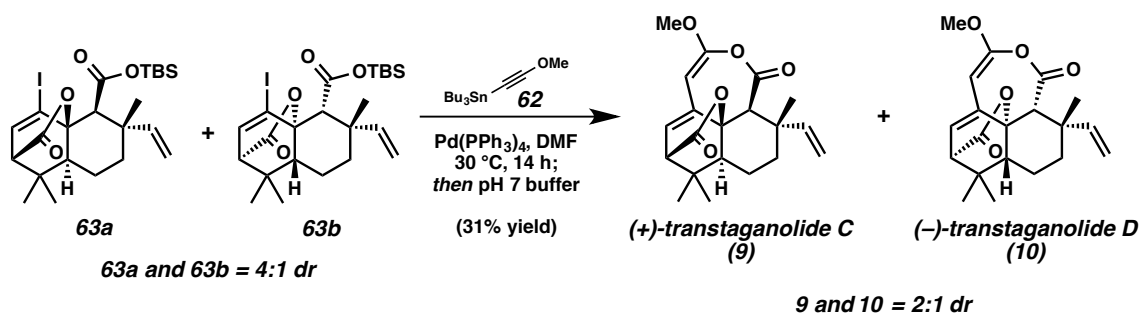




Iodo acids 58a and 58b. To a $23\text{ }^\circ\text{C}$ solution of vinyl silanes **100a** and **100b** (36.5 mg, 0.075 mmol) in MeCN (1.5 mL, 0.05M) was added $\text{HBF}_4(\text{aq})$ (48% w/w, 75 μL , 0.60 mmol). The reaction was stirred for 4.5 h and then diluted with ethyl acetate (15 mL). The organic layer was then washed with 0.02% $\text{HCl}(\text{aq})$ (3 x 5 mL). The aqueous phases were combined and back extracted with ethyl acetate (3 x 5 mL). The combined organic phases were dried over Na_2SO_4 and concentrated by rotary evaporation. Purification by column chromatography (EtOAc in hexanes with 0.1% AcOH , 5% \rightarrow 30% on silica) yielded 27.5 mg (89% yield) of a 4:1 diastereomeric mixture of the desilylated tricycles **58a** and **58b** as white solids. $[\alpha]_{\text{D}}^{20} = +42.73$ (c 1.00 in CHCl_3). All other spectral data matches the literature.²



TBS-esters 63a and 63b. To a 23 °C solution of iodo acids **58a** and **58b** (46 mg, 0.11 mmol,) in DMF (300 μ L, 0.35M) were added sequentially imidazole (76 mg, 1.1 mmol) and TBSCl (84 mg, 0.55 mmol). The reaction was warmed to 40 °C and then stirred for 12 h. The solution was then diluted with saturated brine (1 mL) and extracted with Et₂O/hexane (1:1) (3 x 2 mL). The combined organic extracts were washed with saturated aqueous KHSO₄ (1 mL) and then with saturated brine (3 x 1 mL). The combined organics were dried over Na₂SO₄, and concentrated by rotary evaporation. The crude oil was purified by column chromatography (EtOAc in hexanes 10%→50% on silica) to yield 39 mg (66% yield) of a 4:1 mixture of diastereomers **63a** and **63b** as white powders. $[\alpha]_D^{20} = +41.42$ (*c* 1.00 in CHCl₃). All other spectral data matches the literature.²



Transtaganolides C and D (9 and 10). In a nitrogen filled glovebox, to a solution of esters **63a** and **63b** (13 mg, 0.026 mmol) and Pd(PPh₃)₄ (33 mg, 0.029 mmol) in DMF

(260 μL , 0.1 M) was added tributyl(2-methoxyethyl)stannane (**62**) (34 mg, 0.104 mmol). The reaction was stirred at 30 °C for 14 h. The reaction mixture was then filtered through a Kimwipe plug with Et₂O (1.0 mL) (this removes a large excess of the undissolved Pd(PPh₃)₄) and removed from the glovebox. Outside of the glovebox, the added Et₂O was removed by rotary evaporation, and the reaction was diluted with MeCN (15 mL). To this solution was then added pH 7 phosphate buffer (200 μL) and the reaction was stirred vigorously at 23 °C for 2 h. Upon completion, MeCN was removed by rotary evaporation and the remaining aqueous solution was diluted with EtOAc (4 mL). This was then washed with water (3 x 1 mL) and the combined aqueous washes were back extracted with EtOAc (2 x 1 mL). All organics were pooled, dried with Na₂SO₄, and concentrated by rotary evaporation. The crude oil was purified by normal phase HPLC to yield 1.7 mg (20% yield) of transtaganolide C (**9**) and 0.9 mg (11% yield) of transtaganolide D (**10**) as white powders.

Transtaganolide C (9): ¹H NMR (500 MHz, CDCl₃) δ 6.07 (dd, J = 1.5, 6.5 Hz, 1H), 5.80 (dd, J = 11.0, 17.5 Hz, 1H), 5.07 (d, J = 17.5 Hz, 1H), 5.03 (d, J = 11.0 Hz, 1H), 5.00 (d, J = 1.5 Hz, 1H), 3.71 (s, 3H), 3.23 (s, 1H), 3.06 (d, J = 6.5 Hz, 1H), 1.71–1.63 (m, 3H), 1.60 (s, 3H), 1.44 (m, 1H), 1.30 (m, 1H), 1.08 (s, 3H), 0.97 (s, 3H); ¹³C NMR (125 MHz, CDCl₃) δ 171.8, 162.3, 156.7, 146.5, 138.0, 123.6, 112.8, 87.3, 79.3, 56.3, 53.8, 50.6, 48.1, 38.4, 38.3, 33.3, 29.9, 24.8, 19.9, 19.2; FTIR (Neat Film NaCl) 2965, 2928, 2872, 1791, 1761, 1668, 1619, 1456, 1334, 1267, 1233, 1178, 1115, 970, 954, 828 cm⁻¹; HRMS (Multimode-ESI/APCI) m/z calc'd for C₂₀H₂₄O₅ [M+H]⁺: 345.1697, found 345.1703; $[\alpha]_{\text{D}}^{20}$ = +120.73 (c 0.42, CHCl₃, 96% ee); SFC conditions: 8.0% IPA, 2.5 mL/min, AD-H column, t_{R} (min): major = 12.19, minor = 13.15.

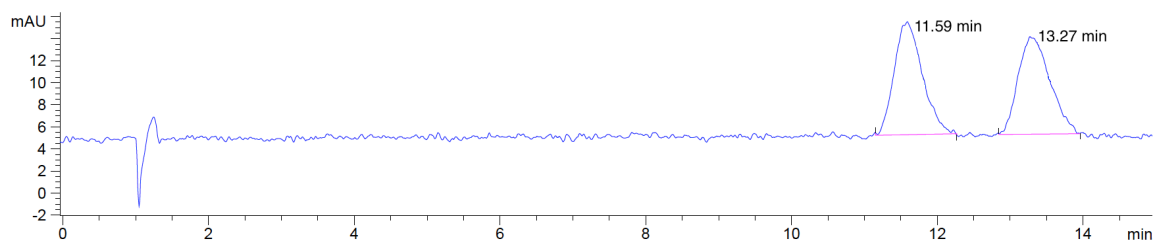
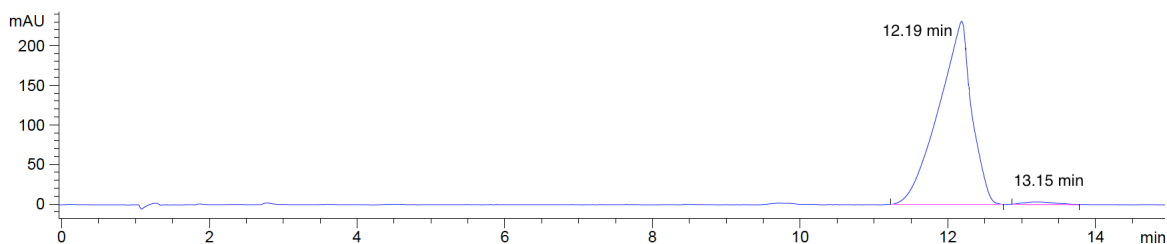


Figure 2.8.6. Enantioenriched SFC trace of transtaganolide C (**9**).



Transtaganolide D (10): ^1H NMR (500 MHz, CDCl_3) δ 7.00 (dd, $J = 11.0, 17.5$ Hz, 1H), 6.09 (dd, $J = 1.0, 6.5$ Hz, 1H), 5.15 (dd, $J = 1.0, 11.0$ Hz, 1H), 5.05 (dd, $J = 1.0, 17.5$ Hz, 1H), 5.02 (d, $J = 1.0$ Hz, 1H), 3.73 (s, 3H), 3.13 (s, 1H), 3.06 (d, $J = 6.5$ Hz, 1H), 1.91 (dt, $J = 3.5, 13.5$ Hz, 1H), 1.64 (dq, $J = 3.0, 13.5$ Hz, 1H), 1.58 (m, 1H), 1.39 (dt, $J = 3.5, 13.5$ Hz, 1H), 1.33 (dd, $J = 4.5, 13.5$ Hz, 1H), 1.22 (s, 3H), 1.04 (s, 3H), 0.97 (s, 3H); ^{13}C NMR (125 MHz, CDCl_3) δ 171.7, 162.6, 156.7, 142.9, 137.7, 123.9, 112.1, 87.3, 79.4, 56.3, 54.0, 53.3, 48.4, 40.5, 38.4, 33.3, 29.9, 28.5, 24.8, 20.5; FTIR (Neat Film NaCl) 2964, 2929, 2872, 1764, 1760, 1738, 1667, 1620, 1467, 1334, 1267, 1235, 1195, 1177, 1106, 1009, 954, 827 cm^{-1} ; HRMS (Multimode-ESI/APCI) m/z calc'd for $\text{C}_{20}\text{H}_{24}\text{O}_5$ $[\text{M}+\text{H}]^+$: 345.1697, found 345.1698; $[\alpha]_{\text{D}}^{20} = -51.55$ (c 0.17, CHCl_3 , 92% ee); SFC conditions: 6.0% IPA, 2.5 mL/min, AD-H column, t_{R} (min): minor = 25.49, major = 28.77.

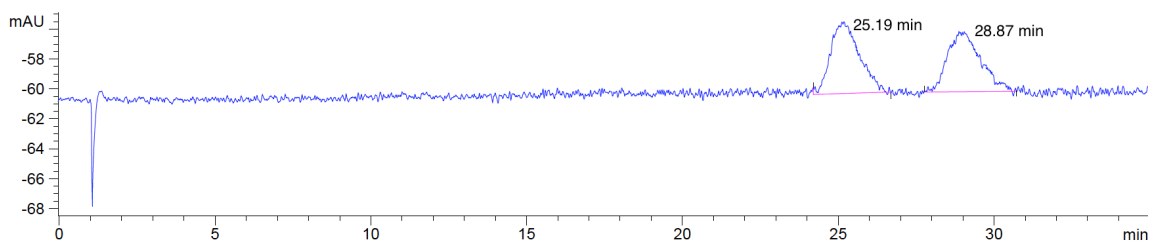
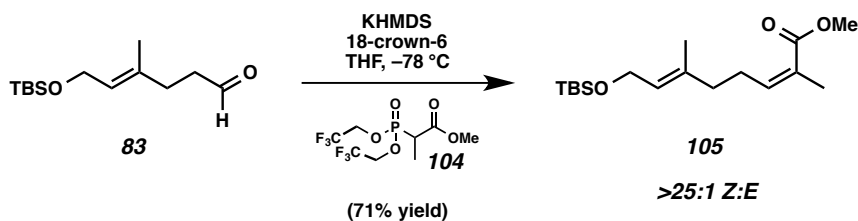
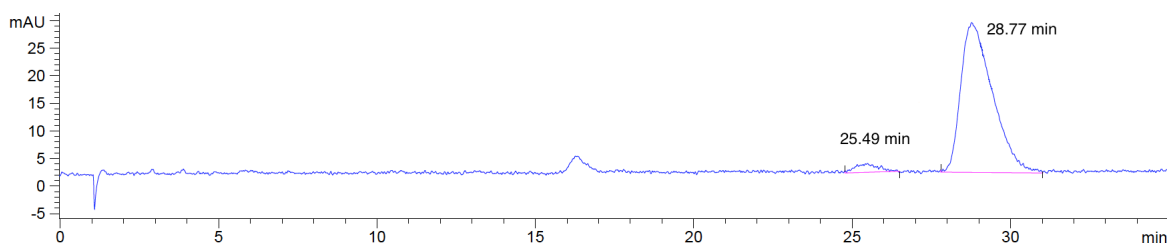
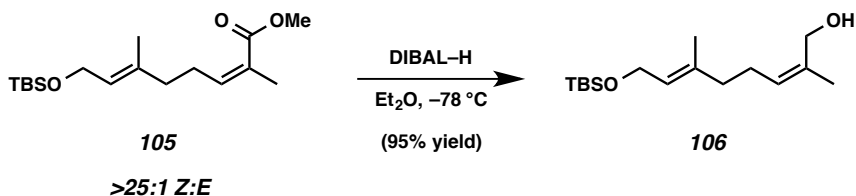


Figure 2.8.8. Enantioenriched SFC trace of transtaganolide D (**10**).



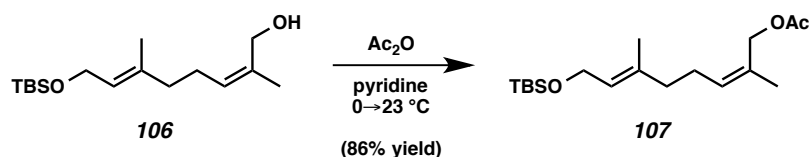
(Z)-methyleneoate **105**. To a $-78\text{ }^{\circ}\text{C}$ solution of KHMDS (2.92 g, 14.6 mmol) in THF (170 mL) was added a solution of phosphonate reagent **104** (4.46 g, 13.4 mmol) and 18-crown-6 (6.45 g, 24.4 mmol) in THF (50 mL). After stirring the reaction mixture for 10 min at $-78\text{ }^{\circ}\text{C}$, a solution of aldehyde **83** (2.96 g, 12.2 mmol) in THF (50 mL) was added. This brings the total volume of THF to 270 mL, which is a 0.05M solution with respect to the Still-Gennari Reagent **104**. The reaction was stirred at $-78\text{ }^{\circ}\text{C}$ for 20 min and then quenched with a saturated NH_4Cl solution (100 mL) at $-78\text{ }^{\circ}\text{C}$. After allowing the reaction mixture to warm to $23\text{ }^{\circ}\text{C}$, the organic layer was washed with saturated NH_4Cl (2 x 100 mL). Aqueous layers were combined and back extracted with Et_2O (2 x

150 mL). The combined organic layers were washed with saturated brine (300 mL), dried over MgSO_4 , and concentrated by rotary evaporation. Purification was accomplished by column chromatography (EtOAc in hexanes 2%→10% on silica) to yield 2.72 g (71% yield) >25:1, Z:E of enoate **105** as a colorless oil; ^1H NMR (500 MHz, CDCl_3) δ 5.92 (tq, $J = 7.3, 1.5$ Hz, 1H), 5.32 (tq, $J = 6.3, 1.3$ Hz, 1H), 4.18 (dq, $J = 6.3, 0.9$ Hz, 2H), 3.73 (s, 3H), 2.61–2.55 (m, 2H), 2.11–2.07 (m, 2H), 1.88 (q, $J = 1.5$ Hz, 3H), 1.62 (d, $J = 1.3$ Hz, 3H), 0.89 (s, 9H), 0.06 (s, 6H); ^{13}C NMR (125 MHz, CDCl_3) δ 168.6, 143.0, 136.2, 127.1, 125.2, 60.4, 51.4, 39.1, 27.8, 26.1, 20.8, 18.5, 16.3, –4.9; FTIR (Neat Film NaCl) 2953, 2930, 2896, 2857, 1721, 1671, 1648, 1472, 1461, 1435, 1383, 1362, 1254, 1214, 1197, 1130, 1106, 1087, 1065, 1006, 837, 776 cm^{-1} ; HRMS (ESI) m/z calc'd for $\text{C}_{17}\text{H}_{32}\text{O}_3\text{SiNa}$ $[\text{M}+\text{Na}]^+$: 335.2020, found 335.2013.



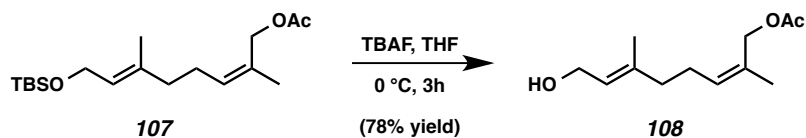
Alcohol 106. To a –78 °C solution of (Z)-methyleneoate **105** (1.76 g, 5.63 mmol) in Et_2O (28 mL, 0.2M) was added DIBAL–H (2.50 mL, 14.1 mmol) dropwise. The reaction mixture was then stirred at –78 °C for 45 min. The reaction mixture was then slowly quenched by the dropwise addition of saturated aqueous Rochelle’s salt (20 mL) at –78 °C. The reaction was then allowed to warm to ambient temperature and stirred vigorously for 1 h. The aqueous layer was separated from the organics and extracted with Et_2O (4 x 15). The organics were combined and dried over MgSO_4 . Solvent was evaporated by rotary evaporation and purification by column chromatography (EtOAc in

hexanes 3.5%→15% on silica) resulted in the isolation of 1.52 g (95% yield) of alcohol **106** as a colorless oil; $^1\text{H NMR}$ (300 MHz, CDCl_3) δ 5.30–5.20 (m, 2H), 4.16 (dq, $J = 6.5, 0.8$ Hz, 2H), 4.07 (s, 2H), 2.16 (q, $J = 7.5$, 2H), 2.00 (t, $J = 7.3$, 2H), 1.78 (q, $J = 1.2$ Hz, 3H), 1.62 (d, $J = 1.4$ Hz, 3H), 0.90 (s, 9H), 0.07 (s, 6H); $^{13}\text{C NMR}$ (75 MHz, CDCl_3) δ 136.7, 135.2, 127.4, 125.0, 61.5, 60.3, 39.4, 26.1, 25.8, 21.3, 18.6, 16.5, –5.0; FTIR (Neat Film NaCl) 3346, 2956, 2930, 2885, 2857, 1472, 1463, 1382, 1361, 1255, 1110, 1066, 1006, 836, 814, 776 cm^{-1} ; HRMS (ESI) m/z calc'd for $\text{C}_{16}\text{H}_{32}\text{O}_2\text{SiNa}$ $[\text{M}+\text{Na}]^+$: 307.2064, found 307.2070.

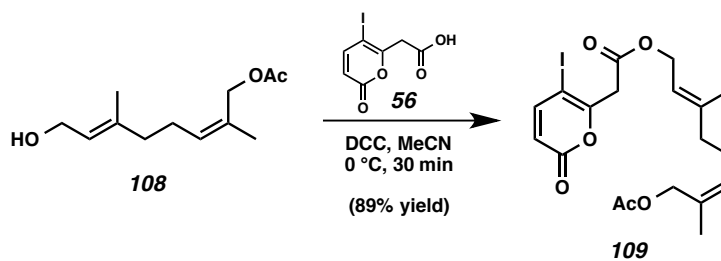


Acetate 107. To a 0 °C solution of alcohol **106** (473 mg, 1.66 mmol) in pyridine (3.5 mL, 0.5 M) was added acetic anhydride (780 μL , 8.32 mmol) dropwise. The reaction was then warmed to ambient temperature and stirred for 3 h. Following reaction completion the mixture was diluted with Et_2O (25 mL) and washed with saturated aqueous CuSO_4 (2 x 10 mL), saturated aqueous NaHCO_3 (2 x 10 mL), saturated aqueous CuSO_4 (1 x 10 mL), and lastly saturated brine (1 x 15 mL). The organic mixture was then dried over MgSO_4 , concentrated by rotary evaporation, and purified by column chromatography (EtOAc in hexanes 1% on silica) to give 466 mg (86% yield) of acetate **107** as a colorless oil; $^1\text{H NMR}$ (300 MHz, CDCl_3) δ 5.41–5.35 (m, 1H), 5.30 (tq, $J = 6.3, 1.3$ Hz, 1H), 4.57 (s, 2H), 4.18 (dq, $J = 6.3, 0.9$ Hz, 2H), 2.19 (q, $J = 7.3$ Hz, 2H), 2.07 (s, 3H), 2.06–1.98 (m, 2H), 1.74 (q, $J = 1.3$ Hz, 3H), 1.61 (d, $J = 1.3$ Hz, 3H), 0.90 (s, 9H),

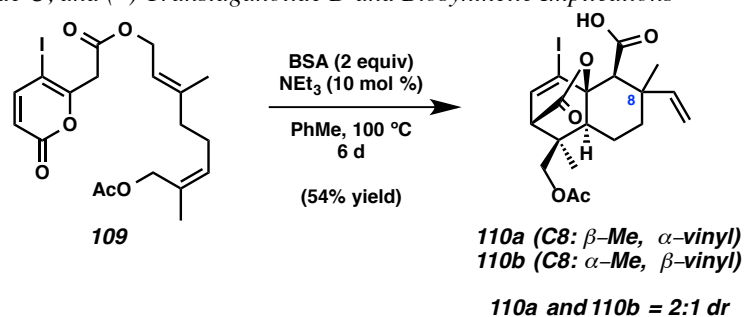
0.07 (s, 6H); ^{13}C NMR (125 MHz, CDCl_3) δ 171.3, 136.3, 130.4, 130.1, 125.1, 63.3, 60.4, 39.6, 26.2, 26.1, 21.6, 21.1, 18.6, 16.4, –4.9; FTIR (Neat Film NaCl) 2951, 2929, 2856, 1740, 1472, 1457, 1381, 1363, 1230, 1110, 1065, 1024, 982, 835, 775 cm^{-1} ; HRMS (ESI) m/z calc'd for $\text{C}_{18}\text{H}_{34}\text{O}_3\text{SiH}$ $[\text{M}+\text{H}]^+$: 327.2350, found 327.2348.



Alcohol 108. To a 0 °C solution of acetate **107** (312 mg, 0.955 mmol) in THF (5 mL, 0.2 M) was added a 1 M solution of TBAF in THF (1.45 mL, 1.45 mmol). The reaction mixture was then stirred at 0 °C for 2 h. After 2 h the reaction appeared to have stalled, so another equiv of 1 M TBAF solution (1 mL, 1 mmol) was added and the reaction stirred at 0 °C for an additional hour. The reaction mixture was quenched at 0 °C by the addition of saturated aqueous NH_4Cl (5 mL) and then allowed to warm to ambient temperature. The aqueous phase was then extracted with Et_2O (3 x 5 mL), the organics were combined, and subsequently washed with saturated brine (1 x 20 mL). The organics were then dried over MgSO_4 , concentrated by rotary evaporation, and purified by column chromatography (EtOAc in hexanes 5%→20% on silica) to give 159 mg (78% yield) of alcohol **108** as a colorless oil; ^1H NMR (300 MHz, CDCl_3) δ 5.45–5.30 (m, 2H), 4.56 (s, 2H), 4.13 (d, $J = 6.9$ Hz, 2H), 2.19 (q, $J = 7.4$ Hz, 2H), 2.06 (s, 3H), 2.08–2.00 (m, 2H), 1.73 (s, 3H), 1.65 (s, 3H); ^{13}C NMR (75 MHz, CDCl_3) δ 171.3, 139.0, 130.2, 130.2, 124.0, 63.3, 59.4, 39.5, 26.1, 21.5, 21.1, 16.4; FTIR (Neat Film NaCl) 3420, 2972, 2922, 2858, 1734, 1672, 1448, 1368, 1233, 1100, 1022, 955, 916 cm^{-1} ; HRMS (ESI) m/z calc'd for $\text{C}_{12}\text{H}_{20}\text{O}_3\text{Na}$ $[\text{M}+\text{Na}]^+$: 235.1305, found 235.1296.



Pyrone ester 109. To a 0 °C solution of alcohol **108** (173 mg, 814 μmol) in MeCN (8.15 mL, 0.1M) was added sequentially iodo-acid **56** (274 mg, 0.977 mmol) and DCC (202 mg, 0.977 mmol). The reaction mixture was stirred at 0 °C for 30 min. The still cold reaction was then filtered through a small pad of celite with MeCN to remove excess urea byproduct. The organics were then concentrated by rotary evaporation and purified by column chromatography (EtOAc in hexanes 6%→12% on silica) to give 344 mg (89% yield) of pyrone ester **109** as a yellow oil; ¹H NMR (300 MHz, CDCl₃) δ 7.46 (d, *J* = 9.7 Hz, 1H), 6.07 (d, *J* = 9.7 Hz, 1H), 5.38–5.30 (m, 2H), 4.66 (d, *J* = 7.2 Hz, 2H), 4.56 (s, 2H), 3.77 (s, 2H), 2.19 (q, *J* = 7.0 Hz, 2H), 2.10–2.02 (m, 2H) 2.06 (s, 3H), 1.74 (d, *J* = 1.4 Hz, 3H), 1.69 (dd, *J* = 1.4, 0.6 Hz, 3H); ¹³C NMR (75 MHz, CDCl₃) δ 171.3, 166.8, 160.5, 158.0, 151.4, 142.7, 130.4, 129.9, 118.1, 116.3, 70.8, 63.2, 62.7, 42.7, 39.5, 26.0, 21.6, 21.1, 16.7; FTIR (Neat Film NaCl) 2966, 2937, 2853, 1732, 1606, 1548, 1445, 1372, 1344, 1328, 1277, 1234, 1165, 1133, 1063, 1016, 959, 867, 821, 767, 728 cm⁻¹; HRMS (ESI) *m/z* calc'd for C₁₉H₂₃IO₆Na [M+Na]⁺: 497.0432, found 497.0413.



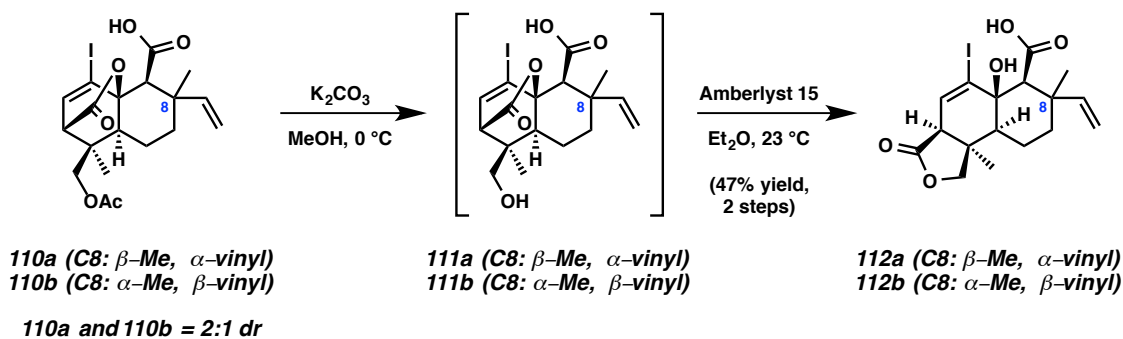
Tricycles 110a and 110b. To a 23 °C solution of pyrone ester **109** (93 mg, 0.197 mmol) in toluene (1.21 mL, 0.17 M) in a 100 mL sealed tube was added BSA (118 μL, 0.484 mmol) and NEt₃ (3.4 μL, 0.024 mmol). The reaction mixture was heated to 110 °C and stirred for 20 min. The mixture was then cooled to 23 °C and diluted with toluene (75 mL). The reaction mixture was then re-heated to 100 °C and stirred for 6 d until completion, which was determined after monitoring by NMR. The reaction mixture was then cooled to 23 °C, a 1% aqueous solution of AcOH was added (5 mL), and the reaction was stirred for an additional 2 min. The reaction was washed with a 1% aqueous solution of AcOH (3 x 20 mL), and the aqueous phases were combined and back extracted with EtOAc (3 x 30 mL), while making sure the pH of the aqueous phase remained acidic. The organics were combined, dried over Na₂SO₄ and solvent was removed by rotary evaporation. Purification by column chromatography (EtOAc in hexanes with 0.1% AcOH, 17%→25% on silica) to give 51 mg (54% yield) of a 2:1 mixture of ICR/DA diastereomers **110a** and **110b** as a white solid.

Major (110a): ¹H NMR (300 MHz, CDCl₃) δ 6.95 (d, *J* = 7.0 Hz, 1H), 6.00 (dd, *J* = 17.5, 10.6 Hz, 1H), 5.13–5.00 (m, 2H), 4.03 (dd, *J* = 100.4, 11.5 Hz, 2H), 3.30 (d, *J* = 7.0 Hz, 1H), 3.00 (s, 1H), 2.08 (s, 3H), 2.02–1.33 (m, 5H), 1.30 (s, 3H), 1.02 (s, 3H); ¹³C

NMR (125 MHz, CDCl₃) δ 173.0, 170.7, 169.8, 147.9, 139.5, 111.8, 99.2, 84.3, 67.7, 59.3, 51.8, 48.8, 40.0, 39.9, 38.2, 24.8, 20.9, 19.0, 18.4.

Minor (110b): ¹H NMR (300 MHz, CDCl₃) δ 6.95 (d, *J* = 7.0 Hz, 1H), 6.32 (dd, *J* = 17.5, 11.0 Hz, 1H), 5.13–5.00 (m, 2H), 4.20–3.81 (m, 2H), 3.29 (d, *J* = 6.9 Hz, 1H), 2.94 (s, 1H), 2.07 (s, 3H), 2.02–1.33 (m, 5H), 1.36 (s, 3H), 1.01 (s, 3H); ¹³C NMR (125 MHz, CDCl₃) δ 173.1, 170.7, 169.8, 140.4, 139.9, 113.8, 98.7, 84.5, 67.7, 60.8, 51.9, 48.8, 40.2, 39.5, 38.6, 29.9, 20.9, 19.0, 18.4.

FTIR (Neat Film NaCl) 3084, 2970, 2932, 2668, 1746, 1455, 1377, 1338, 1315, 1234, 1173, 1124, 1047, 1019, 967, 914, 839, 800, 733 cm⁻¹; HRMS (Multimode-ESI/APCI) *m/z* calc'd for C₁₉H₂₃IO₆H [M+H]⁺: 475.0612, found 475.0595.



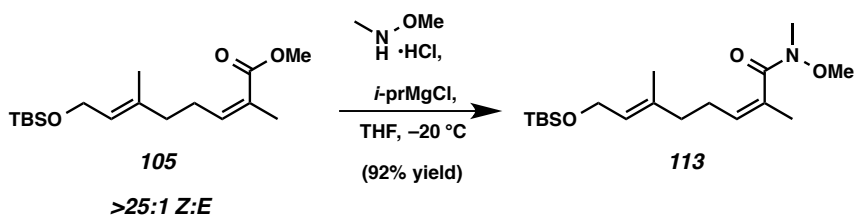
Tricycles 112a and 112b. To a 0 °C solution of tricycles **110a** and **110b** (24 mg, 0.051 mmol) in MeOH (2.5 mL, 0.02 M) was added K₂CO₃ (30 mg, 0.024 mmol). The reaction mixture was then stirred for 2 h at 0 °C. Upon completion of the desired deprotection, the reaction mixture was quenched at 0 °C by the dropwise addition of glacial AcOH until the solution had become acidic, as was ascertained by pH paper. Once acidic, the reaction mixture was concentrated by rotary evaporation to remove the MeOH, and then re-dissolved in EtOAc (5 mL). The organic solution was then washed

with a 1% aqueous solution of AcOH (3 x 5 mL), and the aqueous phases were combined and back extracted with EtOAc (2 x 15 mL), while making sure the pH of the aqueous phase remained acidic. The organics were combined, dried over Na₂SO₄ and solvent was removed by rotary evaporation to give a crude mixture of alcohols **111a** and **111b** along with translactonized products **112a** and **112b**. For the purposes of characterization, the crude mixture of **111a**, **111b**, **112a**, and **112b** was dissolved in Et₂O (3 mL) and stirred at 23 °C over Amberlyst 15 (30 mg) for 12 h. This allowed for complete conversion of alcohols **111a** and **111b** to the translactonized products **112a** and **112b**. The reaction mixture was then filtered through a short pad of celite to remove the Amberlyst 15 resin with EtOAc. Solvent was removed by rotary evaporation and subsequent purification by column chromatography (EtOAc in hexanes with 0.1% AcOH, 17%→25% on silica) to give 10 mg (47% yield) of a 2:1 mixture of tricycles **112a** and **112b** as a white solid.

Major (112a): ¹H NMR (300 MHz, CDCl₃) δ 6.74 (d, *J* = 7.3 Hz, 1H), 5.91 (dd, *J* = 17.3, 10.8 Hz, 1H), 5.60 (bs, 1H), 5.05–4.95 (m, 3H), 3.89 (d, *J* = 9.0 Hz, 1H), 2.98 (d, *J* = 7.2 Hz, 1H), 2.55 (s, 1H), 2.20–1.74 (m, 2H), 1.72–1.40 (m, 3H), 1.28 (s, 3H), 1.25 (s, 3H); ¹³C NMR (125 MHz, CDCl₃) δ 179.6, 176.1, 148.1, 136.3, 111.8, 109.8, 76.1, 74.8, 59.7, 53.4, 51.2, 41.1, 38.8, 38.7, 29.8, 20.0, 19.5.

Minor (112b): ¹H NMR (300 MHz, CDCl₃) δ 6.76 (d, *J* = 7.7 Hz, 1H), 6.44 (dd, *J* = 17.6, 10.8 Hz, 1H), 5.60 (bs, 1H), 5.08–4.94 (m, 3H), 3.87 (d, *J* = 9.1 Hz, 1H), 2.98 (d, *J* = 7.2 Hz, 1H), 2.53 (s, 1H), 2.20–1.74 (m, 2H), 1.72–1.40 (m, 3H), 1.31 (s, 3H), 1.28 (s, 3H); ¹³C NMR (125 MHz, CDCl₃) δ 179.8, 176.1, 141.7, 136.7, 113.4, 109.5, 76.1, 74.9, 61.8, 53.4, 51.8, 40.8, 40.3, 38.8, 29.9, 28.5, 19.5.

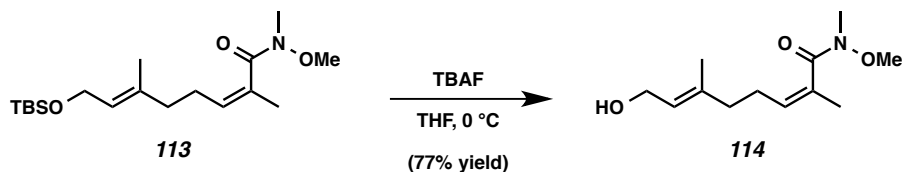
FTIR (Neat Film NaCl) 3362, 3083, 2962, 2923, 2877, 1760, 1690, 1460, 1397, 1379, 1307, 1245, 1205, 1173, 1150, 1090, 1061, 1033, 986, 909, 826, 731 cm^{-1} ; HRMS (Multimode-ESI/APCI) m/z calc'd for $\text{C}_{17}\text{H}_{21}\text{IO}_5\text{Na}$ $[\text{M}+\text{Na}]^+$: 455.0326, found 455.0323.



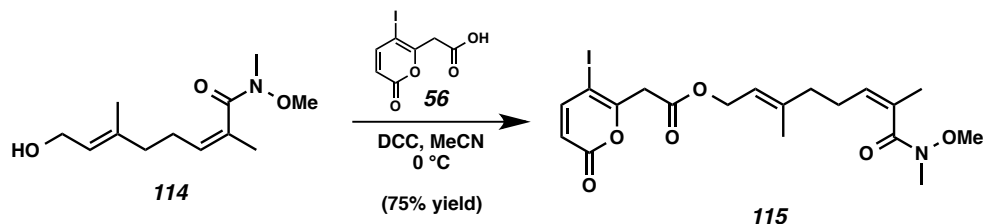
Weinreb amide 113. To a $-20\text{ }^\circ\text{C}$ solution of (Z)-methyleneate **105** (340 mg, 1.09 mmol) in THF (11 mL, 0.1 M) was added sequentially *N,O*-dimethylhydroxyamine hydrochloride (165 mg, 1.69 mmol) and the slow addition of 2 M isopropylmagnesium chloride solution in THF (1.63 mL, 3.26 mmol) dropwise. The reaction mixture was then warmed to $0\text{ }^\circ\text{C}$ and stirred for 3 h. The reaction was then quenched with saturated aqueous NH_4Cl (2.6 mL) at $0\text{ }^\circ\text{C}$ and allowed to warm to ambient temperature. Upon reaching $23\text{ }^\circ\text{C}$, water was added (10 mL) and the aqueous phase separated and back extracted with Et_2O (4 x 15 mL). The organics were combined, washed with saturated brine (40 mL), dried over Na_2SO_4 , and concentrated by rotary evaporation. Purification was accomplished by column chromatography (EtOAc in hexanes 2.5% \rightarrow 10% on silica) to give 340 mg (92% yield) of Weinreb amide **113** as a colorless oil; ^1H NMR (500 MHz, CDCl_3) δ 5.39 (tq, $J = 7.3, 1.6$ Hz, 1H), 5.29 (tq, $J = 6.3, 1.3$ Hz, 1H), 4.17 (d, $J = 6.3$ Hz, 2H), 3.65 (bs, 3H), 3.23 (s, 3H), 2.13 (q, $J = 7.8, 7.4$ Hz, 2H), 2.08–2.02 (m, 2H), 1.88 (s, 3H), 1.59 (s, 3H), 0.89 (s, 9H), 0.05 (s, 6H); ^{13}C NMR (125 MHz, CDCl_3) δ 172.0, 136.0, 131.5, 129.7, 124.9, 61.5, 60.2, 38.9, 32.1, 27.8, 26.0, 20.0, 18.4, 16.2, -5.1 ; FTIR (Neat Film NaCl) 2955, 2930, 2897, 2857, 1652, 1472, 1462, 1414, 1382, 1255, 1180, 1111,

1088, 1063, 1004, 836, 776 cm^{-1} ; HRMS (ESI) m/z calc'd for $\text{C}_{18}\text{H}_{35}\text{NO}_3\text{SiNa}$ $[\text{M}+\text{Na}]^+$:

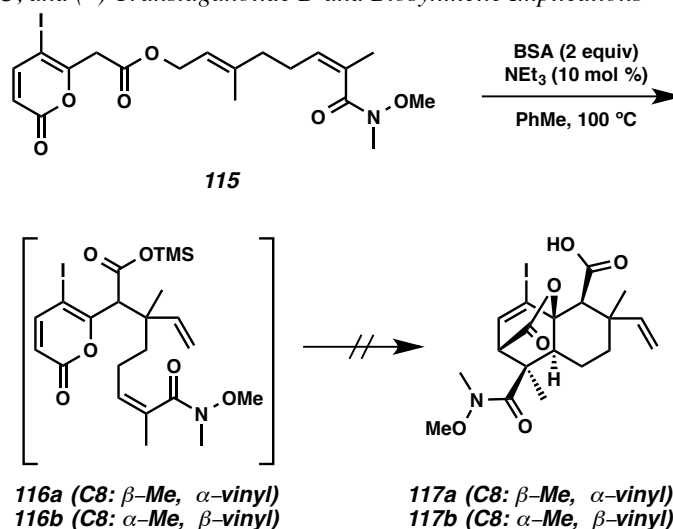
364.2278, found 364.2283.



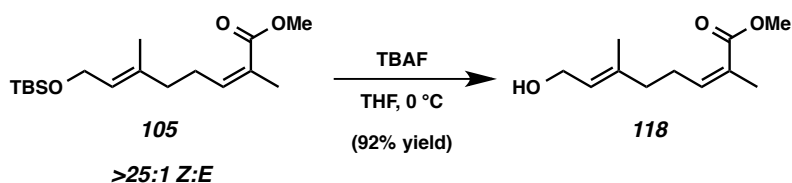
Alcohol 114. To a 0 °C solution of Weinreb amide **113** (217 mg, 0.635 mmol) in THF (6.35 mL, 0.1 M) was slowly added a 1 M TBAF solution in THF (1.27 mL, 1.27 mmol). The reaction mixture was then stirred at 0 °C for 4 h. After the reaction had gone to completion, saturated aqueous NH_4Cl (1 mL) was added at 0 °C and the reaction was warmed to ambient temperature. Water (4 mL) was then added, the aqueous phase was separated from the organics, and the aqueous phase was back extracted with EtOAc (3 x 6 mL). The organics were combined, washed with saturated brine (15 mL), dried over Na_2SO_4 , and concentrated by rotary evaporation. Purification was accomplished by column chromatography (EtOAc in hexanes 17% \rightarrow hexanes in EtOAc 20% on silica) to give 111 mg (77% yield) of alcohol **114** as a colorless oil; ^1H NMR (300 MHz, CDCl_3) δ 5.42–5.33 (bm, 2H), 4.10 (d, $J = 7.1$ Hz, 2H), 3.65 (bs, 3H), 3.22 (s, 1H), 2.18–1.98 (m, 5H), 1.89 (s, 3H), 1.64 (s, 3H); ^{13}C NMR (125 MHz, CDCl_3) δ 172.0, 137.5, 131.4, 129.4, 124.5, 61.5, 58.7, 38.6, 31.9, 27.9, 19.9, 16.1; FTIR (Neat Film NaCl) 3420, 2970, 2935, 2856, 1633, 1440, 1384, 1346, 1325, 1180, 1150, 1103, 1079, 997, 898, 845, 752 cm^{-1} ; HRMS (ESI) m/z calc'd for $\text{C}_{12}\text{H}_{21}\text{NO}_3\text{Na}$ $[\text{M}+\text{Na}]^+$: 250.1414, found 250.1405.



Pyrone 115. To a 0 °C solution of alcohol **114** (92 mg, 0.405 mmol) in MeCN (4 mL, 0.1M) was added sequentially iodo-acid **56** (136 mg, 0.486 mmol) and DCC (100 mg, 0.486 mmol). The reaction was stirred at 0 °C for 30 min. The still cold reaction was then filtered through a small pad of celite with MeCN to remove excess urea byproduct. The solution was then concentrated by rotary evaporation and purified by column chromatography (EtOAc in hexanes 20%→35% on silica) to give 149 mg (75% yield) of pyrone **115** as a yellow oil; ¹H NMR (300 MHz, CDCl₃) δ 7.46 (d, *J* = 9.7 Hz, 1H), 6.07 (d, *J* = 9.7 Hz, 1H), 5.41–5.29 (bm, 2H), 4.65 (d, *J* = 7.1 Hz, 2H), 3.77 (s, 2H), 3.66 (bs, 3H), 3.23 (s, 3H), 2.20–2.05 (m, 5H), 1.89 (s, 3H), 1.69 (s, 3H); ¹³C NMR (126 MHz, CDCl₃) δ 166.6, 160.3, 157.8, 151.3, 142.4, 131.9, 129.2, 118.0, 116.1, 70.7, 62.5, 61.6, 42.6, 38.9, 27.7, 20.1, 16.5; FTIR (Neat Film NaCl) 2969, 2934, 2853, 1742, 1641, 1608, 1546, 1452, 1383, 1344, 1327, 1278, 1205, 1169, 1133, 1088, 1064, 1017, 994, 926, 868, 823, 752 cm⁻¹; HRMS (Multimode-ESI/APCI) *m/z* calc'd for C₁₉H₂₄INO₆H [M+H]⁺: 490.0721, found 490.0761.

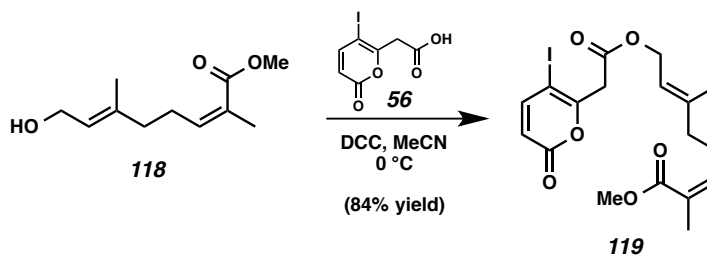


Attempt at tricycle 117a and 117b. To a 23 °C solution of pyrone **115** (44 mg, 0.09 mmol) in toluene (450 μL, 0.2 M) in a 50 mL sealed tube was added BSA (44 μL, 0.18 mmol) and NEt₃ (1.0 μL, 0.007 mmol). The reaction mixture was heated to 110 °C and stirred for 20 min to form Ireland–Claisen products **116a** and **116b**. The mixture was then cooled to 23 °C and diluted with toluene (30 mL). The reaction mixture was then re-heated to 100 °C and stirred indefinitely, and no Diels–Alder product **117a** and **117b** could be observed by NMR even after one month of heating at 100 °C.



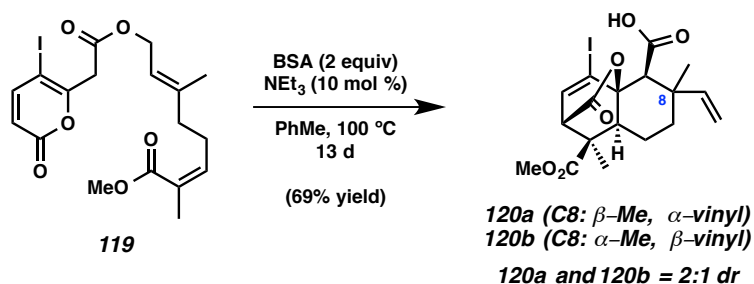
Alcohol 118. To a 0 °C solution of (Z)-methyleneoate **105** (108 mg, 0.346 mmol) in THF (3.5 mL, 0.1 M) was added dropwise a 1 M solution of TBAF in THF (415 μL, 0.415). The reaction was stirred at 0 °C for 2 h. After 2 h more 1 M solution of TBAF in THF (200 μL, 0.200 mmol) was added and the reaction was stirred for 1 h at 0 °C. The

reaction was quenched by the addition of water (3 mL) at 0 °C and the mixture was stirred and allowed to warm to ambient temperature. The aqueous phase was separated and back extracted with Et₂O (3 x 2 mL) and the organics were combined. The combined organics were washed with saturated brine (8 mL), concentrated by rotary evaporation, and purified by column chromatography (EtOAc in hexanes 5%→20% on silica) to give 63 mg (92% yield) of alcohol **118** as a singly isomeric colorless oil; ¹H NMR (300 MHz, CDCl₃) δ 5.91 (tq, *J* = 7.3, 1.5 Hz, 1H), 5.42 (tp, *J* = 6.8, 1.3 Hz, 1H), 4.15 (d, *J* = 6.9 Hz, 2H), 3.73 (s, 3H), 2.63–2.54 (m, 2H), 2.11 (td, *J* = 7.6, 1.0 Hz, 2H), 1.89 (q, *J* = 1.4 Hz, 3H), 1.67 (dd, *J* = 1.4, 0.6 Hz, 3H); ¹³C NMR (125 MHz, CDCl₃) δ 168.6, 142.5, 139.0, 127.4, 124.2, 59.5, 51.4, 39.1, 27.8, 20.8, 16.3; FTIR (Neat Film NaCl) 3365, 2951, 2917, 2853, 1704, 1651, 1457, 1362, 1196, 1128, 1085, 1015, 881, 822, 772 cm⁻¹; HRMS (ESI) *m/z* calc'd for C₁₁H₁₈O₃H [M+H]⁺: 199.1329, found 199.1331.



Pyrone ester 119. To a 0 °C solution of alcohol **118** (198 mg, 1.00 mmol) in MeCN (10 mL, 0.1 M) was added sequentially iodo-acid **56** (337 mg, 1.20 mmol) and DCC (248 mg, 1.20 mmol). The reaction mixture was stirred at 0 °C for 30 min. The still cold reaction was then filtered through a small pad of celite with MeCN to remove excess urea byproduct. The organics were then concentrated by rotary evaporation and purified by column chromatography (EtOAc in hexanes 9%→12% on silica) to give 386 mg (84%

yield) of pyrone ester **119** as a yellow oil; ^1H NMR (300 MHz, CDCl_3) δ 7.46 (d, $J = 9.7$ Hz, 1H), 6.07 (d, $J = 9.7$ Hz, 1H), 5.90 (tq, $J = 7.3, 1.5$ Hz, 1H), 5.35 (tq, $J = 7.1, 1.4$ Hz, 1H), 4.67 (d, $J = 7.1$ Hz, 2H), 3.77 (s, 2H), 3.73 (s, 3H), 2.59 (q, $J = 7.6$ Hz, 2H), 2.13 (t, $J = 7.6$ Hz, 2H), 1.89 (s, 3H), 1.71 (s, 3H); ^{13}C NMR (75 MHz, CDCl_3) δ 168.4, 166.8, 160.5, 158.1, 151.4, 142.7, 142.5, 127.4, 118.2, 116.3, 70.8, 62.7, 51.4, 42.7, 39.0, 27.7, 20.8, 16.6; FTIR (Neat Film NaCl) 3080, 3054, 2975, 2950, 2925, 2857, 1731, 1606, 1548, 1446, 1403, 1367, 1347, 1277, 1243, 1205, 1163, 1131, 1087, 1063, 1045, 1016, 962, 867, 821, 770, 727 cm^{-1} ; HRMS (ESI) m/z calc'd for $\text{C}_{18}\text{H}_{21}\text{IO}_6\text{H}$ $[\text{M}+\text{H}]^+$: 461.0456, found 461.0444.



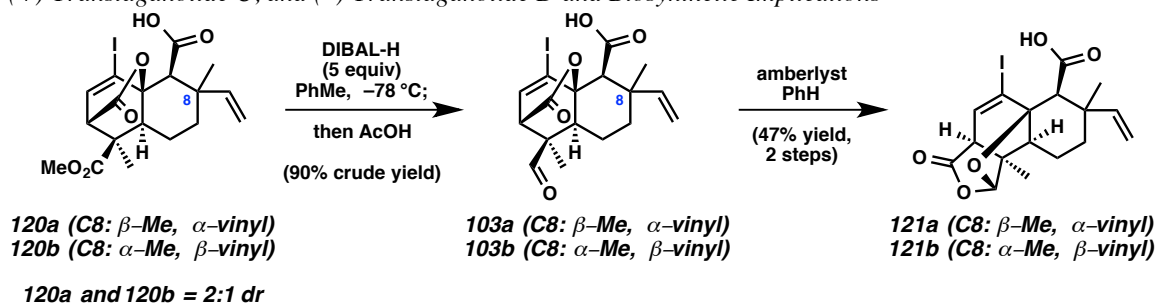
Tricyclic acids 120a and 120b. To a 23 °C solution of pyrone ester **119** (218 mg, 0.474 mmol) in toluene (2.03 mL, 0.233 M) in a 500 mL sealed tube was added BSA (231 μL , 0.948 mmol) and NEt_3 (5.00 μL , 0.047 mmol). The reaction mixture was heated to 110 °C and stirred for 20 min. The mixture was then cooled to 23 °C and diluted with toluene (250 mL). The reaction mixture was then re-heated to 100 °C and stirred for 13 d, until completion, which was determined after monitoring by NMR. The reaction mixture was then cooled to 23 °C and 0.02% $\text{HCl}_{(\text{aq})}$ (20 mL) was added and the mixture stirred vigorously for 1 min. The organic phase was then separated and washed with 0.02% $\text{HCl}_{(\text{aq})}$ (3 x 25 mL). Aqueous phases were then combined and back extracted

with ethyl acetate (3 x 30 mL). The organic phases were combined, dried with Na₂SO₄, and concentrated by rotary evaporation. The crude oil was purified by column chromatography (EtOAc in hexanes with 0.1% AcOH, 5%→30% on silica) to yield 151 mg (69% yield) of a 2:1 mixture of ICR/DA diastereomers **120a** and **120b** as a white solid. It is important to note that compounds **120a** and **120b**, and all subsequent compounds: **103a**, **103b**, **121a**, and **121b** have very poor solubility in most common organic solvents excluding EtOAc. Therefore all transfers of products **120a**, **120b**, **103a**, **103b**, **121a**, and **121b** should be accomplished using EtOAc and vessels should be repeatedly washed.

Major (120a): ¹H NMR (500 MHz, CDCl₃) δ 6.95 (d, *J* = 7.0 Hz, 1H), 5.99 (dd, *J* = 17.2, 10.8 Hz, 1H), 5.09–4.99 (m, 2H), 3.73 (s, 3H), 3.36 (d, *J* = 7.0 Hz, 1H), 2.95 (s, 1H), 1.90–1.38 (m, 5H), 1.28 (s, 3H), 1.26 (s, 3H); ¹³C NMR (125 MHz, CDCl₃) δ 173.5, 173.0, 168.9, 147.8, 139.7, 111.8, 99.9, 83.7, 59.2, 52.7, 51.4, 49.5, 49.2, 40.2, 38.0, 24.5, 20.7, 18.6.

Minor (120b): ¹H NMR (500 MHz, CDCl₃) δ 6.95 (d, *J* = 7.0 Hz, 1H), 6.34 (dd, *J* = 17.4, 11.0 Hz, 1H), 5.09–4.99 (m, 2H), 3.71 (s, 3H), 3.36 (d, *J* = 7.0 Hz, 1H), 2.90 (s, 1H), 1.90–1.38 (m, 5H), 1.35 (s, 3H), 1.26 (s, 3H); ¹³C NMR (125 MHz, CDCl₃) δ 173.4, 173.0, 168.8, 140.3, 140.0, 113.9, 99.4, 83.9, 60.7, 52.7, 51.5, 49.7, 49.3, 39.6, 38.6, 29.6, 24.5, 20.8.

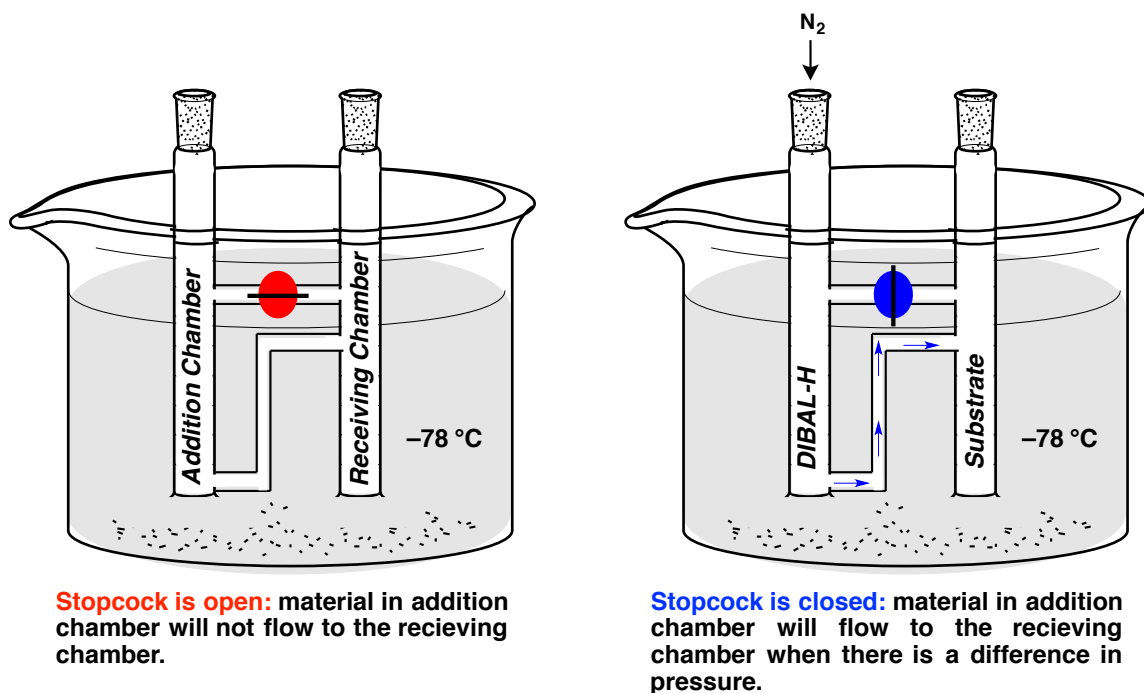
FTIR (Neat Film NaCl) 3083, 2950, 1770, 1732, 1713, 1456, 1434, 1413, 1381, 1309, 1277, 1237, 1165, 1115, 969, 934, 911, 872, 731 cm⁻¹; HRMS (Multimode-ESI/APCI) *m/z* calc'd for C₁₈H₂₁IO₆Na [M+Na]⁺: 483.0275, found 483.0261.



Tetracyclic acetals 121a and 121b. It is important to note that the selective single hydride reduction of the methyl esters of tricyclic acids **120a** and **120b** was only made possible using a glass cannula, as it allows for the precise temperature control necessary to effect the transformation on such a complex molecule bearing many electrophilic carbonyl functionalities (Figure 2.8.9). A solution of acids **120a** and **120b** (25 mg, 0.055 mmol) in toluene (550 μ L, 0.1M) was stirred in the receiving chamber of the glass cannula at -78 $^{\circ}$ C (the entire glass cannula is placed in a -78 $^{\circ}$ C bath submerging both chambers and the cannula itself). A freshly made 1M solution of DIBAL-H (270 μ L, 0.270 mmol) in toluene was added to the addition chamber of the glass cannula, further diluted with toluene (500 μ L), and stirred at -78 $^{\circ}$ C. Once both solutions and the entire glass cannula were sufficiently cooled, the -78 $^{\circ}$ C solution of DIBAL-H was slowly added to acids **120a** and **120b** dropwise. The reaction was stirred for 10 min and then slowly quenched by a -78 $^{\circ}$ C solution of AcOH (100 μ L) in toluene (1.5 mL) via the addition chamber of the glass cannula. Once complete, the reaction vessel was removed from the -78 $^{\circ}$ C bath, allowed to warm to 23 $^{\circ}$ C, and then diluted with ethyl acetate (10 mL). The solution was washed with a 1% aqueous solution of AcOH (3 x 2 mL) and the aqueous phases were combined and back extracted with ethyl acetate (2 x 2 mL). All organic phases were pooled, dried over Na_2SO_4 , and concentrated by rotary evaporation

to give 21 mg (90% crude yield) of the desired aldehydes **103a** and **103b** as an orange-brown solid. **103a** and **103b** were used immediately in the following step without further purification.

Figure 2.8.9. Reaction schematic for the single hydride reduction of tricyclic acids **120a** and **120b** using a glass cannula.



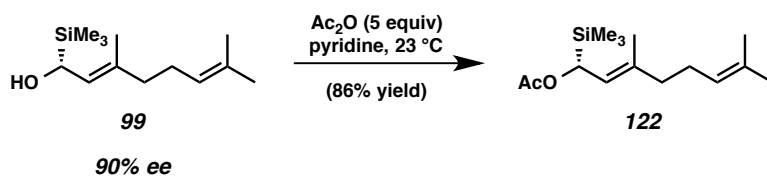
To a 23 °C solution of the crude aldehyde products **103a** and **103b** (21 mg, 0.049 mmol) in benzene (10 mL, 0.005 M) was added Amberlyst 15 (25 mg). The reaction was stirred for at 23 °C for 3 h and then filtered through a small pad of celite with EtOAc to remove the Amberlyst 15 resin. The organics were then washed with pH 2–3 water (0.02% HCl solution) (3 x 3 mL), and the aqueous phases were back extracted with ethyl acetate (2 x 6 mL). All organics were combined, dried over Na₂SO₄, and concentrated by rotary evaporation. Purification was accomplished by column chromatography (EtOAc in hexanes with 0.1% AcOH, 5%→30% on silica) to yield 11 mg (47% yield over two

steps) of a 2:1 mixture of the reduced, cyclized, and diastereomers **121a** and **121b** as a yellow solid.

Major (121a): $^1\text{H NMR}$ (500 MHz, CDCl_3) δ 6.69 (d, $J = 5.8$ Hz, 1H), 6.03 (dd, $J = 17.3, 10.8$ Hz, 1H), 5.75 (s, 1H), 5.10 (d, $J = 10.8$ Hz, 1H), 5.04 (d, $J = 17.4$ Hz, 1H), 3.08 (d, $J = 5.9$ Hz, 1H), 2.92 (s, 1H), 2.21–2.14 (m, 1H), 1.97–1.38 (m, 4H), 1.36 (s, 3H), 1.19 (s, 3H); $^{13}\text{C NMR}$ (125 MHz, CDCl_3) δ 173.1, 169.5, 147.1, 136.1, 112.3, 108.9, 107.3, 87.1, 61.5, 54.7, 49.1, 48.8, 39.7, 36.2, 20.1, 18.8, 15.9.

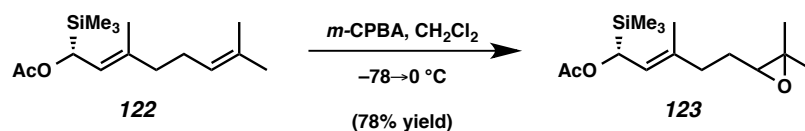
Minor (121b): $^1\text{H NMR}$ (500 MHz, CDCl_3) δ 6.69 (d, $J = 5.9$ Hz, 1H), 6.07 (dd, $J = 17.5, 11.1$ Hz, 1H), 5.67 (s, 1H), 5.12 (d, $J = 11.1$ Hz, 1H), 5.08 (d, $J = 17.5$ Hz, 1H), 3.07 (d, $J = 5.9$ Hz, 1H), 2.88 (s, 1H), 2.21–2.14 (m, 1H), 1.97–1.38 (m, 4H), 1.36 (s, 3H), 1.33 (s, 3H); $^{13}\text{C NMR}$ (125 MHz, CDCl_3) δ 173.2, 169.7, 139.5, 136.3, 114.6, 108.8, 107.0, 87.1, 63.1, 54.7, 49.3, 48.8, 39.4, 36.3, 29.6, 20.0, 15.8.

FTIR (Neat Film NaCl) 3300, 3077, 3007, 2958, 2933, 2873, 1785, 1748, 1708, 1456, 1375, 1286, 1239, 1217, 1199, 1182, 1157, 1115, 1083, 1046, 1034, 992, 964, 957, 910, 895, 873, 829, 814, 796, 752 cm^{-1} ; HRMS (Multimode-ESI/APCI) m/z calc'd for $\text{C}_{17}\text{H}_{20}\text{IO}_5$ $[\text{M}+\text{H}]^+$: 431.0350 found 431.0359; $[\alpha]_{\text{D}}^{20} = +18.71$ (c 0.94 in CHCl_3).



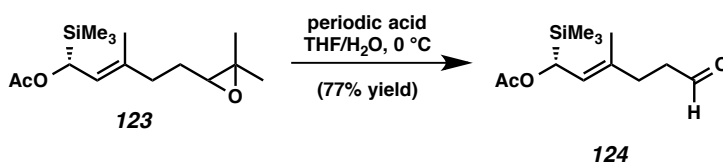
Allyl acetate 122. To a $0\text{ }^\circ\text{C}$ solution of **99** (256 mg, 1.13 mmol) in pyridine (11 mL, 0.1M) was added acetic anhydride ($534\text{ }\mu\text{L}$, 5.65 mmol). The reaction was allowed to warm to $23\text{ }^\circ\text{C}$ and was stirred for 6 h. The solution was then diluted with ethyl acetate

(30 mL) and quenched with saturated NaHCO₃ (10 mL). The organic layer was washed with saturated aqueous CuSO₄ (4 x 10 mL) until the dark blue color no longer persisted in the aqueous phase. This was followed by another saturated NaHCO₃ wash (10 mL), a brine wash (10 mL), and then drying over MgSO₄. Concentration by rotary evaporation gave a crude, colorless oil, which could be taken on without further purification. Purification, if desired, was by column chromatography (EtOAc in hexanes 2→10% on silica) to yield 260 mg (86% yield) of allyl acetate **122** as a colorless oil; ¹H NMR (300 MHz, CDCl₃) δ 5.42 (d, *J* = 10.4 Hz, 1H), 5.16 (dm *J* = 10.4 Hz, 1H), 5.10–5.00 (m, 1H), 2.18–1.94 (m, 7H), 1.66 (s, 6H), 1.59 (s, 3H), 0.02 (s, 9H); ¹³C NMR (125 MHz, CDCl₃) δ 171.1, 137.0, 131.7, 124.2, 121.7, 67.6, 40.0, 26.6, 25.9, 21.4, 17.9, 17.0, –3.7; FTIR (Neat Film NaCl) 2962, 2927, 2856, 1737, 1443, 1368, 1290, 1248, 1237, 1158, 1109, 1014, 957, 842, 750 cm⁻¹; HRMS (ESI) *m/z* calc'd for C₁₅H₂₉O₂Si [M]⁺: 268.1859, found 268.1863; [α]_D²⁰ = +49.50 (*c* 1.00 in CHCl₃).



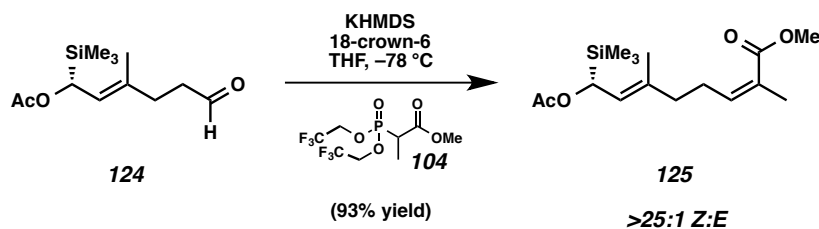
Epoxide 123. To a –78 °C solution of allyl acetate **122** (260 mg, 0.97 mmol) in CH₂Cl₂ (10 mL, 0.1M) was added *m*-CPBA (max 77% by weight) (240 mg, 1.07 mmol). The reaction was warmed to 0 °C and stirred for 30 min until complete, as determined by TLC analysis. The reaction was quenched with 10% aqueous Na₂SO₃ (5 mL) at 0 °C. The organic layer was then separated from the aqueous and washed again with 10% Na₂SO₃ (5 mL). The combined aqueous layers were then combined and back extracted with CH₂Cl₂ (3 x 10 mL). The combined organic layers were washed with saturated

NaHCO₃ (15 mL), brine (15 mL), and dried over MgSO₄. Concentration by rotary evaporation gave a crude oil, which was purified by column chromatography (EtOAc in hexanes 2%→10% on silica) to yield 215 mg (78% yield) of **123** as a colorless oil and a 1:1 mixture of diastereomers; ¹H NMR (500 MHz, CDCl₃) δ 5.40 (d, *J* = 10.3 Hz, 1H), 5.21 (d, *J* = 10.3, 1H), 2.69 (td, *J* = 6.5, 5.3 Hz, 1H), 2.24–2.05 (m, 2H), 2.02 (s, 3H), 1.71–2.05 (m, 3H), 1.68–1.56 (m, 2H), 1.30–1.24 (m, 6H), 0.02 (s, 9H); ¹³C NMR (125 MHz, CDCl₃) δ 171.04, 171.02, 136.3, 136.2, 122.2, 122.1, 67.4, 64.1, 58.49, 58.48, 36.64, 36.56, 27.7, 27.5, 25.03, 25.00, 21.3, 18.9, 18.8, 17.1, 16.9, –3.6; FTIR (Neat Film NaCl) 2960, 2928, 1736, 1732, 1446, 1377, 1369, 1323, 1291, 1248, 1238, 1123, 1046, 1015, 958, 842, 795, 751, 718 cm⁻¹; HRMS (ESI) *m/z* calc'd for C₁₅H₂₈O₃SiNa [M+Na]⁺: 307.1700, found 307.1706; [α]_D²⁰ = +34.03 (*c* 1.00 in CHCl₃).



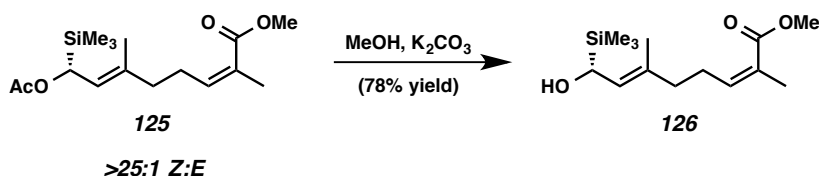
Aldehyde 124. To a solution of epoxide **123** (244 mg, 0.86 mmol) in THF (8.6 mL, 0.1M) and water (4.8 mL, 0.18M) at 0 °C was added periodic acid (391 mg, 1.72 mmol). The reaction was stirred for 7 h, diluted with Et₂O (25 mL), and quenched with saturated NaHCO₃ (10 mL). The aqueous layer was then separated from the organic and back extracted with Et₂O (2 x 10 mL). The combined organics were washed with saturated brine (3 x 15 mL), dried over MgSO₄, and concentrated by rotary evaporation. Purification by column chromatography (EtOAc in hexanes 5%→25% on silica) yielded 161 mg (77% yield) of aldehyde **124** as a colorless oil; ¹H NMR (300 MHz, CDCl₃) δ

9.74 (t, $J = 1.7$ Hz, 1H), 5.37 (d, $J = 10.3$ Hz, 1H), 5.18 (d, $J = 10.3$, 1H), 2.58–2.47 (m, 2H), 2.41–2.28 (m, 2H), 2.01 (s, 3H), 1.68 (s, 3H), 0.00 (s, 9H); ^{13}C NMR (75 MHz, CDCl_3) δ 202.1, 171.0, 134.9, 122.7, 67.3, 42.2, 32.0, 21.3, 17.1, –3.7; FTIR (Neat Film NaCl) 3432, 2958, 2902, 2823, 2720, 2479, 2113, 1732, 1415, 1368, 1291, 1248, 1142, 1115, 1046, 1016, 958, 842, 769, 752, 718 cm^{-1} ; HRMS (ESI) m/z calc'd for $\text{C}_{12}\text{H}_{22}\text{O}_3\text{SiNa}$ $[\text{M}+\text{Na}]^+$: 265.1230, found 265.1232; $[\alpha]_{\text{D}}^{20} = +41.93$ (c 1.00 in CHCl_3).



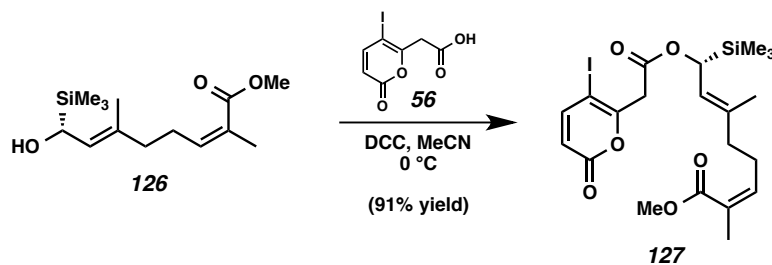
(Z)-Enone 125. To a $-78\text{ }^\circ\text{C}$ solution of KHMDS (35 mg, 0.18 mmol) in THF (2 mL) was added a solution of phosphonate reagent **104** (53.5 mg, 0.16 mmol) and 18-crown-6 (193.5 mg, 0.73 mmol) in THF (600 μL). After stirring the reaction mixture for 10 min at $-78\text{ }^\circ\text{C}$, a solution of aldehyde **124** (35.5 mg, 0.15 mmol) in THF (600 μL) was added. This brings the total volume of THF to 3.2 mL, which is a 0.05M solution with respect to the Still-Gennari Reagent **104**. The reaction was stirred at $-78\text{ }^\circ\text{C}$ for 20 min and then quenched with a saturated NH_4Cl solution (1 mL) at $-78\text{ }^\circ\text{C}$. After allowing the reaction mixture to warm to $23\text{ }^\circ\text{C}$, it was diluted with Et_2O (10 mL) and washed with saturated NH_4Cl (1 x 3 mL). Aqueous layers were combined and back extracted with Et_2O (2 x 3 mL). The combined organic layers were washed with saturated brine (10 mL), dried over MgSO_4 , and concentrated by rotary evaporation. Purification was accomplished by column chromatography (EtOAc in hexanes 2% \rightarrow 10% on silica) to

yield 42.5 mg (93% yield) >25:1, Z:E of enone **125** as a colorless oil; ^1H NMR (300 MHz, CDCl_3) δ 5.88 (t, $J = 7.2$ Hz, 1H), 5.39 (d, $J = 10.3$ Hz, 1H), 5.17 (d, $J = 10.5$ Hz, 1H), 3.72 (s, 3H), 2.58 (q, $J = 7.5$ Hz, 2H), 2.11 (t, $J = 7.3$ Hz, 2H), 2.02 (s, 3H), 1.88–1.85 (m, 3H), 1.67–1.66 (m, 3H), 0.01 (s, 9H); ^{13}C NMR (75 MHz, CDCl_3) δ 168.4, 143.0, 136.3, 127.2, 122.3, 67.4, 51.3, 39.4, 27.9, 21.3, 20.8, 16.9, –3.7; FTIR (Neat Film NaCl) 2954, 2928, 2855, 1722, 1649, 1453, 1434, 1368, 1289, 1248, 1238, 1199, 1131, 1104, 1085, 1015, 958, 842, 769, 751 cm^{-1} ; HRMS (ESI) m/z calc'd for $\text{C}_{16}\text{H}_{28}\text{O}_4\text{SiNa}$ $[\text{M}+\text{Na}]^+$: 335.1649, found 335.1648; $[\alpha]_{\text{D}}^{20} = +49.43$ (c 1.00 in CHCl_3).



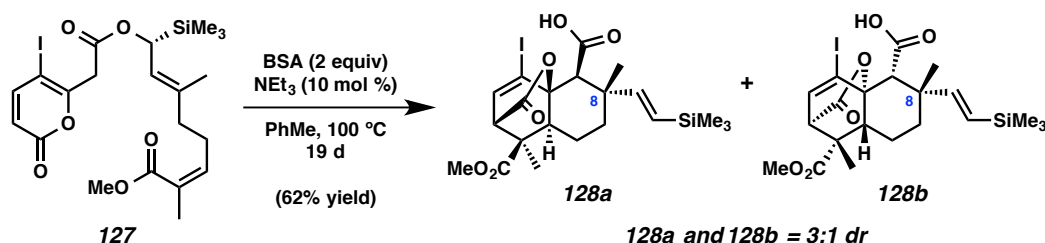
Alcohol 126. To a 23 °C solution of (Z)-enone **125** (143 mg, 0.46 mmol) in MeOH (10 mL, 0.05M) was added K_2CO_3 (32 mg, 0.23 mmol). The resulting suspension was then stirred for 2.5 d until complete deprotection was observed by TLC. Following completion, the reaction was diluted with Et_2O (100 mL) and washed with water (2 x 75 mL). The combined aqueous washes were back extracted with Et_2O (3 x 75 mL). The organic phases were combined, washed with saturated brine (100 mL), dried over MgSO_4 , and concentrated by rotary evaporation. Purification was accomplished by column chromatography (EtOAc in hexanes 5%→10% on silica) to yield 96 mg (78%) of >25:1, Z:E of alcohol **126** as a colorless oil; ^1H NMR (300 MHz, CDCl_3) δ 5.89 (t, $J = 7.3$ Hz, 1H), 5.27 (d, $J = 10.1$ Hz, 1H), 4.16 (d, $J = 10.1$ Hz, 1H), 3.71 (s, 3H), 2.63–2.52 (m, 2H), 2.11 (t, $J = 7.3$ Hz, 2H), 1.88–1.84 (m, 3H), 1.58 (d, $J = 1.2$ Hz, 3H), 0.01 (s,

9H); ^{13}C NMR (75 MHz, CDCl_3) δ 168.5, 142.9, 134.3, 127.2, 126.9, 64.5, 51.4, 39.5, 28.0, 20.8, 16.7, –4.0; FTIR (Neat Film NaCl) 3424, 2953, 2928, 2854, 1719, 1648, 1454, 1437, 1382, 1366, 1331, 1246, 1198, 1129, 1083, 1032, 978, 856, 841, 791, 749 cm^{-1} ; HRMS (ESI) m/z calc'd for $\text{C}_{14}\text{H}_{26}\text{O}_3\text{SiNa}$ $[\text{M}+\text{Na}]^+$: 293.1543, found 293.1538; $[\alpha]_{\text{D}}^{20} = +56.83$ (c 1.00 in CHCl_3).



Pyrone ester 127. To a 0 °C solution of alcohol **126** (297 mg, 1.10 mmol) in MeCN (11mL, 0.1M) were added sequentially pyrone acid **56** (339 mg, 1.21 mmol) and DCC (250 mg, 1.21 mmol). After 20 min at 0 °C the reaction was filtered through a short pad of celite, washing with MeCN. The filtrate was collected and concentrated by rotary evaporation. The crude oil was purified by column chromatography (EtOAc in hexanes 2%→10% on silica) to yield 534 mg (91% yield) of pyrone ester **127** as a yellow oil; ^1H NMR (300 MHz, CDCl_3) δ 7.46 (d, $J = 9.7$ Hz, 1H), 6.06 (d, $J = 9.7$ Hz, 1H), 5.88 (t, $J = 7.2$ Hz, 1H), 5.41 (d, $J = 10.4$ Hz, 1H), 5.16 (d, $J = 10.4$ Hz, 1H), 3.76 (s, 2H), 3.73 (s, 3H), 2.59 (td, $J = 7.3, 7.2$ Hz, 2H), 2.13 (t, $J = 7.3$ Hz, 2H), 1.87 (d, $J = 1.4$ Hz, 3H), 1.67 (d, $J = 1.3$ Hz, 3H), 0.01 (s, 9H); ^{13}C NMR (75 MHz, CDCl_3) δ 166.6, 160.5, 158.5, 151.4, 142.9, 137.3, 127.2, 121.5, 116.1, 70.5, 69.6, 51.4, 43.1, 39.4, 27.9, 20.9, 16.9, –3.7; FTIR (Neat Film NaCl) 2953, 2923, 2854, 1742, 1648, 1607, 1546, 1451, 1434, 1405, 1382, 1365, 1336, 1249, 1202, 1172, 1131, 1085, 1062, 1016, 960, 842, 764, 751,

729 cm⁻¹; HRMS (Multimode-ESI/APCI) m/z calc'd for C₂₁H₂₈IO₆Si [M–H]⁻: 531.0705, found 531.0712; [α]_D²⁰ = +17.79 (c 1.00 in CHCl₃).



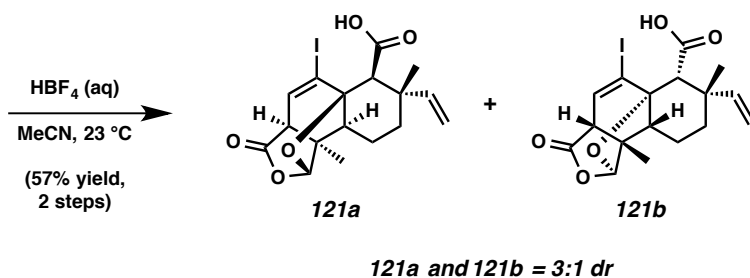
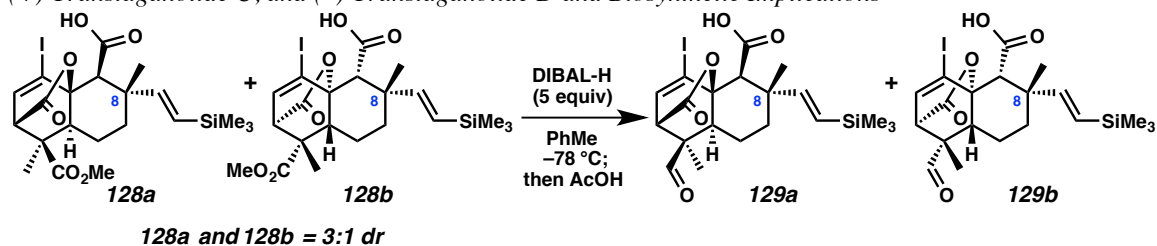
Vinyl silane 128a and 128b. To a 23 °C solution of pyrone ester **127** (298 mg, 0.56 mmol) in toluene (2.8 mL, 0.2M) in a 500 mL sealed tube was added BSA (274 μL, 1.12 mmol) and NEt₃ (8 μL, 0.06 mmol). The reaction mixture was heated to 110 °C and stirred for 20 min. The mixture was then cooled to 23 °C and diluted with toluene (450 mL), leaving ample headspace in the sealed tube to allow for solvent expansion. The reaction mixture was then re-heated to 100 °C and stirred for 19 d, until completion, which was determined after monitoring by NMR. The reaction mixture was then cooled to 23 °C and 0.02% HCl_(aq) (20 mL) was added and the mixture stirred vigorously for 1 min. The organic phase was then separated and washed with 0.02% HCl_(aq) (3 x 25 mL). Aqueous phases were then combined and back extracted with ethyl acetate (3 x 30 mL). The organic phases were combined, dried with Na₂SO₄, and concentrated by rotary evaporation. The crude oil was purified by column chromatography (EtOAc in hexanes with 0.1% AcOH, 5%→30% on silica) to yield 186 mg (62% yield) of a 3:1 mixture of ICR/DA diastereomers **128a** and **128b** as a yellow solid. It is important to note that compounds **128a** and **128b**, and all subsequent compounds **129a**, **129b**, **121a**, **121b**, **130a**, **130b**, **7**, and **8** have very poor solubility in most common organic solvents

excluding EtOAc. Therefore all transfers of products **128a**, **128b**, **129a**, **129b**, **121a**, **121b**, **130a**, **130b**, **7**, and **8** should be accomplished using EtOAc and vessels should be repeatedly washed.

Major (128a): ^1H NMR (500 MHz, CDCl_3) δ 6.96 (d, $J = 7.0$ Hz, 1H), 6.09 (d, $J = 18.8$ Hz, 1H), 5.64 (d, $J = 18.8$ Hz, 1H), 3.74 (s, 3H), 3.36 (d, $J = 7.0$ Hz, 1H), 2.96 (s, 1H), 1.98–1.36 (m, 5H), 1.27 (s, 6H), 0.06 (s, 9H); ^{13}C NMR (125 MHz, CDCl_3) δ 173.5, 172.1, 168.9, 154.9, 139.8, 125.8, 99.8, 83.8, 59.2, 52.7, 51.5, 49.5, 49.2, 41.4, 37.9, 24.6, 20.8, 18.7, –1.0.

Minor (128b): ^1H NMR (500 MHz, CDCl_3) δ 6.95 (d, $J = 6.9$ Hz, 1H), 6.41 (d, $J = 19.1$ Hz, 1H), 5.64 (d, $J = 19.1$ Hz, 1H), 3.70 (s, 3H), 3.34 (d, $J = 7.1$ Hz, 1H), 2.91 (s, 1H), 1.98–1.36 (m, 5H), 1.30 (s, 3H), 1.25 (s, 3H), 0.06 (s, 9H); ^{13}C NMR (125 MHz, CDCl_3) δ 173.3, 171.9, 168.0, 147.5, 140.1, 128.1, 99.2, 83.9, 61.2, 52.5, 51.5, 49.6, 49.0, 40.6, 37.6, 29.6, 24.6, 20.7, –1.1.

FTIR (Neat Film NaCl) 3077, 2952, 1773, 1736, 1611, 1492, 1459, 1453, 1382, 1309, 1276, 1247, 1184, 1161, 1122, 1047, 1019, 989, 970, 935, 870, 838, 783, 754 cm^{-1} ;
HRMS (Multimode-ESI/APCI) m/z calc'd for $\text{C}_{21}\text{H}_{30}\text{IO}_6\text{Si}$ $[\text{M}+\text{H}]^+$: 533.0851, found 533.0847; $[\alpha]_{\text{D}}^{20} = +10.47$ (c 1.00 in CHCl_3).



Tetracyclic acetals 121a and 121b. It is important to note that the selective single hydride reduction of the methyl esters of vinyl silanes **128a** and **128b** was only made possible using a glass cannula, as it allows for the precise temperature control necessary to effect the transformation on such a complex molecule bearing many electrophilic carbonyl functionalities (Figure 2.8.9). A solution of vinyl silanes **128a** and **128b** (31 mg, 0.06 mmol) in toluene (600 μ L, 0.1M) was stirred in the receiving chamber of the glass cannula at -78 $^{\circ}$ C (the entire glass cannula is placed in a -78 $^{\circ}$ C bath submerging both chambers and the cannula itself). A freshly made 1M solution of DIBAL-H (300 μ L, 0.30 mmol) in toluene was added to the addition chamber of the glass cannula, further diluted with toluene (500 μ L), and stirred at -78 $^{\circ}$ C. Once both solutions and the entire glass cannula were sufficiently cooled, the -78 $^{\circ}$ C solution of DIBAL-H was slowly added to vinyl silanes **128a** and **128b** dropwise. The reaction was stirred for 10 min and then slowly quenched by a -78 $^{\circ}$ C solution of AcOH (100 μ L) in toluene (2 mL) via the addition chamber of the glass cannula. Once complete, the reaction vessel was removed from the -78 $^{\circ}$ C bath, allowed to warm to 23 $^{\circ}$ C, and then diluted with ethyl

acetate (10 mL). The solution was washed with a 1% aqueous solution of AcOH (3 x 2 mL) and the aqueous phases were combined and back extracted with ethyl acetate (2 x 2 mL). All organic phases were pooled, dried over Na₂SO₄, and concentrated by rotary evaporation to give the desired aldehydes **129a** and **129b** as an orange-brown solid. **129a** and **129b** were used immediately in the following step without further purification.

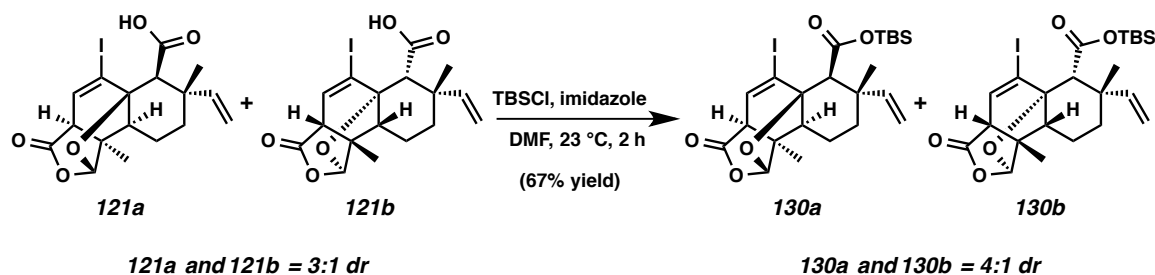
To a 23 °C solution of the crude aldehyde products (**129a** and **129b**) in MeCN (150 µL, 0.4M assuming quantitative yield from the reduction) was added aqueous HBF₄ (48% w/w, 100 µL, 0.78 mmol). The reaction was stirred at 23 °C for 8 h and then diluted with ethyl acetate (5 mL). This was washed with pH 2–3 water (0.02% HCl solution) (3 x 1 mL), and the aqueous phases were back extracted with ethyl acetate (2 x 1 mL). All organics were combined, dried over Na₂SO₄, and concentrated by rotary evaporation. Purification was accomplished by column chromatography (EtOAc in hexanes with 0.1% AcOH, 5%→30% on silica) to yield 15 mg (57% yield over two steps) of a 3:1 mixture of the reduced, cyclized, and desilylated diastereomers **121a** and **121b** as a yellow solid.

Major (121a): ¹H NMR (500 MHz, CDCl₃) δ 6.69 (d, *J* = 5.8 Hz, 1H), 6.03 (dd, *J* = 17.3, 10.8 Hz, 1H), 5.75 (s, 1H), 5.10 (d, *J* = 10.8 Hz, 1H), 5.04 (d, *J* = 17.4 Hz, 1H), 3.08 (d, *J* = 5.9 Hz, 1H), 2.92 (s, 1H), 2.21–2.14 (m, 1H), 1.97–1.38 (m, 4H), 1.36 (s, 3H), 1.19 (s, 3H); ¹³C NMR (125 MHz, CDCl₃) δ 173.1, 169.5, 147.1, 136.1, 112.3, 108.9, 107.3, 87.1, 61.5, 54.7, 49.1, 48.8, 39.7, 36.2, 20.1, 18.8, 15.9.

Minor (121b): ¹H NMR (500 MHz, CDCl₃) δ 6.69 (d, *J* = 5.9 Hz, 1H), 6.07 (dd, *J* = 17.5, 11.1 Hz, 1H), 5.67 (s, 1H), 5.12 (d, *J* = 11.1 Hz, 1H), 5.08 (d, *J* = 17.5 Hz, 1H), 3.07 (d, *J* = 5.9 Hz, 1H), 2.88 (s, 1H), 2.21–2.14 (m, 1H), 1.97–1.38 (m, 4H), 1.36 (s,

3H), 1.33 (s, 3H); ^{13}C NMR (125 MHz, CDCl_3) δ 173.2, 169.7, 139.5, 136.3, 114.6, 108.8, 107.0, 87.1, 63.1, 54.7, 49.3, 48.8, 39.4, 36.3, 29.6, 20.0, 15.8.

FTIR (Neat Film NaCl) 3300, 3077, 3007, 2958, 2933, 2873, 1785, 1748, 1708, 1456, 1375, 1286, 1239, 1217, 1199, 1182, 1157, 1115, 1083, 1046, 1034, 992, 964, 957, 910, 895, 873, 829, 814, 796, 752 cm^{-1} ; HRMS (Multimode-ESI/APCI) m/z calc'd for $\text{C}_{17}\text{H}_{20}\text{IO}_5$ $[\text{M}+\text{H}]^+$: 431.0350 found 431.0359; $[\alpha]_{\text{D}}^{20} = +18.71$ (c 0.94 in CHCl_3).



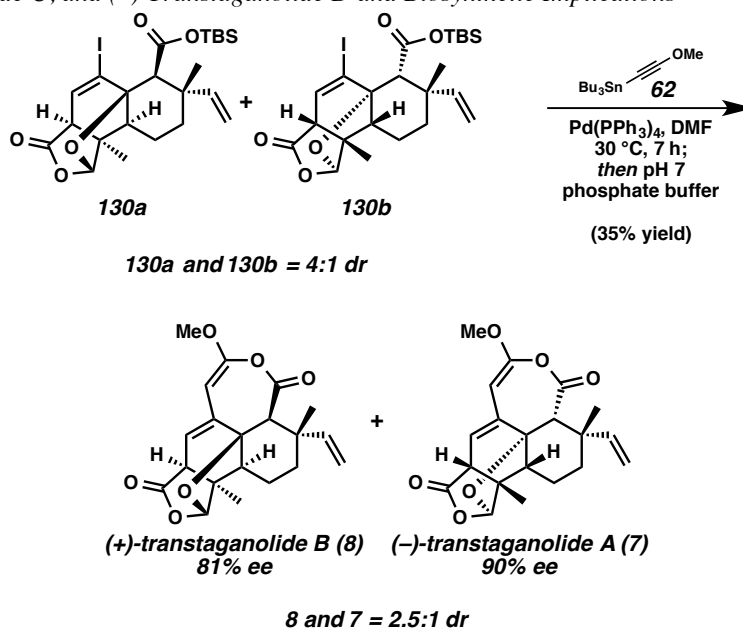
TBS-ester 130a and 130b. To a 23 °C solution of acetals **121a** and **121b** (15 mg, 0.034 mmol) in DMF (600 μL , 0.055M) were added sequentially imidazole (14 mg, 0.21 mmol) and TBSCl (21 mg, 0.14 mmol). The reaction was stirred at 23 °C for 2 h. The reaction mixture was then diluted with saturated brine (2 mL) and extracted with EtOAc/hexanes (1:1) (4 x 3 mL). The combined organic extracts were washed with saturated aqueous NaHCO_3 (3 mL) and then with brine (2 x 3 mL). The combined organics were dried over Na_2SO_4 and concentrated by rotary evaporation. The crude oil was purified by column chromatography (EtOAc in hexanes 10% \rightarrow 50% on silica) to yield 12.5 mg (67% yield) of a 4:1 mixture of diastereomers **130a** and **130b** as a white solid.

Major (130a): ^1H NMR (500 MHz, CDCl_3) δ 6.61 (d, $J = 6.0$ Hz, 1H), 6.00 (dd, $J = 17.4, 10.7$ Hz, 1H), 5.68 (s, 1H), 4.99 (d, $J = 10.7$ Hz, 1H), 4.98 (d, $J = 17.4$ Hz, 1H),

2.98 (dd, $J = 6.0, 0.8$ Hz, 1H), 2.80 (s, 1H), 2.08–2.00 (m, 1H), 1.90–1.35 (m, 4H), 1.29 (s, 3H), 1.18 (s, 3H), 0.92 (s, 9H), 0.31 (s, 3H), 0.25 (s, 3H); ^{13}C NMR (125 MHz, CDCl_3) δ 174.4, 169.7, 149.2, 135.4, 110.9, 110.0, 109.8, 87.0, 61.1, 55.1, 49.5, 48.7, 40.0, 37.4, 25.7, 20.6, 18.2, 17.7, 16.0, –4.7.

Minor (130b): ^1H NMR (500 MHz, CDCl_3) δ 6.61 (d, $J = 6.1$ Hz, 1H), 6.26 (dd, $J = 17.6, 11.0$ Hz, 1H), 5.58 (s, 1H), 5.03 (dd, $J = 11.0, 1.1$ Hz, 1H), 4.97 (dd, $J = 17.6, 1.1$ Hz, 1H), 2.96 (dd, $J = 6.1, 0.9$ Hz, 1H), 2.72 (s, 1H), 2.08–2.00 (m, 1H), 1.90–1.35 (m, 4H), 1.32 (s, 3H), 1.26 (s, 3H), 0.93 (s, 9H), 0.31 (s, 3H), 0.25 (s, 3H); ^{13}C NMR (125 MHz, CDCl_3) δ 174.5, 169.9, 141.4, 135.6, 112.8, 109.9, 109.4, 87.0, 62.6, 55.1, 49.6, 48.9, 39.6, 37.7, 30.4, 25.6, 20.6, 17.6, 15.9, –4.8.

FTIR (Neat Film NaCl) 3083, 2930, 2857, 1784, 1716, 1638, 1601, 1471, 1463, 1413, 1390, 1362, 1338, 1317, 1282, 1250, 1235, 1222, 1196, 1183, 1160, 1144, 1115, 1084, 1049, 1036, 1000, 960, 942, 908, 895, 884, 868, 843, 828, 816, 787, 752 cm^{-1} ; HRMS (Multimode-ESI/APCI) m/z calc'd for $\text{C}_{23}\text{H}_{34}\text{IO}_5\text{Si}$ $[\text{M}+\text{H}]^+$: 545.1215, found 545.1218; $[\alpha]_{\text{D}}^{20} = +49.09$ (c 1.00 in CHCl_3).



Transtaganolides B and A (8 and 7). In a nitrogen filled glovebox, to a solution of TBS-esters **130a** and **130b** (9 mg, 0.0165 mmol) and Pd(PPh₃)₄ (21 mg, 0.018 mmol) in DMF (165 μL, 0.1M) was added tributyl(2-methoxyethyl)stannane (**62**) (22 mg, 0.066 mmol). The heterogeneous reaction mixture was vigorously stirred at 31 °C for 7.5 h. The reaction mixture was then filtered through a Kimwipe with MeCN (1.5 mL) (this removes a large excess of the undissolved Pd(PPh₃)₄) and removed from the glovebox. pH 7 phosphate buffer (75 μL) was added to the MeCN solution, which was then vigorously stirred for 36 h. The reaction was then concentrated by rotary evaporation, so as to remove some of the copious amounts of MeCN, and then diluted with EtOAc (2 mL). This was then washed with water (3 x 750 μL) and the combined aqueous washes were back extracted with EtOAc (2 x 750 μL). All organics were pooled, dried with Na₂SO₄, and concentrated by rotary evaporation. The crude oil was purified by normal phase HPLC to yield 1.5 mg (25% yield) of transtaganolide B (**8**) and 0.6 mg (10% yield) of transtaganolide A (**7**) as white powders.

Transtaganolide B (8): ^1H NMR (500 MHz, CDCl_3) δ 5.80 (dd, $J = 17.4, 10.8$ Hz, 1H), 5.65 (t, 0.8 Hz, 1H), 5.58 (dd, $J = 6.0, 1.1$ Hz, 1H), 5.05 (dd, $J = 17.4, 0.6$ Hz, 1H), 5.02 (d, $J = 10.8, 0.6$ Hz, 1H), 4.96 (t, 0.8 Hz, 1H), 3.68 (s, 3H), 3.12 (dt, $J = 6.0, 0.9$ Hz, 1H), 3.08 (s, 1H), 1.94 (dd, $J = 12.3, 6.3$ Hz, 1H), 1.72 (ddt, $J = 13.1, 6.3, 3.3$ Hz, 1H), 1.63 (ddd, $J = 13.1, 3.9, 2.7$ Hz, 1H), 1.55 (s, 3H), 1.55–1.35 (m, 2H), 1.33 (s, 3H); ^{13}C NMR (125 MHz, CDCl_3) δ 175.6, 163.8, 154.5, 146.7, 144.2, 119.4, 112.7, 109.8, 87.7, 84.4, 56.5, 51.6, 49.8, 49.5, 48.8, 38.1, 37.0, 20.1, 19.4, 15.9; FTIR (Neat Film NaCl) 2948, 2931, 2874, 2855, 1782, 1668, 1447, 1372, 1348, 1324, 1296, 1252, 1237, 1167, 1109, 1059, 1024, 999, 966, 912, 897, 843, 812, 736 cm^{-1} ; HRMS (Multimode-ESI/APCI) m/z calc'd for $\text{C}_{20}\text{H}_{21}\text{O}_6$ $[\text{M}-\text{H}]^-$: 357.1344, found 357.1356; $[\alpha]_{\text{D}}^{20} = +207.93$ (c 0.15, CHCl_3 , 81% ee); SFC conditions: 30% IPA, 2.5 mL/min, AD-H column, t_{R} (min): major = 2.83, minor = 4.68.

Figure 2.8.10. Racemic SFC trace of transtaganolide B (8).

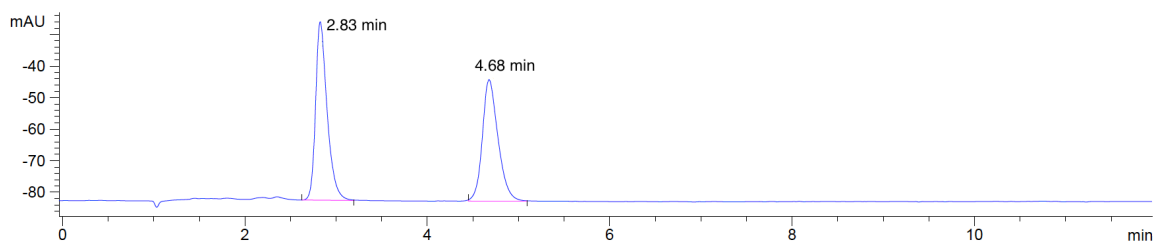
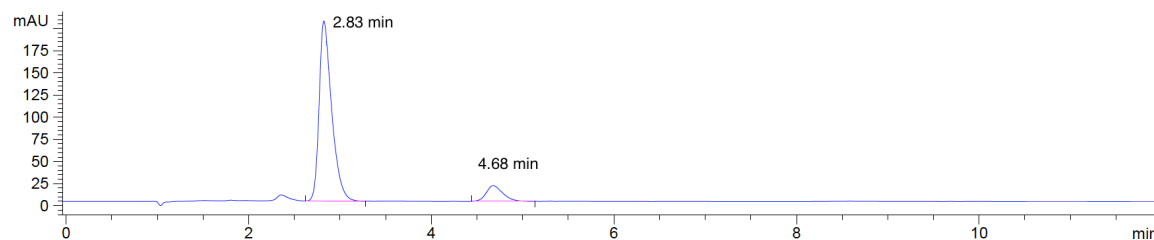


Figure 2.8.11. Enantioenriched SFC trace of transtaganolide B (8).



Transtaganolide A (7): ^1H NMR (500 MHz, CDCl_3) δ 6.90 (dd, $J = 17.9, 11.1$ Hz, 1H), 5.62 (s, 1H), 5.60 (dd, $J = 5.9, 1.0$ Hz, 1H), 5.12 (ddd, $J = 11.1, 1.1, 0.6$ Hz, 1H),

5.03 (dd, $J = 17.9, 1.1$ Hz, 1H), 4.98 (s, 1H), 3.70 (s, 3H), 3.11 (dt, $J = 5.9, 0.8$ Hz, 1H), 2.98 (s, 1H), 1.95 (dd, $J = 12.3, 6.3$ Hz, 1H), 1.83 (ddd, $J = 12.9, 3.7, 2.6$ Hz, 1H), 1.60–1.30 (m, 3H), 1.30 (s, 3H), 1.22 (s, 3H); ^{13}C NMR (125 MHz, CDCl_3) δ 175.6, 164.1, 154.5, 143.9, 143.8, 119.6, 111.8, 109.8, 87.6, 84.5, 56.5, 52.8, 51.6, 49.7, 48.8, 39.4, 38.3, 28.6, 20.1, 15.8; FTIR (Neat Film NaCl) 2963, 2922, 2852, 1780, 1670, 1453, 1348, 1323, 1259, 1236, 1167, 1113, 1058, 1021m 999, 973, 959, 921, 840, 808, 731 cm^{-1} ; HRMS (Multimode-ESI/APCI) m/z calc'd for $\text{C}_{20}\text{H}_{21}\text{O}_6$ $[\text{M}-\text{H}]^-$: 357.1344, found 357.1356; $[\alpha]_{\text{D}}^{20} = -98.76$ (c 0.06, CHCl_3 , 90% ee); SFC conditions: 30% IPA, 2.5 mL/min, AD-H column, t_{R} (min): minor = 3.20, major = 4.97.

Figure 2.8.12. Racemic SFC trace of transtaganolide A (7).

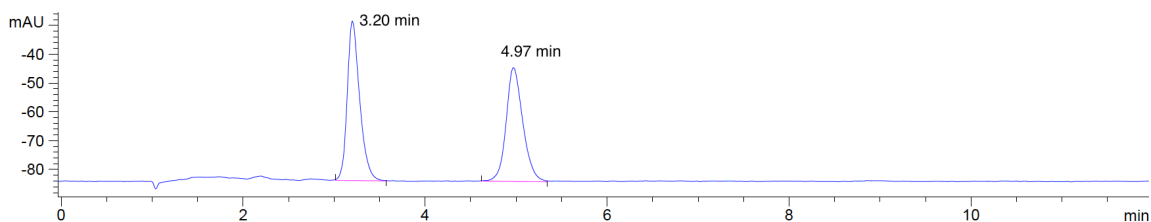
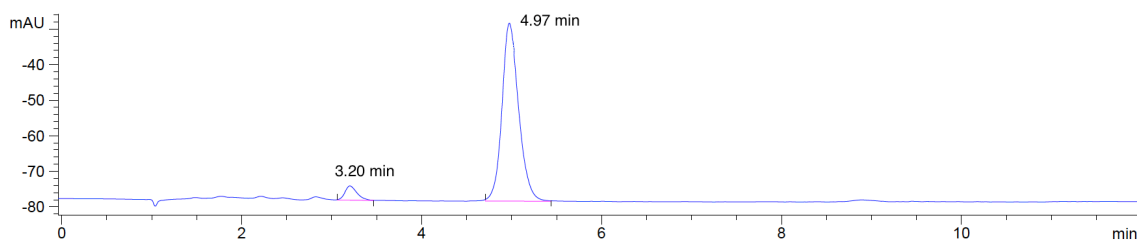
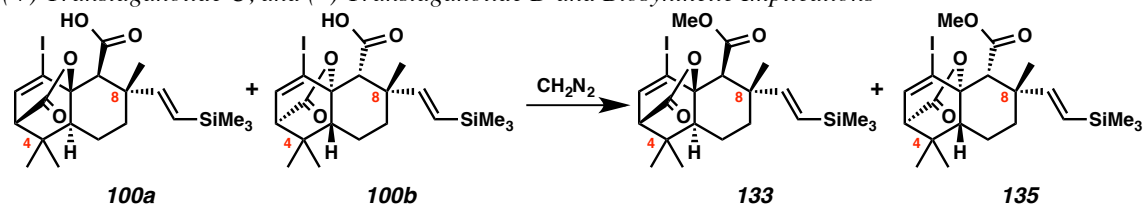


Figure 2.8.13. Enantioenriched SFC trace of transtaganolide A (7).





Methyl esters 133 and 135: Diazomethane in a solution of Et₂O was added dropwise to a 0.1M solution of the acids **100a** and **100b** at 0 °C. This was done using flame polished pipettes, glassware containing no ground glass joints, and open top to avoid detonation. The diazomethane was added until the yellow color of diazomethane persisted in the reaction solution. The reaction was then stirred for an additional 35 min, until the lemon-lime color faded, and all unreacted diazomethane had evaporated into the well-ventilated hood. The reaction was then concentrated by rotary evacuation and purified by preparatory HPLC, to separate diastereomers **133** and **135**. The major diastereomer (**133**) was crystallized by slow evaporation from pentanes in order to obtain crystals suitable for X-ray diffraction.

Major (133): ¹H NMR (500 MHz, CDCl₃) δ 6.92 (d, *J* = 6.8 Hz, 1H), 6.10 (d, *J* = 18.9 Hz, 1H), 5.59 (d, *J* = 18.9 Hz, 1H), 3.61 (s, 3H), 2.97 (s, 1H), 2.94 (d, *J* = 6.8 Hz, 1H), 1.70–1.40 (m, 4H), 1.34 (dd, *J* = 12.0, 5.3 Hz, 1H), 1.23 (s, 3H), 1.08 (s, 3H), 1.00 (s, 3H), 0.08 (s, 9H); ¹³C NMR (125 MHz, CDCl₃) δ 171.0, 169.3, 156.1, 140.3, 124.5, 98.0, 84.7, 59.0, 56.9, 51.2, 48.3, 41.5, 38.2, 37.0, 30.0, 24.7, 20.9, 18.4, –0.9; FTIR (Neat Film NaCl) 2953, 2923, 2848, 1746, 1612, 1464, 1454, 1392, 1386, 1365, 1352, 1302, 1246, 1209, 1196, 1167, 1141, 1052, 1011, 993, 976, 965, 939, 868, 838, 796, 756 cm⁻¹; HRMS (Multimode-ESI/APCI) *m/z* calc'd for C₂₁H₃₂IO₄Si [M+H]⁺: 503.1109 found 503.1113; [α]_D²⁰ = +34.50 (*c* 0.24 in CHCl₃); MP: 125–130 °C.

Minor (135): ^1H NMR (500 MHz, CDCl_3) δ 6.89 (d, $J = 6.8$ Hz, 1H), 6.48 (d, $J = 19.2$ Hz, 1H), 5.57 (d, $J = 19.2$ Hz, 1H), 3.68 (s, 3H), 2.90 (d, $J = 6.8$ Hz, 1H), 2.87 (s, 1H), 1.96 (dt, $J = 13.7, 3.4$ Hz, 1H), 1.66–1.51 (m, 2H), 1.41 (td, $J = 13.5, 3.4$ Hz, 1H), 1.34 (dd, $J = 12.6, 5.0$ Hz, 1H), 1.27 (s, 3H), 1.02 (s, 3H), 0.97 (s, 3H), 0.06 (s, 9H); ^{13}C NMR (125 MHz, CDCl_3) δ 170.4, 169.6, 148.9, 140.4, 126.6, 110.1, 97.7, 84.5, 61.1, 57.0, 51.7, 48.3, 40.8, 38.3, 37.2, 30.0, 24.6, 20.9, –1.1; FTIR (Neat Film NaCl) 2952, 2893, 1760, 1745, 1608, 1455, 1435, 1394, 1372, 1354, 1304, 1246, 1224, 1190, 1168, 1149, 1137, 1102, 1047, 1012, 994, 955, 869, 838, 799, 755, 737, 727 cm^{-1} ; HRMS (Multimode-ESI/APCI) m/z calc'd for $\text{C}_{21}\text{H}_{32}\text{IO}_4\text{Si}$ $[\text{M}+\text{H}]^+$: 503.1109 found 503.1119; $[\alpha]_{\text{D}}^{20} = -82.77$ (c 0.37 in CHCl_3).

2.9 NOTES AND REFERENCES

Note: Portions of this chapter have been published, see: Nelson, H. M.; Gordon, J. R.; Virgil, S. C.; Stoltz, B. M. *Angew. Chem. Int. Ed.* **2013**, *52*, 6699–6703.

- (1) Saouf, A.; Guerra, F. M.; Rubal, J. J.; Moreno-Dorado, F. J.; Akssira, M.; Mellouki, F.; López, M.; Pujadas, A. J.; Jorge, Z. D.; Massanet, G. M. *Org. Lett.* **2005**, *7*, 881–884.
- (2) Nelson, H. M.; Murakami, K.; Virgil, S. C.; Stoltz, B. M. *Angew. Chem. Int. Ed.* **2011**, *50*, 3688–3691.
- (3) (a) Nelson, H. M.; Stoltz, B. M. *Tetrahedron Lett.* **2009**, *50*, 1699–1701; (b) Larsson, R.; Sterner, O.; Johansson, M. *Org. Lett.* **2009**, *11*, 657–660.
- (4) Rubal, J. J.; Moreno-Dorado, F. J.; Guerra, F. M.; Jorge, Z. D.; Saouf, A.; Akssira, M.; Mellouki, F.; Romero-Garrido, R.; Massanet, G. M. *Phytochemistry* **2007**, *68*, 2480–2486.
- (5) All attempts to utilize reported methods for asymmetric ester-enolate-Claisen rearrangements were unsuccessful: (a) Corey, E. J.; Lee, D. H. *J. Am. Chem. Soc.* **1991**, *113*, 4026–4028; (b) Kazmaier, U.; Krebs, A. *Angew. Chem. Int. Ed.* **1995**, *34*, 2012–2014.
- (6) Ireland, R. E.; Varney, M. D. *J. Am. Chem. Soc.* **1984**, *106*, 3668–3670.
- (7) (a) Zeng, W.; Fröhlich, R.; Hoppe, D. *Tetrahedron* **2005**, *61*, 3281–3287; (b) Hoppe has reported that longer reaction times result in higher yields but lower ee's: i.e. 1.5 h = 37% yield, 87% ee; and 3 h = 76% yield, 77% ee. In our hands, using the 3 h procedure outlined by Hoppe and coworkers, we observed

consistently higher ee's for this extended reaction time, which is necessary to drive the reaction to completion. Reproducibility was somewhat of a challenge as ee's varied from values as high as 90% ee and as low as 82% ee for the 3 h reaction time. In all reactions the (–)-sparteine was dried and distilled from CaH₂ by kugelrohr distillation. We believe the variability in ee results directly from the quality of the distilled (–)-sparteine used in the reaction.

- (8) Even under mild esterification conditions, i.e., low-temperature DCC coupling, olefin isomerization would occur. Compounding the issue was a difficult separation of the *E* and *Z* isomers via chromatography. Ultimately, the isomers were separated by HPLC, however, any attempts to induce the Ireland–Claisen rearrangement resulted in isomerization as well.
- (9) (a) Gordon, J.; Hamilton, C.; Hooper, A. M.; Ibbotson, H. C.; Kurosawa, S.; Mori, K.; Muto, S.; Pickett, J. A. *Chem. Comm.* **1999**, 2335–2336; (b) Imamura, Y.; Takikawa, H.; Mori, K. *Tetrahedron Lett.* **2002**, *43*, 5743–5746.
- (10) Still, W. C.; Gennari, C. *Tetrahedron Lett.* **1983**, *24*, 4405–4408.
- (11) Snyder, S. A.; Treitler, D. S. *Angew. Chem. Int. Ed.* **2009**, *48*, 7899–7903.
- (12) Fillion, E.; Beingessner, R. L. *J. Org. Chem.* **2003**, *68*, 9485–9488.
- (13) Sogo, S. G.; Widlanski, T. S.; Hoare, J. H.; Grimshaw, C. E.; Berchtold, G. A.; Knowles, J. R. *J. Am. Chem. Soc.* **1984**, *106*, 2701–2703.
- (14) Batista, J. M.; López, S. N.; Da Silva Mota, J.; Vanzolini, K. L.; Cass, Q. B.; Rinaldo, D.; Vilegas, W.; Da Silva Bolzani, V.; Kato, M. J.; Furlan, M. *Chirality* **2009**, *21*, 799–801.

- (15) Kozytska, M. V.; Dudley, G. B. *Tetrahedron Lett.* **2008**, *49*, 2899–2901.
- (16) (a) Ireland, R. E.; Wipf, P.; Xiang, J. N. *J. Org. Chem.* **1991**, *56*, 3572–3582; (b) Gul, S.; Schoenebeck, F.; Aviyente, V.; Houk, K. N. *J. Org. Chem.* **2010**, *75*, 2115–2118.
- (17) Comparison of CD spectra to the bulk material confirmed that the mounted crystal represented the major enantiomer in the 90% ee bulk.
- (18) Appendino, G.; Prosperini, S.; Valdivia, C.; Ballero, M.; Colombano, G.; Billington, R. A.; Genazzani, A. A.; Sterner, O. *J. Nat. Prod.* **2005**, *68*, 1213–1217.
- (19) Subsequent to submission of this manuscript Prof. Giovanni Appendino generously provided our group with an authentic sample of the structurally, and presumably biosynthetically, related basiliolide B (**11**).¹⁷ Comparison to racemic synthetic basiliolide B (see ref. 16b) by chiral phase chromatography clearly demonstrated that naturally occurring basiliolide B is enantiopure upon isolation. Furthermore, consistent in magnitude with the enantioenriched synthetic transtaganolides, the specific rotation of natural basiliolide B was measured as -173° (0.24 c).
- (20) Extensive efforts were made to obtain authentic samples of **7–10** from the isolation chemists to no avail.

APPENDIX 4

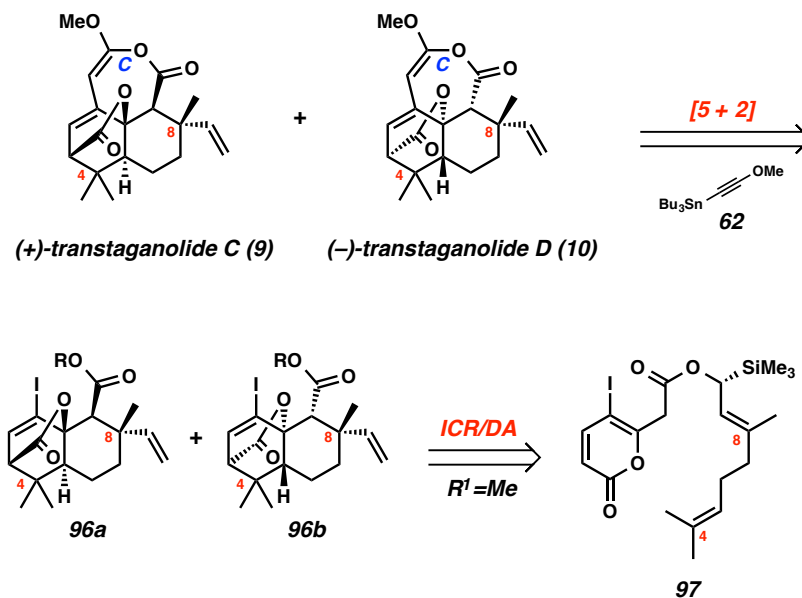
Synthetic Summary for (–)-Transtaganolide A, (+)-Transtaganolide B,

(+)-Transtaganolide C, and (–)-Transtaganolide D:

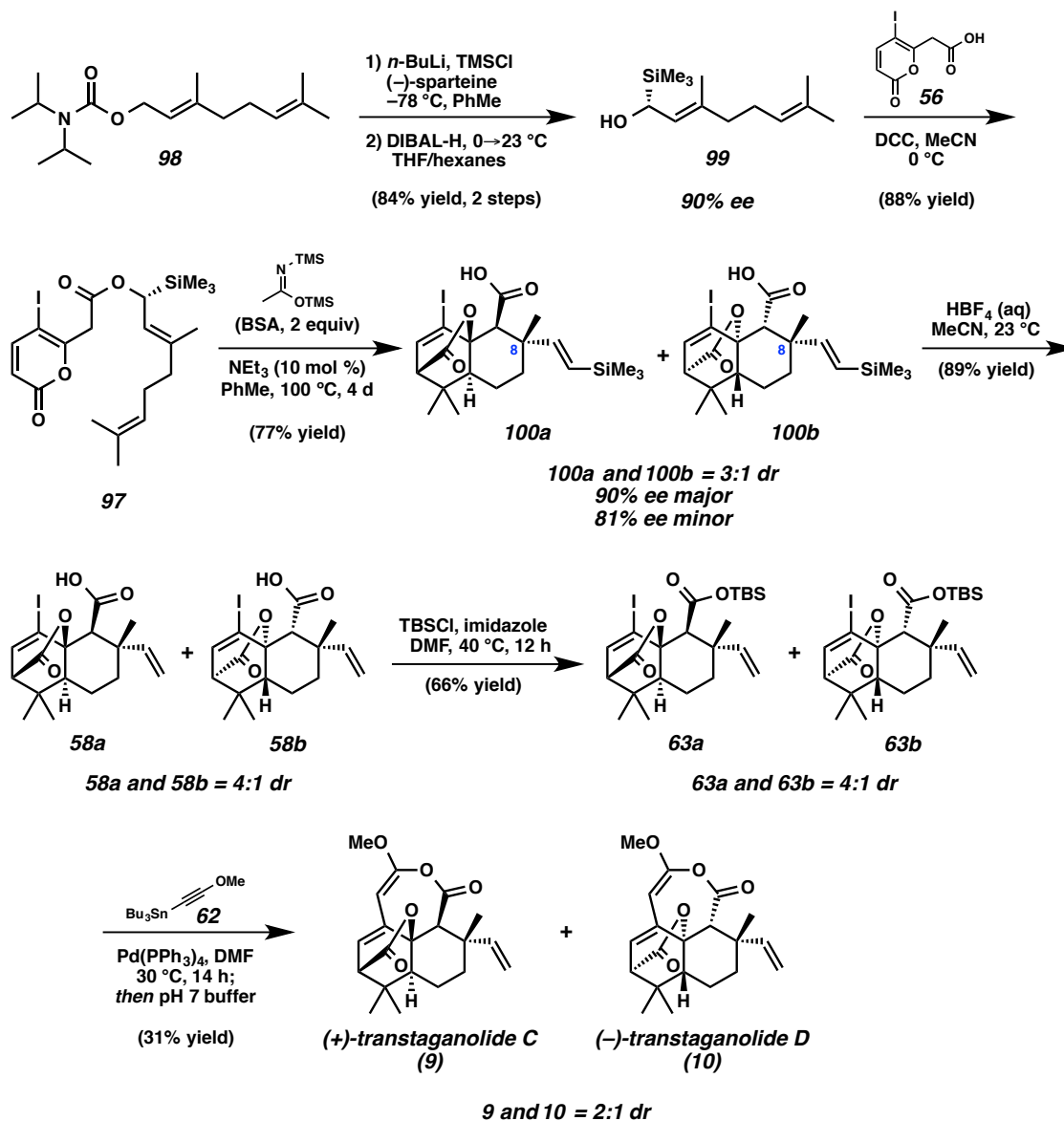
Relevant to Chapter 2

A4.1 SYNTHETIC SUMMARY FOR (+)-TRANSTAGANOLIDE C AND (–)- TRANSTAGANOLIDE D

Scheme 4.1.1. Retrosynthetic analysis for (+)-transtaganolide C (**9**) and (–)-transtaganolide D (**10**).

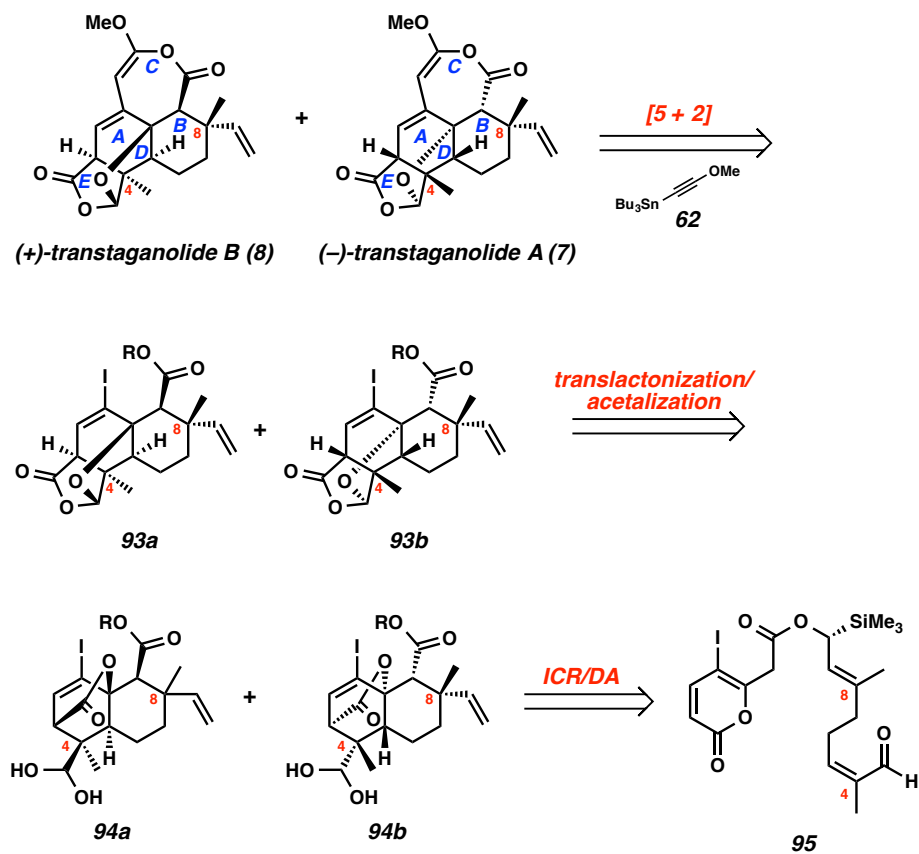


Scheme 4.1.2. Syntheses of (+)-transtaganolide C (**9**) and (–)-transtaganolide D (**10**).

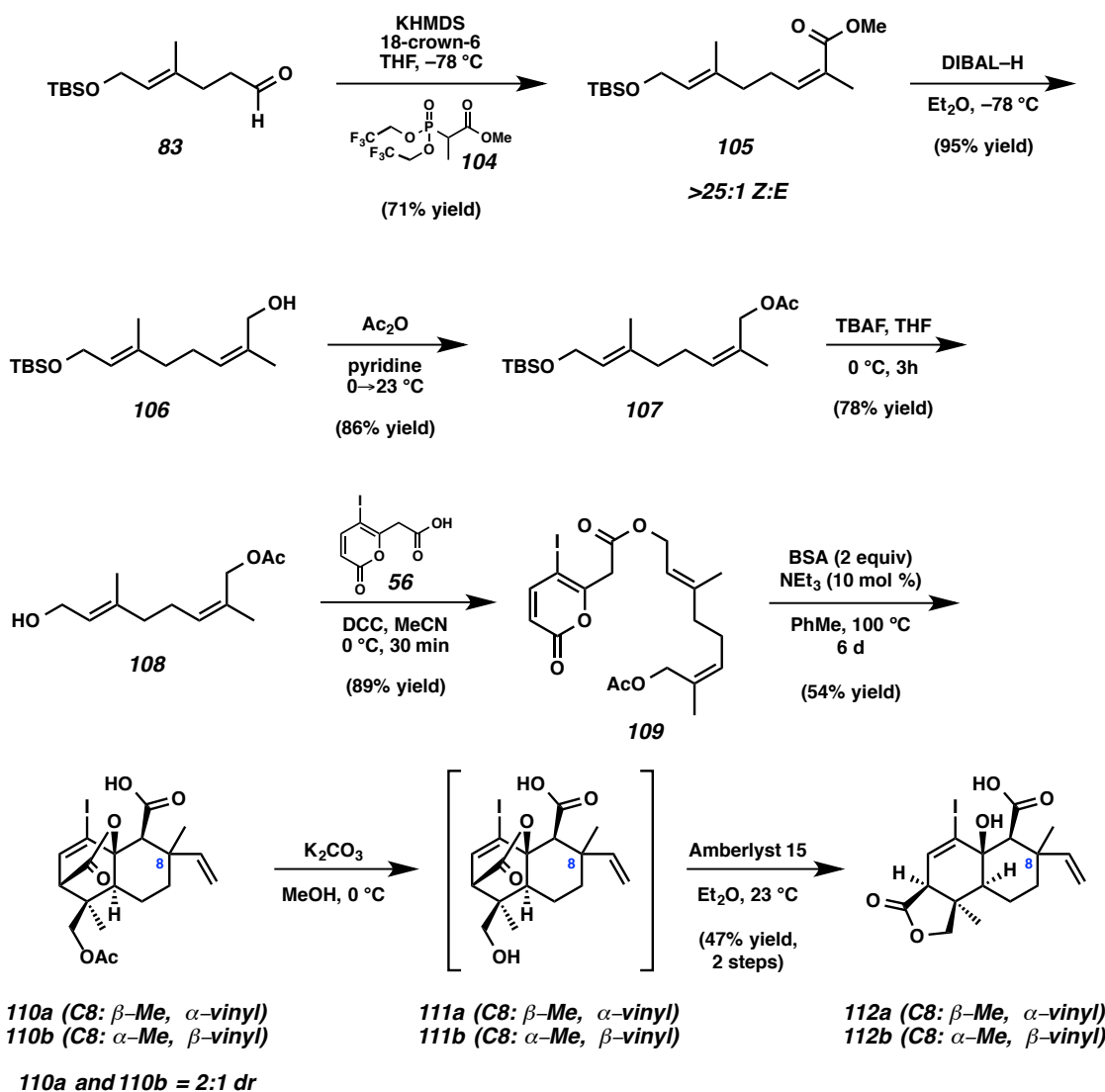


A4.2 SYNTHETIC SUMMARY FOR (–)-TRANSTAGANOLIDE A AND (+)-TRANSTAGANOLIDE B

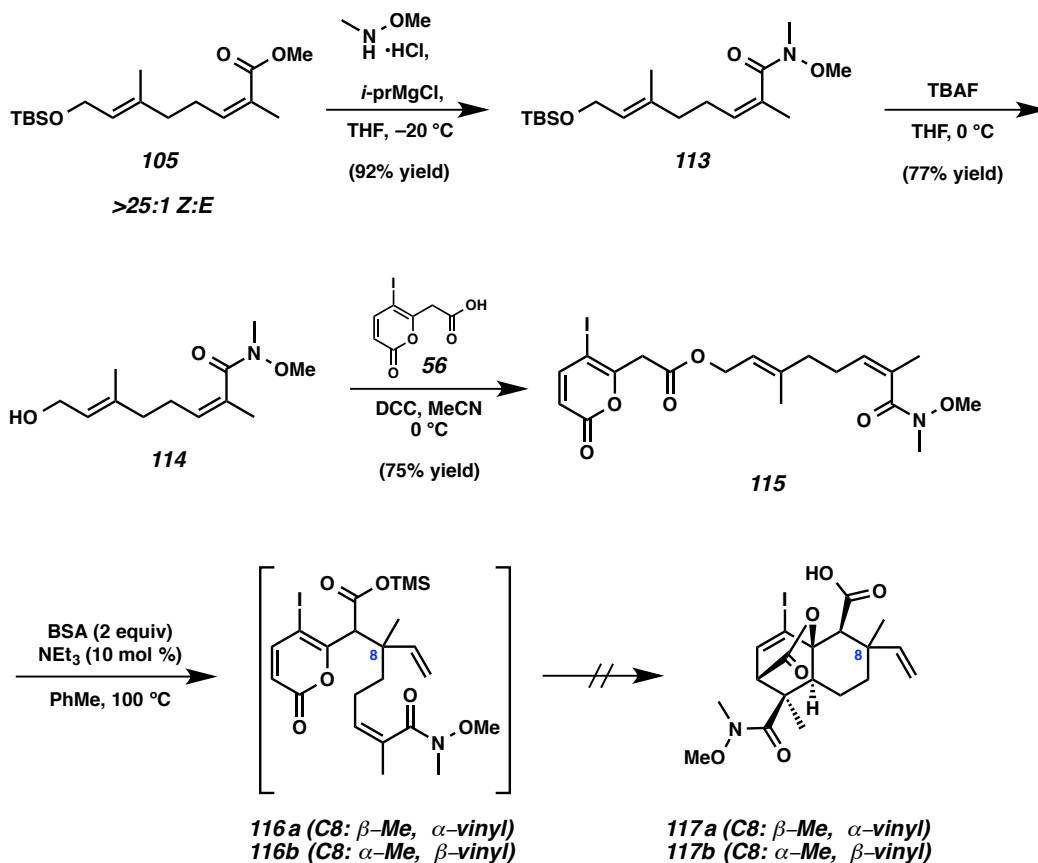
Scheme 4.2.1. Retrosynthetic analysis for (–)-transtaganolide A (**7**) and (+)-transtaganolide B (**8**).



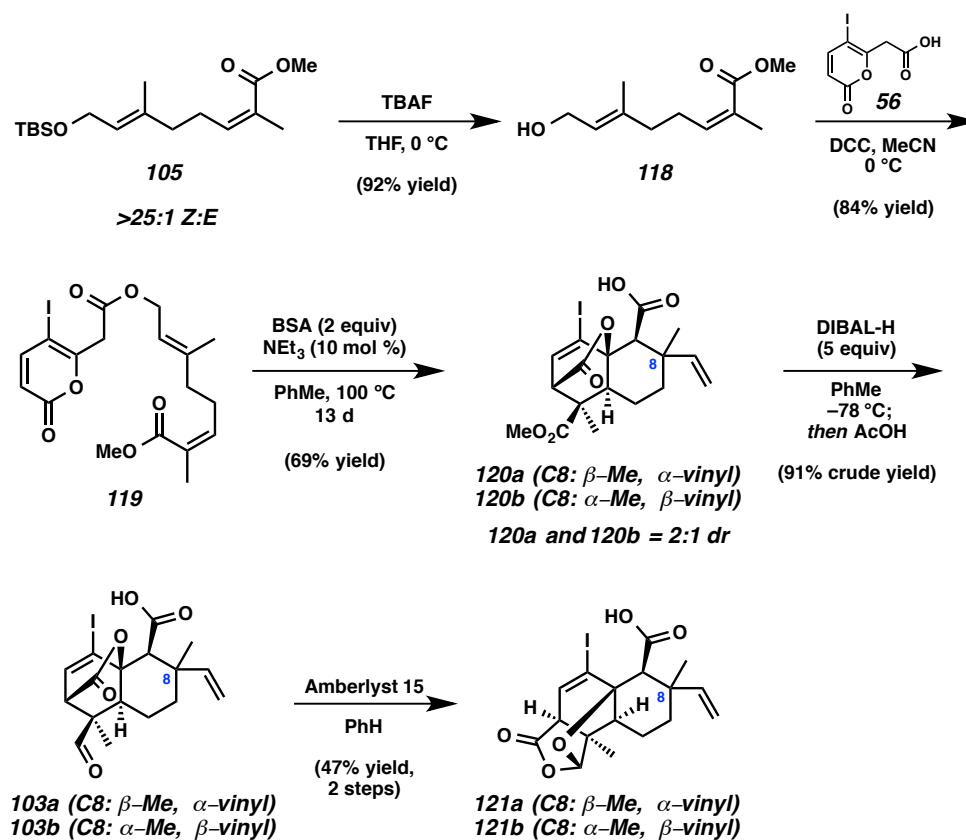
Scheme 4.2.2. First attempt to synthesize (±)-transtaganolide A and B (7–8) tetracyclic core via protected alcohol **109**.



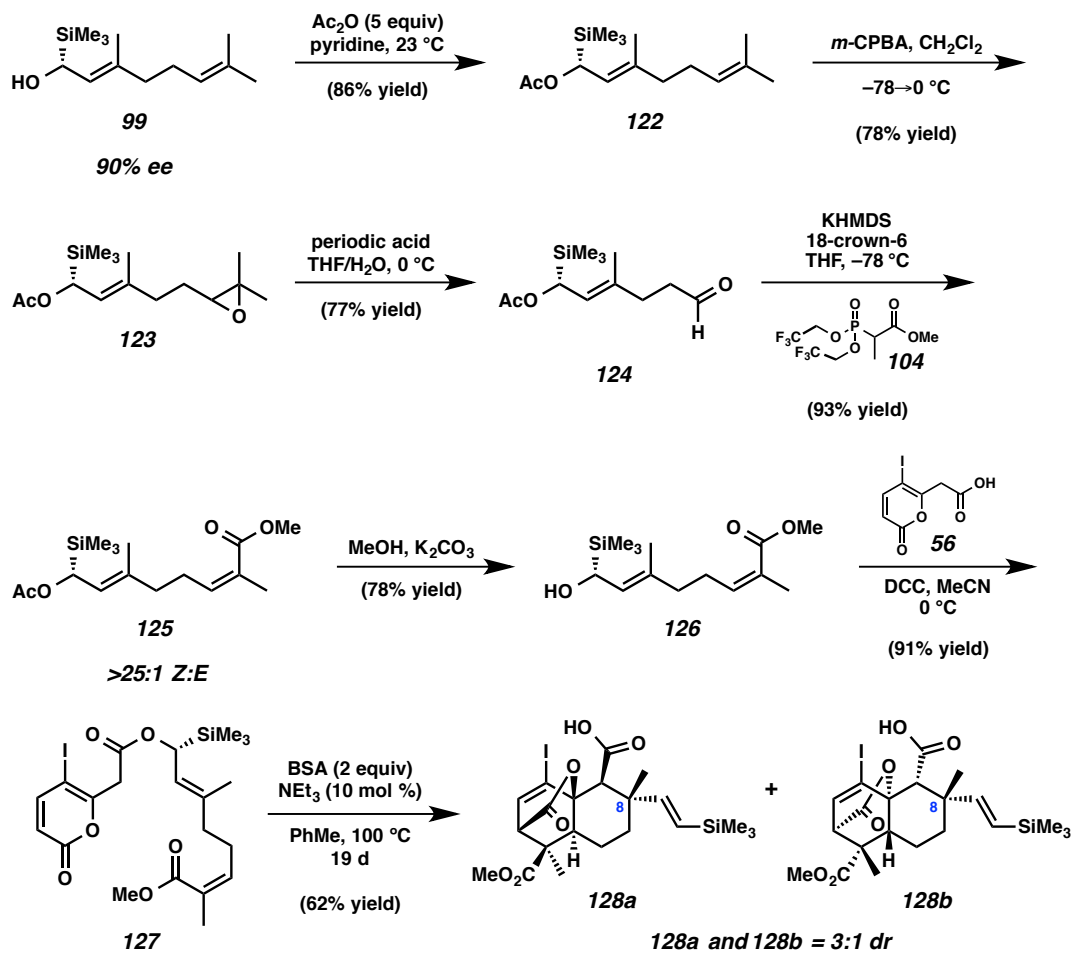
Scheme 4.2.3. Second attempt to synthesize (±)-transtaganolide A and B (7–8) tetracyclic core via Weinreb amide **115**.



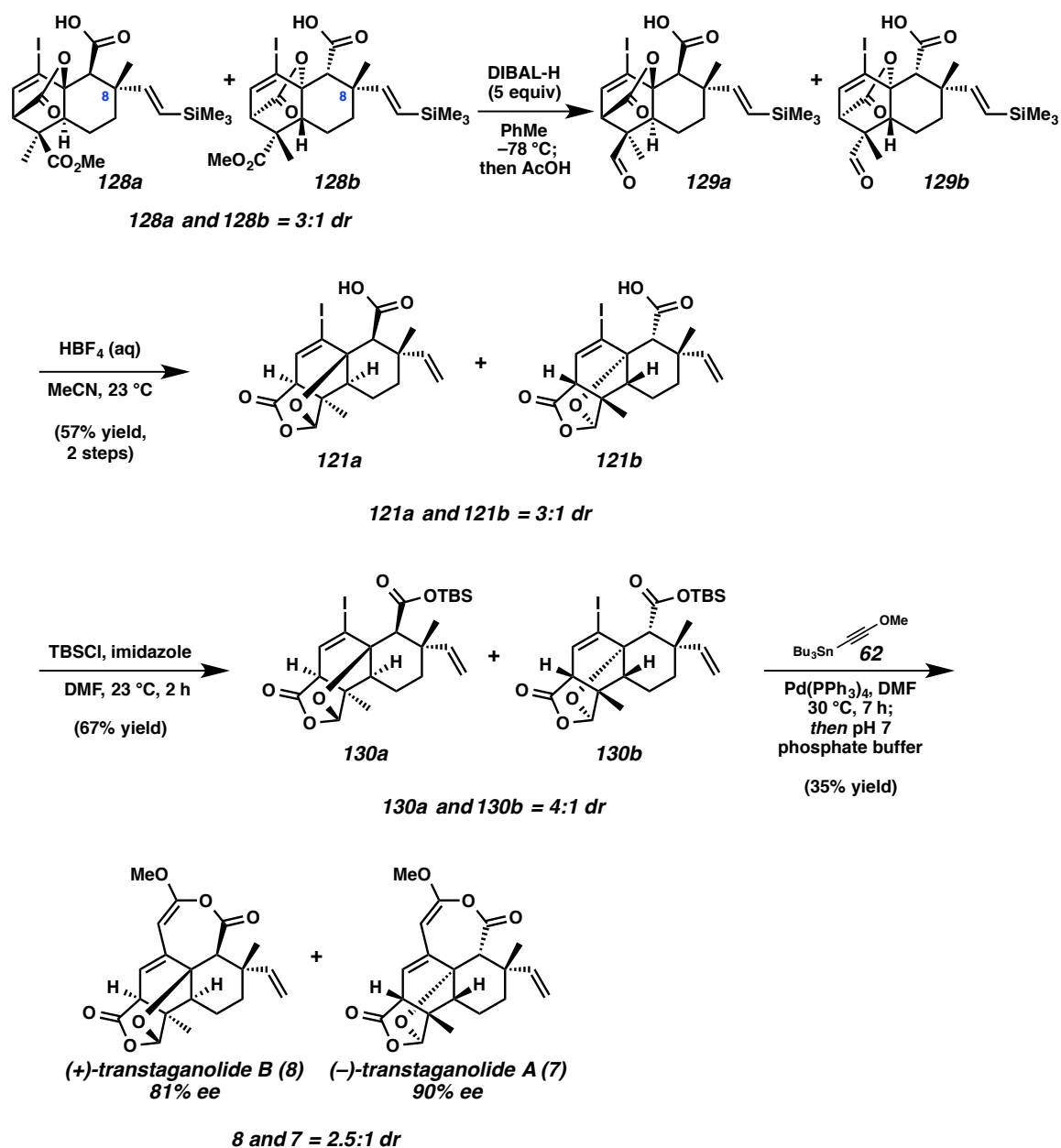
Scheme 4.2.4. Third attempt to synthesize (±)-transtaganolide A and B (7–8) tetracyclic core via methylester **119**.



Scheme 4.2.5. Forward syntheses of (–)-transtaganolide A (**7**) and (+)-transtaganolide B (**8**).



Scheme 4.2.6. Continued forward syntheses of (–)-transtaganolide A (**7**) and (+)-transtaganolide B (**8**).



APPENDIX 5

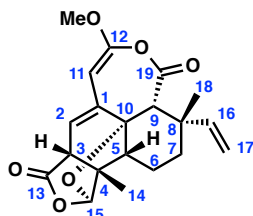
Comparison of Spectral Data for Synthetic and Reported

Transtaganolides A–D, as well as CD Spectra:

Relevant to Chapter 2

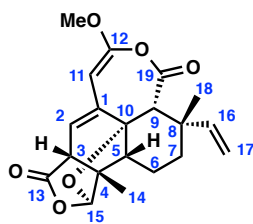
A5.1 COMPARISON OF ¹H NMR AND ¹³C NMR FOR SYNTHETIC AND REPORTED TRANSTAGANOLIDE A

Table A5.1.1. Comparison of ¹H NMR data for synthetic and reported natural¹ transtaganolide A (7).



Assignment	Synthetic δ (ppm)	Multiplicity, J (Hz)	Natural δ (ppm)	Multiplicity, J (Hz)
C1	—	—	—	—
C2	5.60	dd, 5.9, 1.0	5.60	dd, 5.9, 1.1
C3	3.11	dt, 5.9, 0.8	3.11	d, 6.0
C4	—	—	—	—
C5	1.95	dd, 12.3, 6.3	1.96	dd, 12.1, 6.2
C6	1.60–1.30	m	1.60	dddd, 13.3, 6.2, 2.7, 2.2
	1.60–1.30	m	1.47	dddd, 13.3, 13.3, 12.3, 2.3
C7	1.60–1.30	m	1.39	ddd, 13.3, 13.3, 2.7
	1.83	ddd, 12.9, 3.7, 2.6	1.82	ddd, 12.7, 3.7, 2.3
C8	—	—	—	—
C9	2.98	s	2.99	s
C10	—	—	—	—
C11	4.98	s	4.99	bs
C12	—	—	—	—
C13	—	—	—	—
C14	1.30	s	1.30	s
C15	5.62	s	5.61	s
C16	6.90	dd, 17.9, 11.1	6.89	dd, 17.9, 11.2
C17	5.12	ddd, 11.1, 1.1, 0.6	5.11	ddt, 11.1, 1.1, 0.6
	5.03	dd, 17.9, 1.1	5.03	dd, 17.8, 1.1
C18	1.22	s	1.22	s
OMe	3.70	s	3.70	s

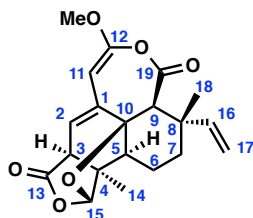
Table A5.1.2. Comparison of ^{13}C NMR data for synthetic and reported natural¹ transtaganolide A (7).



Assignment	Synthetic 7 (ppm)	Natural 7 (ppm)
C1	143.8	143.7
C2	119.6	119.4
C3	51.6	51.3
C4	48.8	48.6
C5	49.7	49.4
C6	20.1	19.9
C7	39.4	39.1
C8	38.3	38.1
C9	52.8	52.5
C10	87.6	87.5
C11	84.5	84.1
C12	154.5	154.4
C13	175.6	175.5
C14	15.8	15.6
C15	109.8	109.6
C16	143.9	143.7
C17	111.8	111.5
C18	28.6	28.3
C19	164.1	164.0
OMe	56.5	56.3

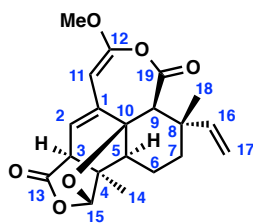
A5.2 COMPARISON OF ¹H NMR AND ¹³C NMR FOR SYNTHETIC AND REPORTED TRANSTAGANOLIDE B

Table A5.2.1. Comparison of ¹H NMR data for synthetic and reported natural¹ transtaganolide B (**8**).



Assignment	Synthetic 8 (ppm)	Multiplicity, J (Hz)	Natural 8 (ppm)	Multiplicity, J (Hz)
C1	—	—	—	—
C2	5.58	dd, 6.0, 1.1	5.58	dd, 6.0, 1.1
C3	3.12	dt, 6.0, 0.9	3.12	dt, 6.0, 0.9
C4	—	—	—	—
C5	1.94	dd, 12.3, 6.3	1.95	dd, 12.1, 6.3
C6	1.72 1.55–1.35	ddt, 13.1, 6.3, 3.3 m	1.73 1.51	dddd, 12.9, 6.2, 3.7, 2.5 dddd, 13.0, 13.0, 13.0, 2.4
C7	1.55–1.35 1.63	m ddd, 13.1, 3.9, 2.7	1.43 1.63	ddd, 13.3, 11.9, 2.3 ddd, 13.3, 3.7, 2.3
C8	—	—	—	—
C9	3.08	s	3.09	s
C10	—	—	—	—
C11	4.96	t, 0.8	4.97	t, 0.8
C12	—	—	—	—
C13	—	—	—	—
C14	1.33	s	1.33	s
C15	5.65	t, 0.8	5.66	t, 0.7
C16	5.80	dd, 17.4, 10.8	5.81	dd, 17.4, 10.8
C17	5.05 5.02	dd, 17.4, 0.6 dd, 10.8, 0.6	5.09 5.06	dd, 10.8, 0.7 dd, 17.4, 0.7
C18	1.55	s	1.55	s
OMe	3.68	s	3.68	s

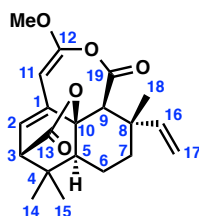
Table A5.2.2. Comparison of ^{13}C NMR data for synthetic and reported natural¹ transtaganolide B (**8**).



Assignment	Synthetic 8 (ppm)	Natural 8 (ppm)
C1	144.2	144.0
C2	119.4	119.2
C3	51.6	51.4
C4	48.8	48.6
C5	49.5	49.3
C6	19.4	19.2
C7	37.0	36.8
C8	38.1	37.9
C9	49.8	49.6
C10	87.7	87.5
C11	84.4	84.2
C12	154.5	154.3
C13	175.6	175.5
C14	15.9	15.7
C15	109.8	109.6
C16	146.7	146.5
C17	112.7	112.5
C18	20.1	19.9
C19	163.8	163.7
OMe	56.5	56.3

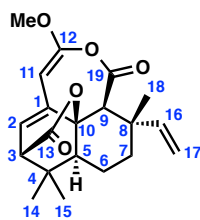
A5.3 COMPARISON OF ¹H NMR AND ¹³C NMR FOR SYNTHETIC AND REPORTED TRANSTAGANOLIDE C

Table A5.3.1. Comparison of ¹H NMR data for synthetic and reported natural¹ transtaganolide C (9).



Assignment	Synthetic 9 (ppm)	Multiplicity, J (Hz)	Natural 9 (ppm)	Multiplicity, J (Hz)
C1	—	—	—	—
C2	6.07	dd, 6.5, 1.5	6.08	dd, 6.5, 1.1
C3	3.06	d, 6.5	3.07	d, 6.5
C4	—	—	—	—
C5	1.34–1.27	m	1.30	dd, 11.5, 6.5
C6	1.71–1.63	m	1.70–1.60	m
	1.71–1.63	m	1.70–1.60	m
C7	1.48–1.39	m	1.44	ddd, 13.0, 13.0, 3.3
	1.71–1.63	m	1.65	m
C8	—	—	—	—
C9	3.23	s	3.24	s
C10	—	—	—	—
C11	5.00	d, 1.5	5.01	d, 1.1
C12	—	—	—	—
C13	—	—	—	—
C14	0.97	s	0.98	s
C15	1.08	s	1.09	s
C16	5.80	dd, 17.5, 11.0	5.81	dd, 17.4, 10.8
C17	5.03	d, 11.0	5.05	br d, 10.7
	5.07	d, 17.5	5.08	br d, 17.4
C18	1.60	s	1.61	s
C19	—	—	—	—
OMe	3.71	s	3.72	s

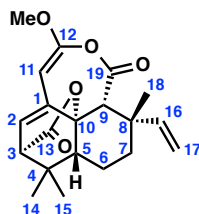
Table A5.3.2. Comparison of ^{13}C NMR data for synthetic and reported natural¹ transtaganolide C (9).



Assignment	Synthetic 9 (ppm)	Natural 9 (ppm)
C1	138.0	131.9
C2	123.6	123.5
C3	53.8	53.8
C4	33.3	33.2
C5	48.1	47.9
C6	19.9	19.8
C7	38.3	38.3
C8	38.4	38.4
C9	50.6	50.4
C10	87.3	87.4
C11	79.3	79.1
C12	156.7	156.7
C13	171.8	172.0
C14	29.9	29.6
C15	24.8	24.8
C16	146.5	146.5
C17	112.8	112.8
C18	19.2	19.1
C19	162.3	162.5
OMe	56.6	56.3

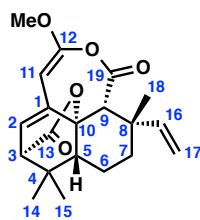
A5.4 COMPARISON OF ¹H NMR AND ¹³C NMR FOR SYNTHETIC AND REPORTED TRANSTAGANOLIDE D

Table A5.4.1. Comparison of ¹H NMR data for synthetic and reported natural¹ transtaganolide D (10).



Assignment	Synthetic 10 (ppm)	Multiplicity, J (Hz)	Natural 10 (ppm)	Multiplicity, J (Hz)
C1	—	—	—	—
C2	6.09	dd, 6.5, 1.0	6.08	dd, 6.5, 1.2
C3	3.06	d, 6.5	3.04	d, 6.6
C4	—	—	—	—
C5	1.33	dd, 13.5, 3.5	1.34	dd, 12.6, 5.3
C6	1.64	dquint, 13.5, 3.0	1.65–1.53	m
	1.59–1.56	m	1.65–1.53	m
C7	1.39	dt, 13.5, 3.5	1.39	ddd, 13.0, 13.0, 3.3
	1.91	dt, 13.5, 3.5	1.89	ddd, 13.0, 3.3, 3.3
C8	—	—	—	—
C9	3.13	s	3.14	s
C10	—	—	—	—
C11	5.02	d, 1.0	5.02	d, 1.1
C12	—	—	—	—
C13	—	—	—	—
C14	0.97	s	0.96	s
C15	1.04	s	1.02	s
C16	7.00	dd, 17.5, 11.0	6.98	dd, 17.8, 11.2
C17	5.15	dd, 11.0, 1.0	5.11	dd, 11.1, 1.1
	5.05	dd, 17.5, 1.0	5.03	dd, 17.8, 1.1
C18	1.22	s	1.21	s
C19	—	—	—	—
OMe	3.73	s	3.72	s

Table A5.4.2. Comparison of ^{13}C NMR data for synthetic and reported natural¹ transtaganolide D (**10**).

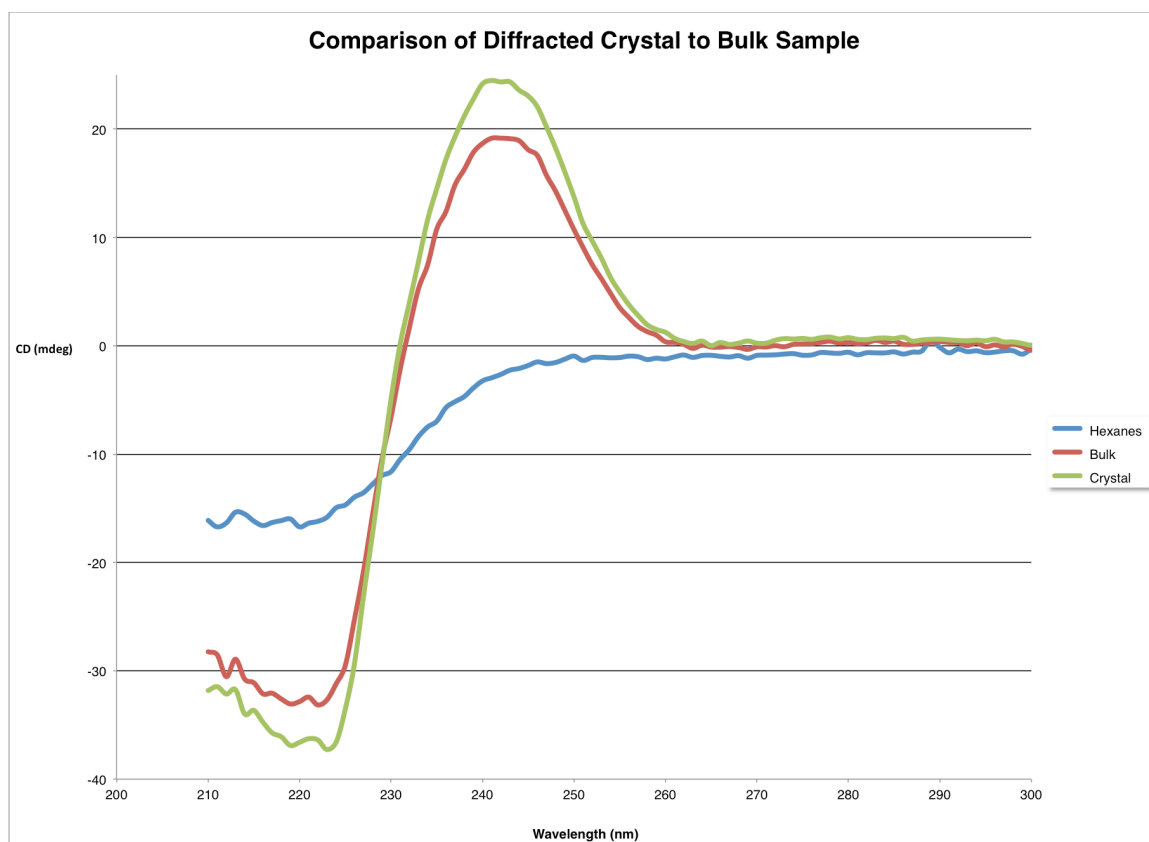


Assignment	Synthetic 10 (ppm)	Natural 10 (ppm)
C1	137.7	137.5
C2	123.9	123.8
C3	54.0	53.9
C4	33.3	33.2
C5	48.4	48.2
C6	20.5	20.3
C7	40.5	40.3
C8	38.4	38.3
C9	53.3	53.1
C10	87.3	87.4
C11	79.4	79.2
C12	156.7	156.6
C13	171.7	171.9
C14	29.9	29.8
C15	24.8	24.7
C16	142.9	142.9
C17	112.1	111.9
C18	28.5	28.4
C19	162.6	162.7
OMe	56.3	56.3

A5.5 CD SPECTRA OF DIFFRACTED CRYSTAL **133**

The circular dichroism (CD) spectra of crystal **133** (in green, Figure A5.5.1) and the CD spectra of the bulk material from which crystal **133** was obtained (in red, Figure A5.5.1) were compared. Since crystal **133** was grown from 90% enantiomeric excess (ee) material it was possible that crystal **133** could have been the crystallized minor enantiomer (**135**). Figure A5.5.1 demonstrates that the CD spectra of the bulk material (**133** and **135**) and crystal **133** are quite similar and therefore confirms that crystal **133** is representative of the major enantiomer.

Figure A5.5.1. CD spectral comparison of diffracted crystal **133** to 90% enantioenriched bulk sample of **133** and **135**.



A5.6 NOTES AND REFERENCES

- (1) Saouf, A.; Guerra, F. M.; Rubal, J. J.; Moreno-Dorado, F. J.; Akssira, M.; Mellouki, F.; López, M.; Pujadas, A. J.; Jorge, Z. D.; Massanet, G. M. *Org. Lett.* **2005**, *7*, 881–884.

APPENDIX 6

Spectra Relevant to Chapter 2:

Total Syntheses of (–)-Transtaganolide A, (+)-Transtaganolide B, (+)-Transtaganolide C, and (–)-Transtaganolide D and Biosynthetic Implications

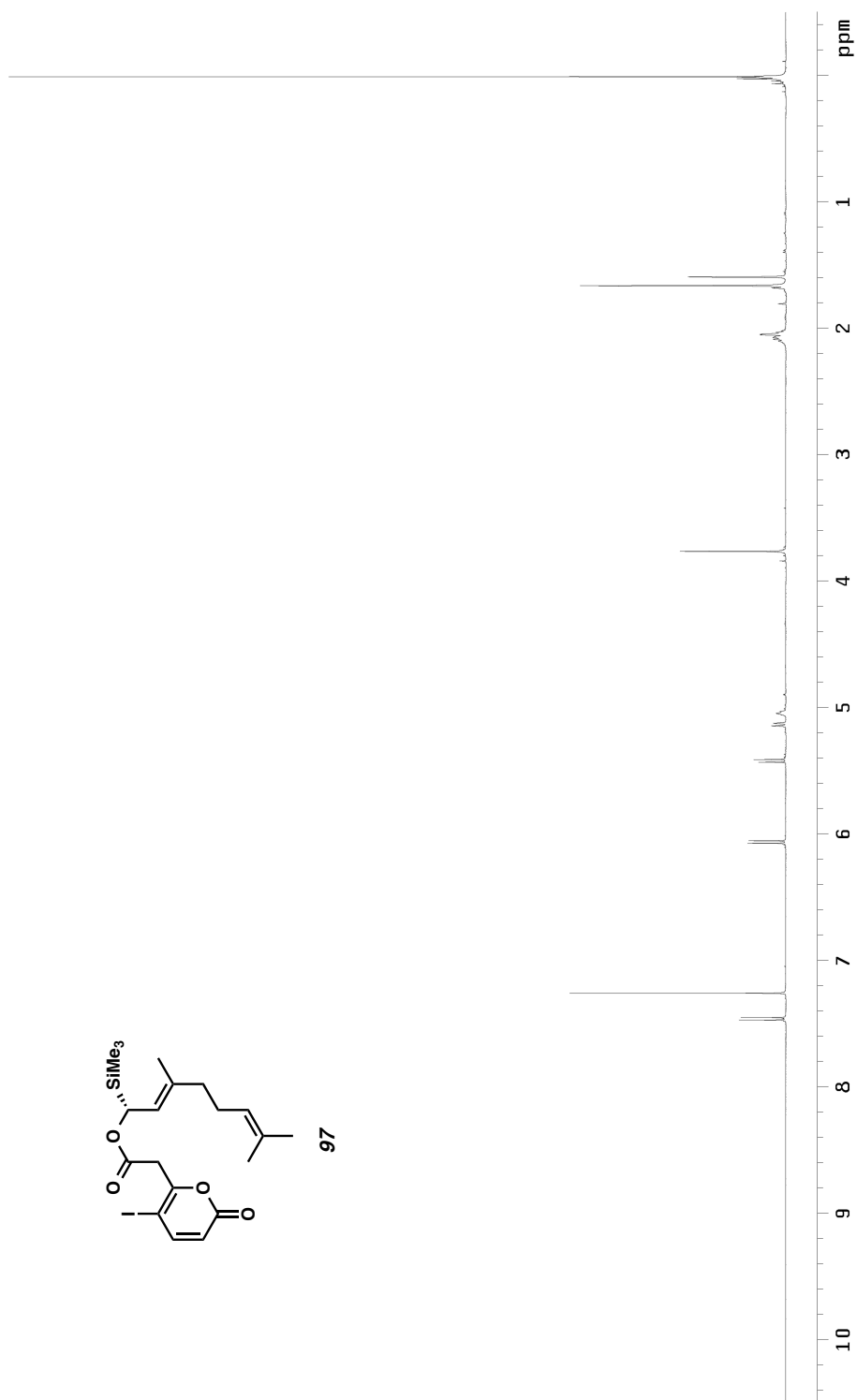


Figure A6.1.1 ¹H NMR (500 MHz, CDCl₃) of compound 97.

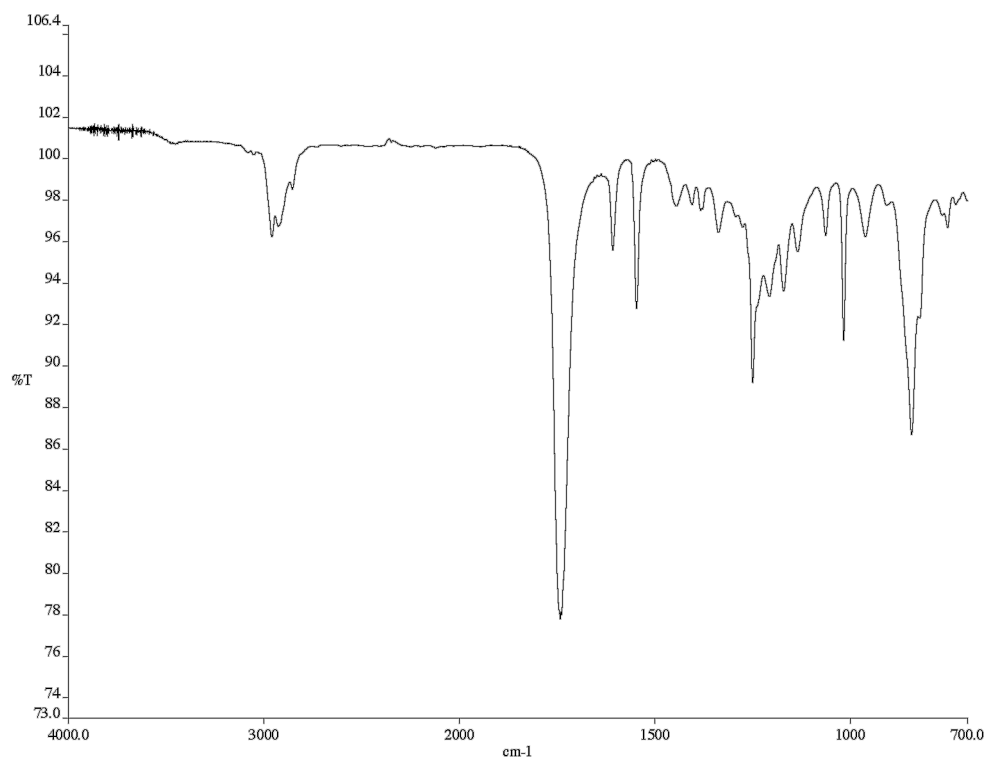


Figure A6.1.2 infrared spectrum (Thin Film, NaCl) of compound **97**.

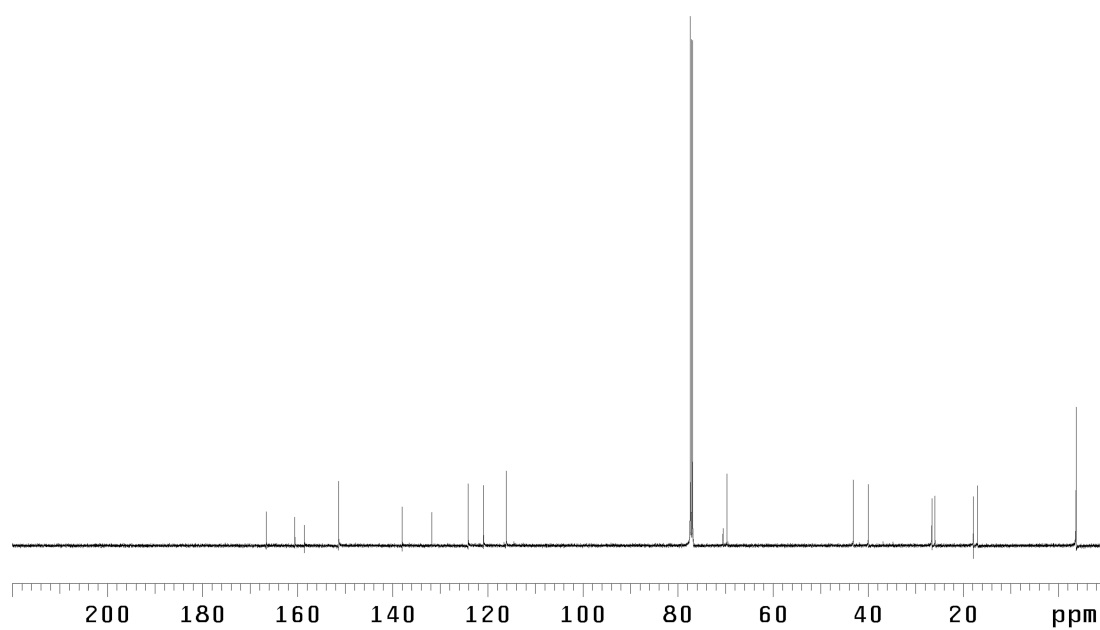


Figure A6.1.3 ¹³C NMR (125 MHz, CDCl₃) of compound **97**.

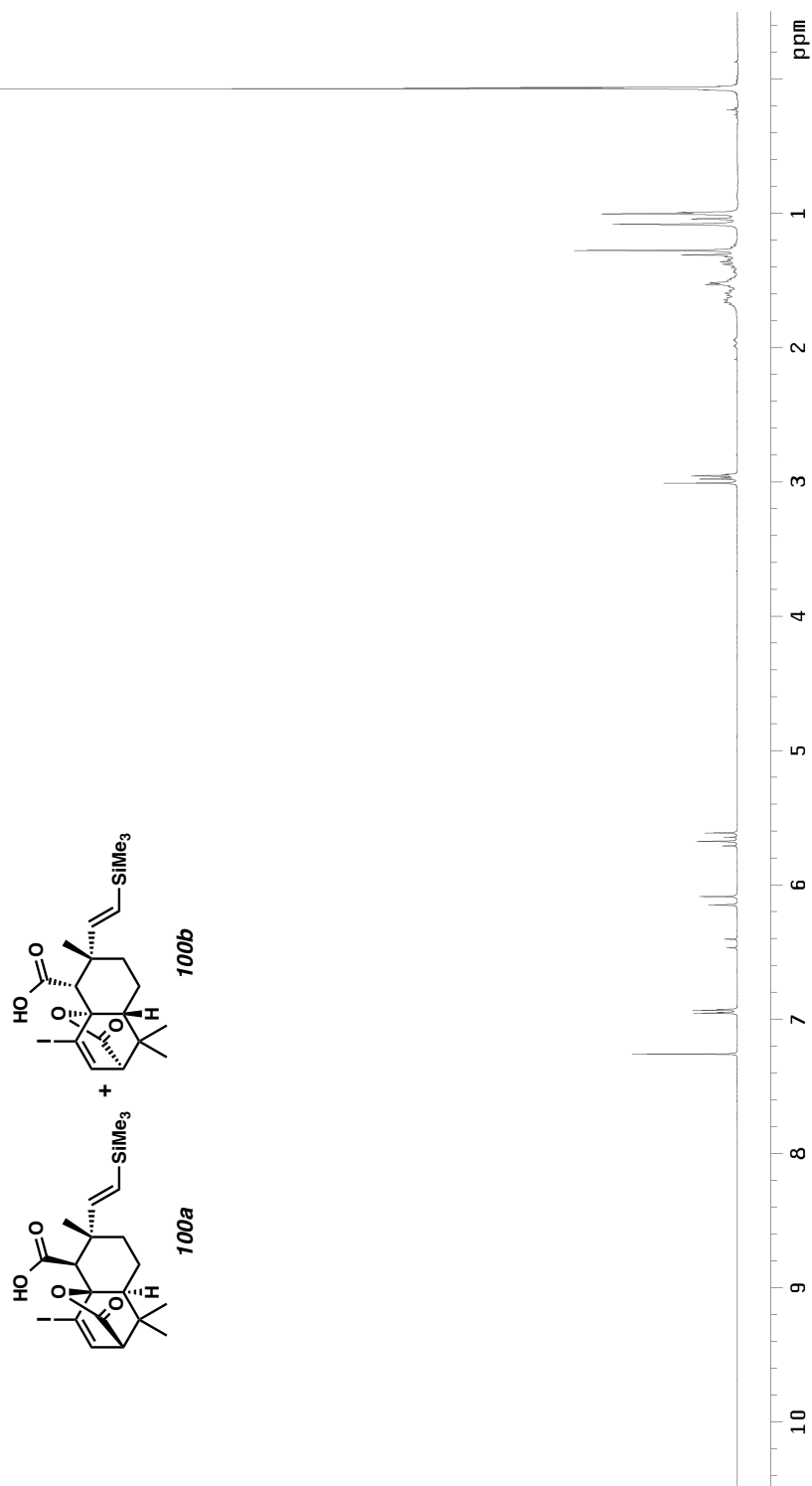


Figure A6.2.1 ^1H NMR (500 MHz, CDCl_3) of compounds **100a** and **100b**.

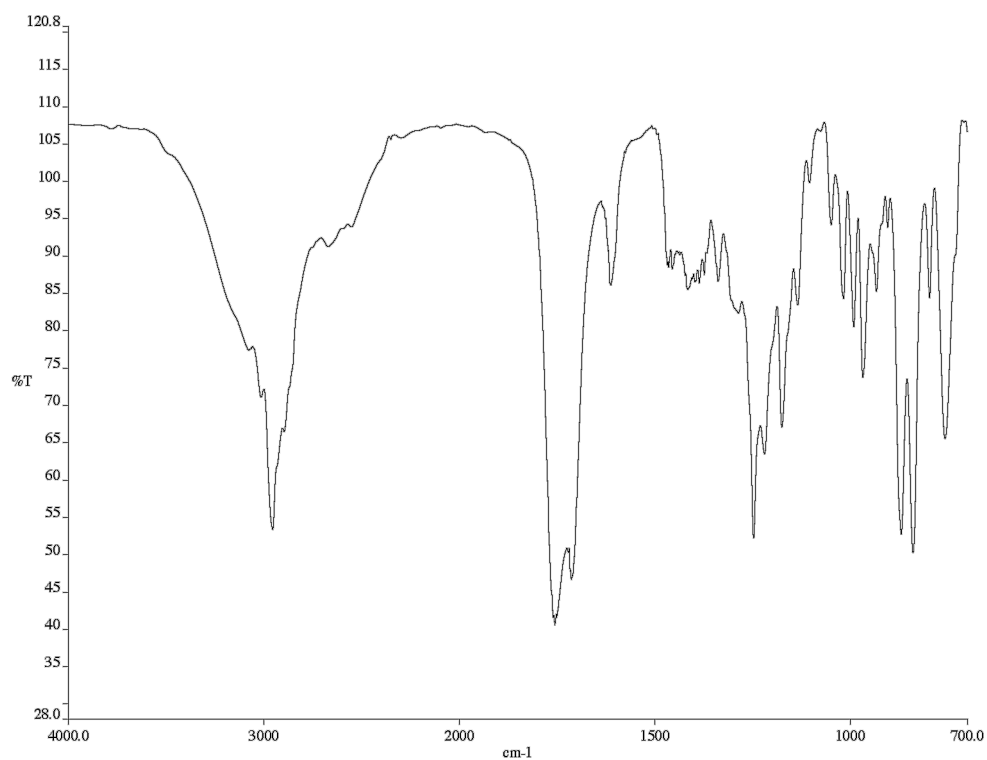


Figure A6.2.2 infrared spectrum (Thin Film, NaCl) of compounds **100a** and **100b**.

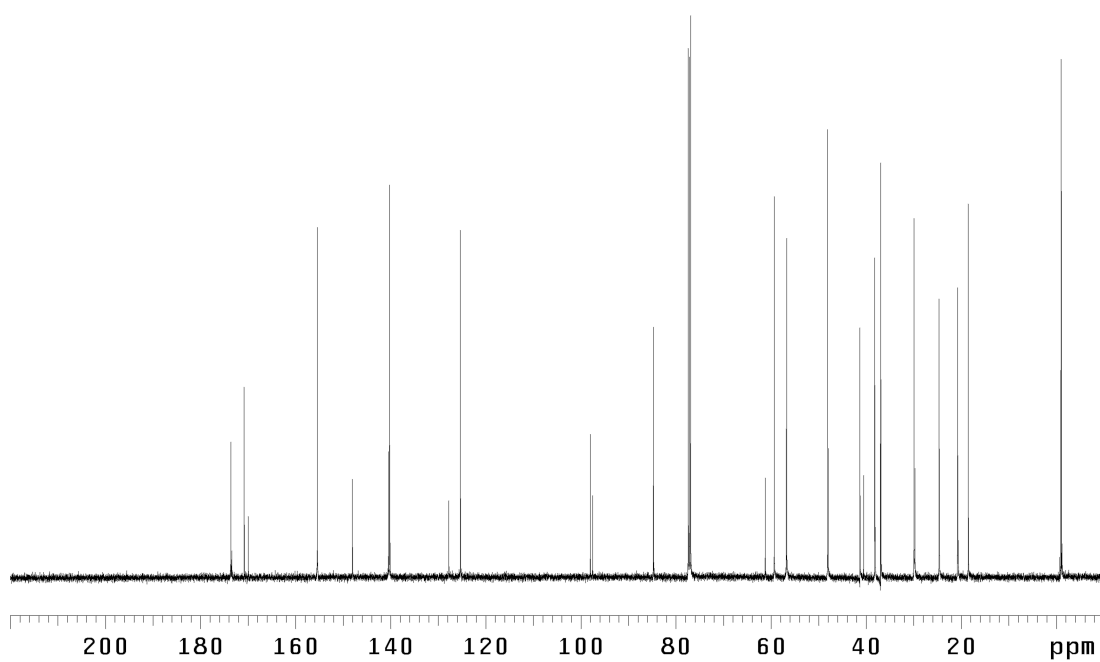


Figure A6.2.3 ¹³C NMR (125 MHz, CDCl₃) of compounds **100a** and **100b**.

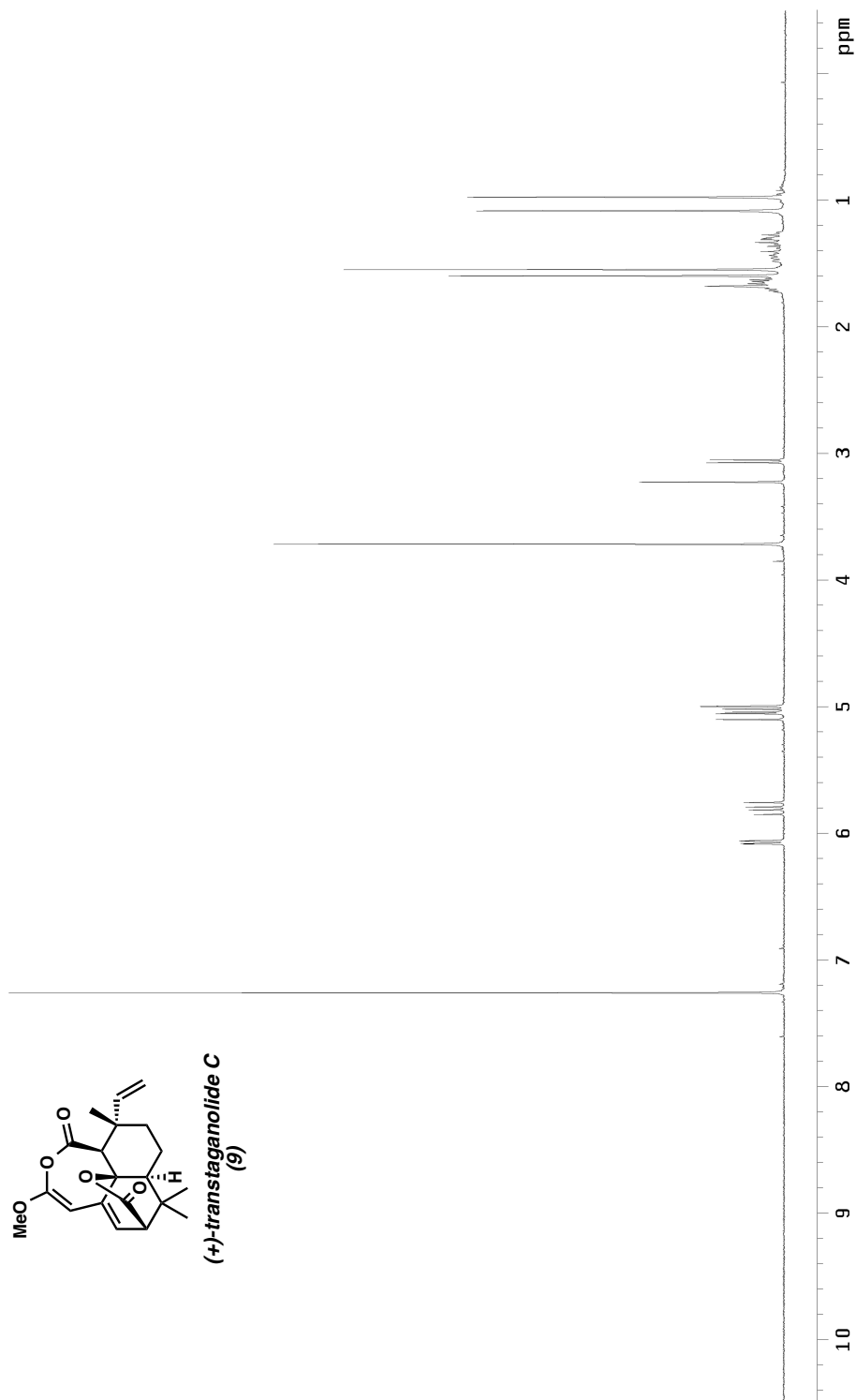


Figure A6.3.1 ¹H NMR (500 MHz, CDCl₃) of transtaganolide C (9).

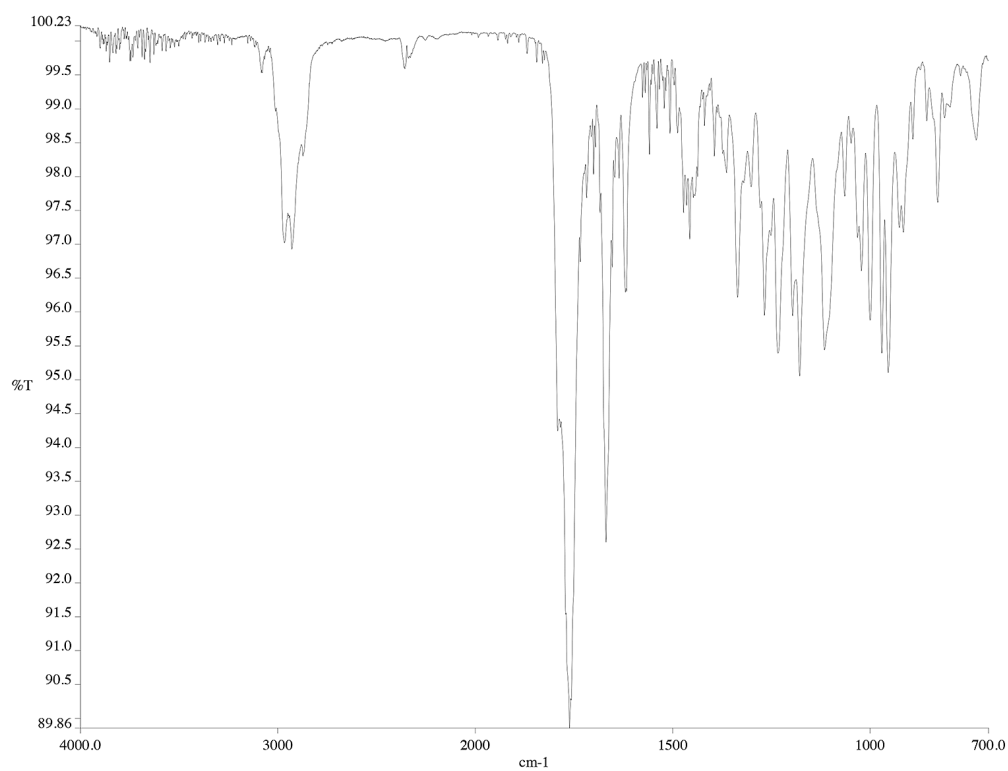


Figure A6.3.2 infrared spectrum (Thin Film, NaCl) of transtaganolide C (9).

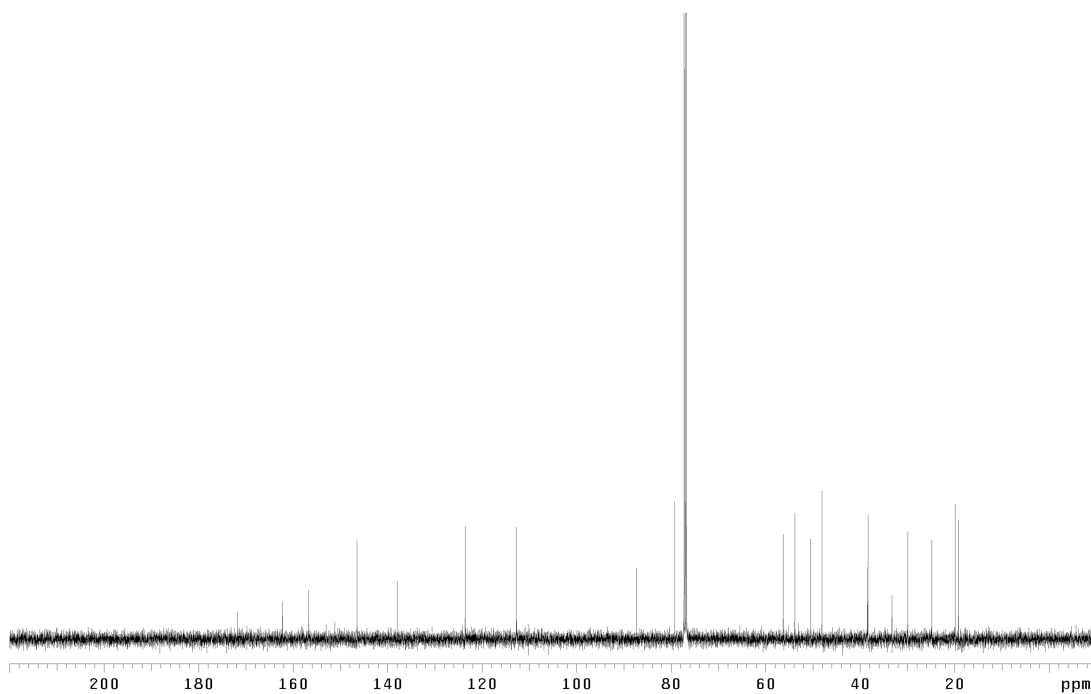


Figure A6.3.3 ¹³C NMR (125 MHz, CDCl₃) of transtaganolide C (9).

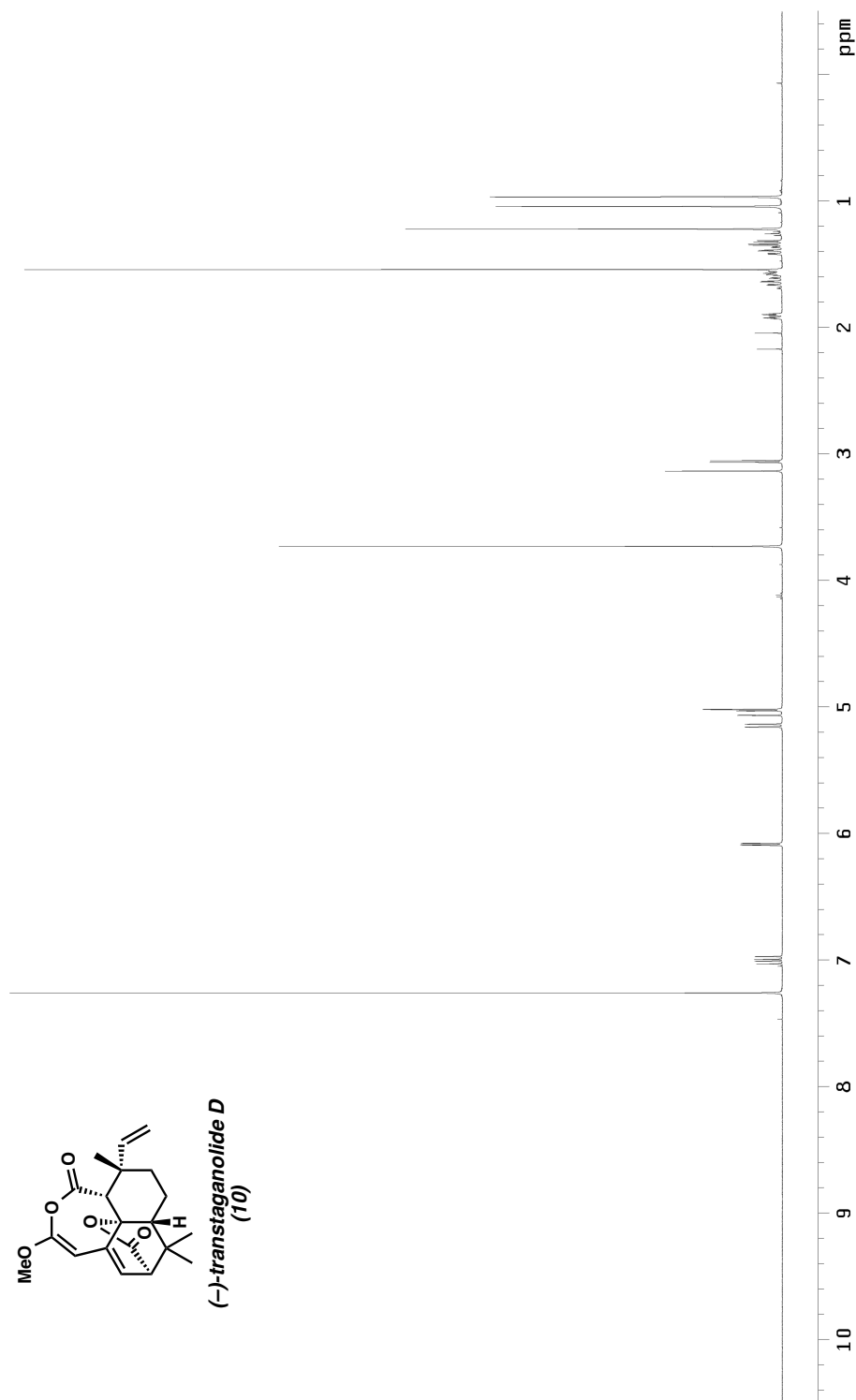


Figure A6.4.1 ¹H NMR (500 MHz, CDCl₃) of transtaganolide D (10).

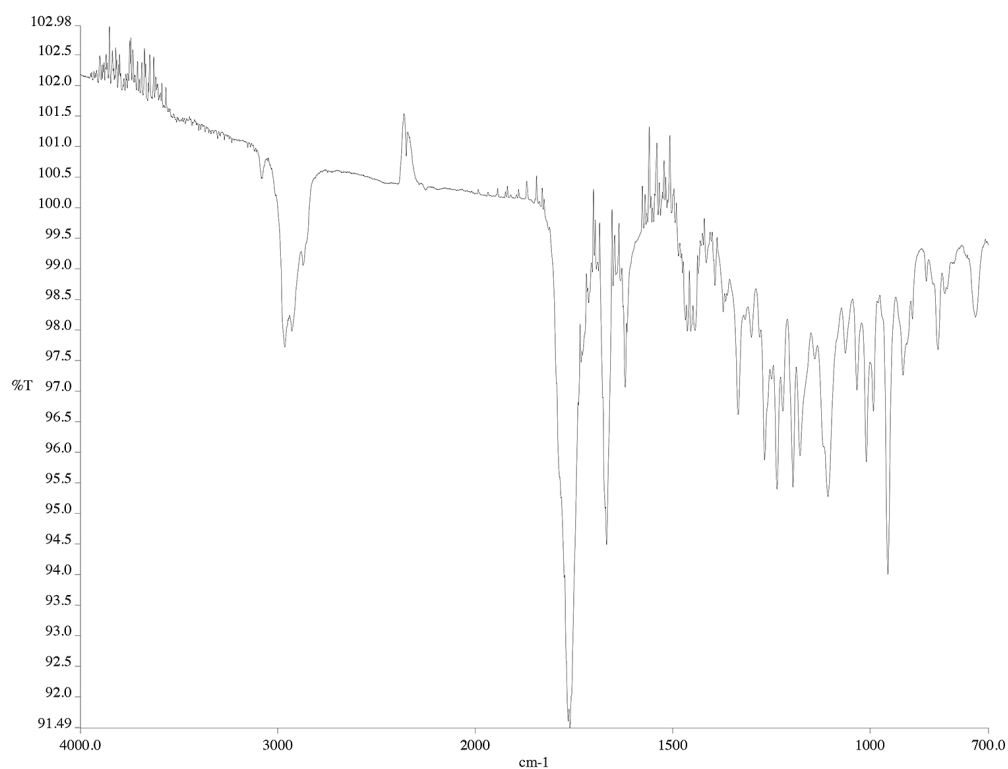


Figure A6.4.2 infrared spectrum (Thin Film, NaCl) of transtaganolide D (10).

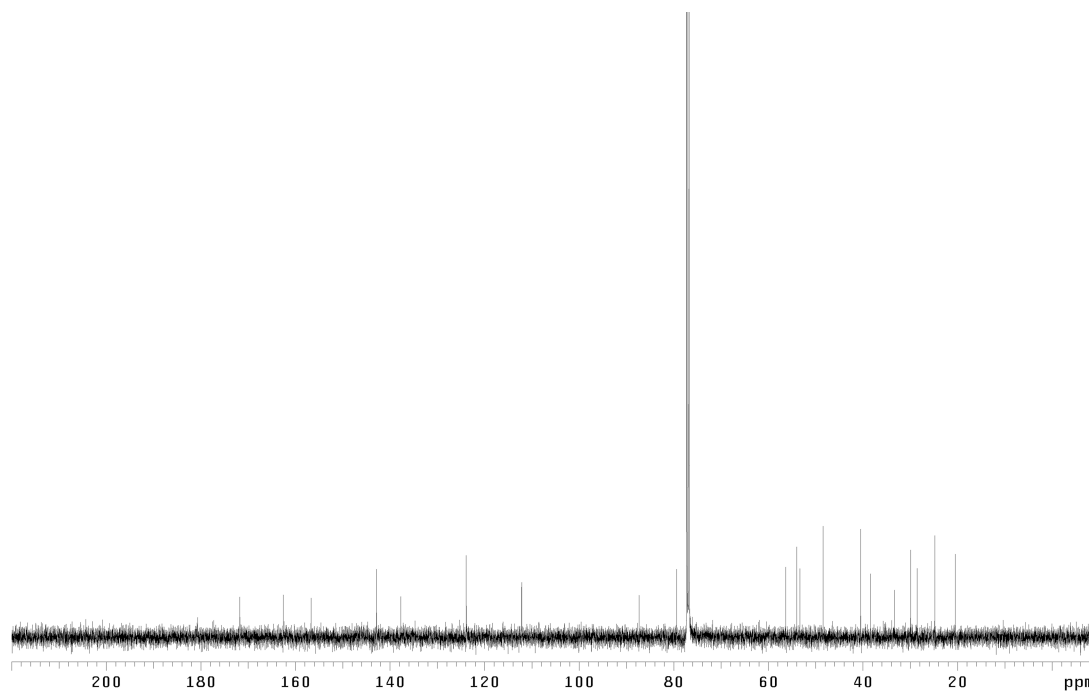


Figure A6.4.3 ^{13}C NMR (125 MHz, CDCl_3) of transtaganolide D (10).

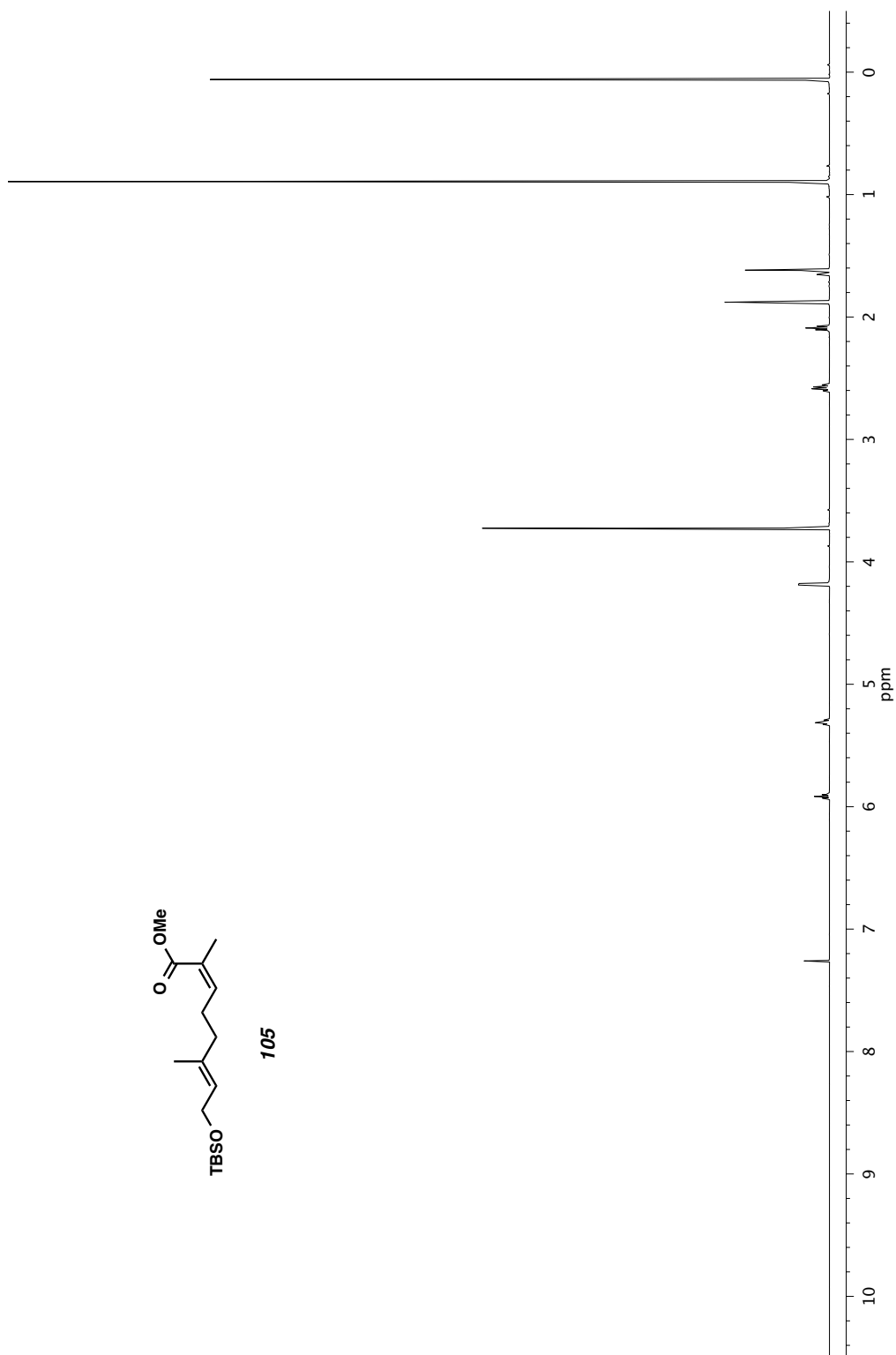


Figure A6.5.1 ¹H NMR (500 MHz, CDCl₃) of compound **105**.

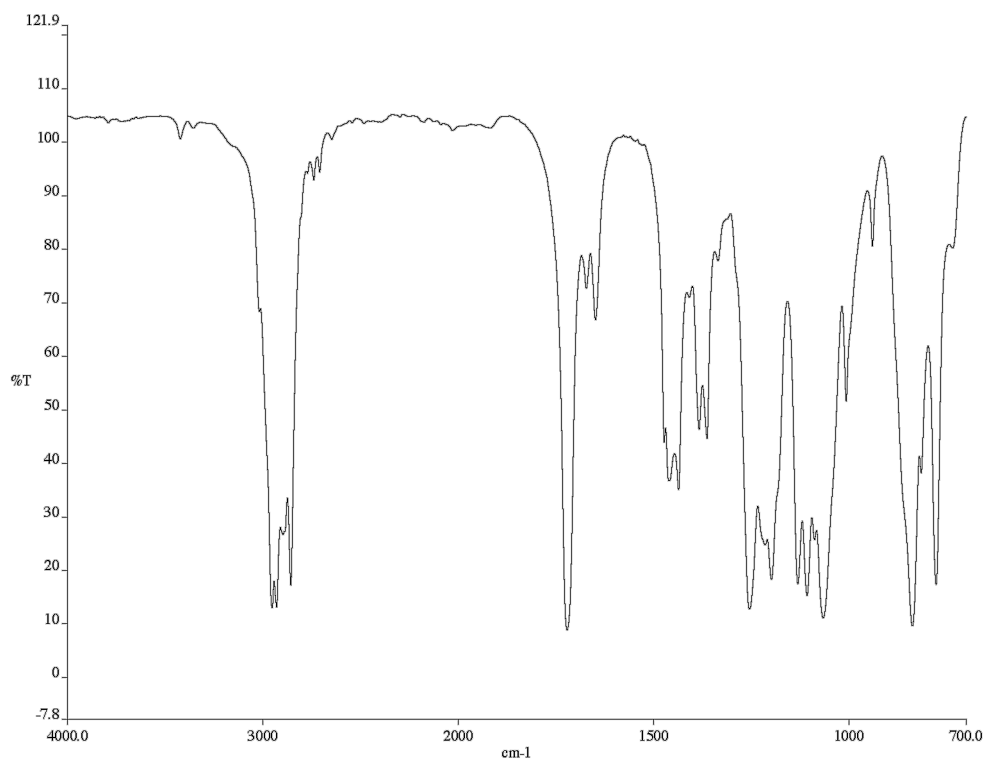


Figure A6.5.2 infrared spectrum (Thin Film, NaCl) of compound **105**.

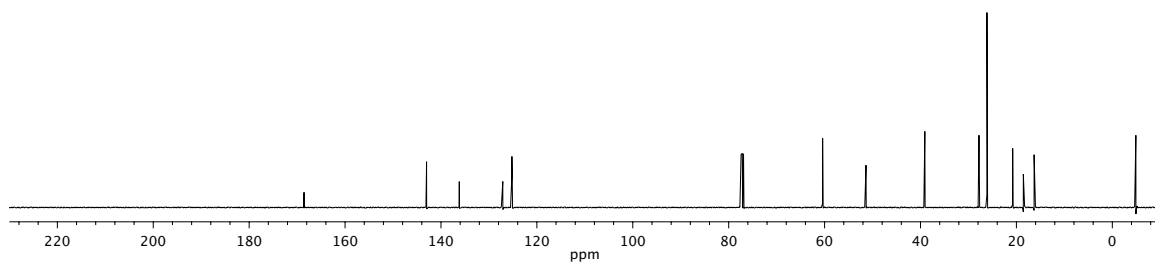


Figure A6.5.3 ¹³C NMR (125 MHz, CDCl₃) of compound **105**.

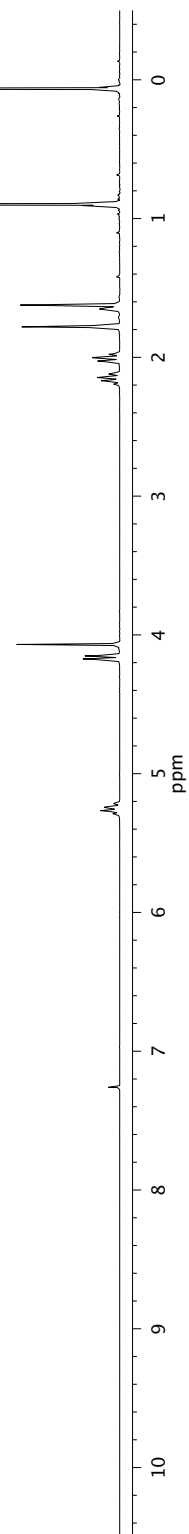
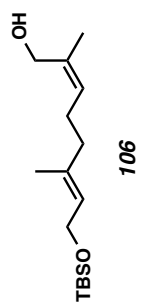


Figure A6.6.1 ¹H NMR (300 MHz, CDCl₃) of compound **106**.

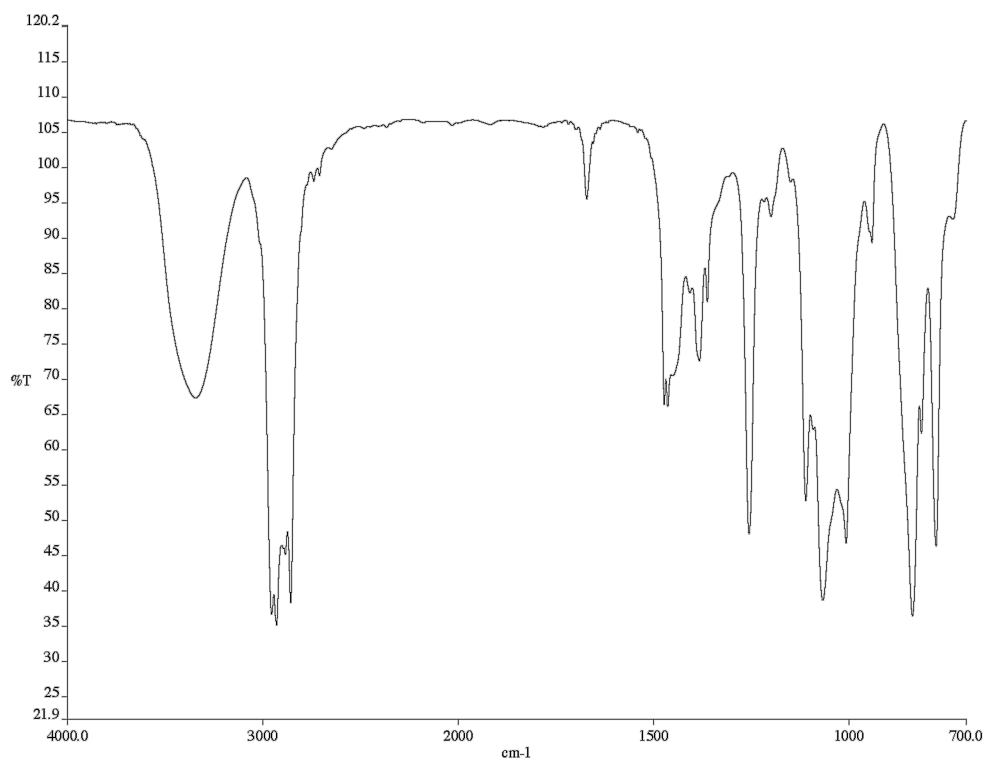


Figure A6.6.2 infrared spectrum (Thin Film, NaCl) of compound **106**.

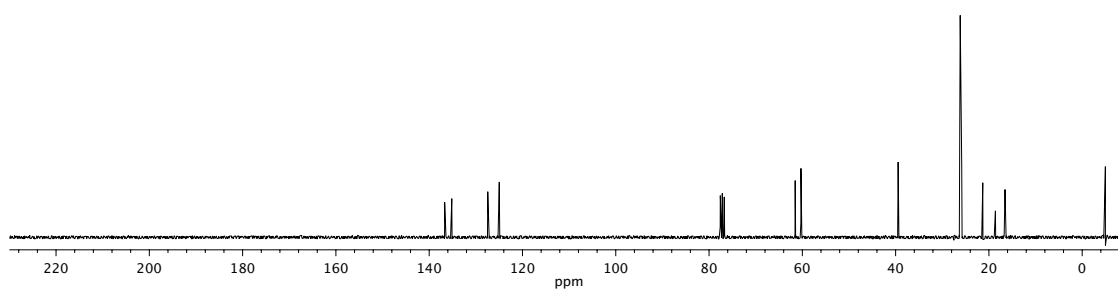


Figure A6.6.3 ¹³C NMR (75 MHz, CDCl₃) of compound **106**.

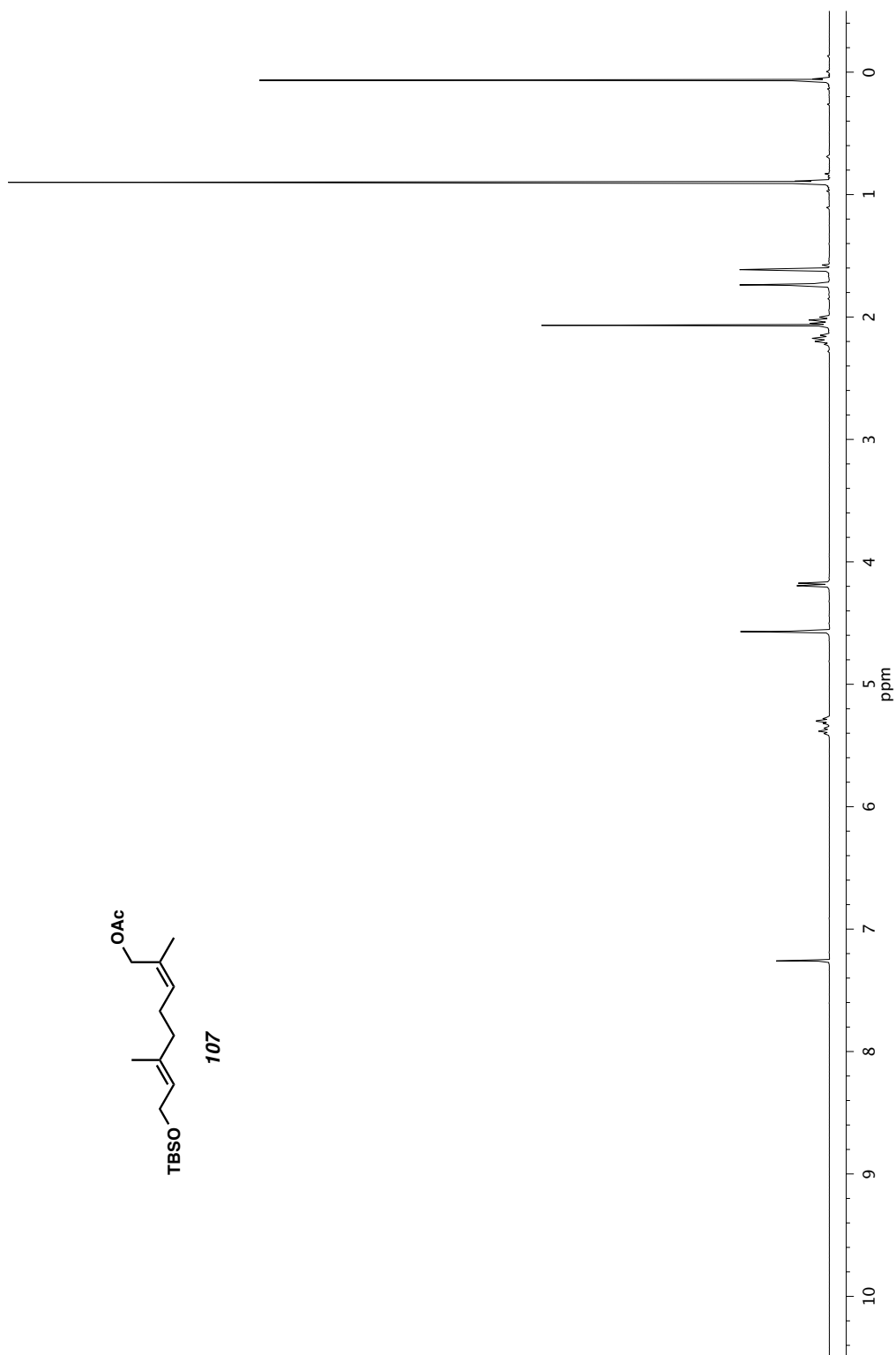


Figure A6.7.1 ¹H NMR 300 MHz, CDCl₃) of compound **107**.

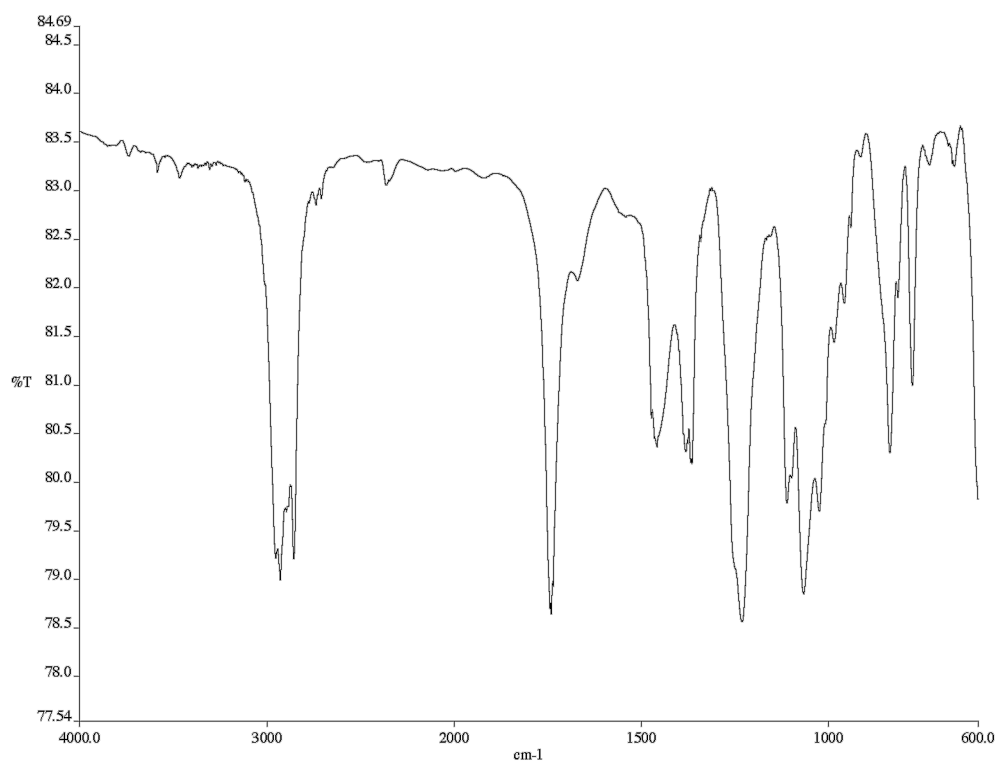


Figure A6.7.2 infrared spectrum (Thin Film, NaCl) of compound **107**.

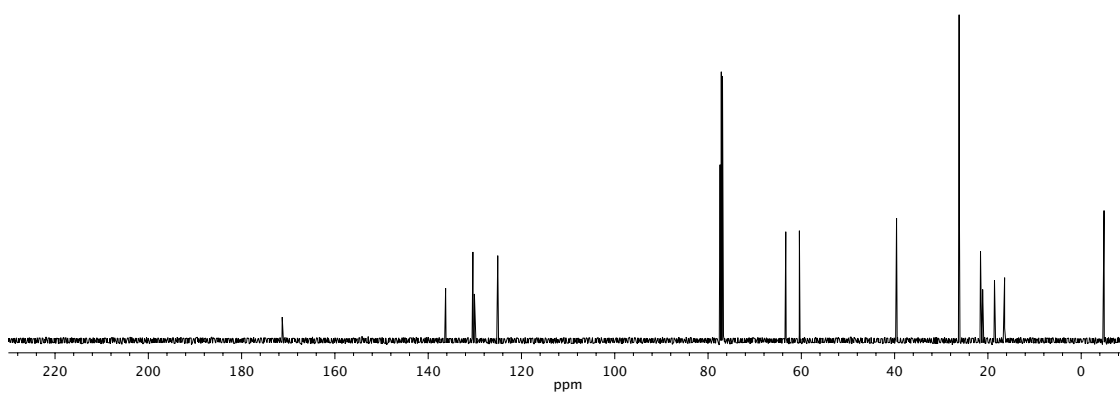


Figure A6.7.3 ¹³C NMR (125 MHz, CDCl₃) of compound **107**.

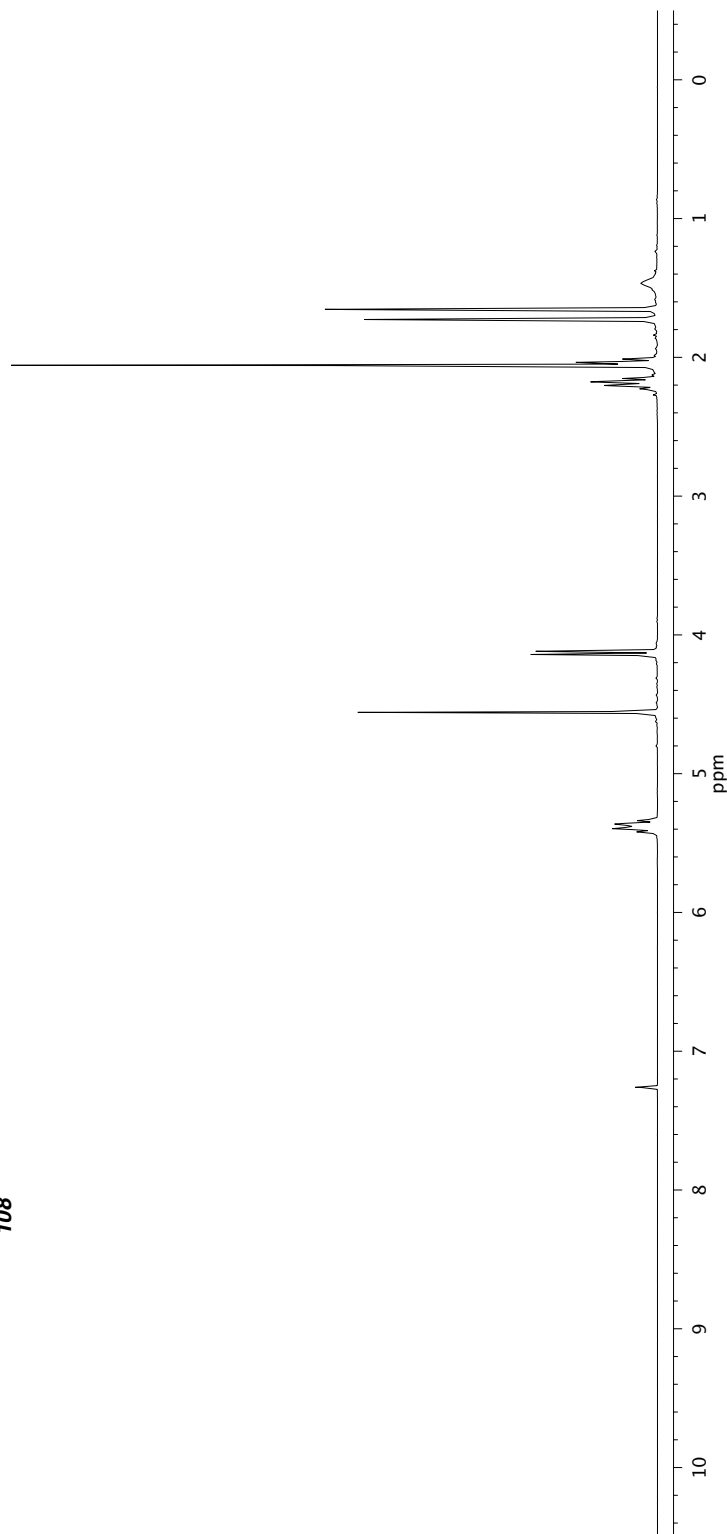
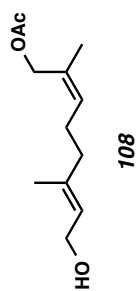


Figure A6.8.1 ¹H NMR (300 MHz, CDCl₃) of compound **108**.

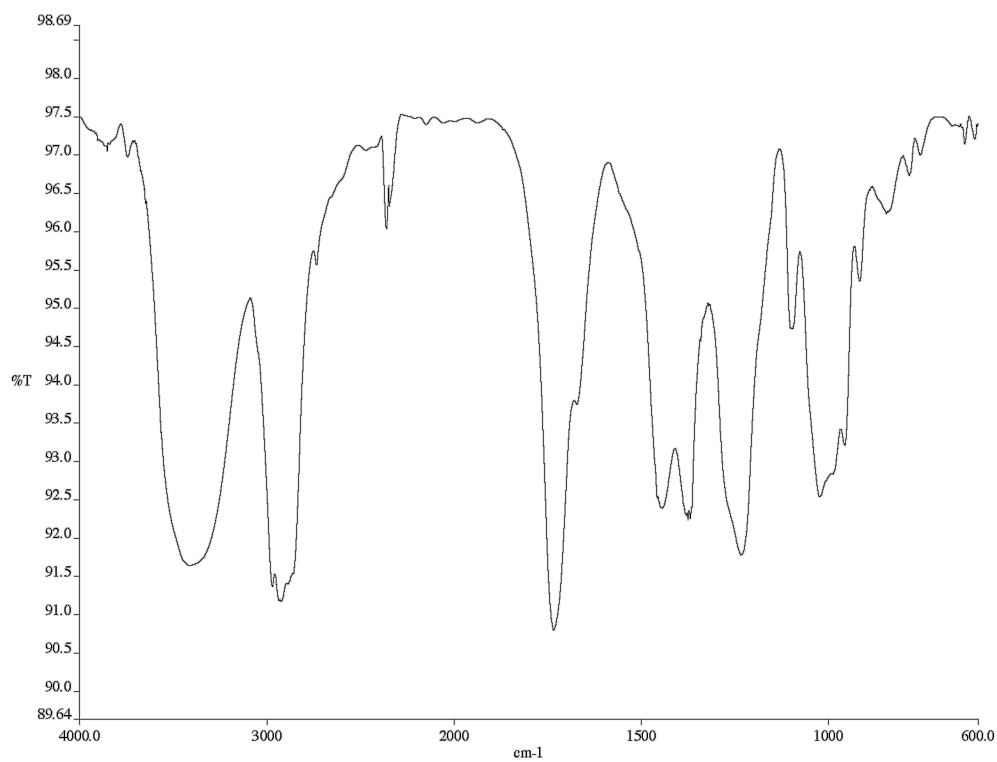


Figure A6.8.2 infrared spectrum (Thin Film, NaCl) of compound 108.

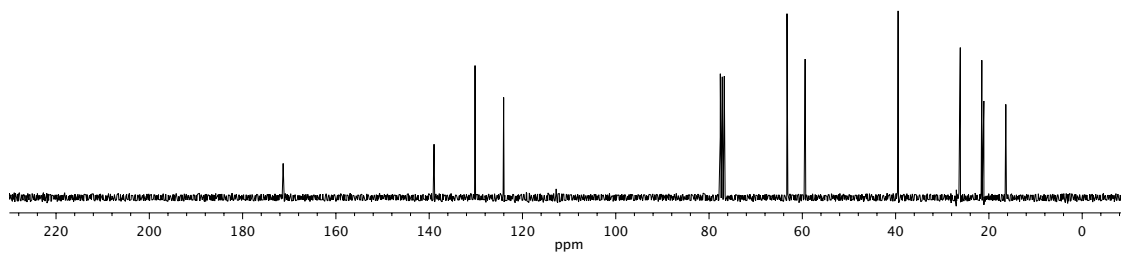


Figure A6.8.3 ^{13}C NMR (75 MHz, CDCl_3) of compound 108.

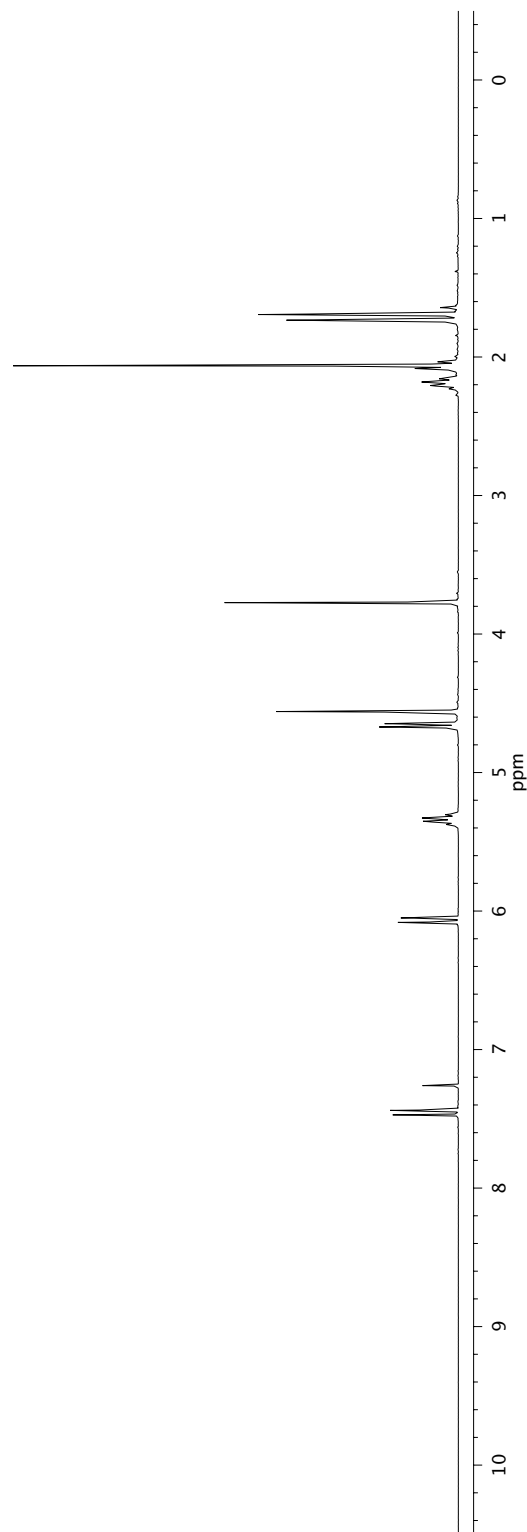
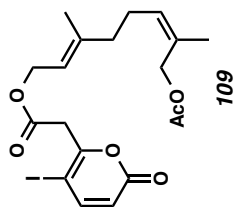


Figure A6.9.1 ¹H NMR (300 MHz, CDCl₃) of compound **109**.

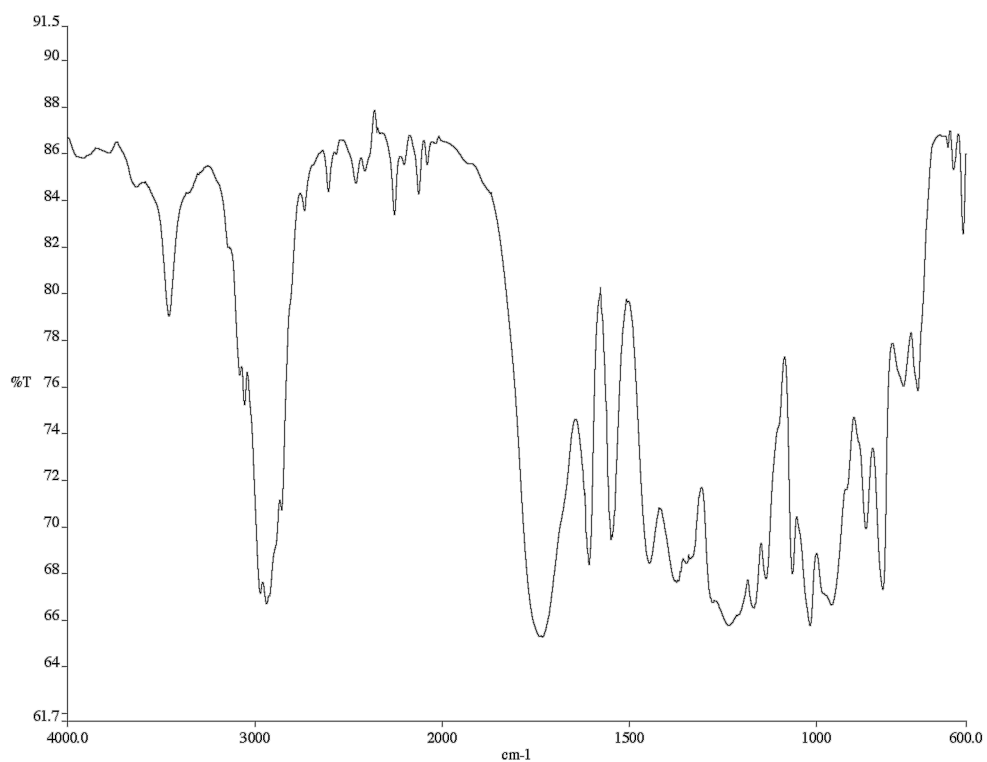


Figure A6.9.2 infrared spectrum (Thin Film, NaCl) of compound **109**.

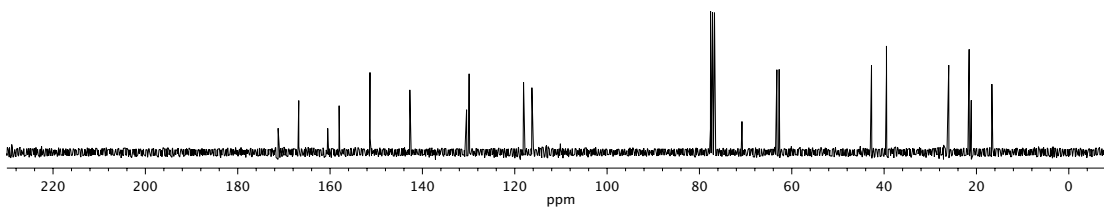
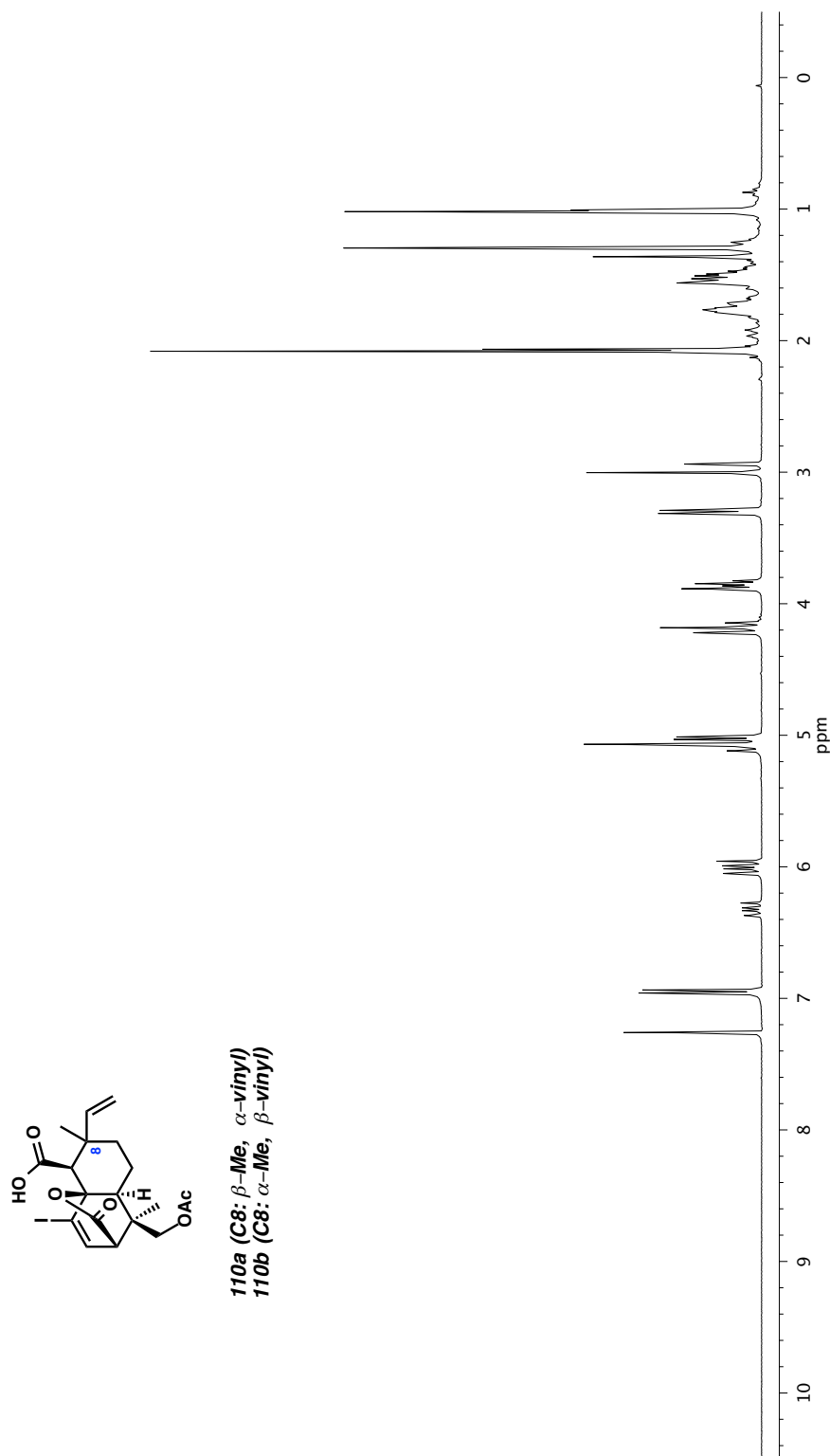


Figure A6.9.3 ¹³C NMR (75 MHz, CDCl₃) of compound **109**.



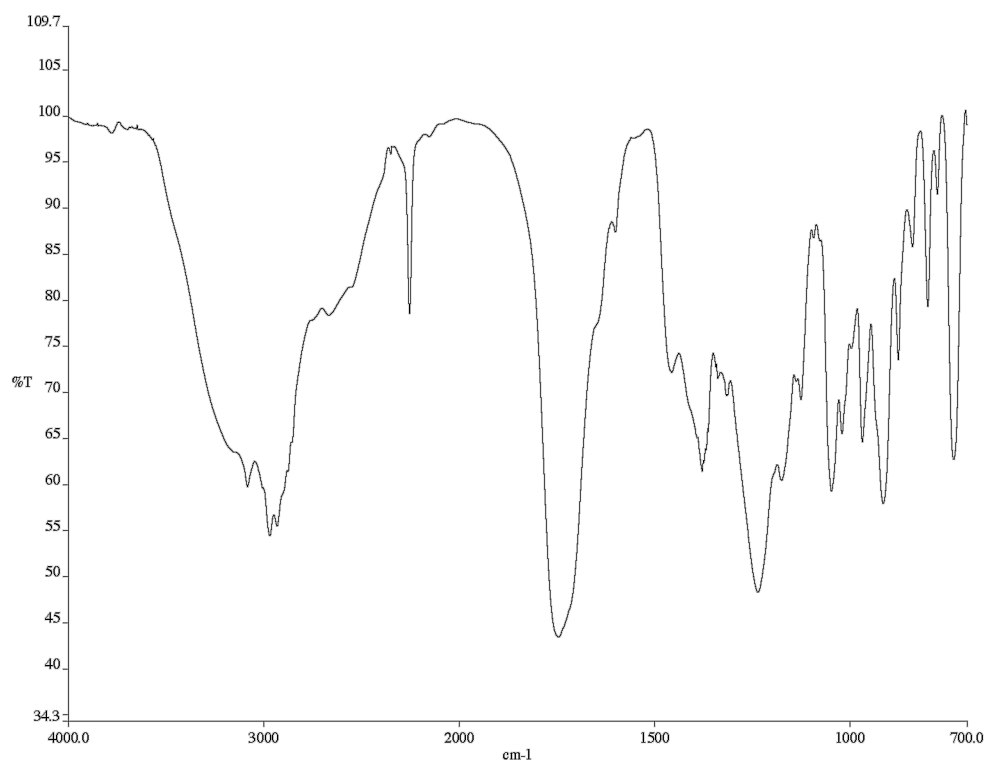


Figure A6.10.2 infrared spectrum (Thin Film, NaCl) of compounds **110a** and **110b**.

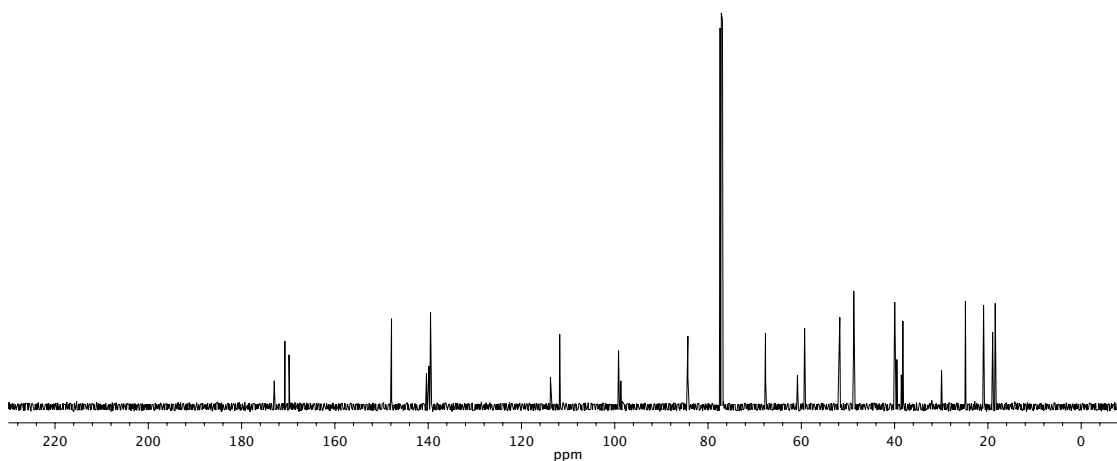
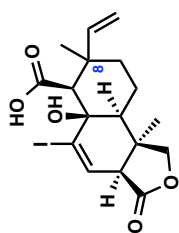


Figure A6.10.3 ^{13}C NMR (125 MHz, CDCl_3) of compounds **110a** and **110b**.



112a (C8: β -Me, α -vinyl)
112b (C8: α -Me, β -vinyl)

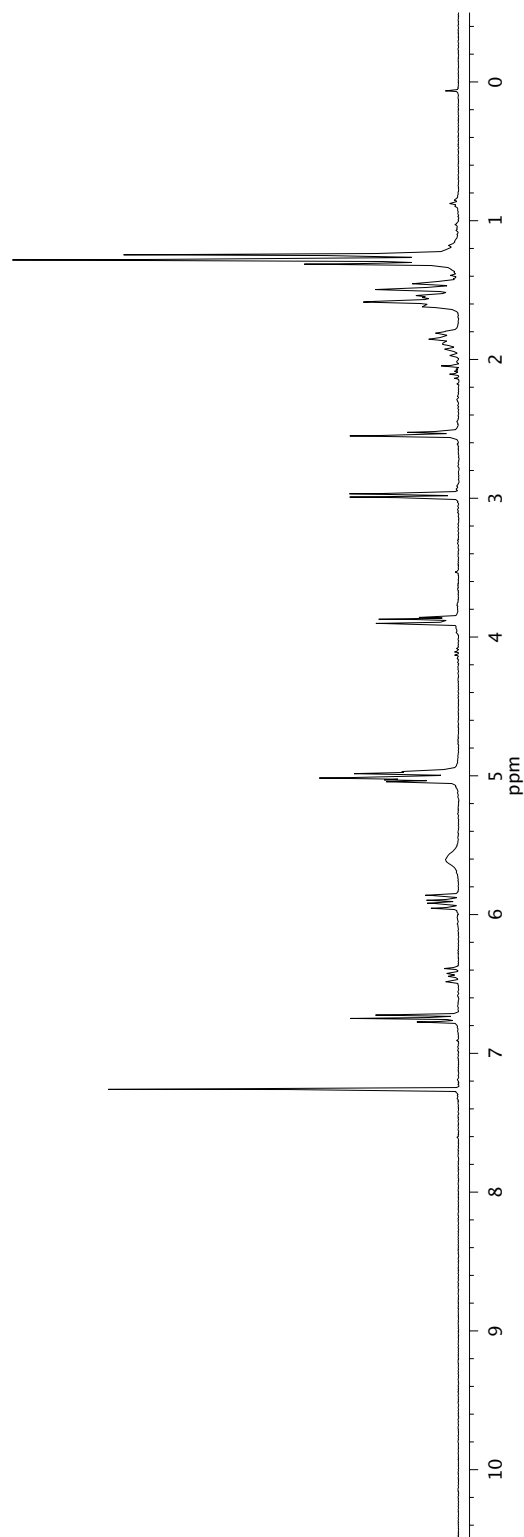


Figure A6.11.1 ^1H NMR (300 MHz, CDCl_3) of compounds **112a** and **112b**.

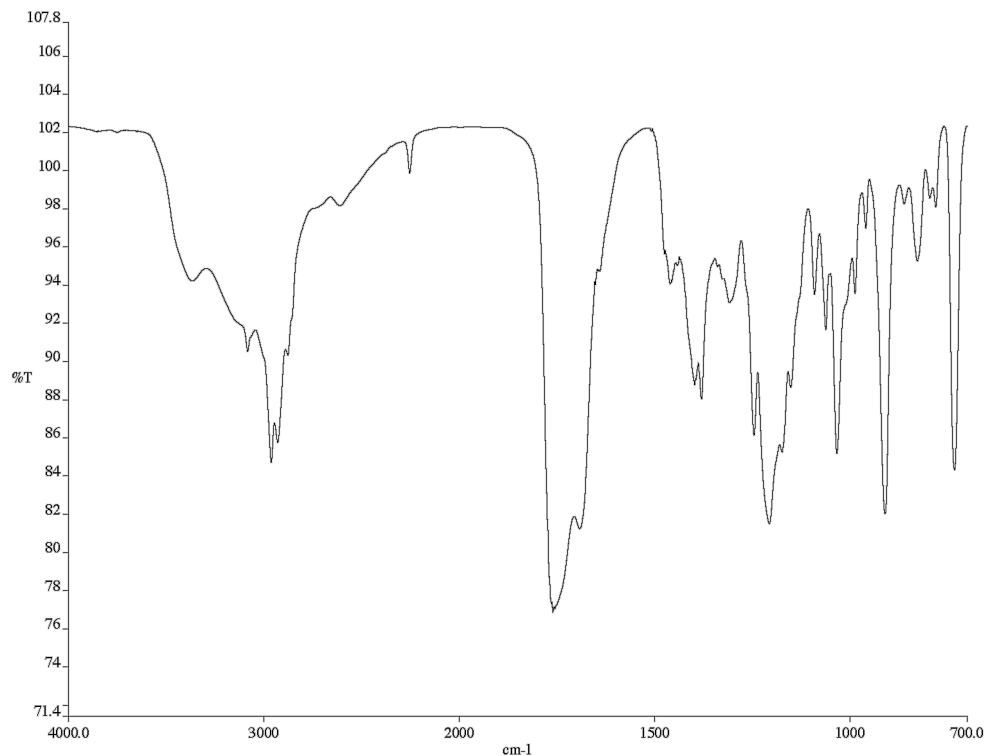


Figure A6.11.2 infrared spectrum (Thin Film, NaCl) of compounds **112a** and **112b**.

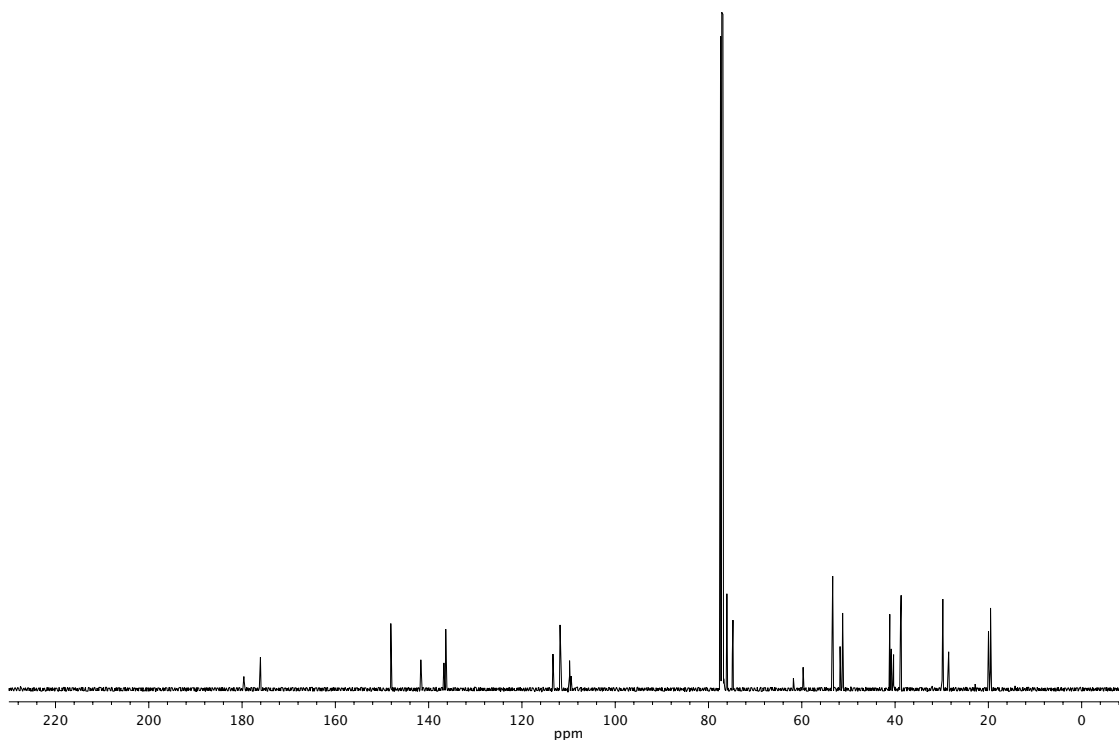
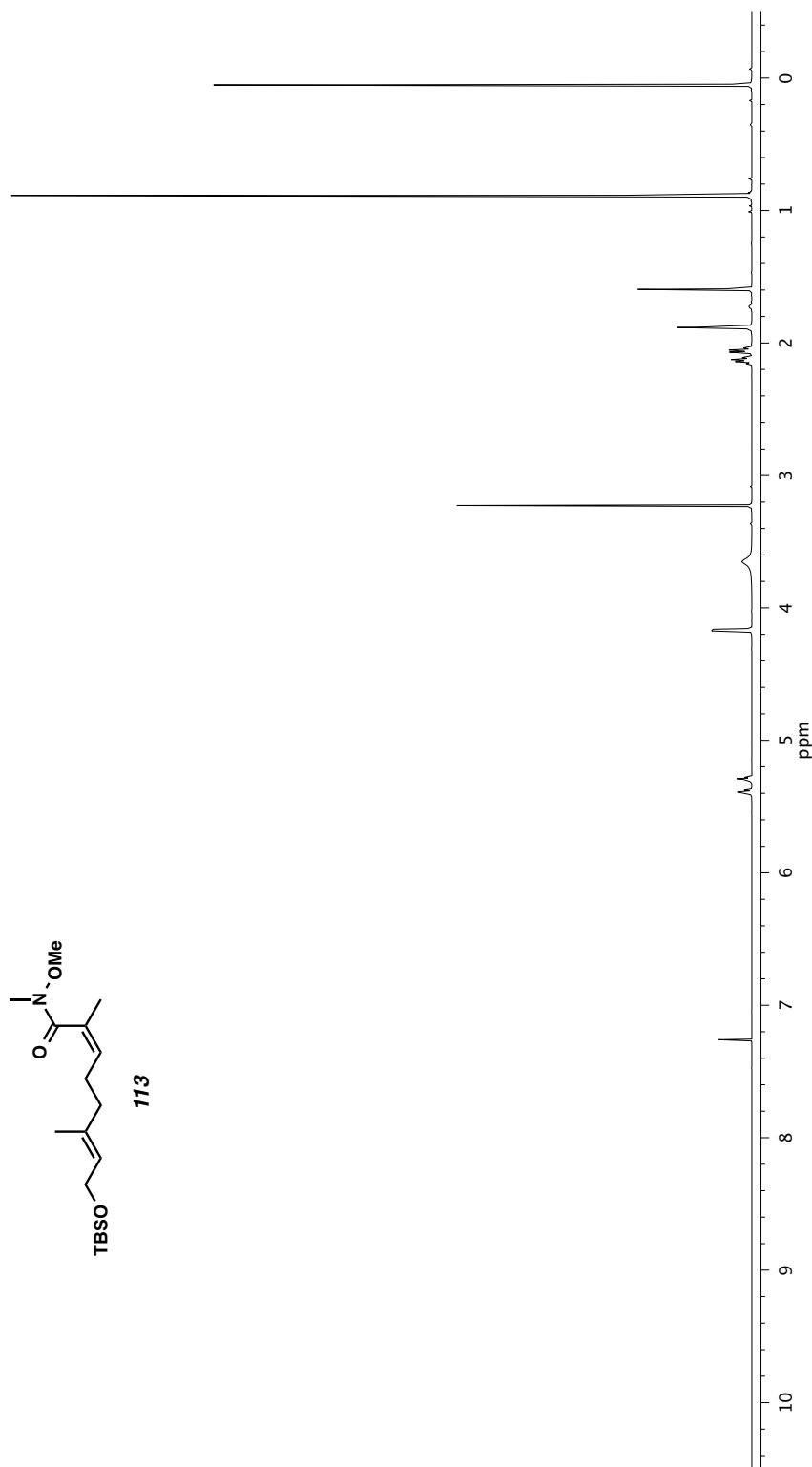


Figure A6.11.3 ¹³C NMR (125 MHz, CDCl₃) of compounds **112a** and **112b**.



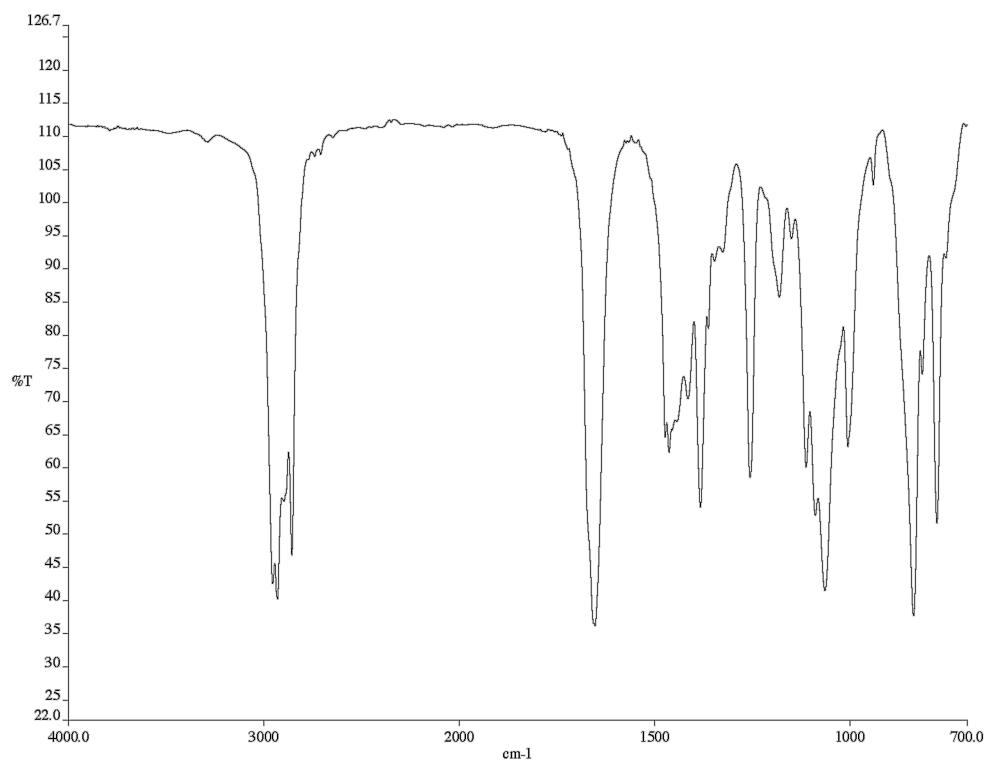


Figure A6.12.2 infrared spectrum (Thin Film, NaCl) of compound **113**.

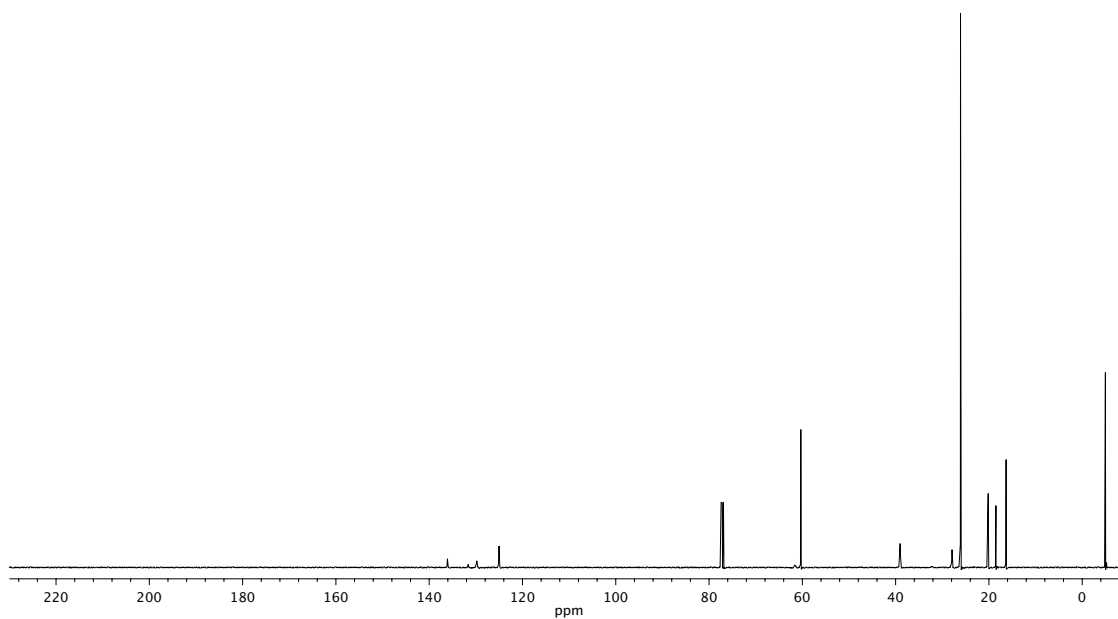


Figure A6.12.3 ^{13}C NMR (125 MHz, CDCl_3) of compound **113**.

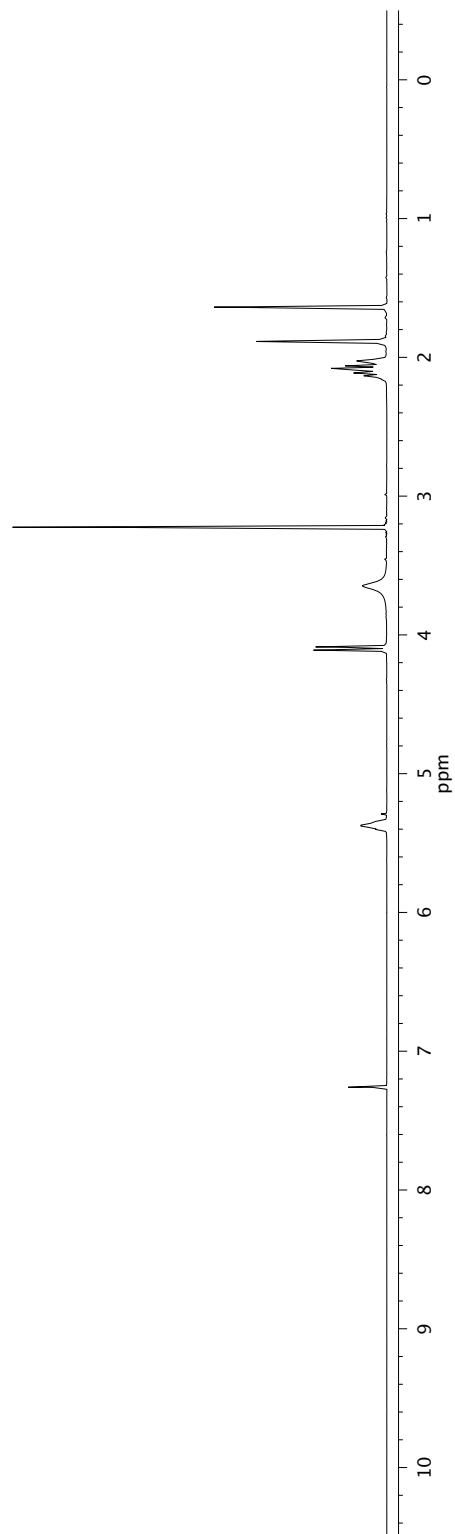
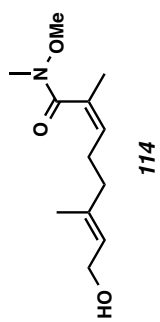


Figure A6.13.1 ¹H NMR (300 MHz, CDCl₃) of compound **114**.

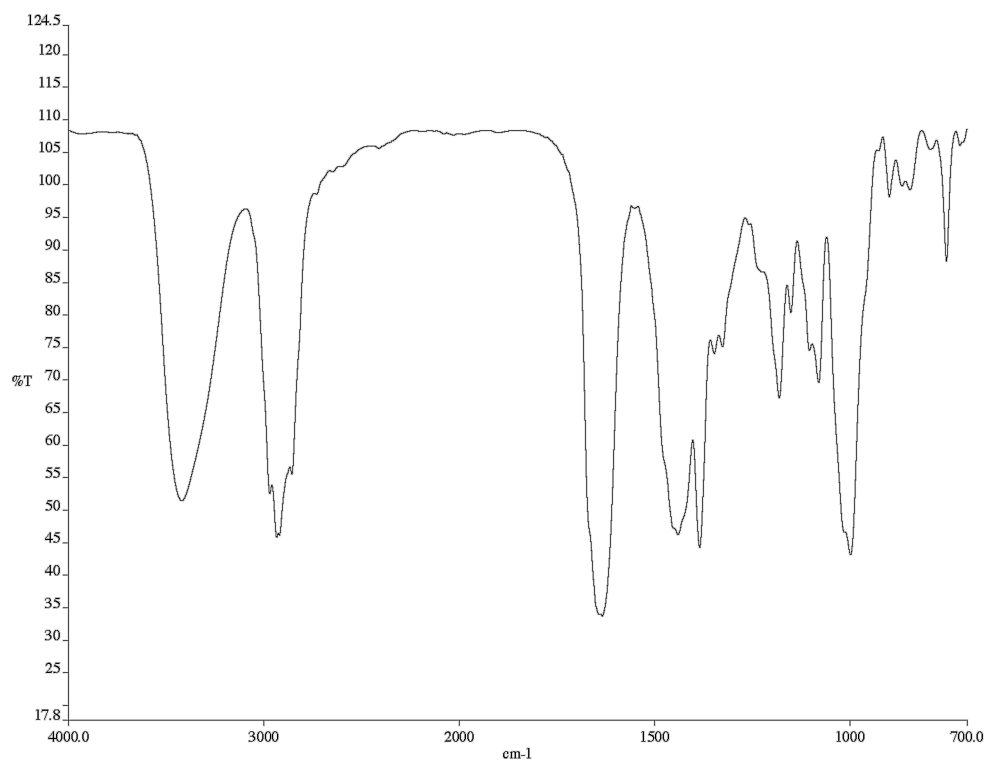


Figure A6.13.2 infrared spectrum (Thin Film, NaCl) of compound **114**.

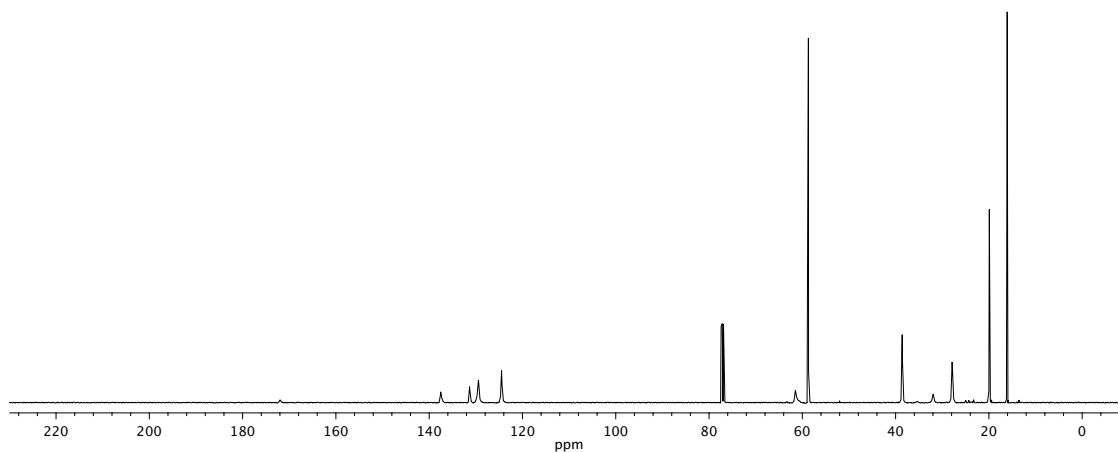


Figure A6.13.3 ¹³C NMR (125 MHz, CDCl₃) of compound **114**.

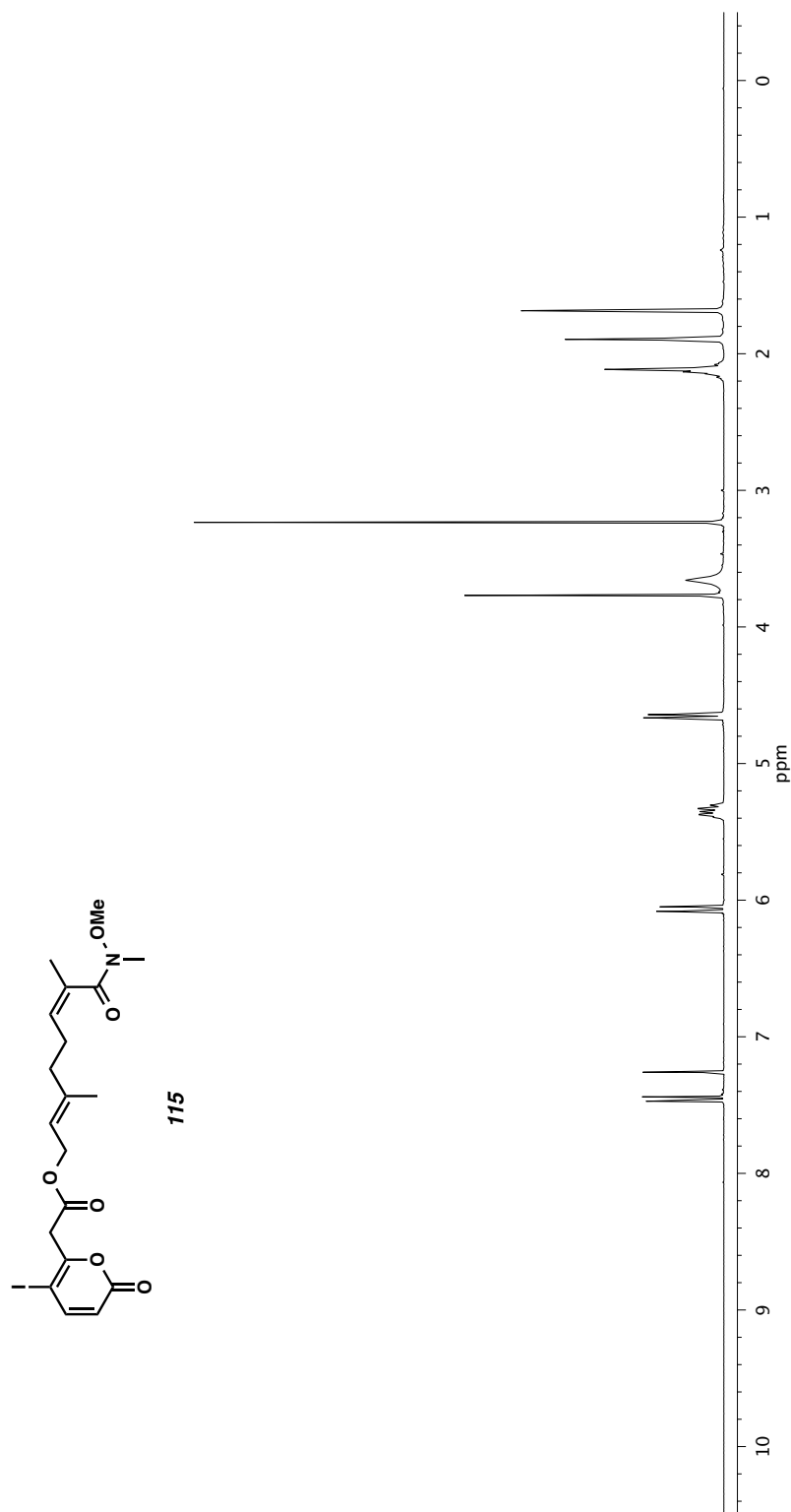


Figure A6.14.1 ¹H NMR (300 MHz, CDCl₃) of compound **115**.

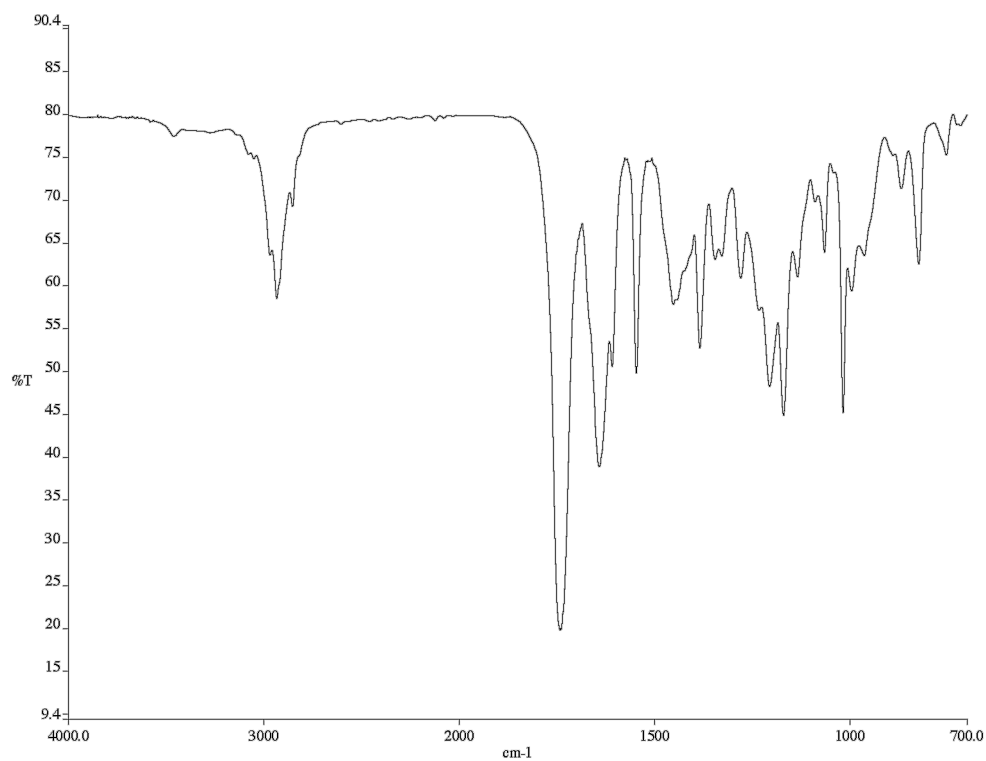


Figure A6.14.2 infrared spectrum (Thin Film, NaCl) of compound **115**.

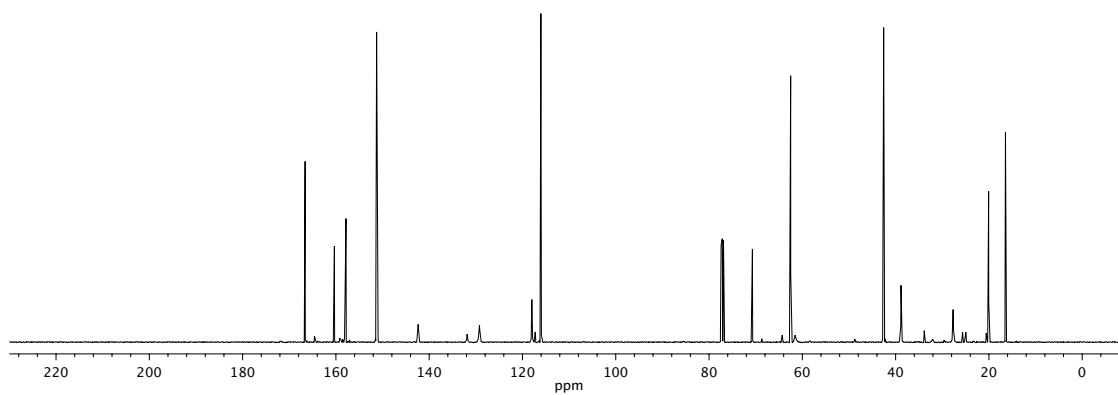


Figure A6.14.3 ¹³C NMR (125 MHz, CDCl₃) of compound **115**.

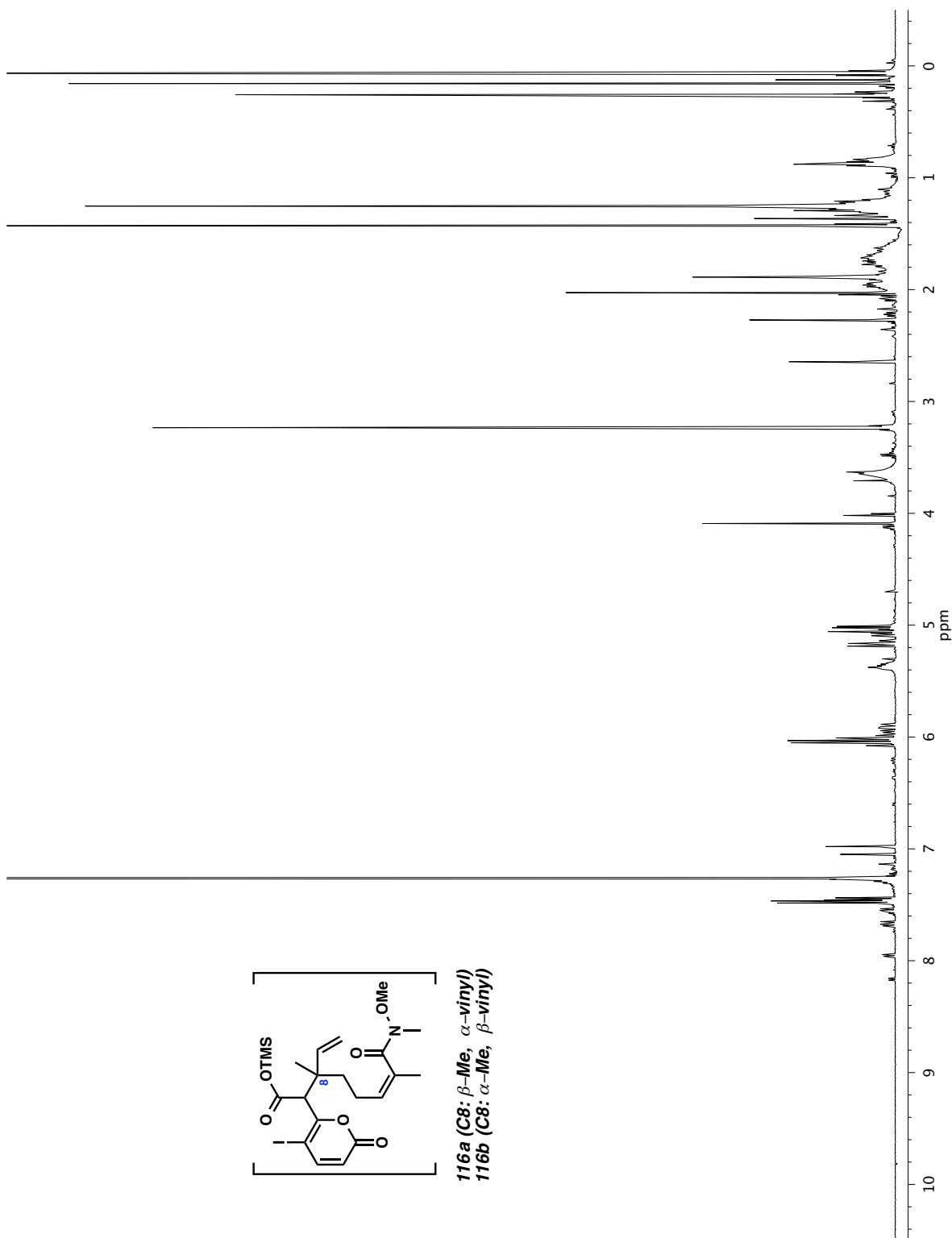


Figure A6.15.1 ^1H NMR (500 MHz, CDCl_3) of a crude mixture of compounds **116a** and **116b**.

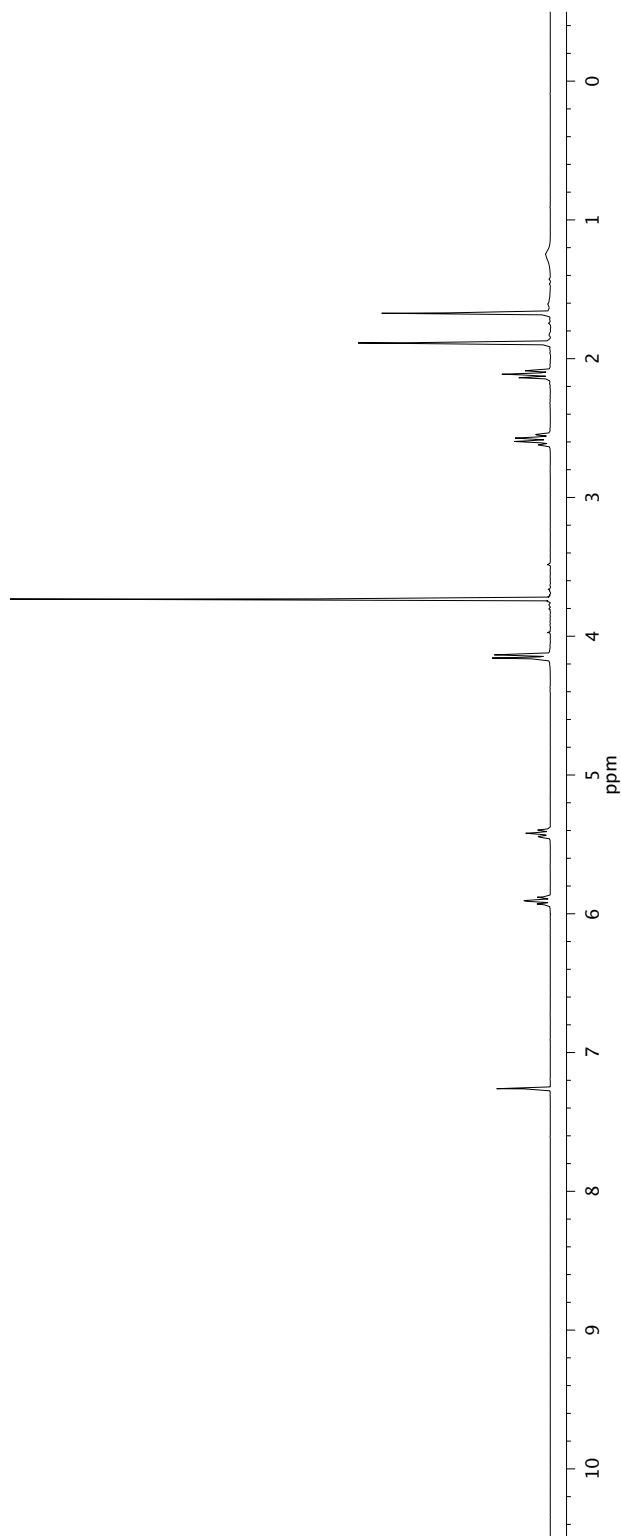
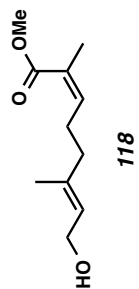


Figure A6.16.1 ¹H NMR (300 MHz, CDCl₃) of compound **118**.

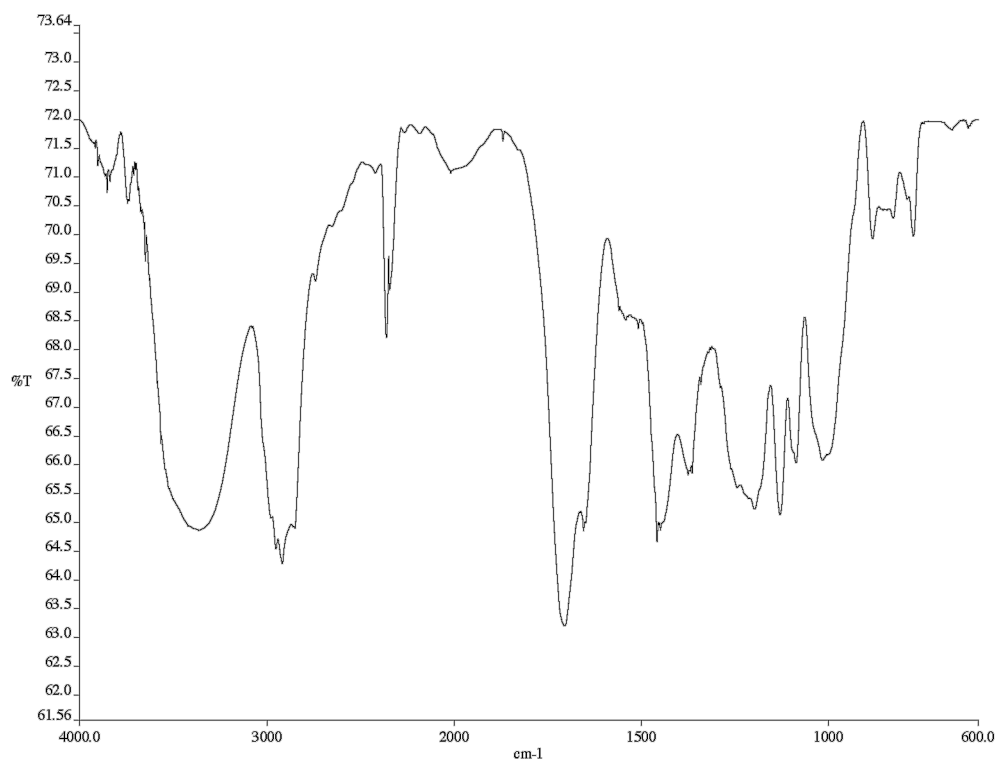


Figure A6.16.2 infrared spectrum (Thin Film, NaCl) of compound **118**.

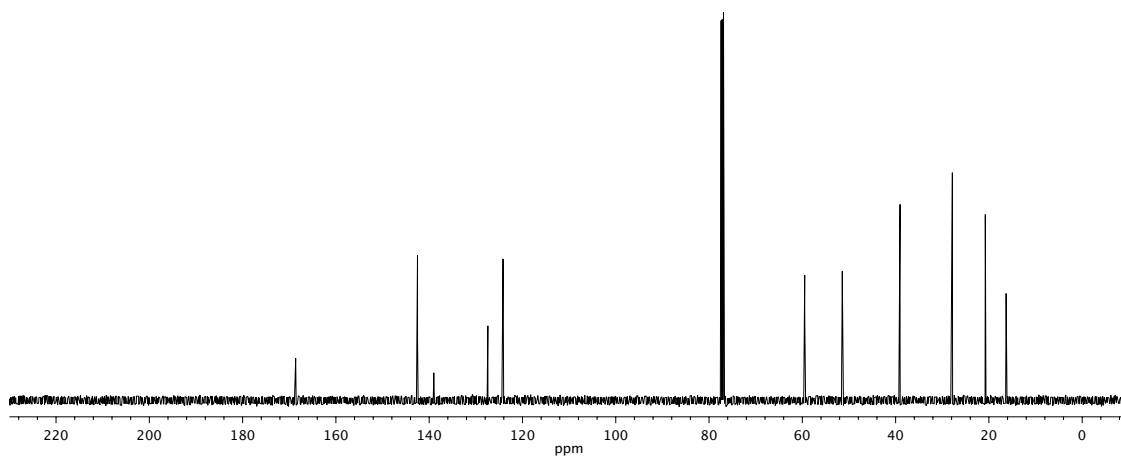


Figure A6.16.3 ¹³C NMR (125 MHz, CDCl₃) of compound **118**.

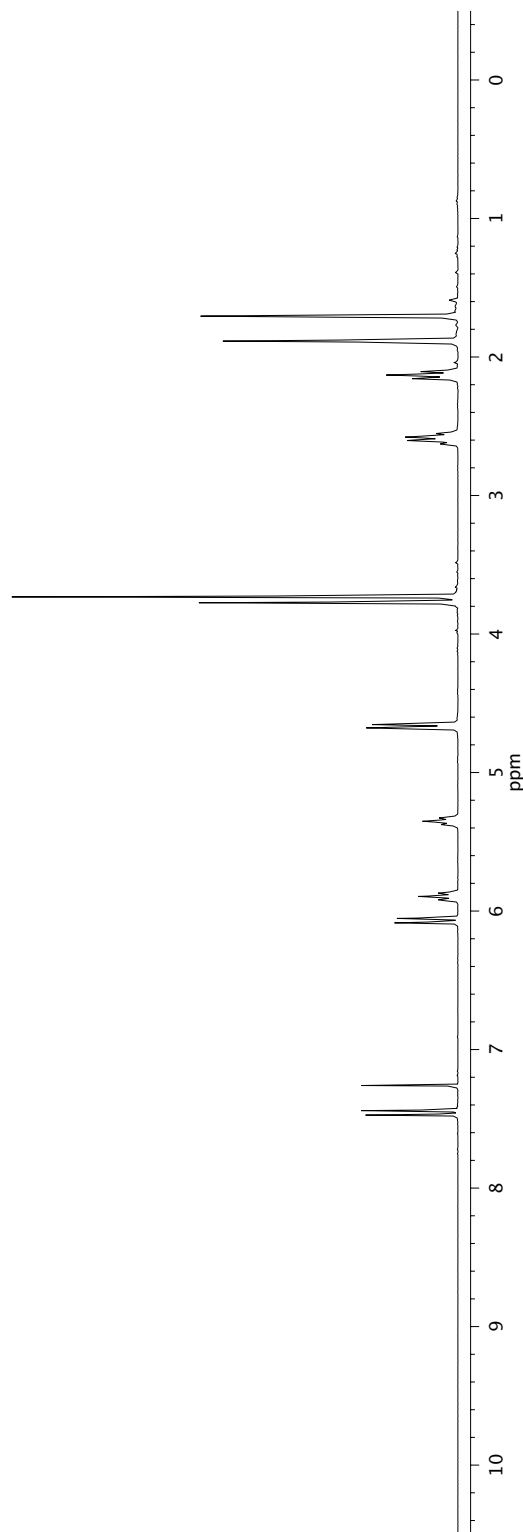
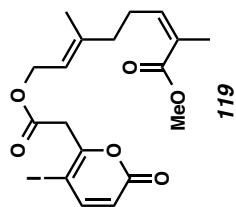


Figure A6.17.1 ¹H NMR (300 MHz, CDCl₃) of compound **119**.

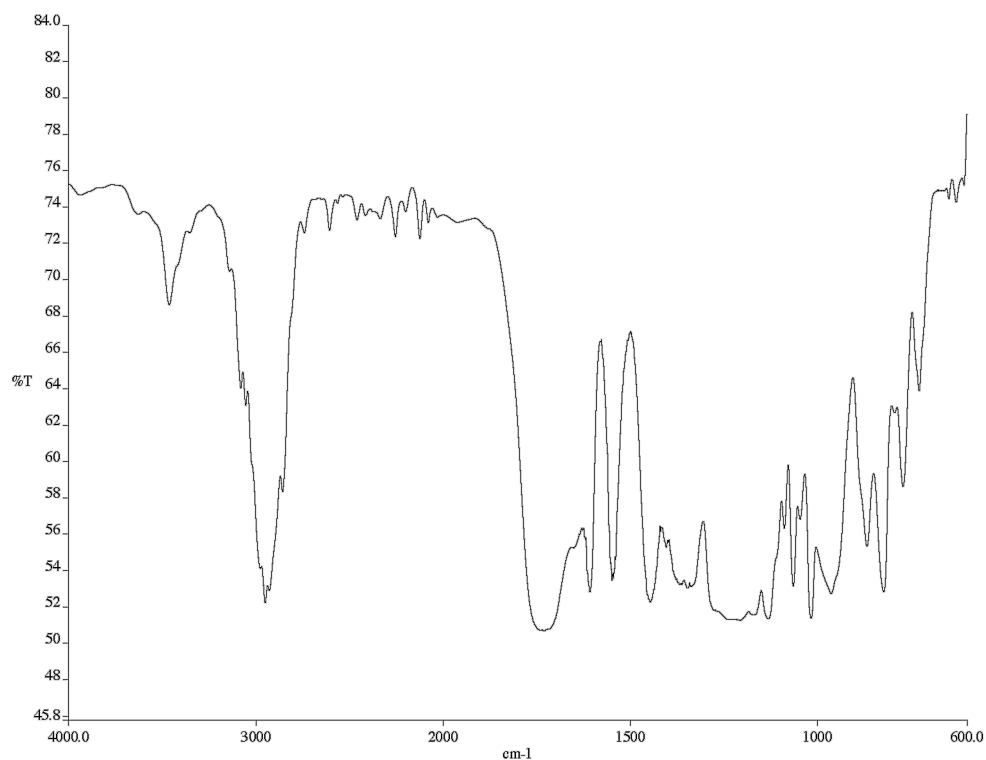


Figure A6.17.2 infrared spectrum (Thin Film, NaCl) of compound **119**.

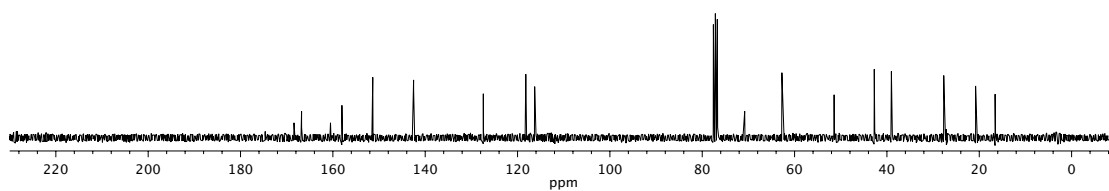


Figure A6.17.3 ¹³C NMR (75 MHz, CDCl₃) of compound **119**.

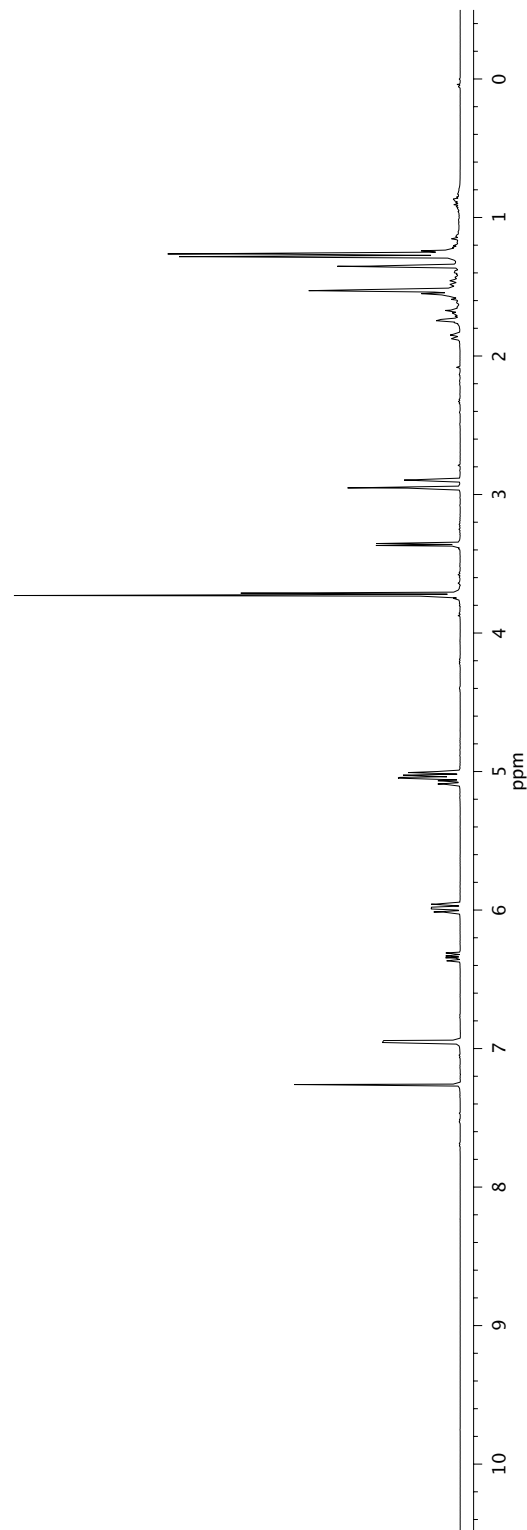
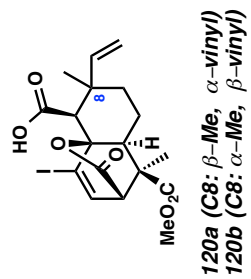


Figure A6.18.1 ^1H NMR (500 MHz, CDCl_3) of compounds **120a** and **120b**.

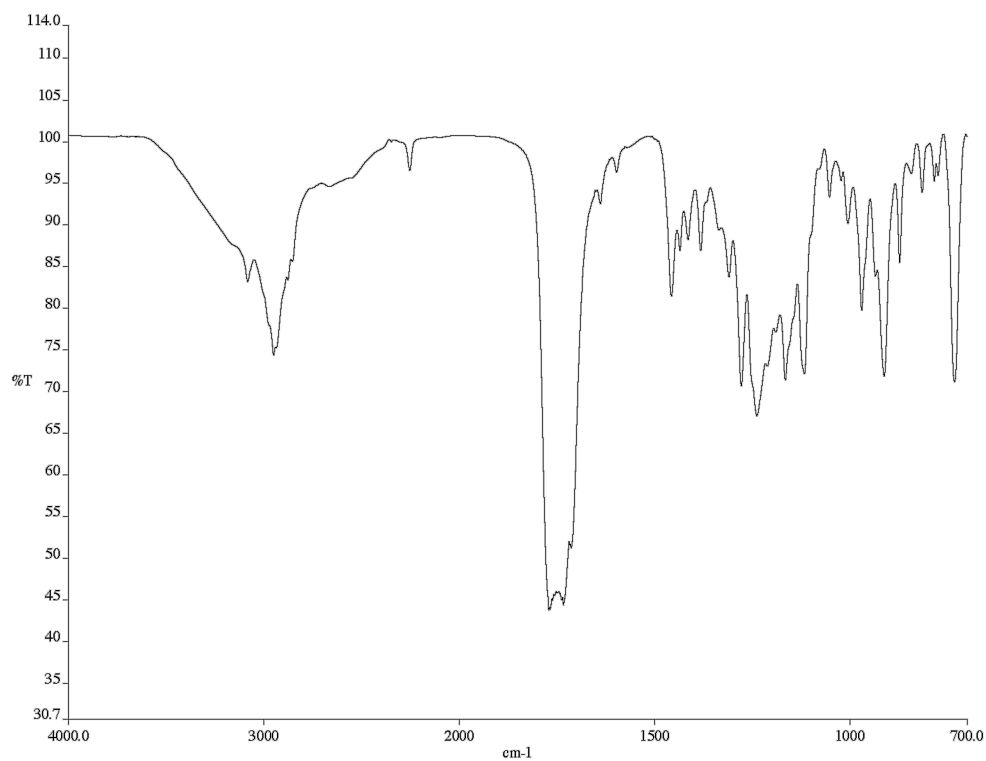


Figure A6.18.2 infrared spectrum (Thin Film, NaCl) of compounds **120a** and **120b**.

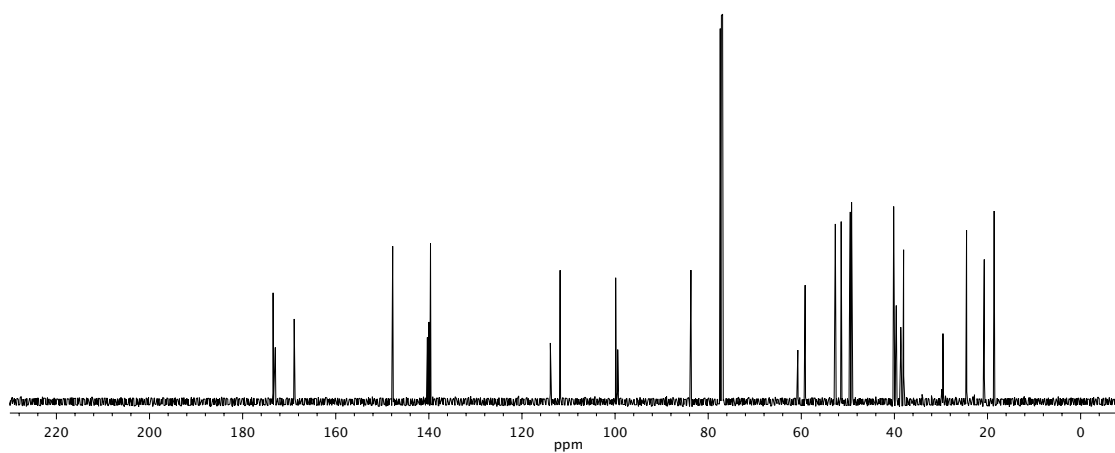


Figure A6.18.3 ¹³C NMR (125 MHz, CDCl₃) of compounds **120a** and **120b**.

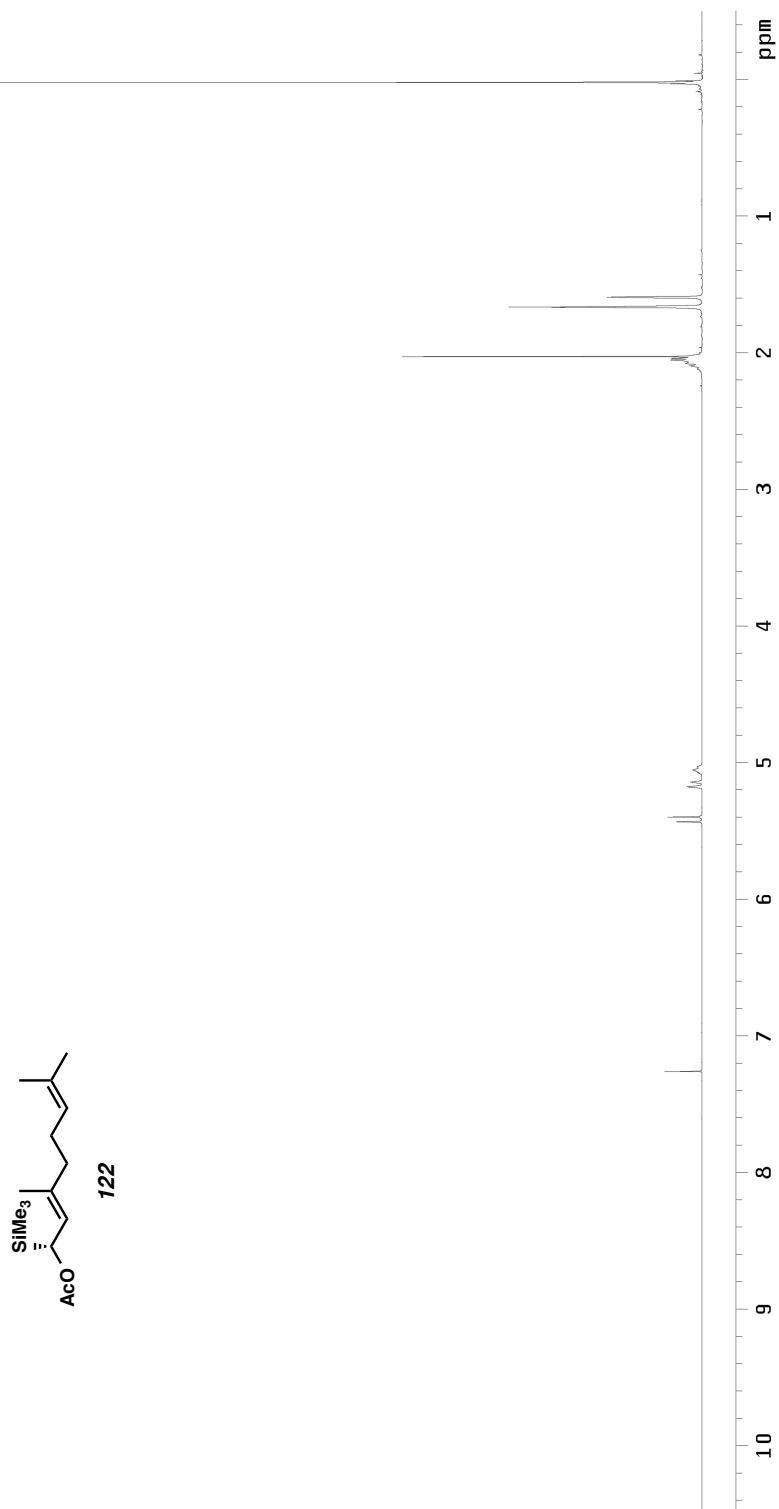


Figure A6.19.1 ¹H NMR (300 MHz, CDCl₃) of compound **122**.

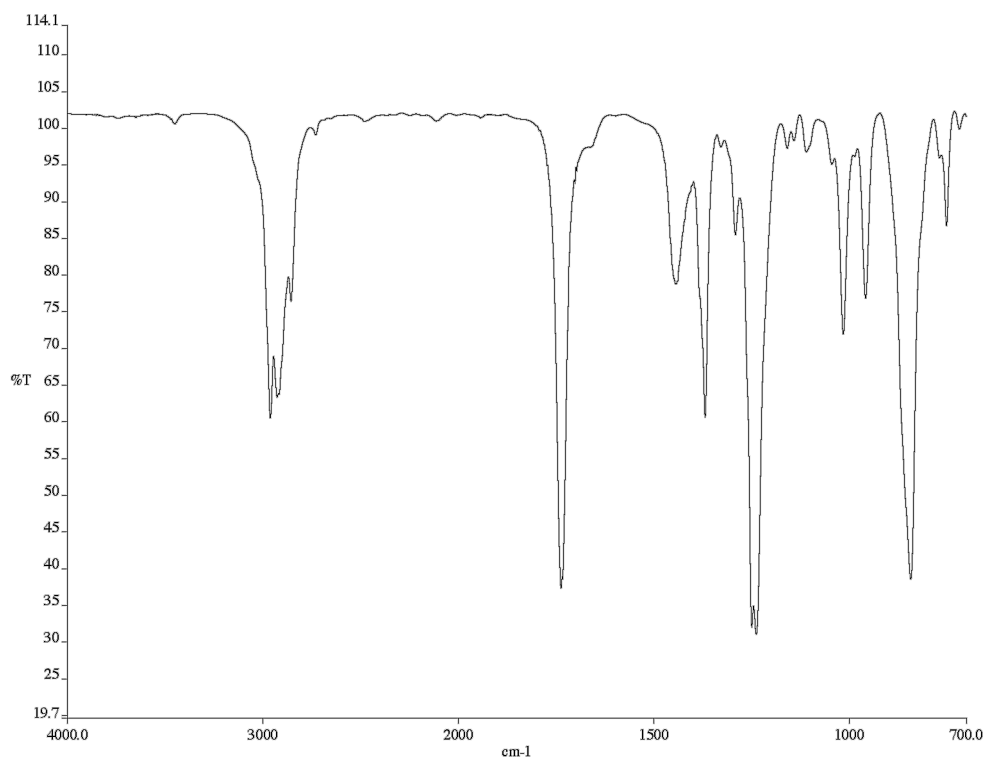


Figure A6.19.2 infrared spectrum (Thin Film, NaCl) of compound **122**.

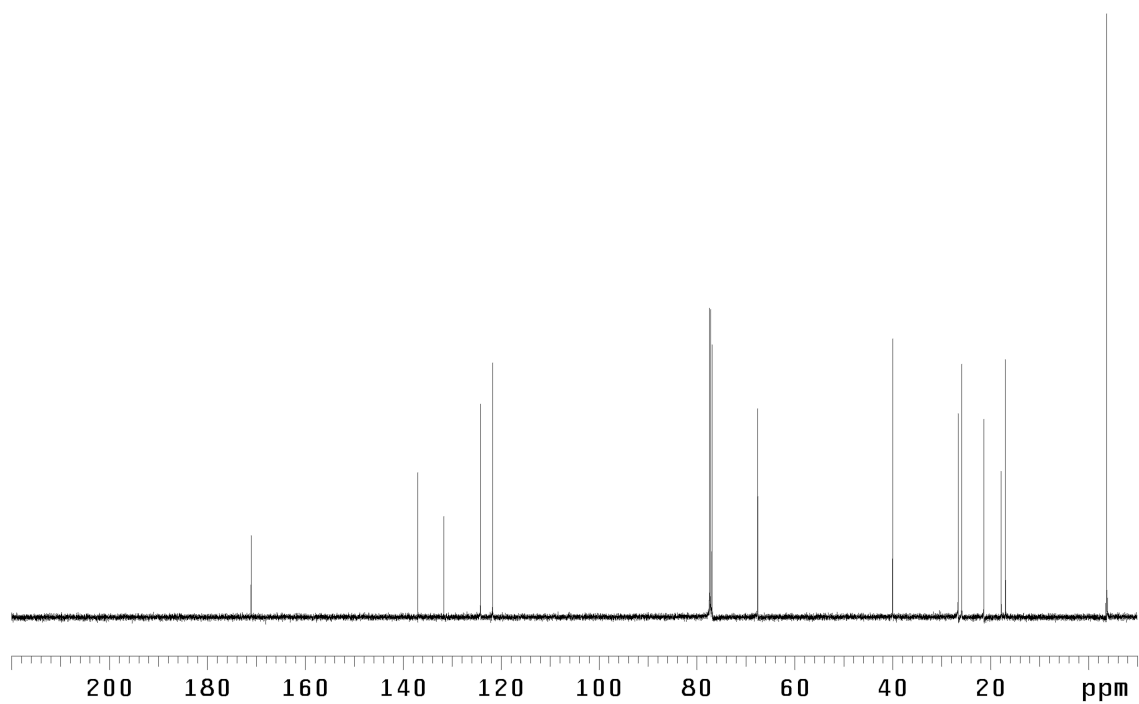


Figure A6.19.3 ¹³C NMR (75 MHz, CDCl₃) of compound **122**.

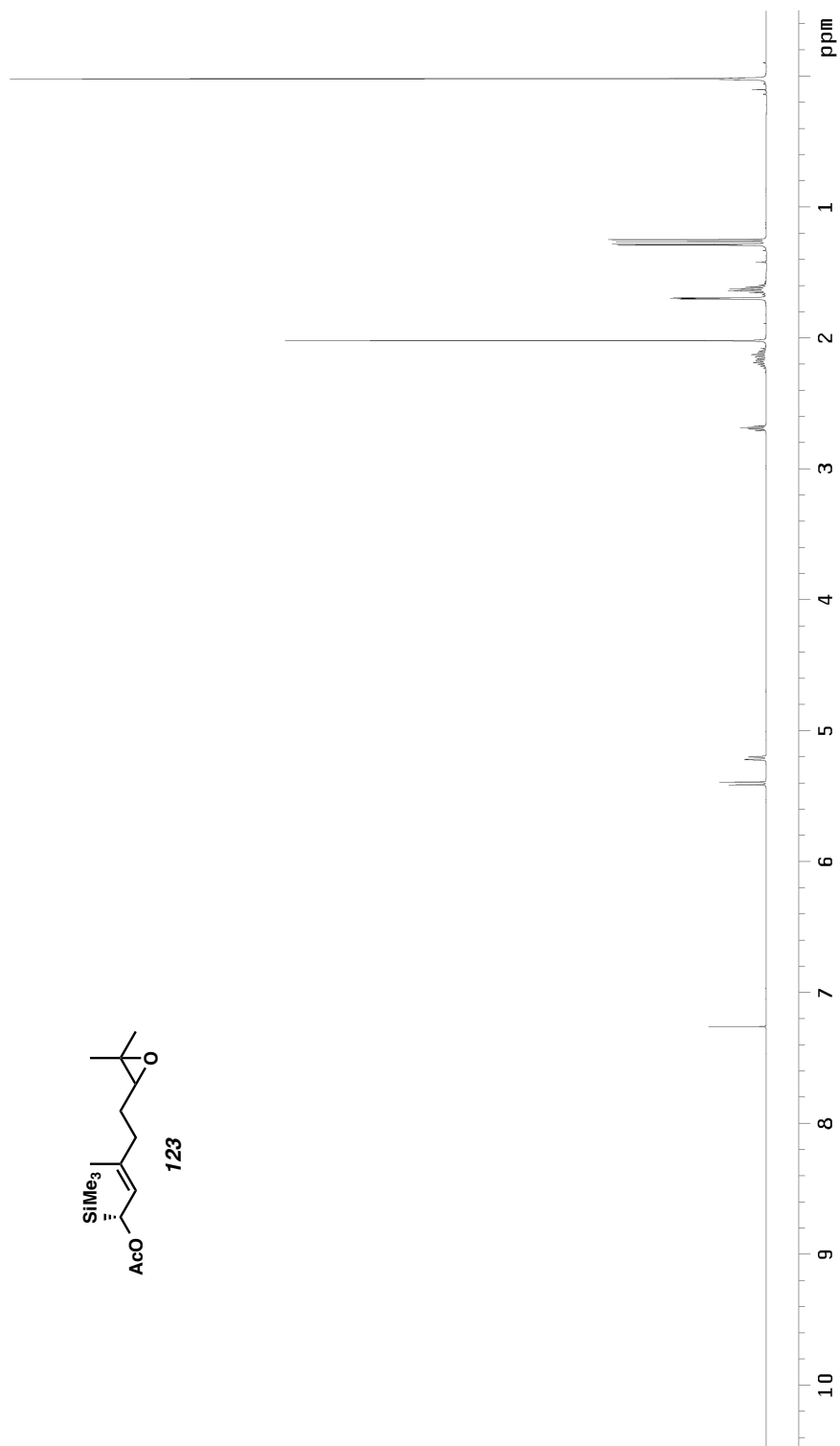
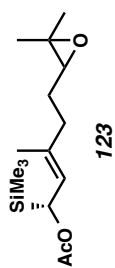


Figure A6.20.1 ¹H NMR (500 MHz, CDCl₃) of compound **123**.

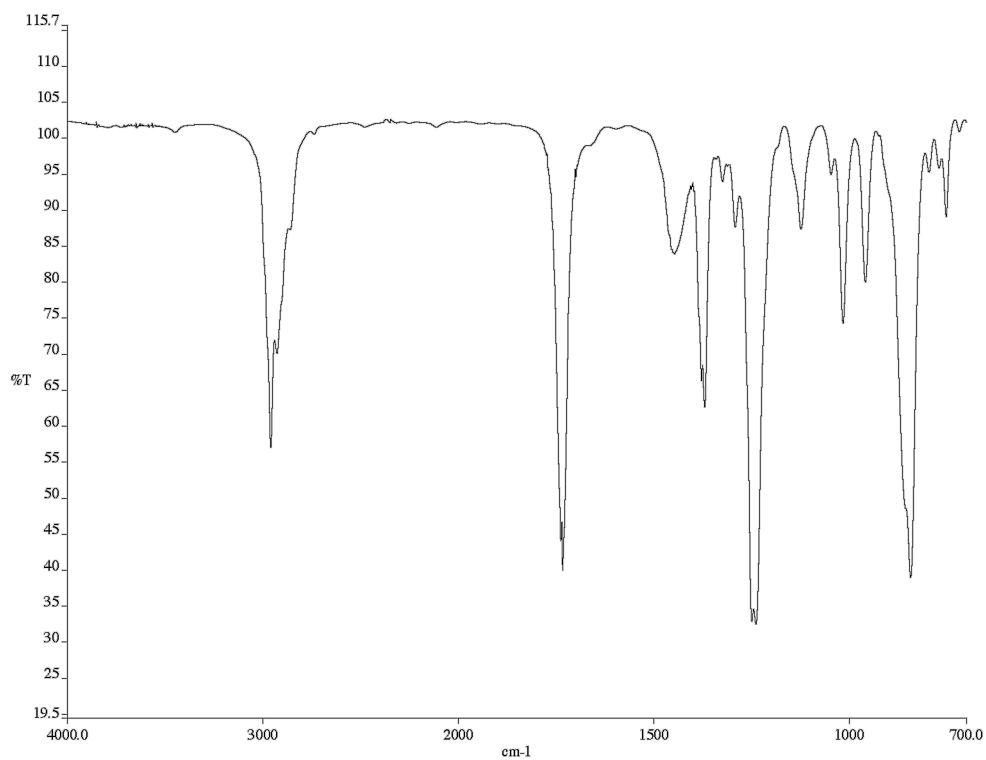


Figure A6.20.2 infrared spectrum (Thin Film, NaCl) of compound **123**.

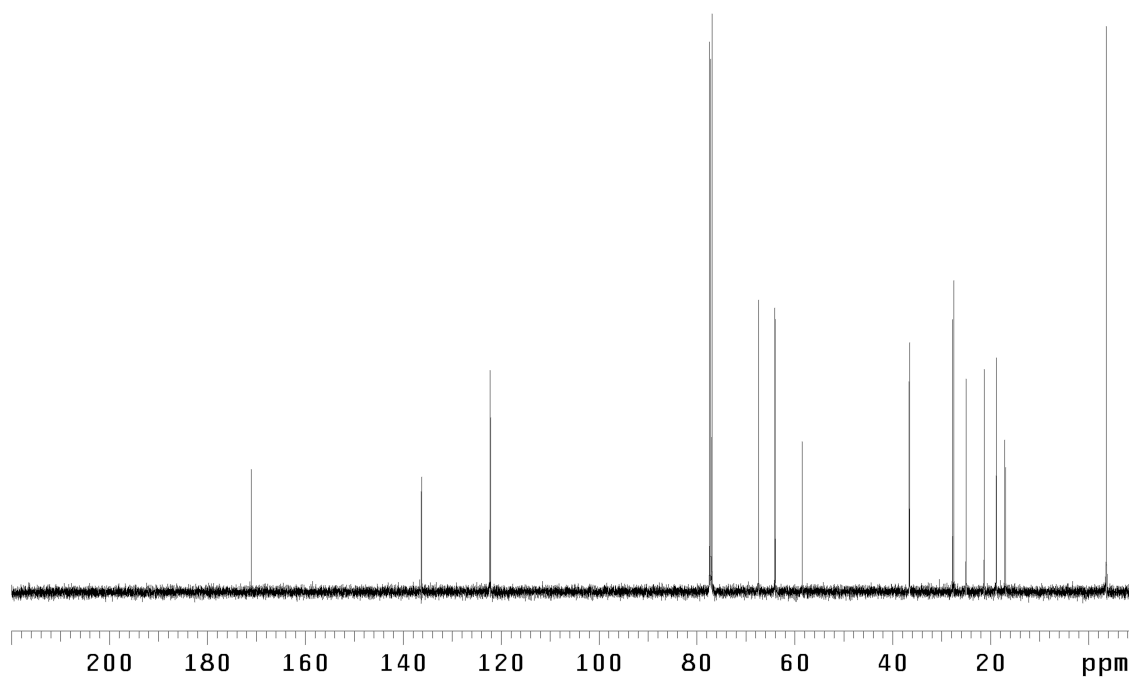


Figure A6.20.3 ^{13}C NMR (125 MHz, CDCl_3) of compound **123**.

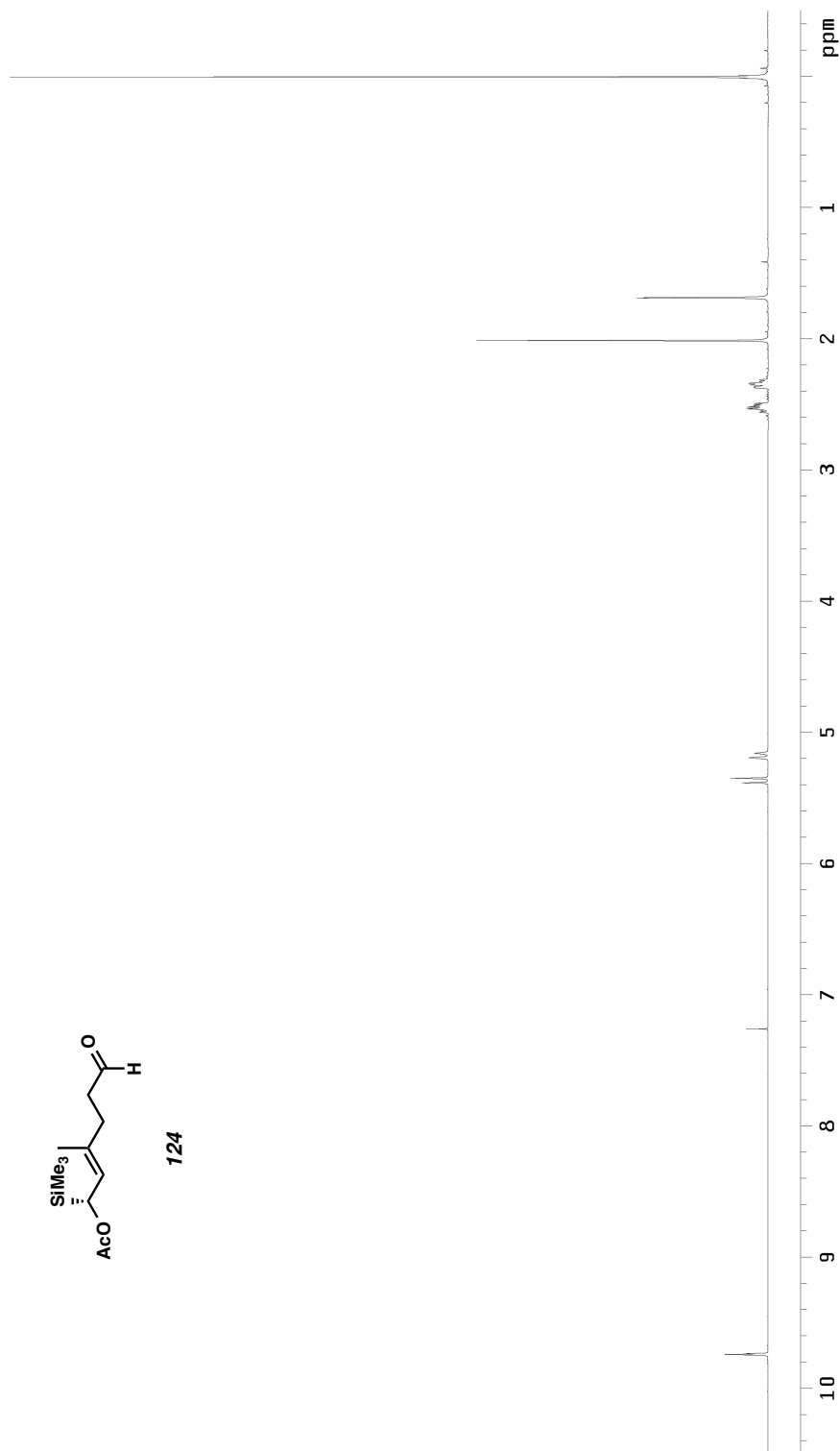


Figure A6.21.1 ¹H NMR (300 MHz, CDCl₃) of compound **124**.

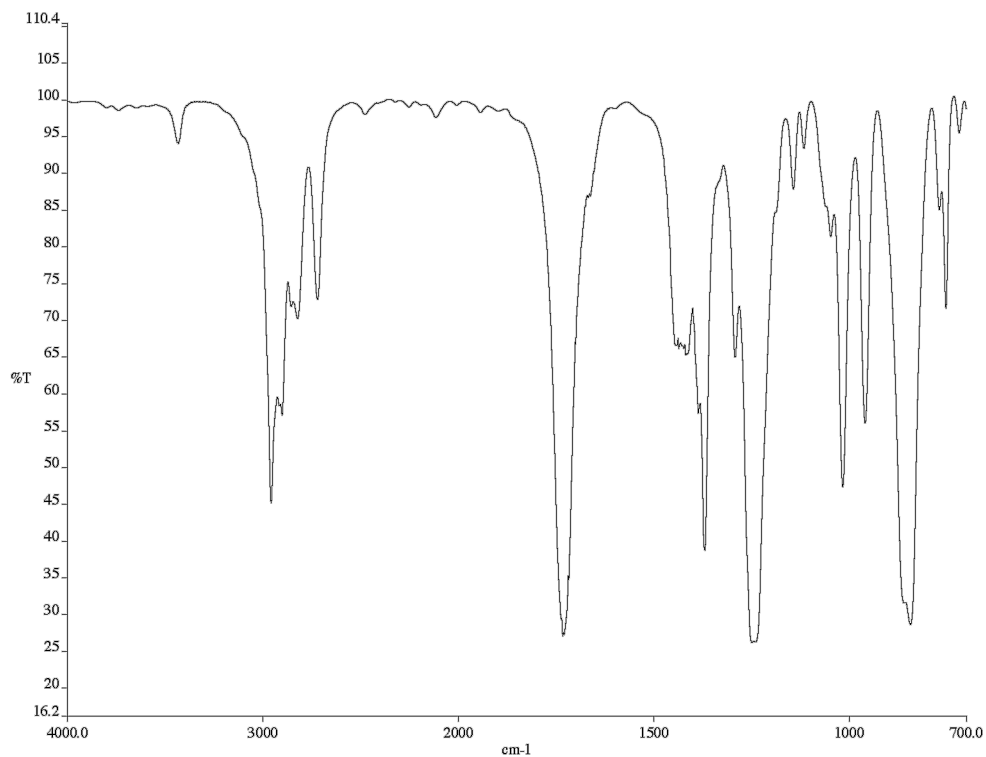


Figure A6.21.2 infrared spectrum (Thin Film, NaCl) of compound **124**.

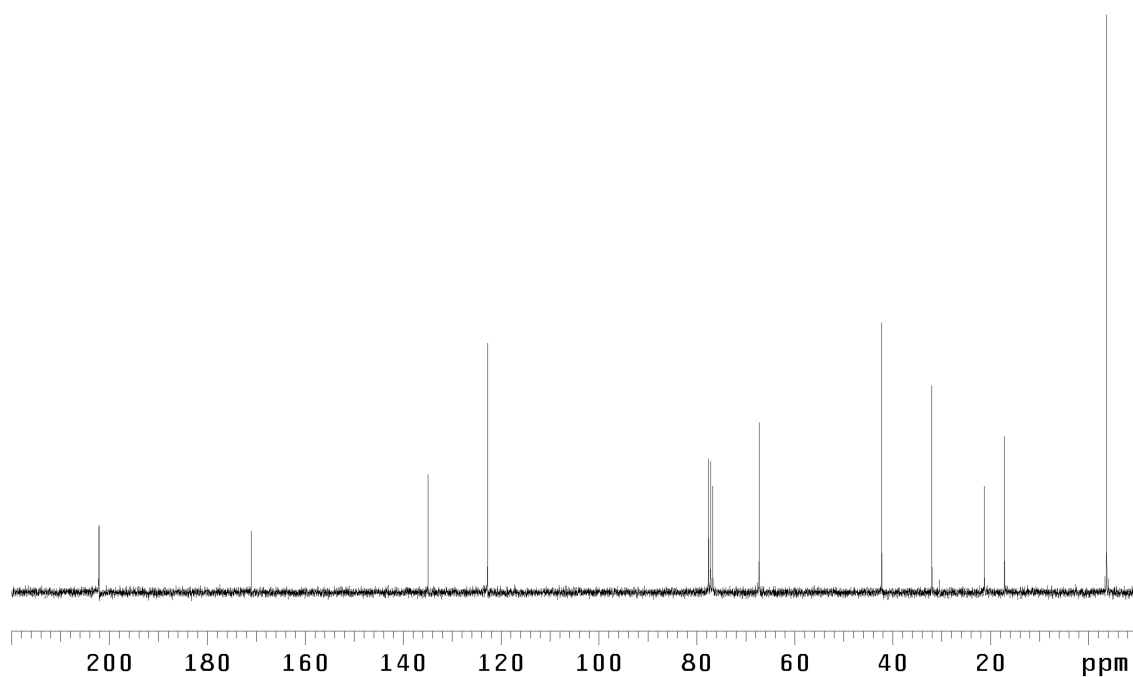


Figure A6.21.3 ¹³C NMR (75 MHz, CDCl₃) of compound **124**.

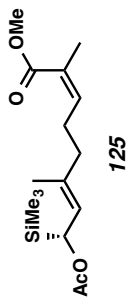
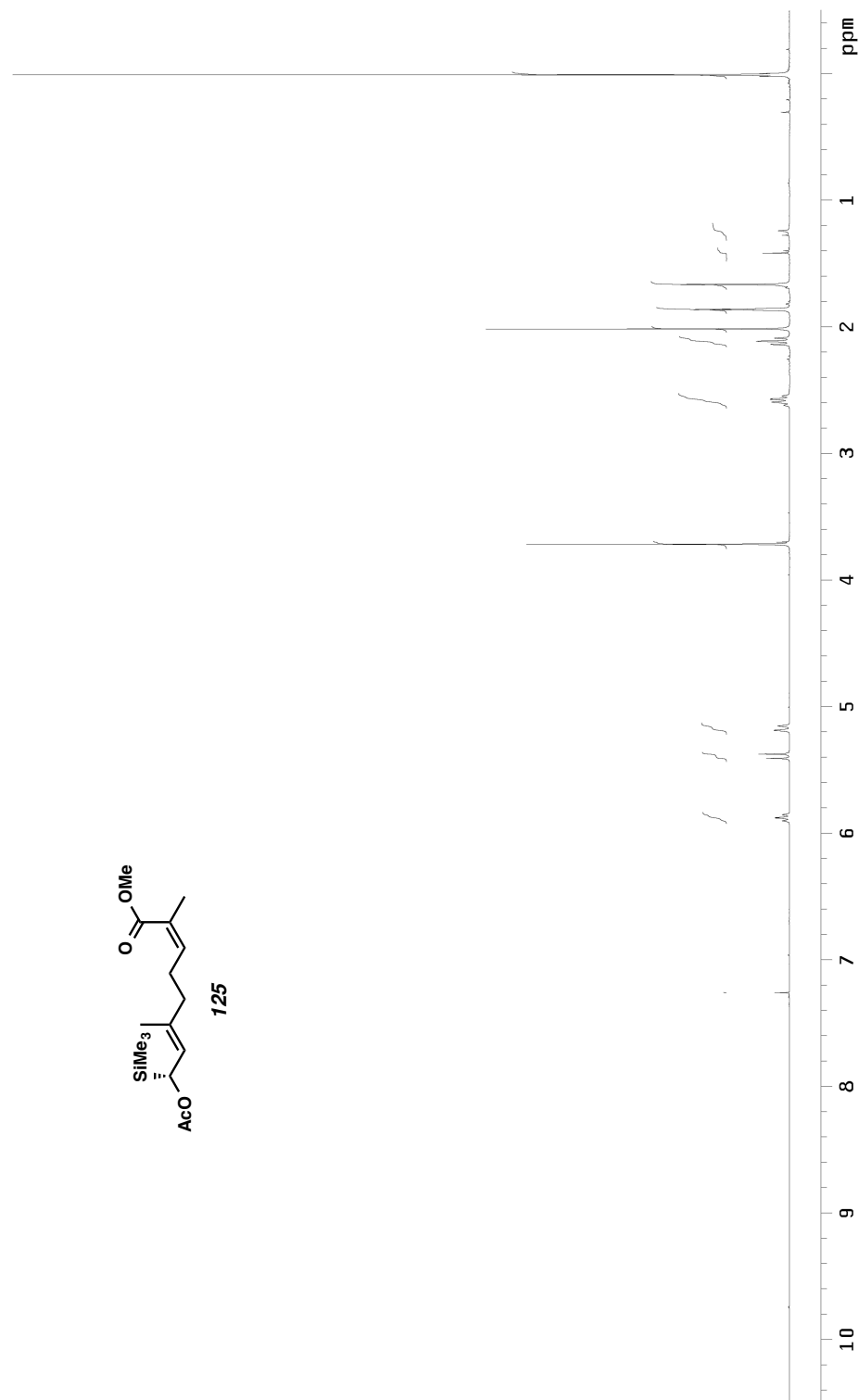


Figure A6.22.1 ¹H NMR (300 MHz, CDCl₃) of compound 125.

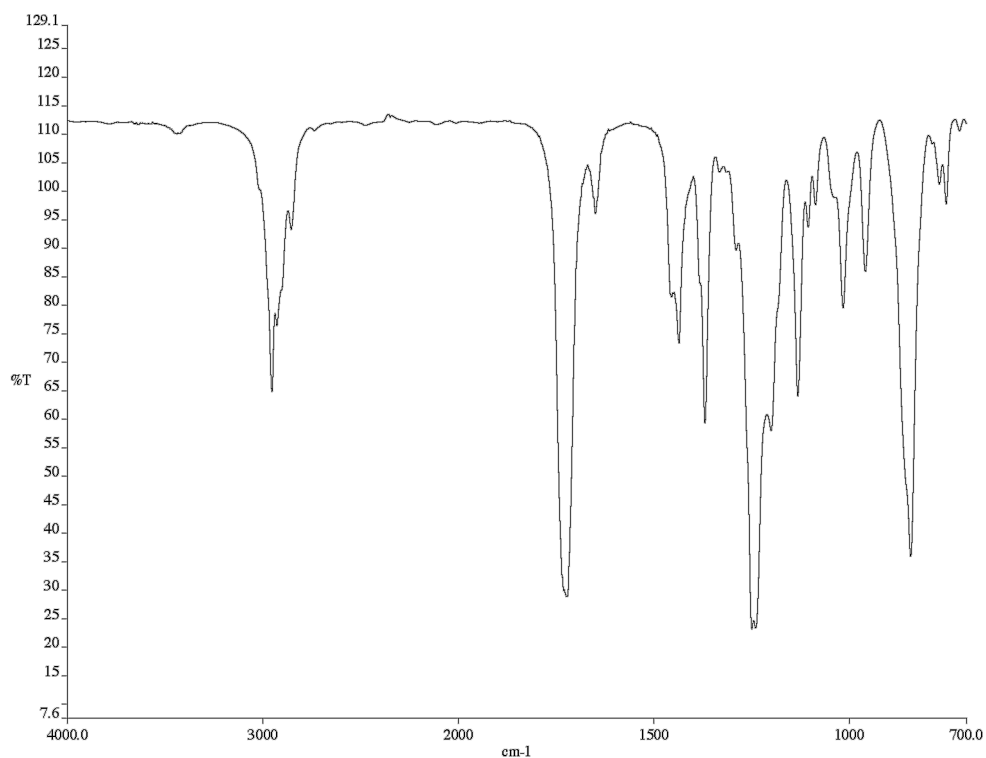


Figure A6.22.2 infrared spectrum (Thin Film, NaCl) of compound **125**.

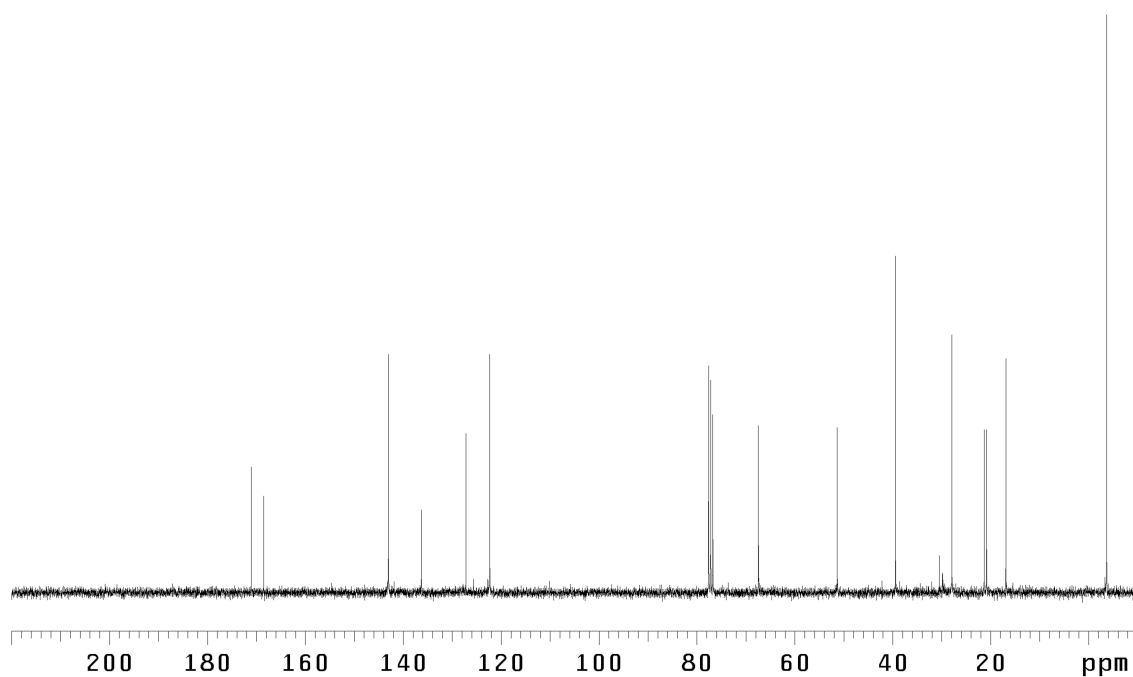


Figure A6.22.3 ^{13}C NMR (75 MHz, CDCl_3) of compound **125**.

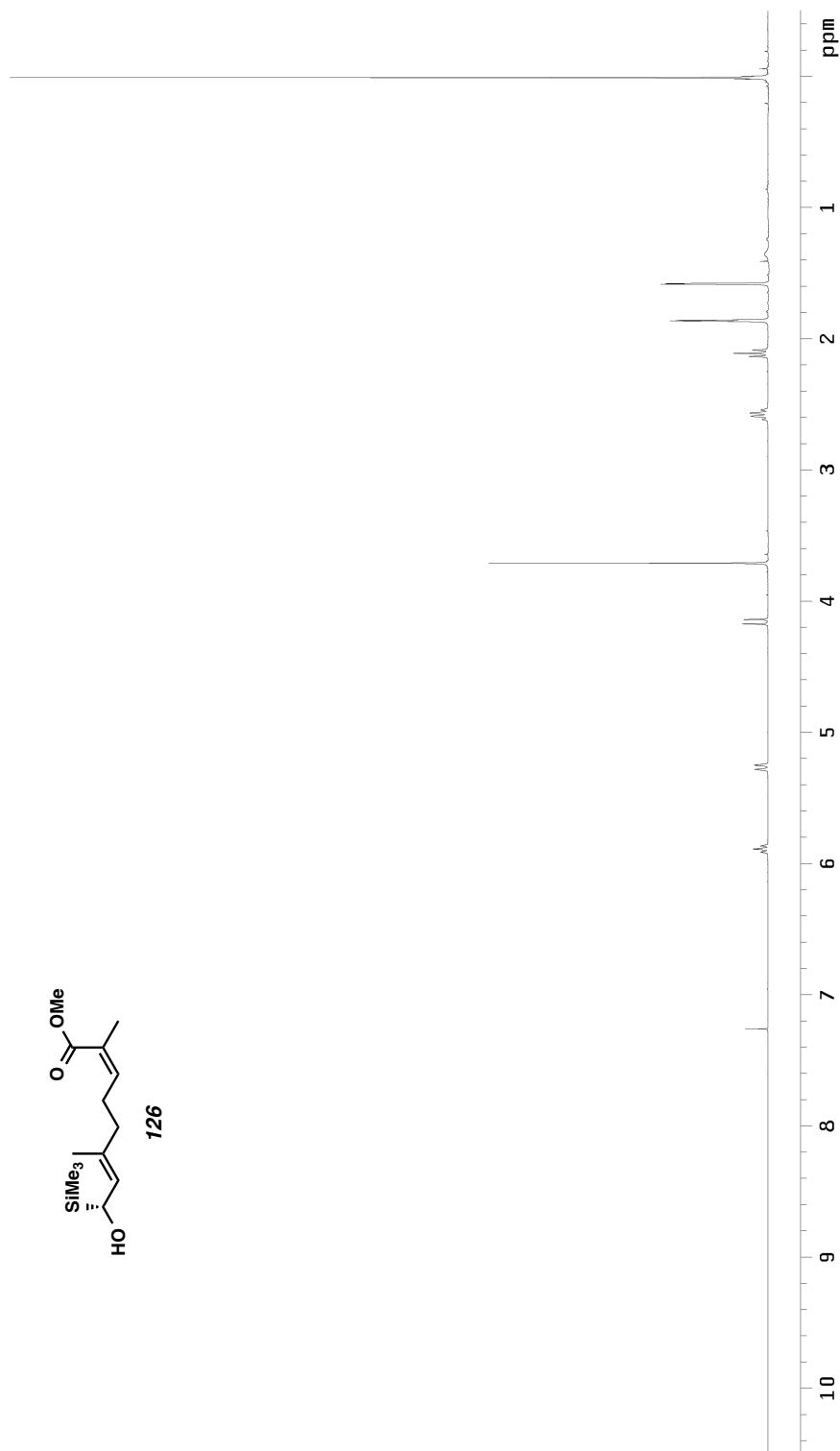


Figure A6.23.1 ¹H NMR (300 MHz, CDCl₃) of compound **126**.

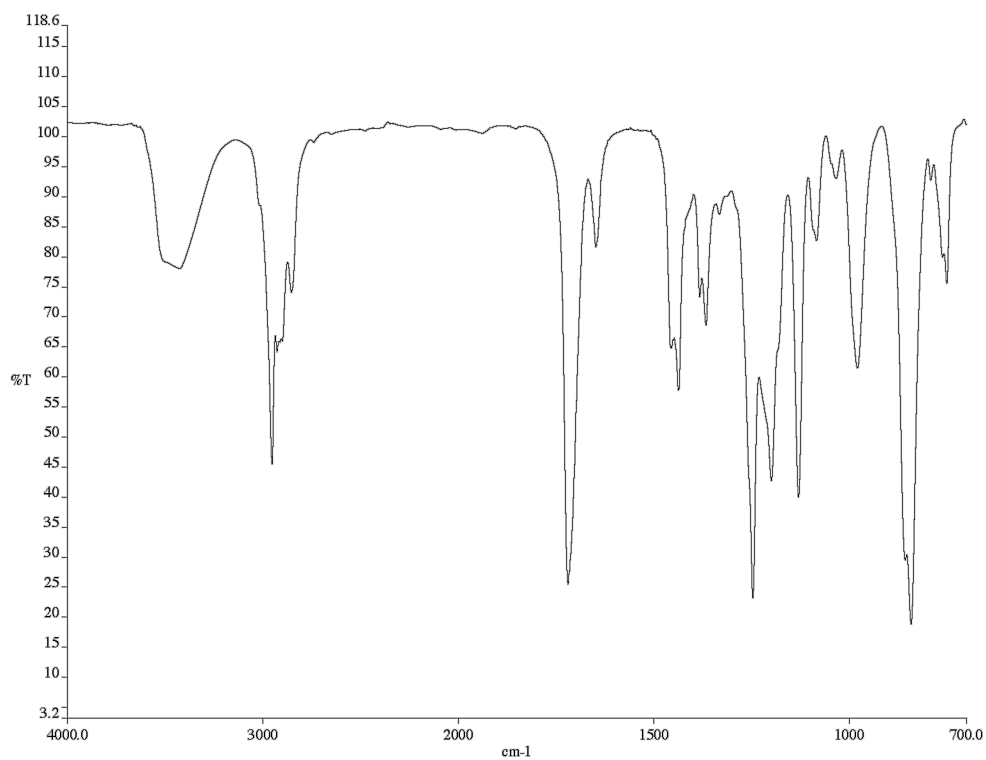


Figure A6.23.2 infrared spectrum (Thin Film, NaCl) of compound **126**.

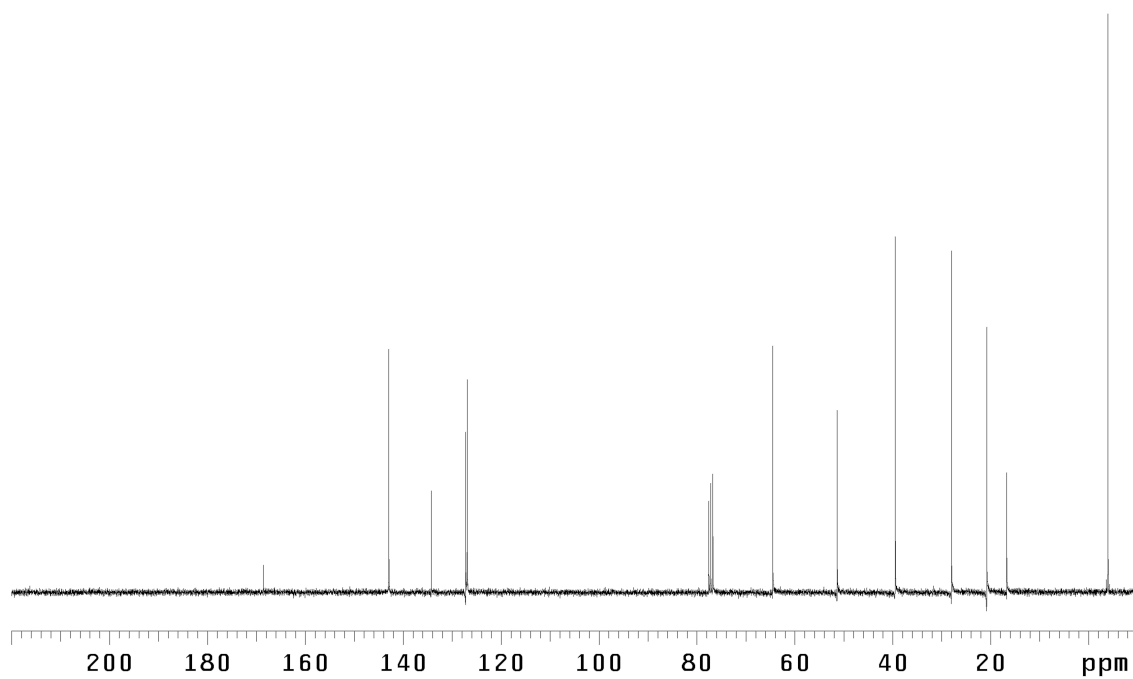


Figure A6.23.3 ^{13}C NMR (75 MHz, CDCl_3) of compound **126**.

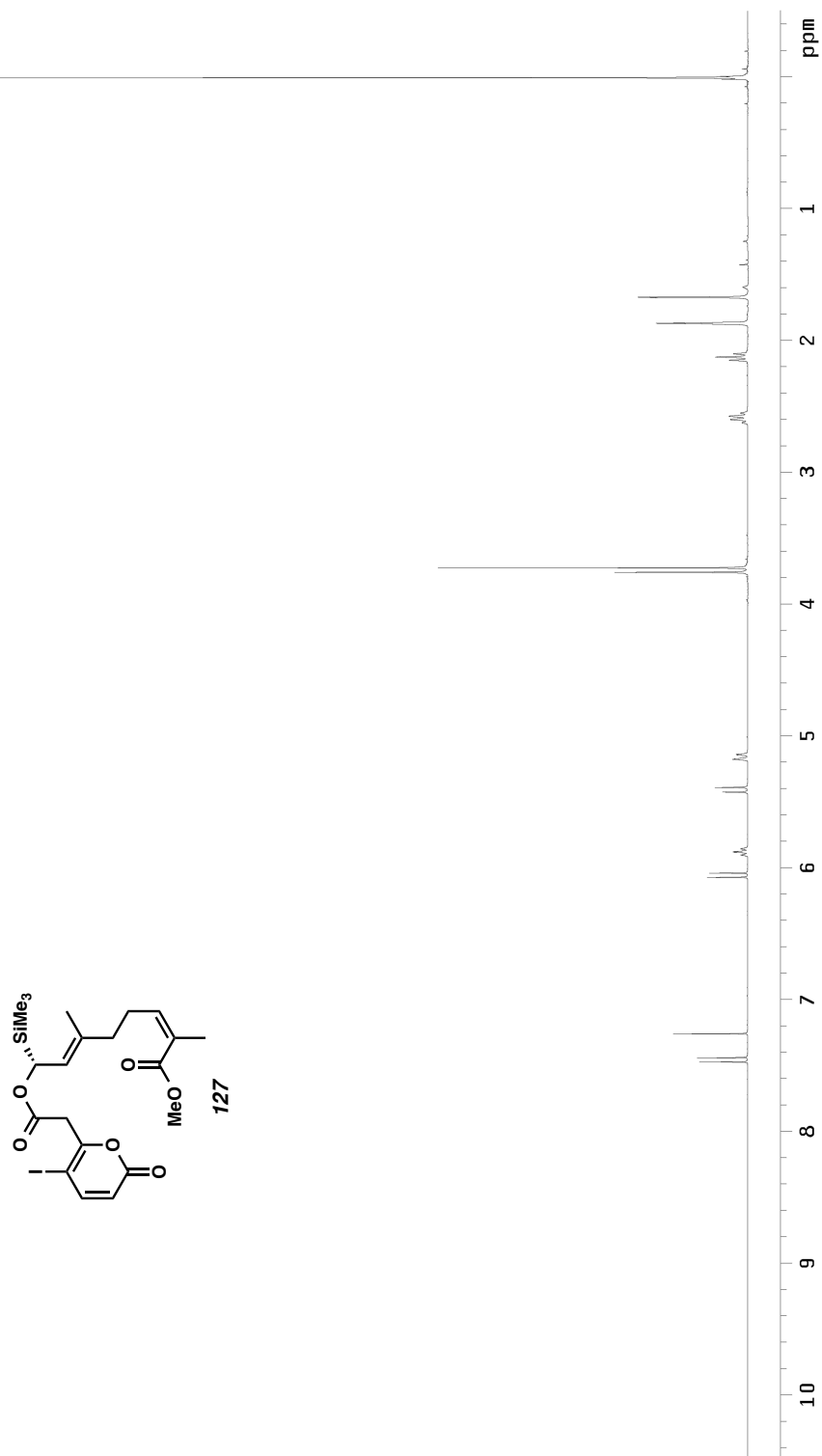


Figure A6.24.1 ¹H NMR (300 MHz, CDCl₃) of compound **127**.

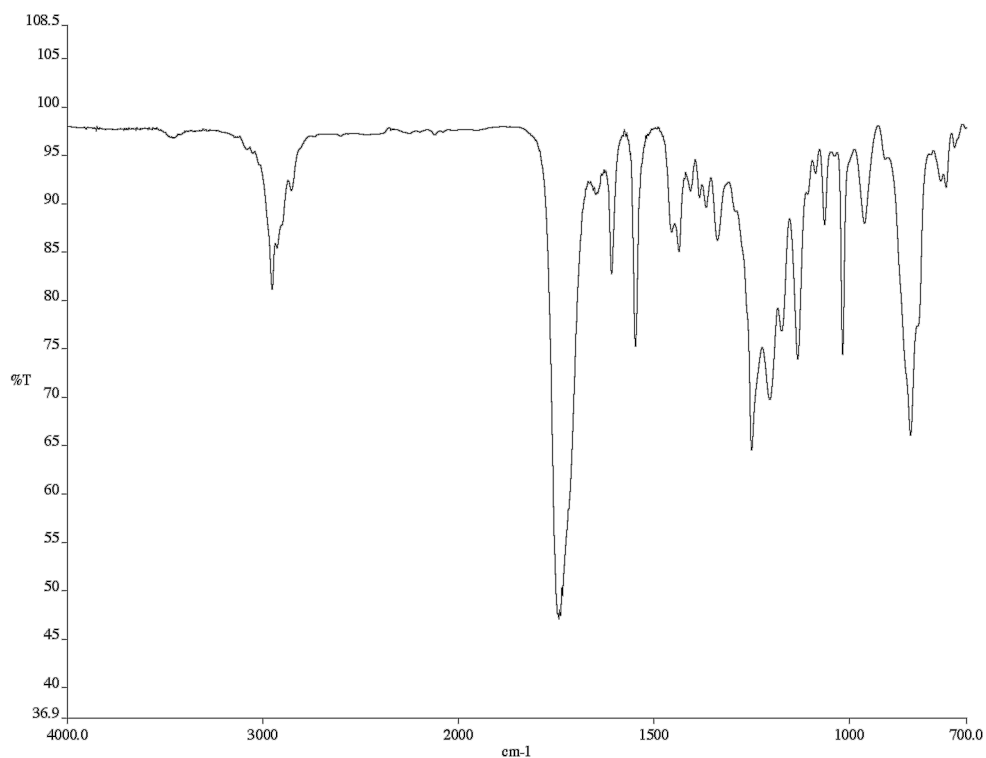


Figure A6.24.2 infrared spectrum (Thin Film, NaCl) of compound **127**.

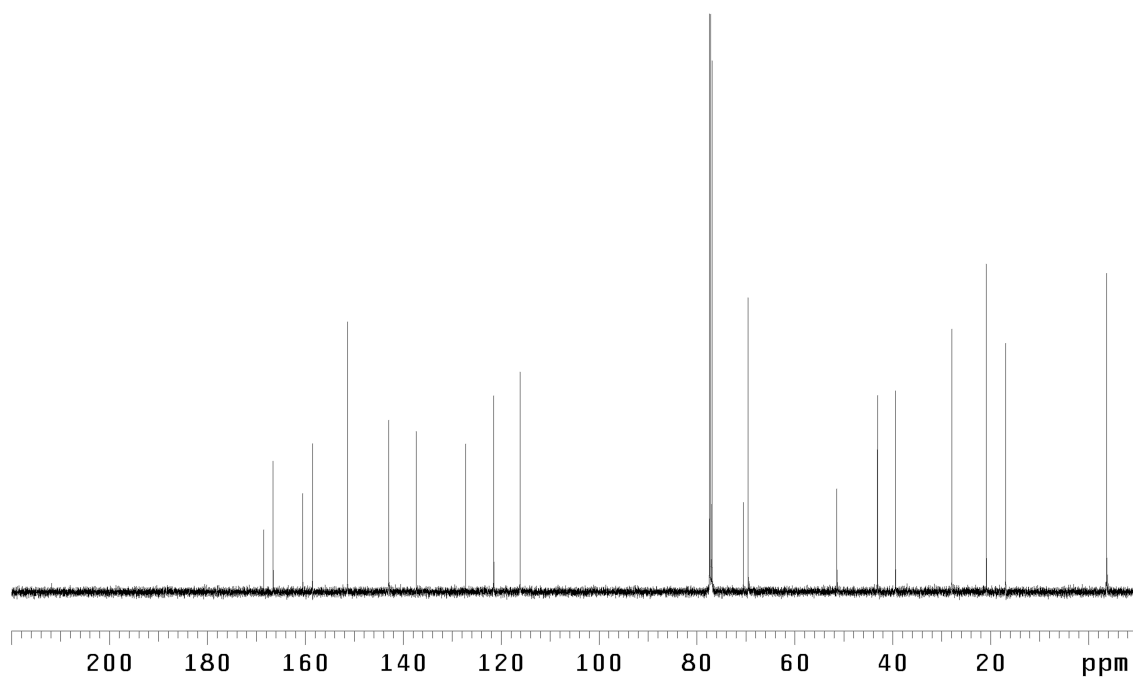


Figure A6.24.3 ^{13}C NMR (125 MHz, CDCl_3) of compound **127**.

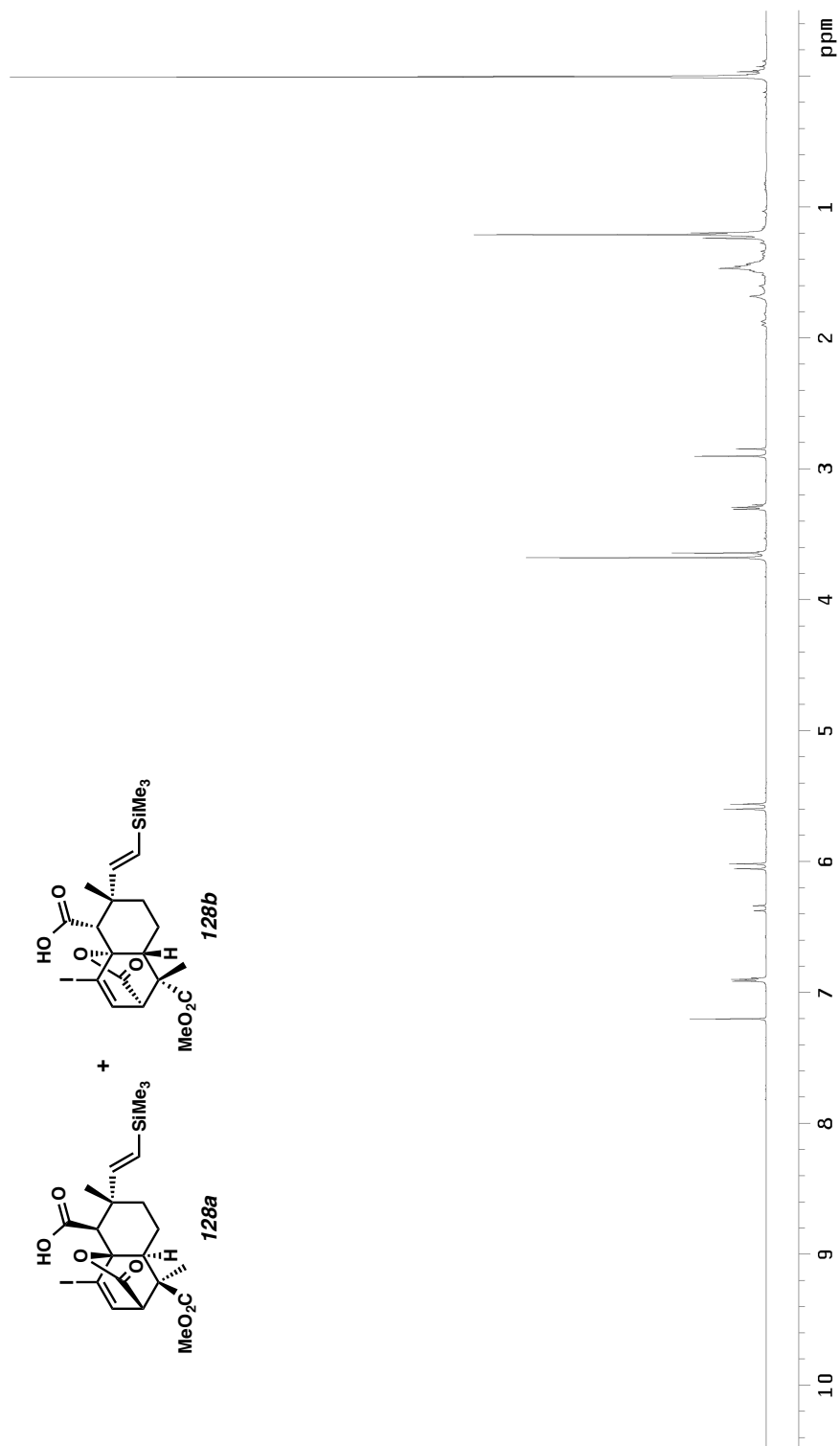


Figure A6.25.1 ¹H NMR (500 MHz, CDCl₃) of compounds **128a** and **128b**.

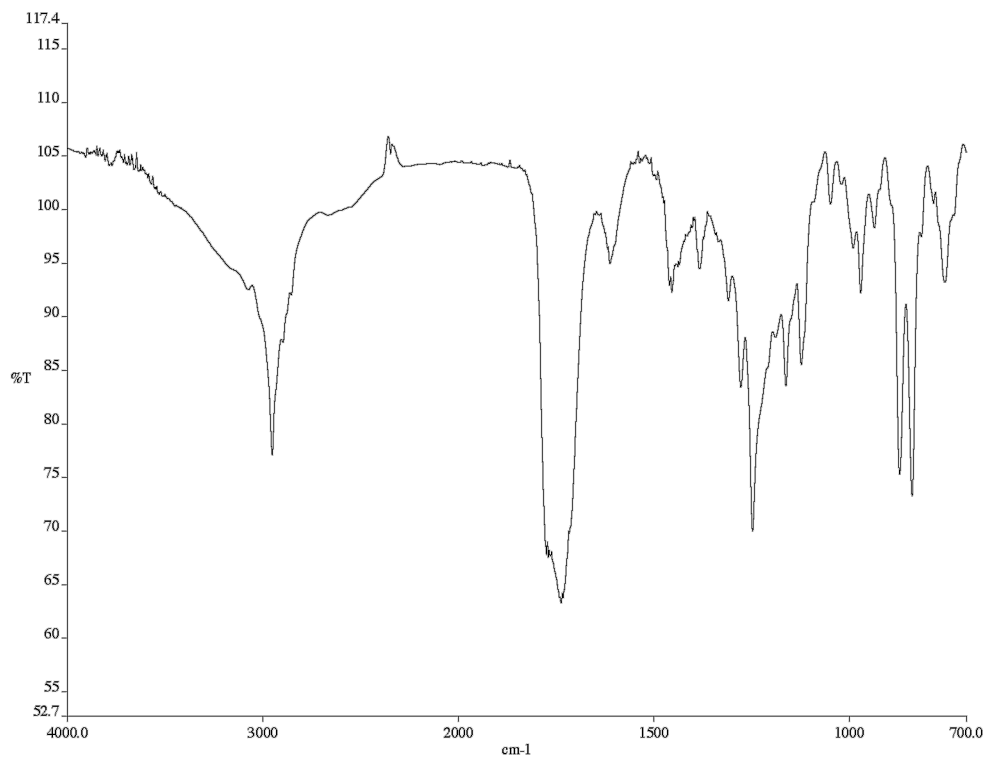


Figure A6.25.2 infrared spectrum (Thin Film, NaCl) of compounds **128a** and **128b**.

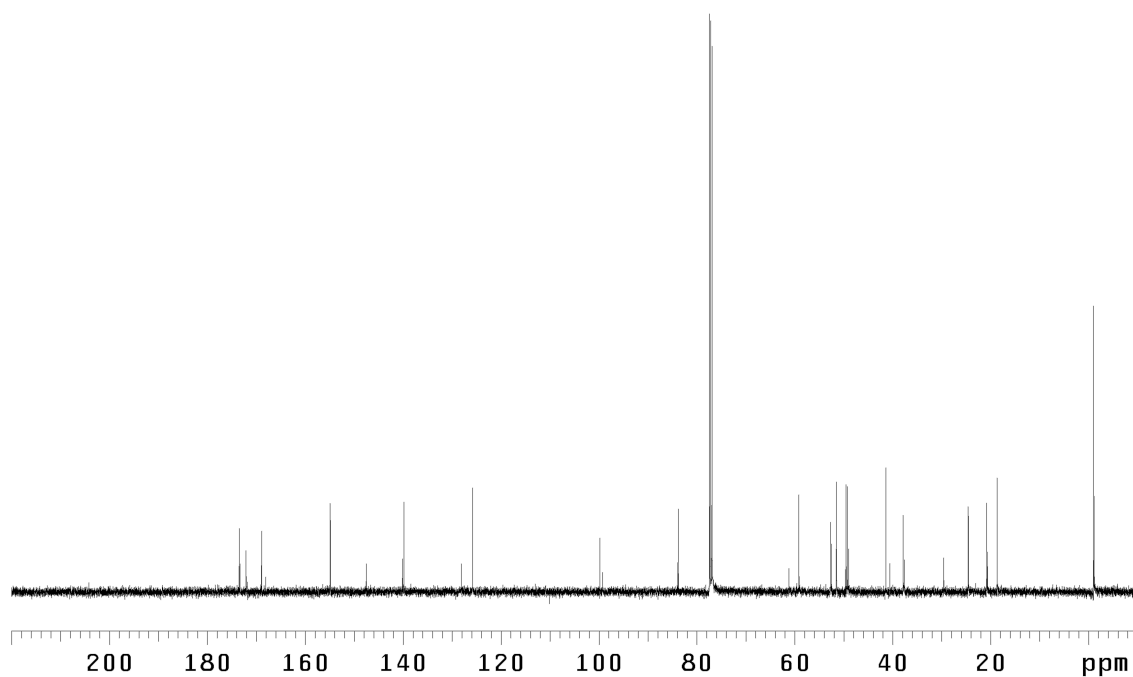


Figure A6.25.3 ¹³C NMR (125 MHz, CDCl₃) of compounds **128a** and **128b**.

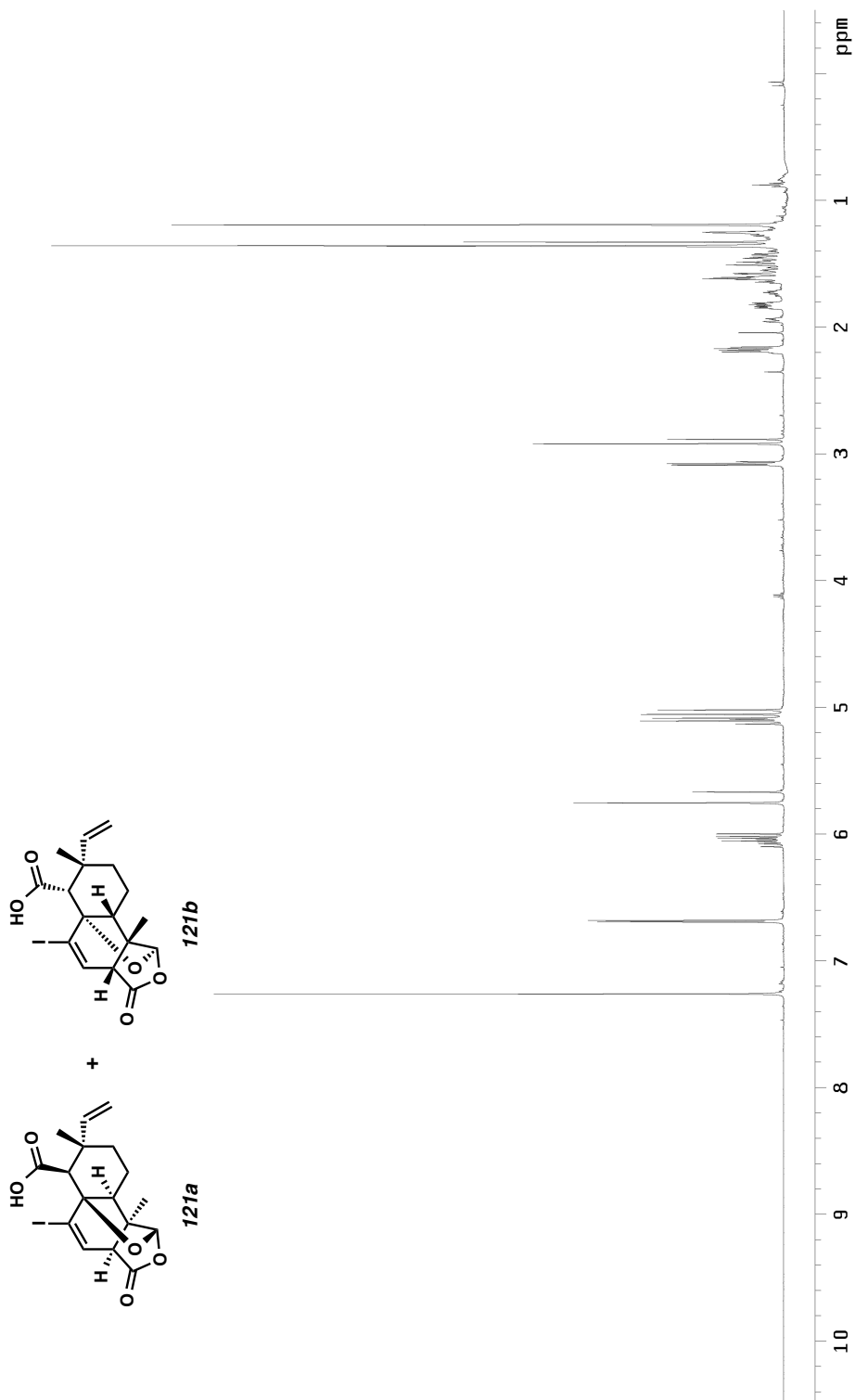


Figure A6.26.1 ¹H NMR (500 MHz, CDCl₃) of compounds **121a** and **121b**.

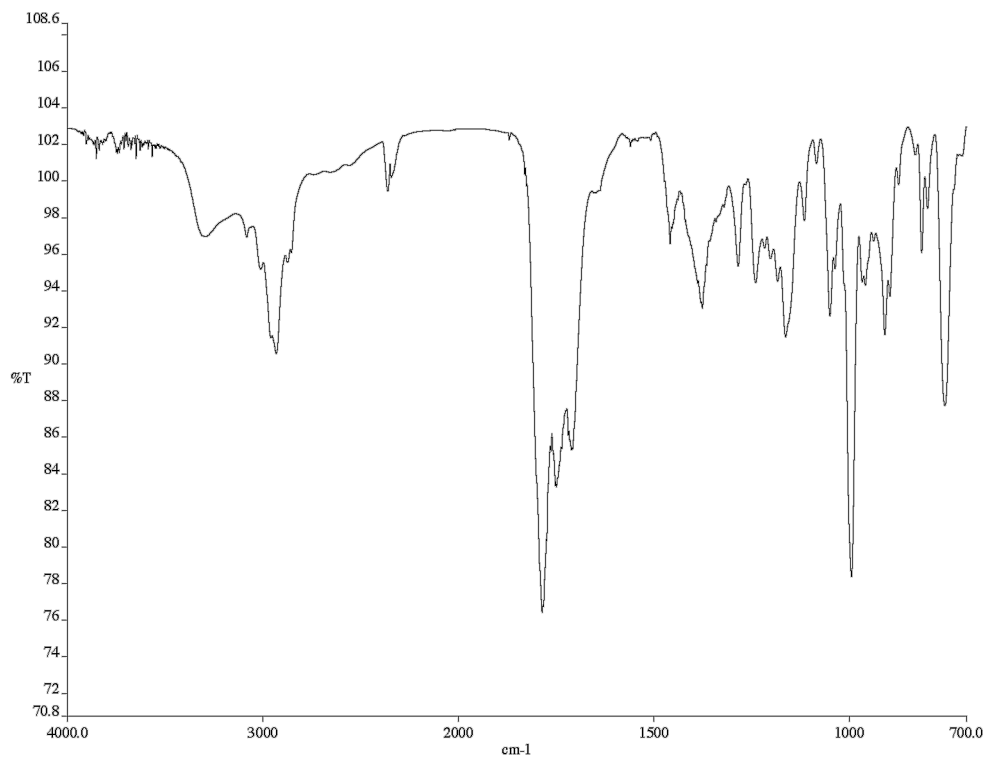


Figure A6.26.2 infrared spectrum (Thin Film, NaCl) of compounds **121a** and **121b**.

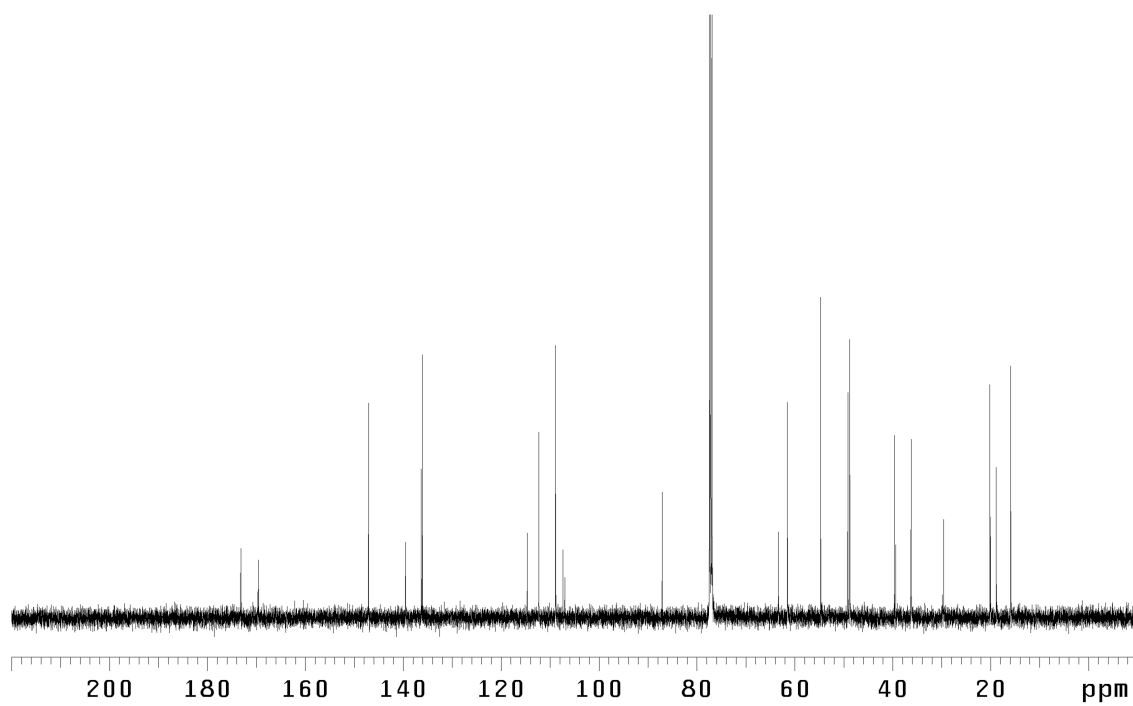


Figure A6.26.3 ¹³C NMR (125 MHz, CDCl₃) of compounds **121a** and **121b**.

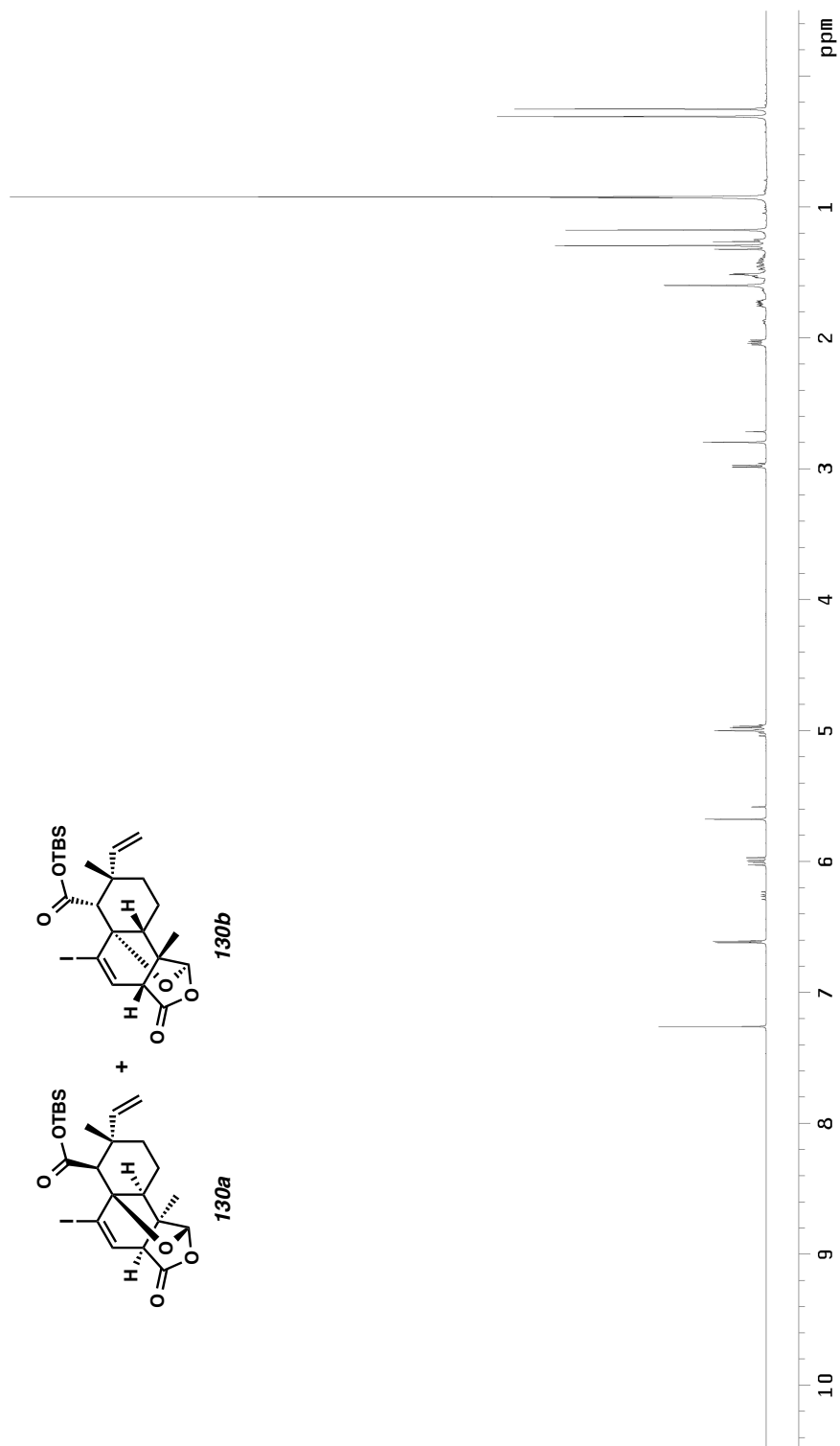


Figure A6.27.1 ^1H NMR (500 MHz, CDCl_3) of compounds **130a** and **130b**.

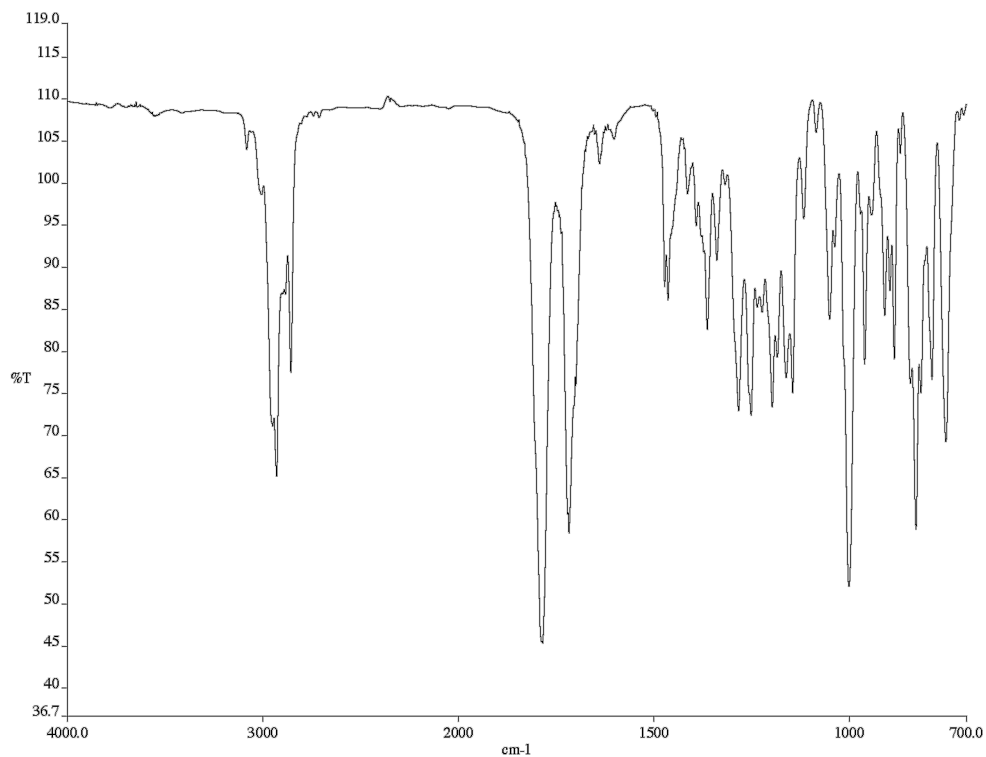


Figure A6.27.2 infrared spectrum (Thin Film, NaCl) of compounds **130a** and **130b**.

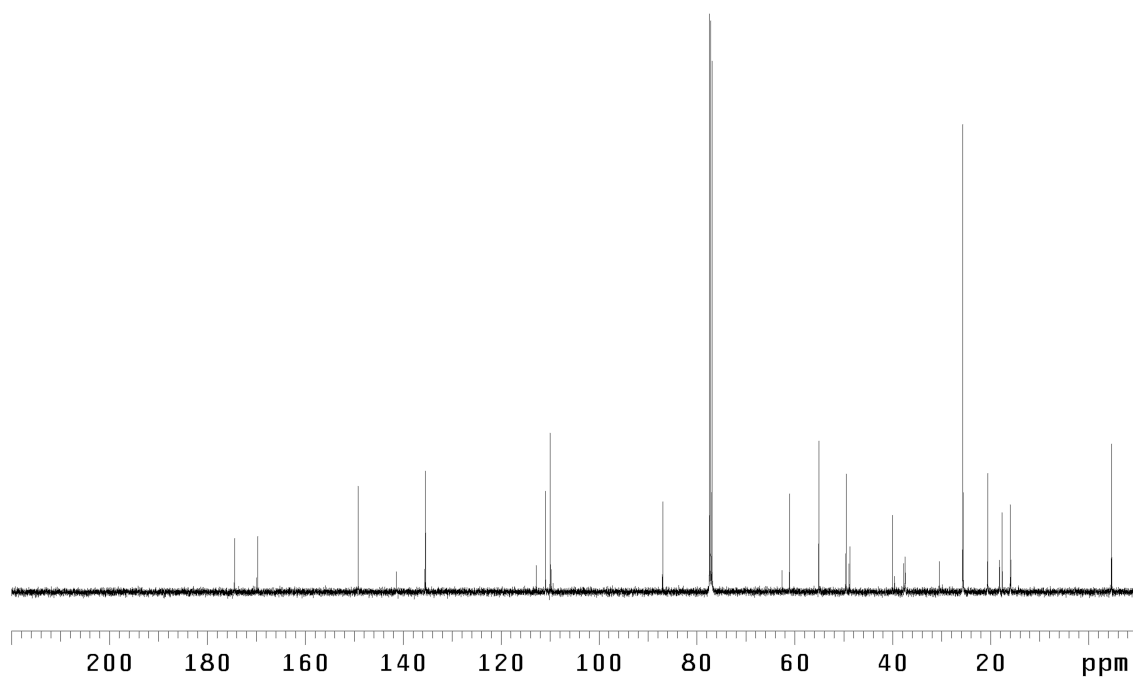


Figure A6.27.3 ¹³C NMR (125 MHz, CDCl₃) of compounds **130a** and **130b**.

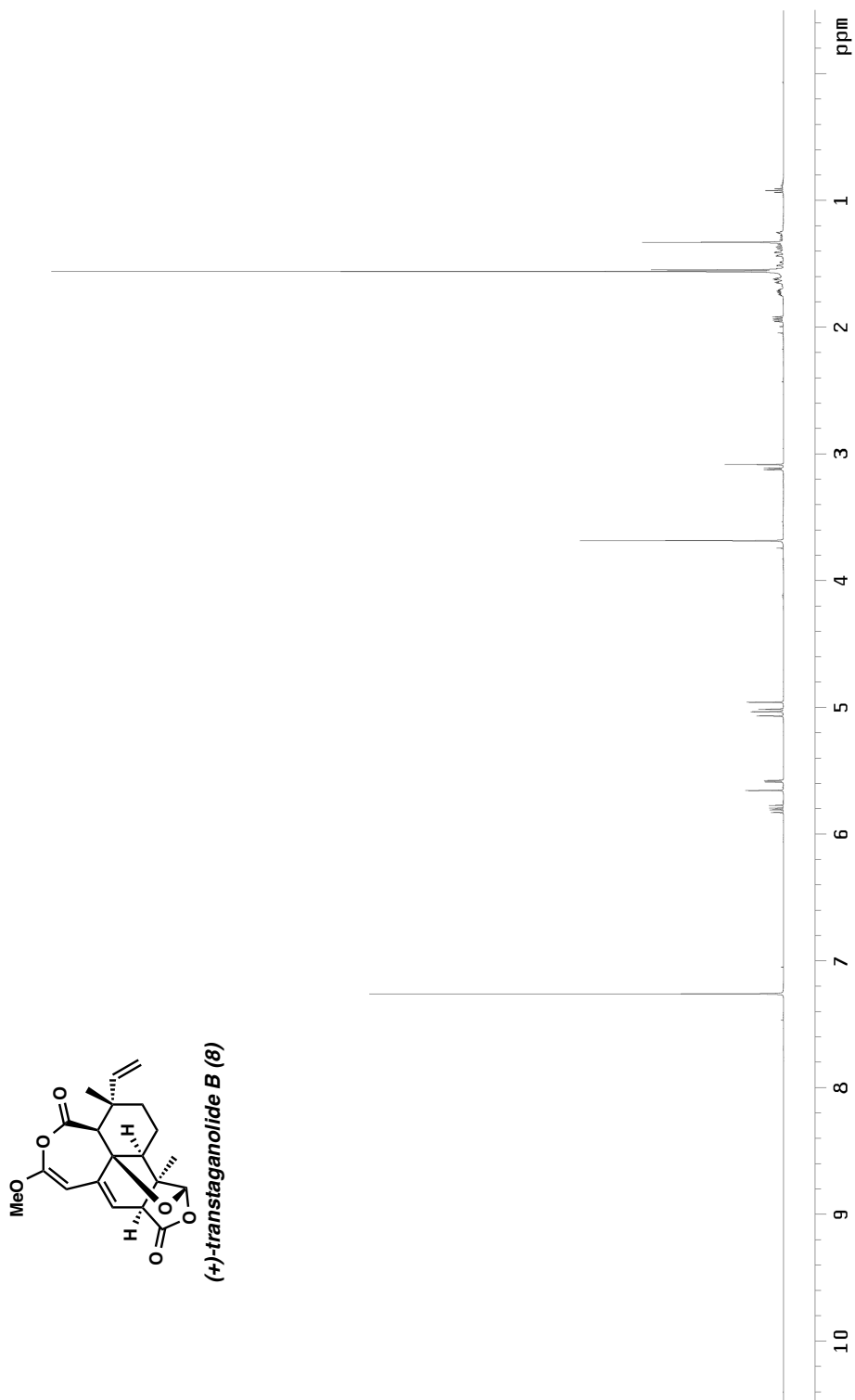


Figure A6.28.1 ¹H NMR (500 MHz, CDCl₃) of transtaganolide B (8).

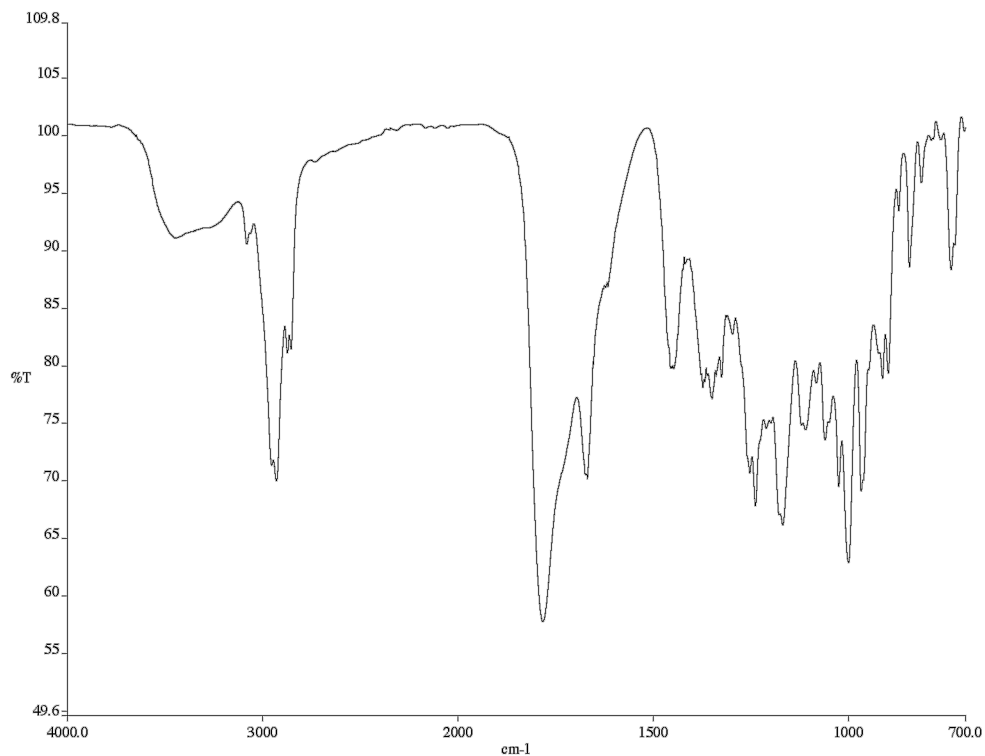


Figure A6.28.2 infrared spectrum (Thin Film, NaCl) of transtaganolide B (**8**).

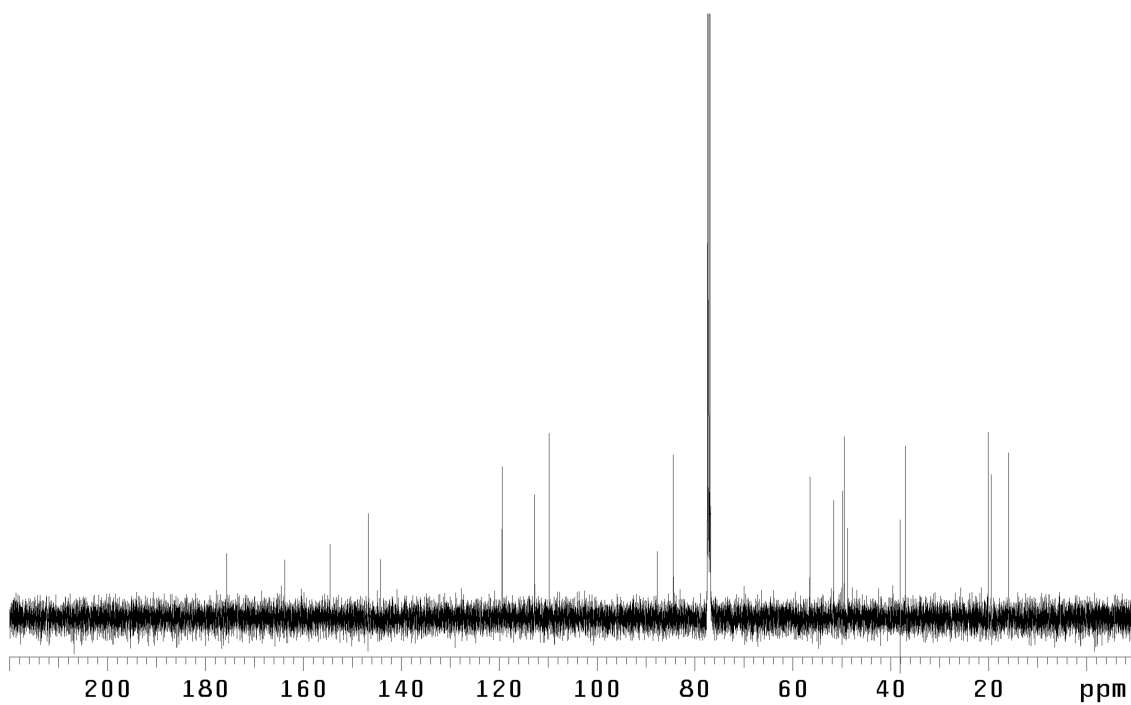


Figure A6.28.3 ¹³C NMR (125 MHz, CDCl₃) of transtaganolide B (**8**).

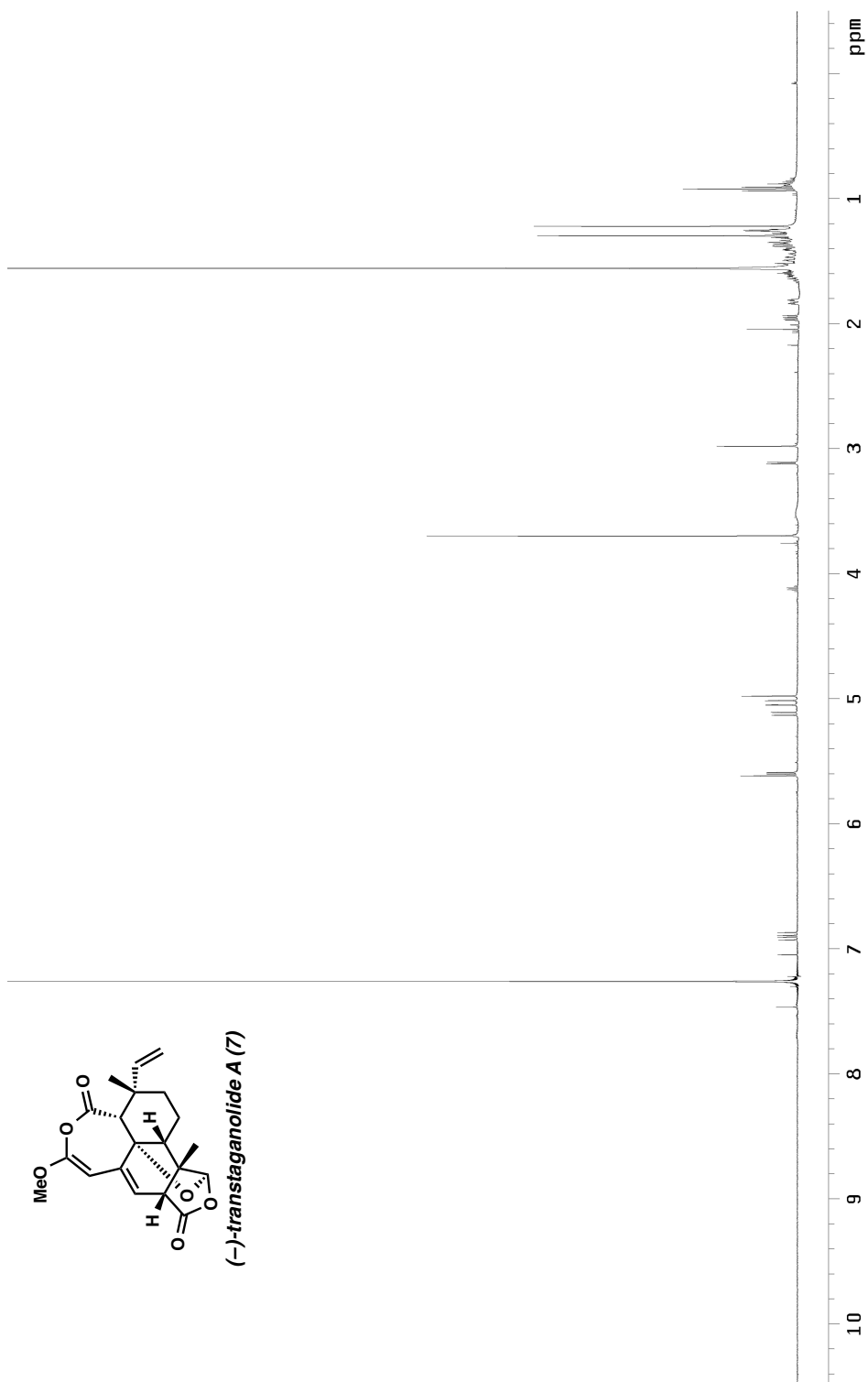


Figure A6.29.1 ¹H NMR (500 MHz, CDCl₃) of transtaganolide A (7).

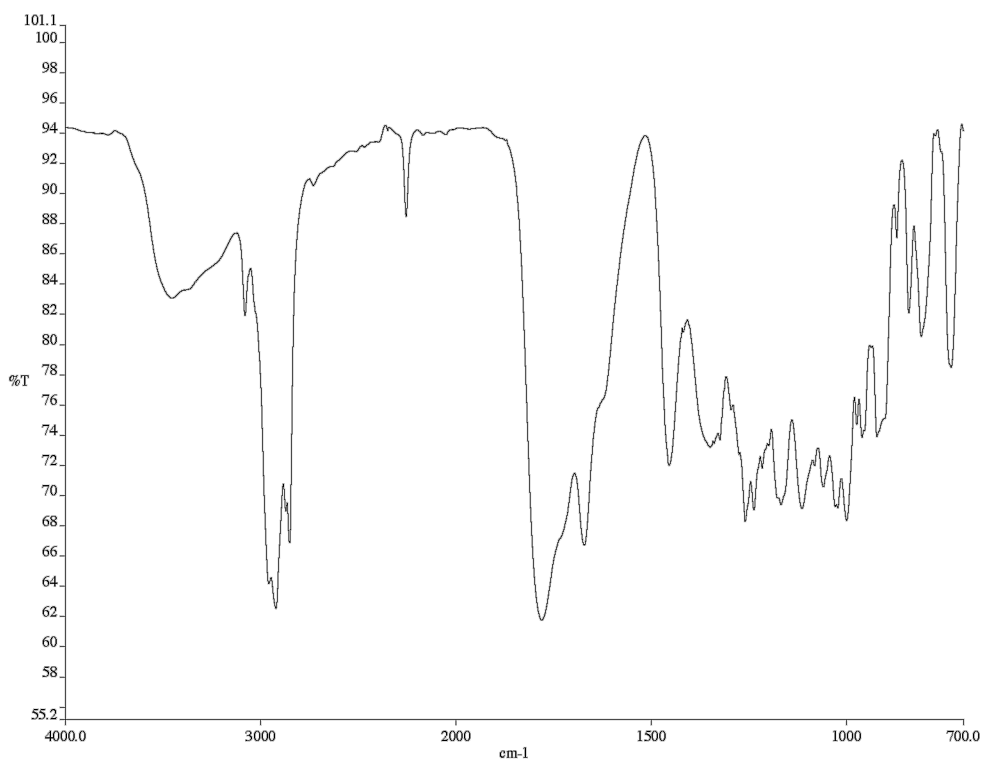


Figure A6.29.2 infrared spectrum (Thin Film, NaCl) of transtaganolide A (7).

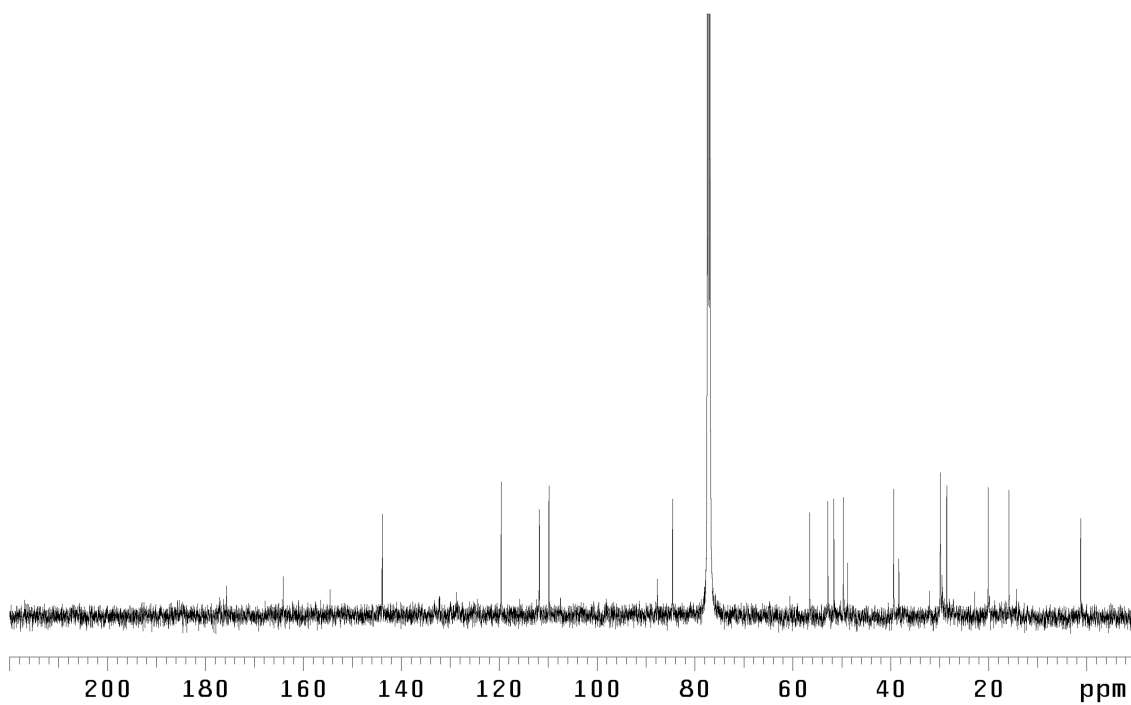


Figure A6.29.3 ¹³C NMR (125 MHz, CDCl₃) of transtaganolide A (7).

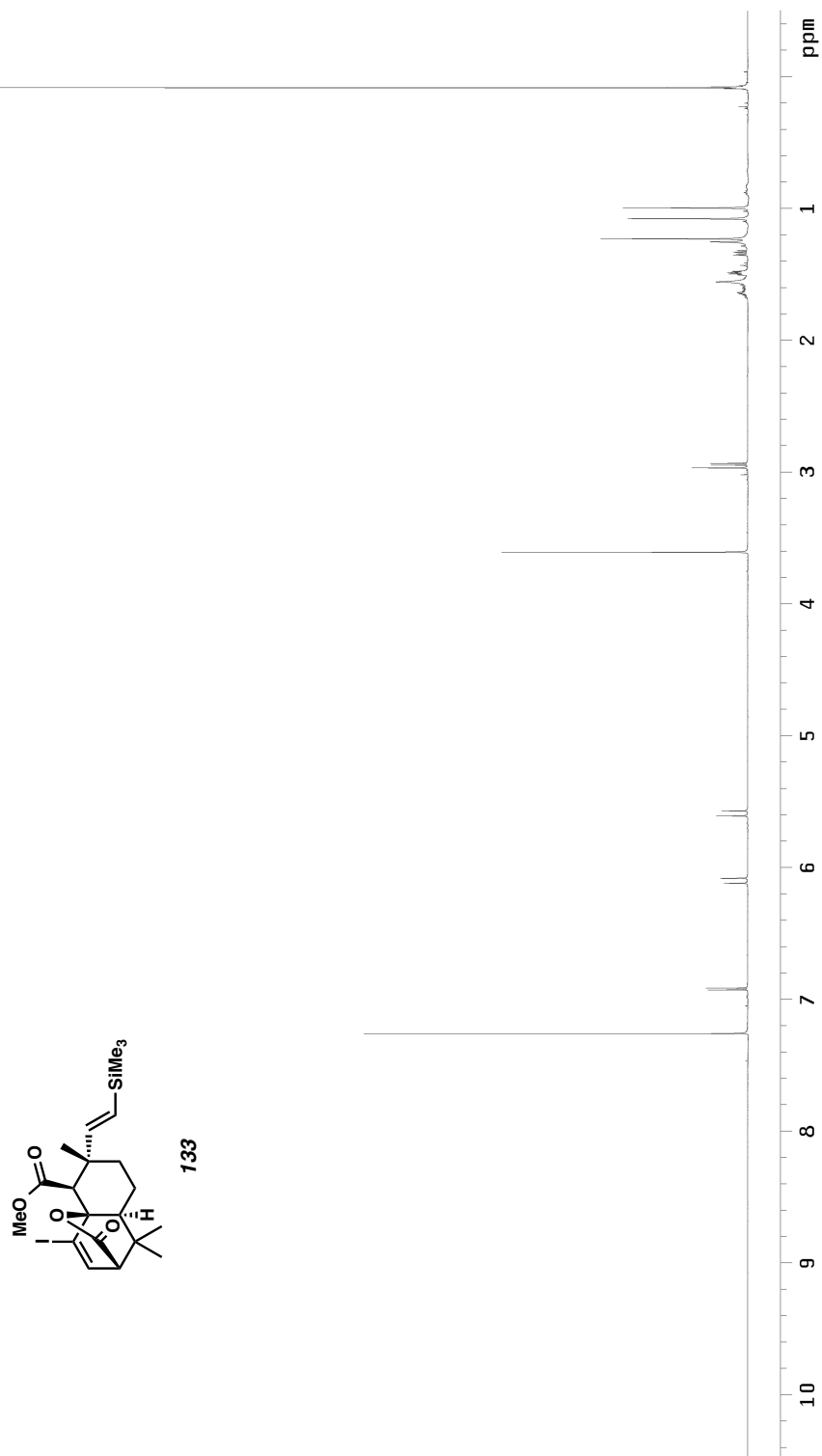


Figure A6.30.1 ¹H NMR (500 MHz, CDCl₃) of compound **133**.

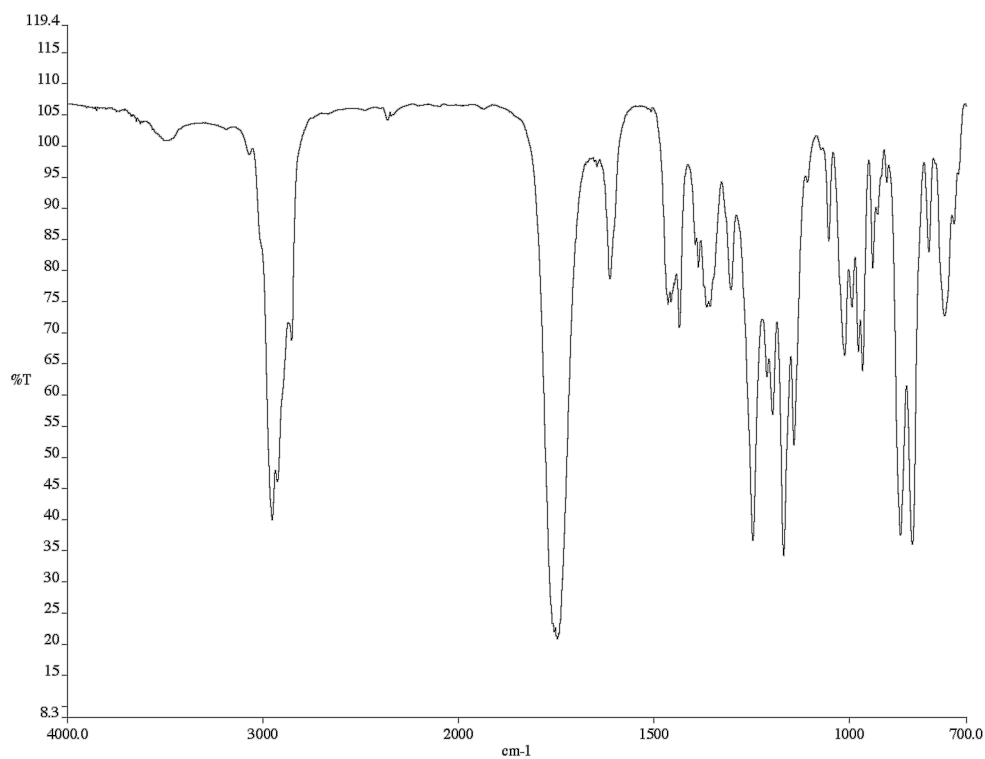


Figure A6.30.2 infrared spectrum (Thin Film, NaCl) of compound **133**.

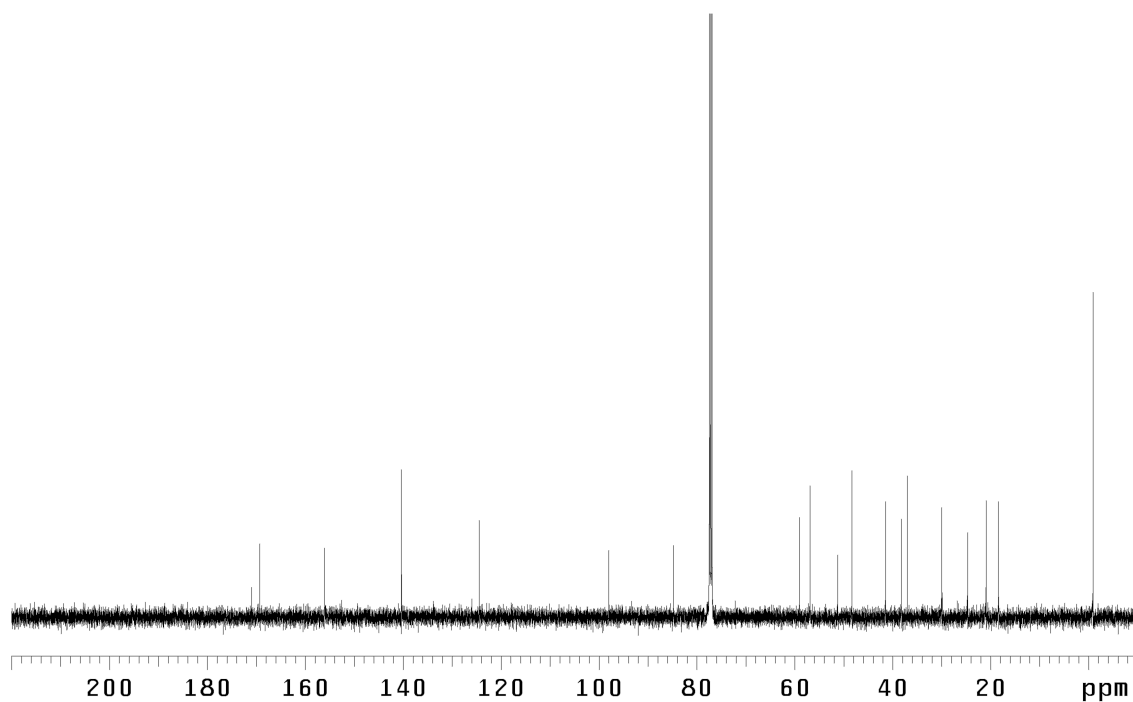


Figure A6.30.3 ¹³C NMR (125 MHz, CDCl₃) of compound **133**.

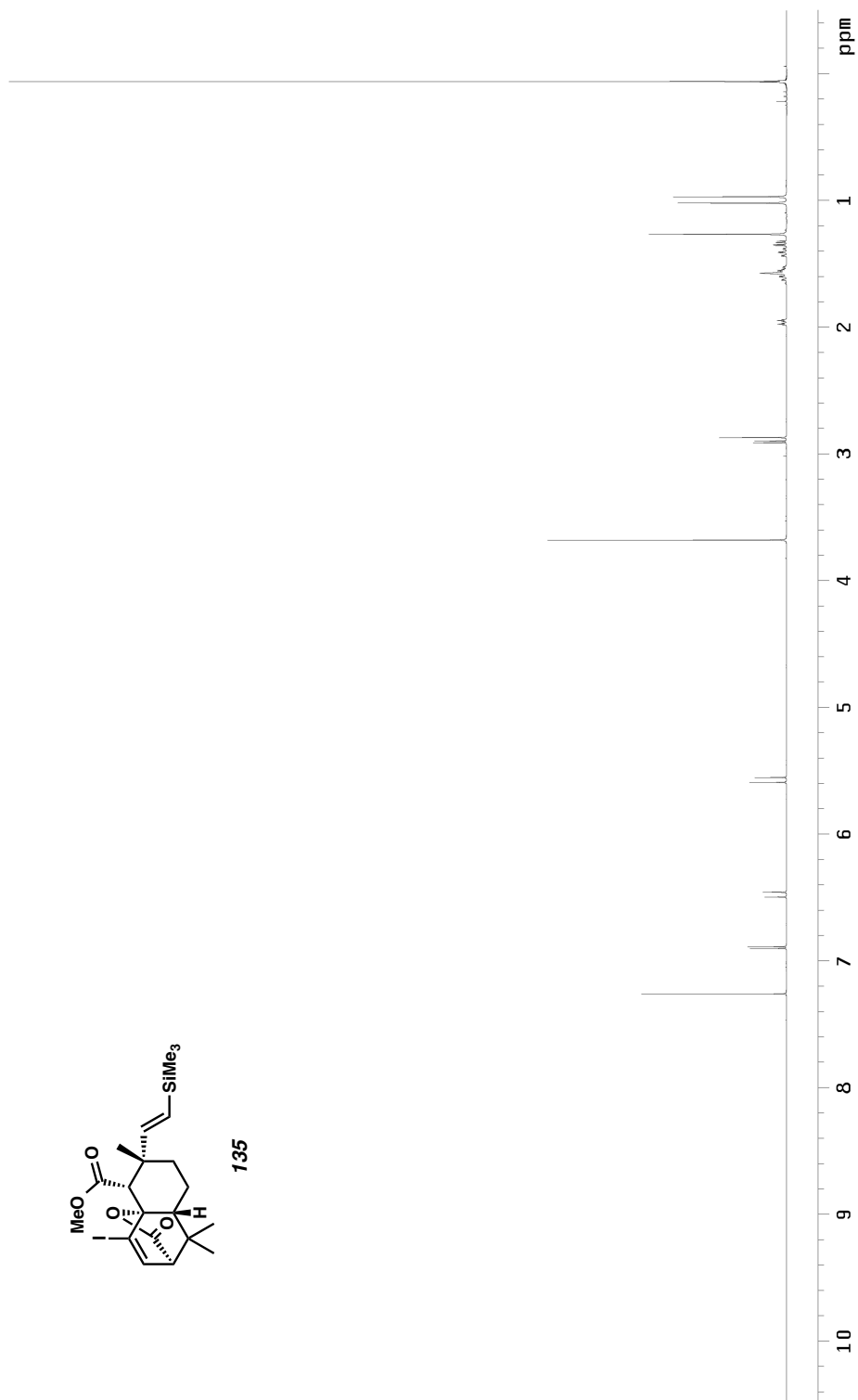
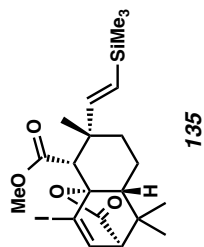


Figure A6.31.1 ¹H NMR (500 MHz, CDCl₃) of compound 135.

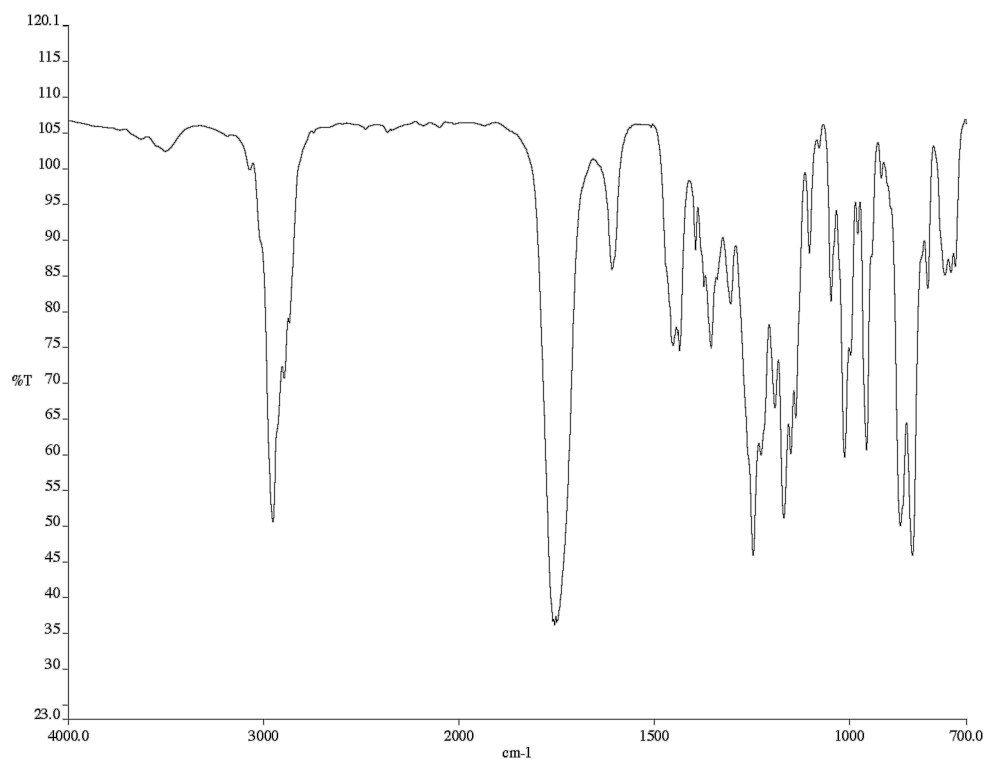


Figure A6.31.2 infrared spectrum (Thin Film, NaCl) of compound **135**.

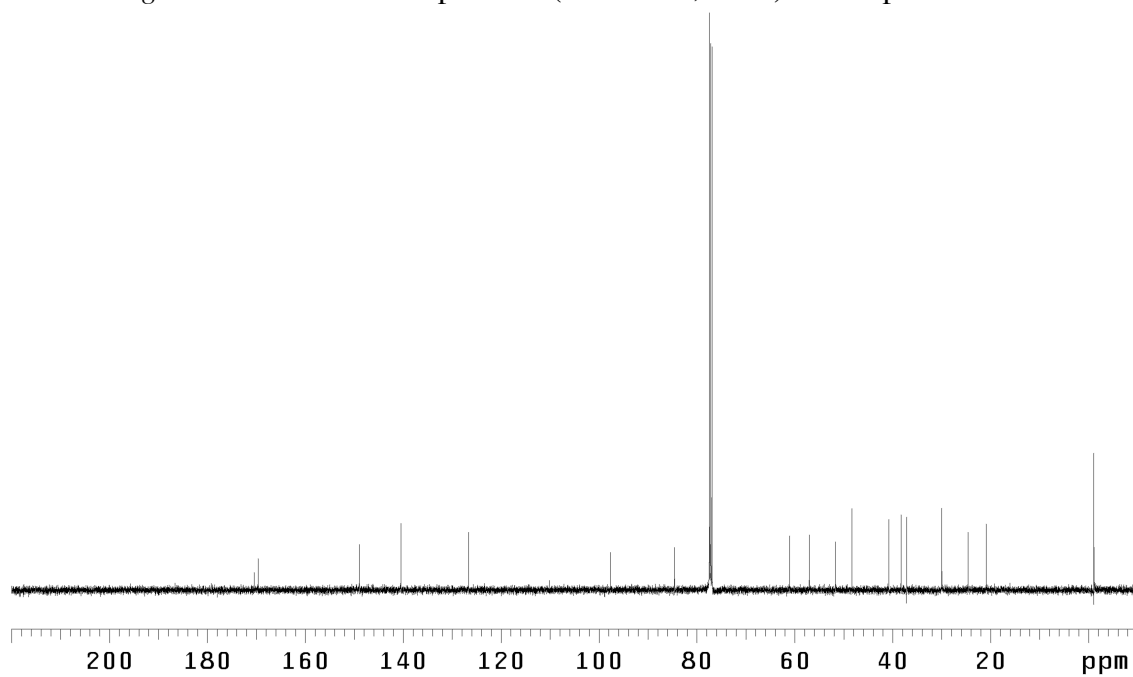


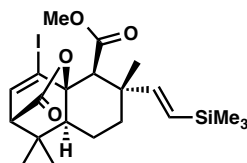
Figure A6.31.3 ¹³C NMR (125 MHz, CDCl₃) of compound **135**.

APPENDIX 7

X-ray Crystallography Reports:

Relevant to Chapter 2

A7.1 CRYSTAL STRUCTURE ANALYSIS FOR COMPOUND 133



133

By Larry Henling 128 Beckman ext. 2735

e-mail: xray@caltech.edu

Contents

Table A7.1.1. Crystal data

Table A7.1.2. Atomic coordinates

Table A7.1.3. Full bond distances and angles

Table A7.1.4. Anisotropic displacement parameters

Table A7.1.5. Hydrogen atomic coordinates

Figure A7.1.1. Ortep diagram of **133**. The crystallographic data have been deposited in the Cambridge Database (CCDC) and placed on hold pending further instructions.

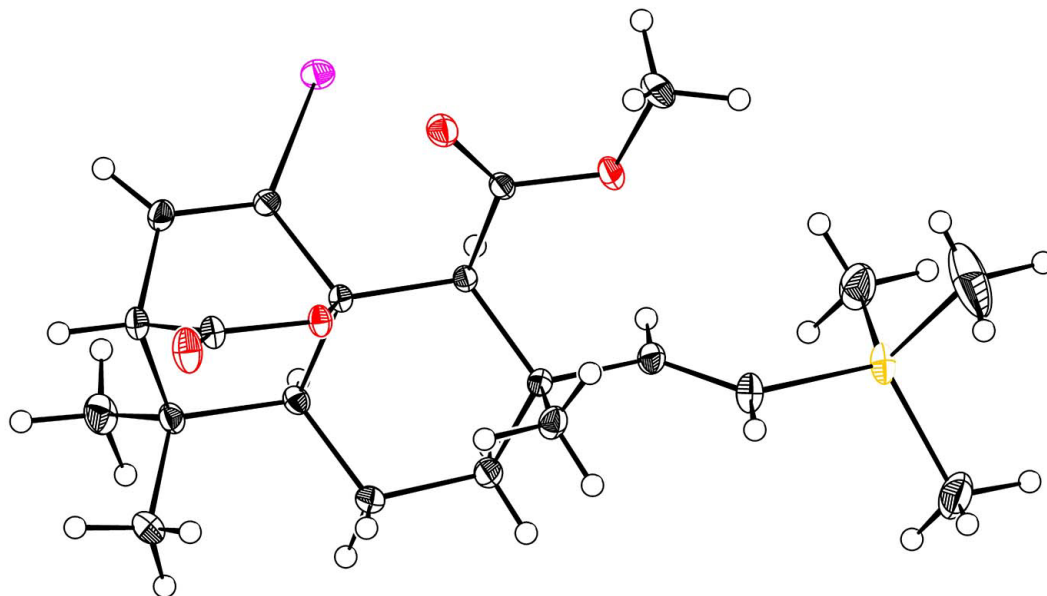


Table A7.1.1. Crystal data and structure analysis details for **133**.

Empirical formula	$C_{21} H_{31} I O_4 Si$
Formula weight	502.45
Crystallization solvent	Hexanes/Pentane
Crystal shape	block
Crystal color	colorless
Crystal size	0.28 x 0.3 x 0.38 mm

Data Collection

Preliminary photograph(s)	rotation
Type of diffractometer	Bruker APEX-II CCD
Wavelength	$0.71073 \approx MoK$
Data collection temperature	100 K
Theta range for 9418 reflections used in lattice determination	2.69 to 49.27°
Unit cell dimensions	$a = 7.8106(6) \approx$ $\alpha = 90^\circ$ $b = 9.9557(9) \approx$ $\beta = 90^\circ$ $c = 29.925(3) \approx$ $\gamma = 90^\circ$
Volume	$2326.9(3) \approx^3$
Z	4
Crystal system	orthorhombic
Space group	P 21 21 21 (# 19)

Density (calculated)	1.434 g/cm ³
F(000)	1024
Theta range for data collection	2.2 to 51.0°
Completeness to theta = 25.00°	99.9%
Index ranges	-16 ≤ h ≤ 8, -21 ≤ k ≤ 21, -61 ≤ l ≤ 65
Data collection scan type	and scans
Reflections collected	91039
Independent reflections	24693 [R _{int} = 0.0329]
Reflections > 2σ(I)	22910
Average σ(I)/(net I)	0.0301
Absorption coefficient	1.45 mm ⁻¹
Absorption correction	Semi-empirical from equivalents
Max. and min. transmission	0.8799 and 0.8128

Structure Solution and Refinement

Primary solution method	dual
Secondary solution method	difmap
Hydrogen placement	geom
Refinement method	Full-matrix least-squares on F ²
Data / restraints / parameters	24693 / 0 / 368
Treatment of hydrogen atoms	refall
Goodness-of-fit on F ²	1.71

Final R indices [$I > 2\sigma(I)$, 22910 reflections]	R1 = 0.0322, wR2 = 0.0520
R indices (all data)	R1 = 0.0364, wR2 = 0.0525
Type of weighting scheme used	calc
Weighting scheme used	calc $w=1/[\sigma^2(F_o^2)]$
Max shift/error	0.002
Average shift/error	0.000
Absolute structure parameter	-0.001(5)
Largest diff. peak and hole	2.58 and -2.43 $e\text{\AA}^{-3}$

Programs Used

Cell refinement	SAINT V8.18C (Bruker-AXS, 2007)
Data collection	APEX2 2012.2-0 (Bruker-AXS, 2007)
Data reduction	SAINT V8.18C (Bruker-AXS, 2007)
Structure solution	SHELXS-97 (Sheldrick, 1990)
Structure refinement	SHELXL-97 (Sheldrick, 1997)
Graphics	DIAMOND 3 (Crystal Impact, 1999)

Table A7.1.2. Atomic coordinates ($\times 10^4$) and equivalent isotropic displacement parameter ($\text{\AA}^2 \times 10^3$) for **133**. $U(\text{eq})$ is defined as one third of the trace of the orthogonalized U^{ij} tensor

	x	y	z	U_{eq}
I(1)	3229(1)	3273(1)	1007(1)	15(1)
Si(1)	8286(1)	9598(1)	296(1)	18(1)
O(1)	5867(1)	5072(1)	2118(1)	11(1)
O(2)	5592(1)	4487(1)	2829(1)	19(1)
O(3)	3205(1)	6242(1)	1658(1)	17(1)
O(4)	4368(1)	7639(1)	1154(1)	18(1)
C(1)	6046(1)	4527(1)	1664(1)	10(1)
C(2)	6004(1)	5727(1)	1341(1)	10(1)
C(3)	7647(1)	6616(1)	1326(1)	12(1)
C(4)	9209(1)	5673(1)	1298(1)	17(1)
C(5)	9286(1)	4665(1)	1680(1)	15(1)
C(6)	7759(1)	3724(1)	1662(1)	12(1)
C(7)	7701(1)	2636(1)	2044(1)	13(1)
C(8)	5895(1)	2726(1)	2272(1)	13(1)
C(9)	4551(1)	2554(1)	1916(1)	14(1)
C(10)	4638(1)	3483(1)	1598(1)	12(1)
C(11)	5751(1)	4138(1)	2445(1)	12(1)
C(12)	4363(1)	6542(1)	1412(1)	11(1)

C(13)	2917(1)	8524(1)	1196(1)	21(1)
C(14)	7682(1)	7423(1)	893(1)	14(1)
C(15)	8219(1)	8682(1)	840(1)	17(1)
C(16)	7633(2)	8455(1)	-168(1)	29(1)
C(17)	6799(3)	11047(2)	328(1)	51(1)
C(18)	10497(2)	10244(2)	195(1)	31(1)
C(19)	7776(1)	7534(1)	1736(1)	15(1)
C(20)	9053(1)	2839(1)	2411(1)	20(1)
C(21)	7953(1)	1234(1)	1846(1)	20(1)

Table A7.1.3. Bond lengths [\AA] and angles [$^\circ$] for **133**.

I(1)-C(10)	2.0931(7)
Si(1)-C(15)	1.8650(8)
Si(1)-C(16)	1.8677(12)
Si(1)-C(17)	1.8543(14)
Si(1)-C(18)	1.8672(13)
O(1)-C(1)	1.4684(9)
O(1)-C(11)	1.3539(10)
O(2)-C(11)	1.2063(11)
O(3)-C(12)	1.2049(10)
O(4)-C(12)	1.3363(10)
O(4)-C(13)	1.4404(11)
C(1)-C(2)	1.5377(11)
C(1)-C(6)	1.5580(11)
C(1)-C(10)	1.5261(11)
C(2)-H(2)	1.015(14)
C(2)-C(3)	1.5596(10)
C(2)-C(12)	1.5307(10)
C(3)-C(4)	1.5419(12)
C(3)-C(14)	1.5258(11)
C(3)-C(19)	1.5320(12)
C(4)-H(4A)	1.008(15)

C(4)-H(4B)	0.875(17)
C(4)-C(5)	1.5223(12)
C(5)-H(5A)	1.052(15)
C(5)-H(5B)	0.959(14)
C(5)-C(6)	1.5178(12)
C(6)-H(6)	1.030(13)
C(6)-C(7)	1.5739(12)
C(7)-C(8)	1.5698(11)
C(7)-C(20)	1.5367(12)
C(7)-C(21)	1.5297(13)
C(8)-H(8)	1.004(16)
C(8)-C(9)	1.5052(12)
C(8)-C(11)	1.5022(12)
C(9)-H(9)	0.930(16)
C(9)-C(10)	1.3303(11)
C(13)-H(13A)	0.951(16)
C(13)-H(13B)	0.993(14)
C(13)-H(13C)	0.904(18)
C(14)-H(14)	0.928(14)
C(14)-C(15)	1.3312(13)
C(15)-H(15)	0.997(18)
C(16)-H(16A)	0.915(17)
C(16)-H(16B)	1.04(2)

C(16)-H(16C)	1.020(18)
C(17)-H(17A)	0.80(3)
C(17)-H(17B)	1.01(2)
C(17)-H(17C)	0.99(2)
C(18)-H(18A)	1.020(18)
C(18)-H(18B)	0.93(2)
C(18)-H(18C)	0.88(2)
C(19)-H(19A)	0.904(15)
C(19)-H(19B)	0.952(15)
C(19)-H(19C)	0.886(16)
C(20)-H(20A)	0.920(16)
C(20)-H(20B)	0.950(17)
C(20)-H(20C)	0.924(16)
C(21)-H(21A)	1.003(14)
C(21)-H(21B)	0.889(18)
C(21)-H(21C)	0.987(16)
C(15)-Si(1)-C(16)	110.06(5)
C(15)-Si(1)-C(18)	109.60(5)
C(17)-Si(1)-C(15)	108.59(6)
C(17)-Si(1)-C(16)	109.91(9)
C(17)-Si(1)-C(18)	108.64(10)
C(18)-Si(1)-C(16)	110.01(6)
C(11)-O(1)-C(1)	114.95(6)

C(12)-O(4)-C(13)	116.59(7)
O(1)-C(1)-C(2)	106.94(6)
O(1)-C(1)-C(6)	105.89(6)
O(1)-C(1)-C(10)	107.66(6)
C(2)-C(1)-C(6)	114.54(6)
C(10)-C(1)-C(2)	115.60(6)
C(10)-C(1)-C(6)	105.64(6)
C(1)-C(2)-H(2)	105.4(8)
C(1)-C(2)-C(3)	116.17(6)
C(3)-C(2)-H(2)	107.3(8)
C(12)-C(2)-C(1)	110.08(6)
C(12)-C(2)-H(2)	103.7(8)
C(12)-C(2)-C(3)	113.09(6)
C(4)-C(3)-C(2)	107.88(7)
C(14)-C(3)-C(2)	109.73(6)
C(14)-C(3)-C(4)	105.03(6)
C(14)-C(3)-C(19)	111.41(7)
C(19)-C(3)-C(2)	111.72(6)
C(19)-C(3)-C(4)	110.80(7)
C(3)-C(4)-H(4A)	109.0(8)
C(3)-C(4)-H(4B)	108.2(11)
H(4A)-C(4)-H(4B)	110.6(13)
C(5)-C(4)-C(3)	113.04(7)

C(5)-C(4)-H(4A)	109.2(8)
C(5)-C(4)-H(4B)	106.8(10)
C(4)-C(5)-H(5A)	110.4(8)
C(4)-C(5)-H(5B)	106.8(8)
H(5A)-C(5)-H(5B)	109.1(12)
C(6)-C(5)-C(4)	110.45(7)
C(6)-C(5)-H(5A)	111.9(8)
C(6)-C(5)-H(5B)	108.1(8)
C(1)-C(6)-H(6)	106.3(7)
C(1)-C(6)-C(7)	109.03(6)
C(5)-C(6)-C(1)	111.02(7)
C(5)-C(6)-H(6)	108.4(7)
C(5)-C(6)-C(7)	114.99(7)
C(7)-C(6)-H(6)	106.6(7)
C(8)-C(7)-C(6)	107.59(6)
C(20)-C(7)-C(6)	114.06(7)
C(20)-C(7)-C(8)	107.40(7)
C(21)-C(7)-C(6)	110.09(7)
C(21)-C(7)-C(8)	109.68(7)
C(21)-C(7)-C(20)	107.94(7)
C(7)-C(8)-H(8)	110.6(9)
C(9)-C(8)-C(7)	108.20(6)
C(9)-C(8)-H(8)	114.9(9)

C(11)-C(8)-C(7)	105.71(7)
C(11)-C(8)-H(8)	109.7(9)
C(11)-C(8)-C(9)	107.34(7)
C(8)-C(9)-H(9)	119.6(9)
C(10)-C(9)-C(8)	113.10(7)
C(10)-C(9)-H(9)	127.0(9)
C(1)-C(10)-I(1)	123.83(5)
C(9)-C(10)-I(1)	120.64(6)
C(9)-C(10)-C(1)	114.63(7)
O(1)-C(11)-C(8)	112.82(6)
O(2)-C(11)-O(1)	119.90(8)
O(2)-C(11)-C(8)	127.25(8)
O(3)-C(12)-O(4)	123.87(7)
O(3)-C(12)-C(2)	125.54(7)
O(4)-C(12)-C(2)	110.58(6)
O(4)-C(13)-H(13A)	107.9(10)
O(4)-C(13)-H(13B)	110.3(8)
O(4)-C(13)-H(13C)	110.2(12)
H(13A)-C(13)-H(13B)	109.1(12)
H(13A)-C(13)-H(13C)	114.6(15)
H(13B)-C(13)-H(13C)	104.8(14)
C(3)-C(14)-H(14)	113.4(9)
C(15)-C(14)-C(3)	127.14(8)

C(15)-C(14)-H(14)	119.3(9)
Si(1)-C(15)-H(15)	116.0(10)
C(14)-C(15)-Si(1)	125.05(7)
C(14)-C(15)-H(15)	118.5(10)
Si(1)-C(16)-H(16A)	108.5(10)
Si(1)-C(16)-H(16B)	110.7(10)
Si(1)-C(16)-H(16C)	113.9(11)
H(16A)-C(16)-H(16B)	106.6(15)
H(16A)-C(16)-H(16C)	112.0(15)
H(16B)-C(16)-H(16C)	104.8(15)
Si(1)-C(17)-H(17A)	105(2)
Si(1)-C(17)-H(17B)	110.7(13)
Si(1)-C(17)-H(17C)	103.4(14)
H(17A)-C(17)-H(17B)	103(2)
H(17A)-C(17)-H(17C)	126(2)
H(17B)-C(17)-H(17C)	108.5(18)
Si(1)-C(18)-H(18A)	111.1(11)
Si(1)-C(18)-H(18B)	109.9(13)
Si(1)-C(18)-H(18C)	104.1(16)
H(18A)-C(18)-H(18B)	109.8(16)
H(18A)-C(18)-H(18C)	108.5(18)
H(18B)-C(18)-H(18C)	113(2)
C(3)-C(19)-H(19A)	112.9(10)

C(3)-C(19)-H(19B)	112.8(9)
C(3)-C(19)-H(19C)	110.1(9)
H(19A)-C(19)-H(19B)	104.8(13)
H(19A)-C(19)-H(19C)	105.1(13)
H(19B)-C(19)-H(19C)	110.7(13)
C(7)-C(20)-H(20A)	107.2(10)
C(7)-C(20)-H(20B)	110.3(10)
C(7)-C(20)-H(20C)	110.6(9)
H(20A)-C(20)-H(20B)	107.5(13)
H(20A)-C(20)-H(20C)	111.0(14)
H(20B)-C(20)-H(20C)	110.3(14)
C(7)-C(21)-H(21A)	107.9(8)
C(7)-C(21)-H(21B)	114.7(12)
C(7)-C(21)-H(21C)	113.7(9)
H(21A)-C(21)-H(21B)	110.7(12)
H(21A)-C(21)-H(21C)	109.6(12)
H(21B)-C(21)-H(21C)	100.0(14)

Symmetry transformations used to generate equivalent atoms:

Table A7.1.4. Anisotropic displacement parameters ($\text{\AA}^2 \times 10^4$) for **133**. The anisotropic displacement factor exponent takes the form: $-2\pi^2 [h^2 a^{*2} U^{11} + \dots + 2 h k a^* b^* U^{12}]$

	U ¹¹	U ²²	U ³³	U ²³	U ¹³	U ¹²
I(1)	153(1)	162(1)	141(1)	-20(1)	-36(1)	-19(1)
Si(1)	248(1)	130(1)	151(1)	45(1)	40(1)	16(1)
O(1)	155(2)	82(2)	85(2)	0(2)	5(2)	6(2)
O(2)	318(4)	150(3)	106(2)	8(2)	23(2)	13(2)
O(3)	139(2)	179(3)	181(2)	39(2)	29(2)	33(2)
O(4)	154(2)	162(3)	233(3)	93(2)	1(2)	34(2)
C(1)	116(2)	85(3)	86(2)	1(2)	-1(2)	3(2)
C(2)	110(2)	91(3)	94(2)	6(2)	-6(2)	-1(2)
C(3)	120(2)	109(3)	117(3)	16(2)	-6(2)	-15(2)
C(4)	117(3)	181(4)	200(4)	68(3)	24(2)	9(2)
C(5)	106(3)	166(4)	192(3)	48(3)	-7(2)	8(2)
C(6)	119(2)	112(3)	115(3)	6(2)	5(2)	24(2)
C(7)	148(3)	98(3)	148(3)	17(2)	-11(2)	20(2)
C(8)	167(3)	90(3)	131(3)	22(2)	-1(2)	2(2)
C(9)	149(3)	98(3)	160(3)	5(2)	2(2)	-15(2)
C(10)	115(2)	103(3)	128(3)	-4(2)	-16(2)	-9(2)
C(11)	161(3)	103(3)	108(3)	14(2)	5(2)	7(2)
C(12)	118(2)	99(3)	118(3)	7(2)	-19(2)	9(2)

C(13)	192(4)	165(4)	271(4)	34(3)	–35(3)	58(3)
C(14)	151(3)	149(3)	115(3)	23(2)	9(2)	–11(2)
C(15)	237(3)	132(3)	147(3)	26(2)	28(3)	–6(3)
C(16)	380(6)	294(6)	191(4)	60(4)	–41(3)	–109(4)
C(17)	732(12)	401(8)	403(8)	181(7)	221(8)	366(9)
C(18)	363(6)	296(6)	274(5)	104(5)	–16(4)	–138(5)
C(19)	190(3)	143(3)	124(3)	8(3)	–24(2)	–49(3)
C(20)	189(3)	211(4)	188(4)	57(3)	–58(3)	5(3)
C(21)	238(4)	119(3)	256(4)	–9(3)	21(3)	51(3)

Table A7.1.5. Hydrogen coordinates ($\times 10^3$) and isotropic displacement parameters ($\text{\AA}^2 \times 10^3$) for **133**.

	x	y	z	U _{iso}
H(2)	585(2)	532(1)	103(1)	16(3)
H(4A)	917(2)	517(1)	100(1)	18(3)
H(4B)	1014(2)	616(2)	132(1)	23(4)
H(5A)	937(2)	517(2)	199(1)	20(3)
H(5B)	1030(2)	414(1)	164(1)	11(3)
H(6)	779(2)	321(1)	136(1)	10(3)
H(8)	581(2)	208(2)	253(1)	24(4)
H(9)	384(2)	181(2)	192(1)	22(3)
H(13A)	197(2)	811(2)	105(1)	28(4)
H(13B)	316(2)	940(1)	105(1)	16(3)
H(13C)	273(2)	872(2)	149(1)	38(5)
H(14)	735(2)	693(2)	64(1)	17(3)
H(15)	848(2)	923(2)	111(1)	37(5)
H(16A)	657(2)	812(2)	-11(1)	30(4)
H(16B)	845(2)	763(2)	-19(1)	40(5)
H(16C)	768(2)	889(2)	-48(1)	42(5)
H(17A)	587(4)	1072(3)	33(1)	80(10)
H(17B)	680(3)	1156(2)	4(1)	65(6)

H(17C)	731(3)	1162(2)	56(1)	59(6)
H(18A)	1056(2)	1077(2)	-10(1)	37(5)
H(18B)	1127(3)	953(2)	19(1)	48(6)
H(18C)	1068(3)	1080(2)	42(1)	58(6)
H(19A)	875(2)	802(2)	174(1)	22(4)
H(19B)	777(2)	705(2)	201(1)	23(4)
H(19C)	694(2)	814(2)	173(1)	21(3)
H(20A)	885(2)	220(2)	263(1)	23(4)
H(20B)	892(2)	370(2)	255(1)	25(4)
H(20C)	1014(2)	275(2)	229(1)	24(4)
H(21A)	910(2)	121(2)	170(1)	14(3)
H(21B)	714(2)	98(2)	166(1)	31(4)
H(21C)	788(2)	50(2)	207(1)	25(4)

CHAPTER 3

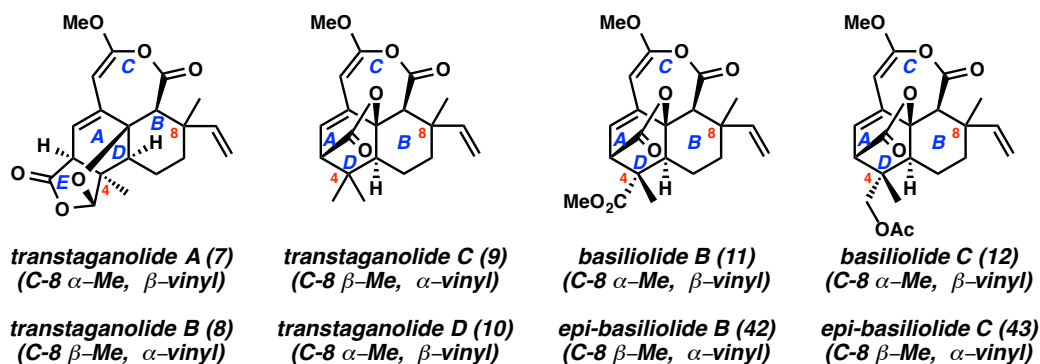
Negishi Cross-Coupling of Zinc Methoxyacetylides and Protecting-Group-Free Total Syntheses of Basiliopyrone And Transtaganolides C and D

3.1 INTRODUCTION

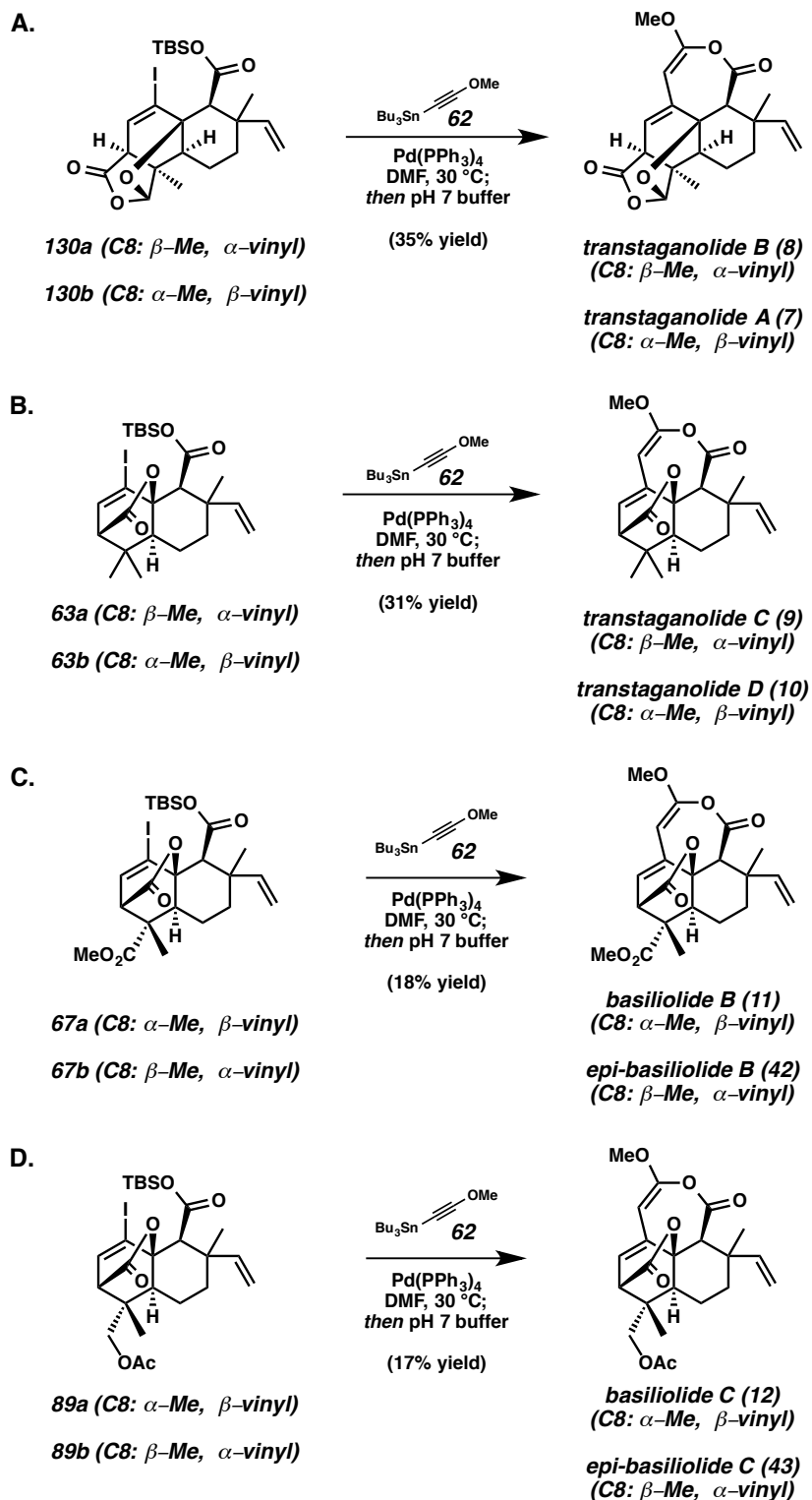
Having successfully synthesized transtaganolides A–B (**7–10**, Figure 3.1.1) (basiliolide B (**11**), epi-basiliolide B (**42**), basiliolide C (**12**), and epi-basiliolide C (**43**)) by means of a concise general synthetic strategy, we once again revisited this general synthetic strategy, aiming to further improve upon it.¹ Our approach employed an Ireland–Claisen, Diels–Alder cycloaddition cascade (ICR/DA) to build the ABD tricyclic core followed by formal [5+2] annulation strategy to build the 7-membered C-ring. Although our strategy allowed for rapid assembly of the transtaganolide and basiliolide natural products, the key formal [5+2] annulation, which builds the ketene-acetal containing 7-membered C-ring, was inefficient, a trend observed in all of our reported total syntheses. Transtaganolides A and B (**7** and **8**) proceeded in 35% combined yield from tetracycles **130a** and **130b** (Scheme 3.1.1A). Transtaganolides C and D (**9** and **10**) proceeded in 31% combined yield from tricycles **63a** and **63b** (Scheme 3.1.1B).

Basiliolide B (**11**) and epi-basiliolide B (**42**) were formed in 18% combined yield from silyl esters **67a** and **67b** (Scheme 3.1.1C). Lastly, basiliolide C (**12**) and epi-basiliolide C (**43**) were formed in 17% combined yield from tricycles **89a** and **89b** (Scheme 3.1.1D). Furthermore, these transformations require stoichiometric palladium and superstoichiometric quantities of the organostannane. To date, similar cross-coupling reactions of organostannanes have not been accomplished on substrates of such complexity, and few examples are known that utilize stannyl oxy-acetylides.² Therefore, we sought to improve the efficiency of this challenging cross-coupling through improved yield, reduced catalyst loading, and reduction or elimination of equivalents of stannane utilized.

Figure 3.1.1. Transtaganolides and basiliolides (**7–12**, **42**, and **43**).



Scheme 3.1.1. A) Cross-coupling to form transtaganolides A and B (**7** and **8**). B) Cross-coupling to form transtaganolides C and D (**9** and **10**). C) Cross-coupling to form basiliolide B (**11**) and epi-basiliolide B (**42**). D) Cross-coupling to form basiliolide C (**12**) and epi-basiliolide C (**43**).

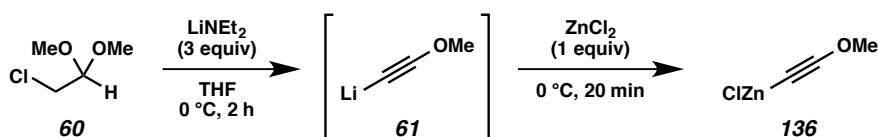


3.2 MODEL CROSS-COUPLING REACTIONS OF ZINC METHOXYACETYLIDES

In 1992, Himbert and Löffler reported a palladium-catalyzed cross-coupling of zinc alkoxyacetylides to simple aryl iodides.³ Inspired by this precedent, we began investigations of palladium catalyzed cross-coupling reactions of a zinc alkoxyacetylide to form the characteristic C-ring of the series.

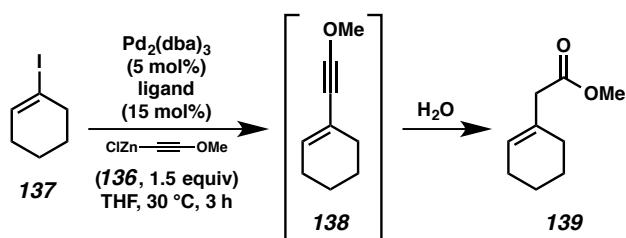
Synthesis of the precedented zinc alkoxyacetylide (**136**) proceeded via known treatment of 1,1-dimethoxy-2-chloro-acetaldehyde (**60**) with 3 equivalents of lithium diethyl amide to form the putative lithium acetylide **61**⁴, which is then trapped as the zinc acetylide **136** by the addition of anhydrous zinc chloride (Scheme 3.2.1). The methoxyethynyl zinc chloride (**136**) was stored at 0 °C as the crude solution and always used within hours of preparation.⁵

Scheme 3.2.1. Synthesis of methoxyethynyl zinc chloride (**136**).



As a model system, Pd-catalyzed coupling of organozinc **136** to iodo-cyclohexene (**137**)⁶ was evaluated (Table 3.2.1). Initially, we investigated a variety of bidentate ligands, as well as those conditions described by Himbert and Löffler. Spontaneous hydration of the cross-coupled product **138** on work-up yielded methyl ester **139**, which could be quantified to determine the overall yield of the process. We found that the conditions reported by Himbert and Löffler (Table 3.2.1, entry 1) did not extend readily from aryl iodides to vinyl iodides such as iodo-cyclohexene (**137**). The use of an N,N-

ligand, bipyridine (entry 2) as well as a P,N-ligand, H₂PHOX (entry 3) resulted in approximately 50% consumption of the vinyl iodide **137**, giving 0% or 10% yield of the product **139**, respectively. This large discrepancy between substrate **137** conversion and the calculated of yield **139** is general and attributed to the rapid decomposition of the cross-coupled product **138** under the reaction conditions. Among the diphosphines tested, BINAP (entry 4) gave 40% conversion of iodo-cyclohexene (**137**), but unfortunately provided the product **139** in a mere 6% yield. Dppe (entry 6) was found to provide no reactivity, whereas dpp-benzene (entry 5) and dppp (entry 7) gave minimal conversions (13% and 22%, respectively) and poor yields (6% and 7%, respectively). Lastly dppb (entry 8) and dppf (entry 9) gave the highest yields (13% and 17%, respectively) and 100% conversion of iodo-cyclohexene (**137**). Although the yields were quite low, we were delighted to have found conditions that employ substoichiometric quantities of palladium for this challenging cross-coupling reaction.

Table 3.2.1. Ligand screen for the cross-coupling of methoxyethynyl zinc chloride (**136**) and iodo-cyclohexene (**137**).

entry	ligand	structure	conversion (%) ^c	yield of 139 (%) ^c
1 ^a	PPh_3 ^b	—	47	5
2	Bipy		54	0
3	H_2PHOX		46	10
4	BINAP		40	6
5	dpp-benzene		13	6
6	dppe		0	0
7	dppp		22	7
8	dppb		100	13
9	dppf		100	17

^a Utilized *n*-BuLi reduction of 10 mol% Pd(II) source $[\text{Cl}_2\text{Pd}(\text{Ph}_3)_2]$, to generate catalyst as described by Himbert and Löffler. ^b Ligand loading was 50 mol%. ^c Determined by GC using tridecane internal standard.

3.3 LIGAND BITE ANGLES AND THE RELATIONSHIP TO ORGANOZINC CROSS-COUPLING OF METHOXYETHYNYL ZINC CHLORIDE

In our reported cross-coupling reactions of organostannanes, as well as the studies reported by others, the major decomposition pathway was Heck polymerization of the

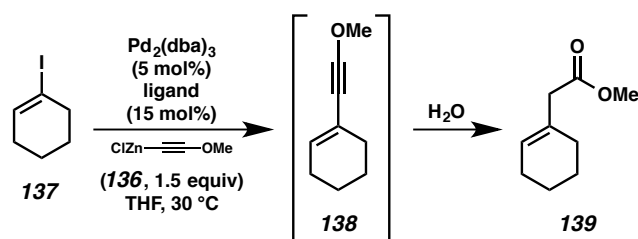
alkoxy alkynyl moiety.³ We posited that the non-productive polymerization pathway led to degradation of the metal methoxyacetylide (i.e., **62** or **136**), degradation of the intermediate eneyne (e.g., **138**), and degradation of the catalyst. We reasoned that these non-productive pathways necessitated stoichiometric quantities of palladium in our [5+2] annulation. Thus, we were pleased to find that dppb and dppf (Table 3.2.1, entry 8 and 9, respectively) could accomplish the coupling of organozinc **136** to iodide **137** utilizing substoichiometric quantities of palladium.

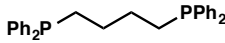

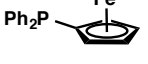
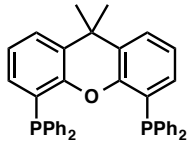
The superior reactivity demonstrated by both dppb and dppf were attributed to their relatively large bite angles (98° and 96° bite angles, respectively).⁷ It has been shown that bidentate ligands with large bite angles are poor catalysts for ethylene carbonylative polymerization reactions,⁸ which require an inner-sphere *cis*-geometry of monomers. We therefore envisioned that *trans*-chelating ligands could improve the efficiency of our reaction through the attenuation of acetylide polymerization, the putative catalyst, and substrate decomposition pathway. Thus, we were eager to investigate Xantphos (Table 3.3.1, entries 9–12) within our reaction manifold, because of its large bite angle (111°) and demonstrated propensity for *trans*-chelation.^{7,8}

We probed this hypothesis again through cross-coupling reactions of methoxyethynyl zinc chloride (**136**) and iodo-cyclohexene (**137**, Table 3.3.1), tabulating the conversion and yield as a function of time for dppb (Table 3.3.1, entries 1–4), dppf (entries 5–8), and Xantphos (entries 9–12). Consistent with our hypothesis, dppb and dppf (entries 1–4 and 5–8 respectively) with similar bite angles of 98° and 96° gave similar yields, 35% and 31% respectively. Xantphos (entries 9–12) with a considerably larger bite angle of 111° provided the product in 48% yield. Furthermore, for all three ligand-catalyst frameworks

we observed product decomposition by the end of the 4 h window that the reactions were monitored, suggesting polymerization was possibly still a competing pathway.

Table 3.3.1. Comparing *dppb*, *dppf*, and *Xantphos* as ligands for catalyzing the cross-coupling of methoxyethynyl zinc chloride (**136**) and iodo-cyclohexene (**137**) as a function of time.



entry	ligand	rxn time	conversion (%) ^a	yield of 139 (%) ^a
1		15 min	21	3
2		1 h	78	35
3	<i>dppb</i>	2.5 h	94	29
4		4 h	100	26
5		15 min	46	3
6		1 h	81	30
7	<i>dppf</i>	2.5 h	98	31
8		4 h	100	29
9		15 min	59	40
10		1 h	87	48
11		2.5 h	91	39
12	<i>Xantphos</i>	4 h	96	44

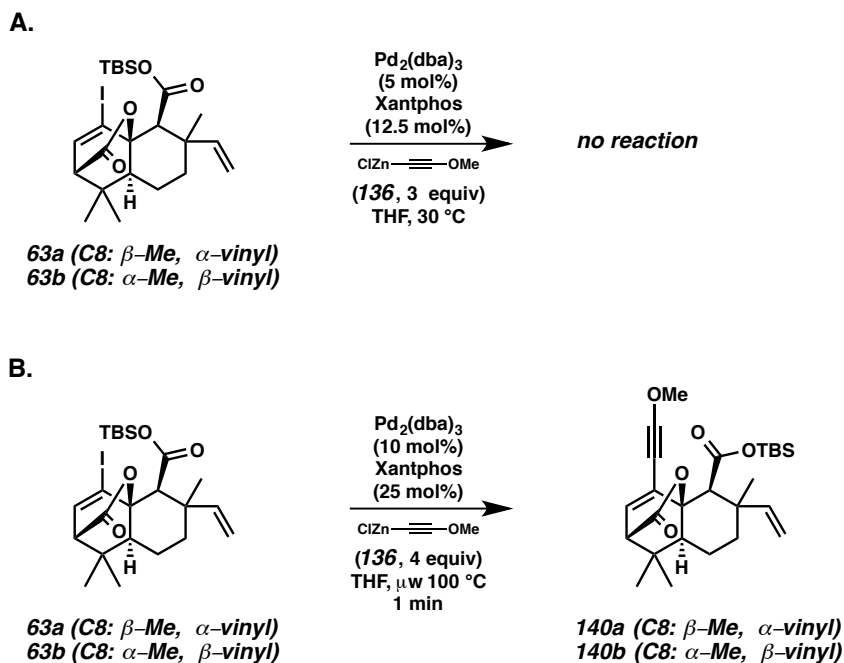
^aDetermined by GC using a tridecane internal standard.

3.4 APPLICATIONS OF ORGANOZINC CROSS-COUPPLINGS TO THE SYNTHESSES OF TRANSTAGANOLIDE NATURAL PRODUCTS

Having found *Xantphos* to be optimal for achieving the cross-coupling of acetylide **136** to vinyl iodide **137**, we moved from the model iodide **137** to the tricyclic transtaganolide core **63a** and **63b**. Unfortunately, our procedure did not readily translate to the more complex vinyl iodide (**63a** and **63b**) utilized in the total synthesis (Scheme 3.4.1A). Under these conditions we observed minimal substrate consumption and no

noticeable product formation; surprisingly, use of stoichiometric palladium loading led to trace product formation. We attribute this poor reactivity to the demanding steric environment of the substrate when compared to the simple cyclohexene **137** utilized in the model studies. In an effort to overcome the putative kinetic barrier, we explored heating of the reaction mixture. Ultimately, we found that microwave heating (100 °C) for short durations (<1 min) led to observable product formation (**140a** and **140b**, Scheme 3.4.1B). However, because of the rapid rate of product **140a** and **140b** decomposition at 100 °C, as well as the very short reaction time, the coupling could not be scaled and had poor reproducibility.

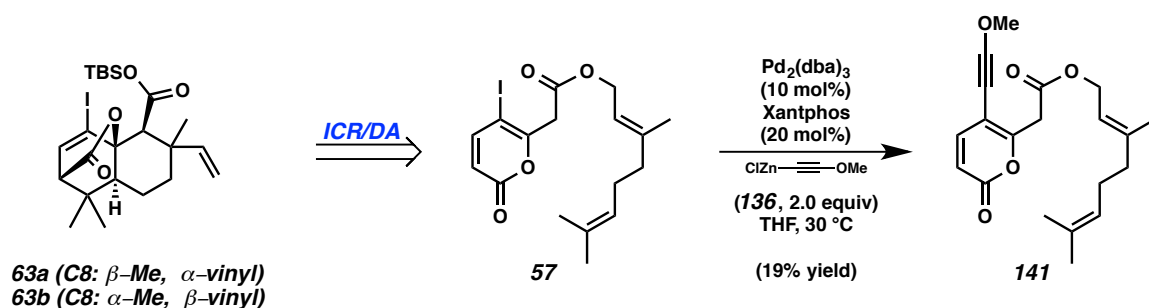
Scheme 3.4.1. A) Cross-coupling of tricycles **63a** and **63b** using the palladium Xantphos catalytic conditions developed on model cross-couplings to iodo-cyclohexene (**137**). B) Cross-coupling of tricycles **63a** and **63b** facilitated by microwave irradiation.



With no clear means to overcome the steric congestion of **63a** and **63b**, we reevaluated our retrosynthetic analysis, noting that prior to the ICR/DA cascade, pyrone

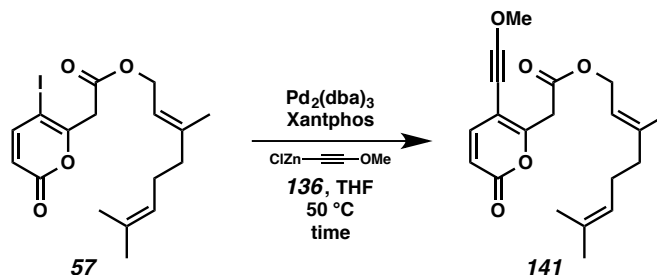
ester **57** bears a heteroaromatic iodine far more accessible for cross-coupling (Scheme 3.4.2). To our delight, palladium catalyzed cross-coupling of ICR/DA precursor **57** and methoxyacetylide **136** proceeded in 19% yield. Furthermore, we were pleased to find that the eneyne **141** could be purified by silica column chromatography without hydration or decomposition.

Scheme 3.4.2. Retrosynthetic Analysis illuminates a viable cross-coupling substrate pyrone ester **57**.



With a viable cross-coupling partner in pyrone **57**, we proceeded with optimization of the reaction conditions. Initial optimization was accomplished in a nitrogen filled glovebox at 50 °C (Table 3.4.1). We investigated organozinc **136** equivalents, catalyst loading, and concentration as they pertain to yield of the cross-coupled product **141** as a function of time. First off, more equivalents of organozinc (comparing entries 1–6 to entries 7–12) gave much higher yields. Lower catalyst loading (comparing entries 1–6 to entries 13–18) gave longer reaction times and lower yields. And lastly, lower concentration (comparing entries 13–18 to entries 19–24) greatly reduced the overall efficacy of the transformation, cutting the yield in half. Furthermore, as was observed in previous cross-coupling reactions, the cross-coupled product **141** decomposes under the reaction conditions.

Table 3.4.1. Comparing methoxyethynyl zinc chloride (**136**) equivalents, catalyst loading, and concentration as they effect the cross-coupling reaction at 50 °C of organozinc **136** and pyrone **57** as a function of time.



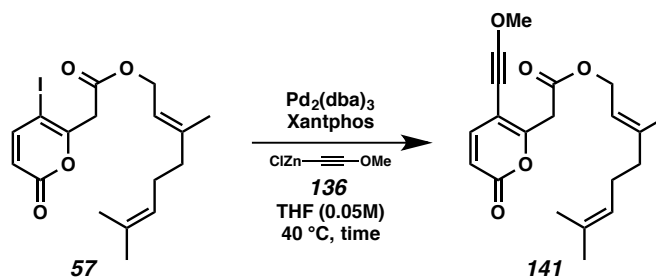
entry	mol% $\text{Pd}_2(\text{dba})_3$	mol% Xantphos	equiv 136	concentration	time	yield of 141 (%) ^a
1	10	20	2.0	0.05 M	15 min	46
2	10	20	2.0	0.05 M	30 min	35
3	10	20	2.0	0.05 M	45 min	— ^b
4	10	20	2.0	0.05 M	1 h	31
5	10	20	2.0	0.05 M	1.5 h	22
6	10	20	2.0	0.05 M	2.5 h	12
7	10	20	1.2	0.05 M	15 min	21
8	10	20	1.2	0.05 M	30 min	12
9	10	20	1.2	0.05 M	45 min	15
10	10	20	1.2	0.05 M	1 h	— ^b
11	10	20	1.2	0.05 M	1.5 h	4
12	10	20	1.2	0.05 M	2.5 h	0
13	5	10	2.0	0.05 M	15 min	38
14	5	10	2.0	0.05 M	30 min	39
15	5	10	2.0	0.05 M	45 min	27
16	5	10	2.0	0.05 M	1 h	— ^b
17	5	10	2.0	0.05 M	1.5 h	25
18	5	10	2.0	0.05 M	2.5 h	— ^b
19	5	10	2.0	0.02 M	15 min	20
20	5	10	2.0	0.02 M	30 min	21
21	5	10	2.0	0.02 M	45 min	17
22	5	10	2.0	0.02 M	1 h	16
23	5	10	2.0	0.02 M	1.5 h	15
24	5	10	2.0	0.02 M	2.5 h	— ^b

^a Determined by SFC using diphenylether internal standard. ^b SFC failed and no data could be collected at the time point. Resubmission was not a viable option as SFC sample would degrade over time.

In our second optimization screen, reactions were performed at 40 °C (Table 3.4.2). 3.0 equivalents of organozinc **136** (entries 4–6) gave higher yields than 2.0 equivalents (entries 1–3). Lower catalyst loadings (comparing entries 7–12 to entries 1–6) gave lower yields similar to experiments executed at 50 °C (Table 3.4.1). Furthermore, when comparing reactions carried out at 40 °C (Table 3.4.2, entries 1–3) to those conducted at

50 °C (Table 3.4.1, entries 1–6), reactions times were slower, as expected, and yields only slightly differed. For this reason, all remaining cross-coupling reactions were executed at 50 °C for substrate **57**.

Table 3.4.2. Comparing methoxyethynyl zinc chloride (**136**) equivalents and catalyst loading as they effect the cross-coupling reaction at 40 °C of organozinc **136** and pyrone **57** as a function of time.



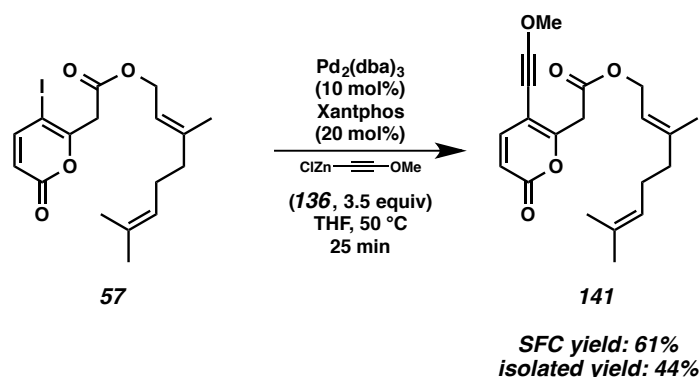
entry	mol% $\text{Pd}_2(\text{dba})_3$	mol% Xantphos	equiv 136	time	yield of 141 (%) ^a
1	10	20	2.0	15 min	29
2	10	20	2.0	30 min	42
3	10	20	2.0	1 h	32
4	10	20	3.0	15 min	37
5	10	20	3.0	30 min	52
6	10	20	3.0	1 h	35
7	5	10	2.0	15 min	22
8	5	10	2.0	30 min	27
9	5	10	2.0	1 h	27
10	5	10	3.0	15 min	27
11	5	10	3.0	30 min	34
12	5	10	3.0	1 h	28

^aDetermined by SFC using diphenylether internal standard.

Having accomplished two rounds of optimization for the cross-coupling reaction of pyrone **57** and methoxyethynyl zinc chloride (**136**), we applied what we had learned from the optimization and performed the cross-coupling on a larger scale (Scheme 3.4.3). To our delight, using 10 mol% $\text{Pd}_2(\text{dba})_3$, 20 mol% Xantphos, and 3.5 equivalents of methoxyacetylide **136**, we formed product **141** in 25 min of 50 °C heating in 61% yield, as determined by SFC and 44% isolated yield. The discrepancy between the 61% yield

as determined by SFC and the 44% isolated yield was not unexpected. Even though eneyne **141** could be isolated by column chromatography, it was clear that product **141** decomposed over time, and therefore we expected to observe some decomposition during purification.

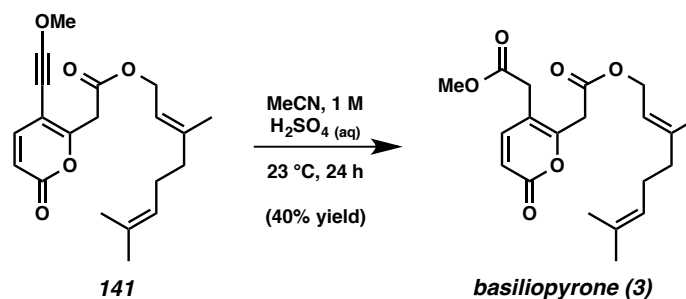
*Scheme 3.4.3. Cross-coupling of pyrone **57** and methoxyethynyl zinc chloride (**136**) using our optimized reaction conditions.*



3.5 PROTECTING-GROUP-FREE SYNTHESSES OF BASILIOPYRONE AND TRANSTAGANOLIDES C AND D

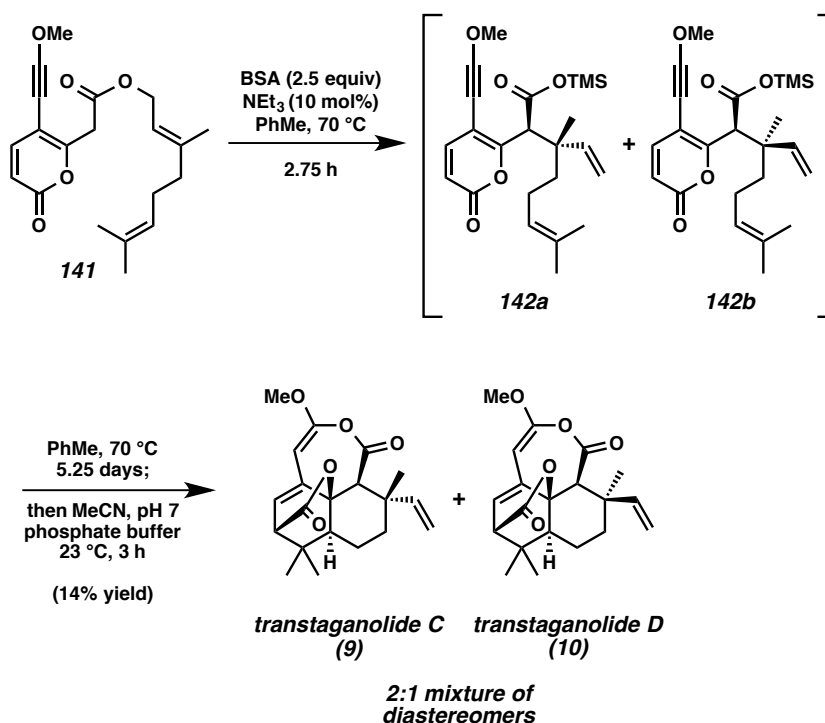
Having developed an acceptable method for the palladium catalyzed Negishi cross-coupling of methoxyethynyl zinc chloride (**136**) and pyrone ester **57**, we could successfully form eneyne **141**, which could be taken on to transtaganolides C and D (**9** and **10**) as well as basiliopyrone (**3**). If desired, eneyne **141** could be hydrated by treatment with aqueous sulfuric acid in acetonitrile to cleanly furnish basiliopyrone (**3**) in 40% yield (Scheme 3.5.1). The total synthesis of basiliopyrone (**3**) required seven steps (longest linear sequence) from commercially available material.

Scheme 3.5.1. Acid catalyzed hydration of **141** allows for the formation of basiliopyrone (**3**).



Finally, minor modification of our reported ICR/DA cascade conditions allowed direct access to transtaganolides C and D (**9** and **10**) in a single step from the alkynyl pyrone ester **141** as a 2:1 mixture of diastereomers in 14% combined yield (Scheme 3.5.2). Because of the thermal instability of the substrate (**141**) the cascade was performed at a lower temperature (70 °C) than our standard conditions and in a nitrogen filled glovebox to ensure the absolute exclusion of adventitious water. Furthermore, the Ireland–Claisen step of the cascade proceeded smoothly, but the Ireland–Claisen products (**142a** and **142b**) we found to be unstable and prone to decomposition. Nevertheless, we were satisfied to observe the successful [4+2] cycloaddition of a substrate (**142a** or **142b**) bearing an electron-donating methoxy alkynyl moiety on the pyrone ring (all prior pyrone Diels–Alder cycloadditions had required electron-withdrawing substituents). While low yielding, this one-pot procedure forms three rings, two all-carbon quaternary centers, and four tertiary stereocenters from a simple monocyclic, achiral precursor (**141**). Finally, the success of this cascade process further implicates the Ireland–Claisen/Diels–Alder sequence as a potential biosynthetic route.

Scheme 3.5.2. A one-pot synthesis of transtaganolides C and D (**9** and **10**) from alkynyl pyrone **141**.



3.6 CONCLUSION

In conclusion, we have improved our previously disclosed [5+2] annulation of methoxy acetyl stannane **62** by obviating the need for organotin reagents and developing a complimentary Negishi cross-coupling of methoxyacetylde **136**. This methodology, which employs catalytic quantities of a Xantphos palladium complex, was used to furnish the alkynyl pyrone ester **141**. The cross-coupled product **141** could be hydrated to furnish basiliopyrone (**3**) or, to our delight, transformed in a single step cascade process into transtaganolides C and D (**9** and **10**).

3.7 EXPERIMENTAL SECTION

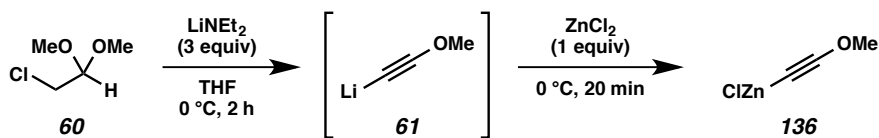
3.7.1 Materials and Methods

Unless otherwise stated, reactions were performed in flame-dried glassware under an argon or nitrogen atmosphere using dry deoxygenated solvents. Solvents were dried by passage through an activated alumina column under argon. Chemicals were purchased from Sigma-Aldrich Chemical Company and used as received. Pd(PPh₃)₄ was prepared using known methods. Thin layer chromatography (TLC), both preparatory and analytical, was performed using E. Merck silica gel 60 F254 precoated plates (0.25 mm) and visualized by UV fluorescence quenching, *p*-anisaldehyde, I₂, or KMnO₄ staining. Analytical super critical fluid (SFC) chromatography was performed using a Thar SFC and either Chiralpak IA or AD-H columns. Preparatory SFC was performed with a Jasco SFC and a prep AD-H column (21 x 250 mm, 5mic part# 19445). ICN Silica gel (particle size 0.032–0.063 mm) was used for flash chromatography. ¹H NMR and ¹³C NMR spectra were recorded on a Varian Mercury 300 (at 300 MHz) or on a Varian Unity Inova 500 (at 500 MHz). ¹H NMR spectra are reported relative to CDCl₃ (7.26 ppm). Data for ¹H NMR spectra are reported as follows: chemical shift (ppm), multiplicity, coupling constant (Hz), and integration. Multiplicities are reported as follows: s = singlet, d = doublet, t = triplet, q = quartet, sept. = septet, m = multiplet, bs = broad singlet, bm = broad multiplet. ¹³C NMR spectra are reported relative to CDCl₃ (77.16 ppm). FTIR spectra were recorded on a Perkin Elmer SpectrumBX spectrometer and are reported in frequency of absorption (cm⁻¹). HRMS were acquired using an Agilent 6200 Series TOF with an Agilent G1978A Multimode source in electrospray ionization (ESI),

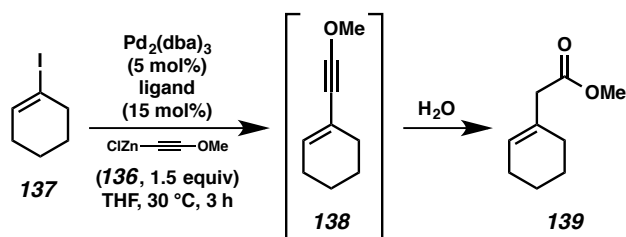
atmospheric pressure chemical ionization (APCI), or multimode-ESI/APCI.

Crystallographic data were obtained from the Caltech X-Ray Diffraction Facility.

3.7.2 PREPARATIVE PROCEDURES

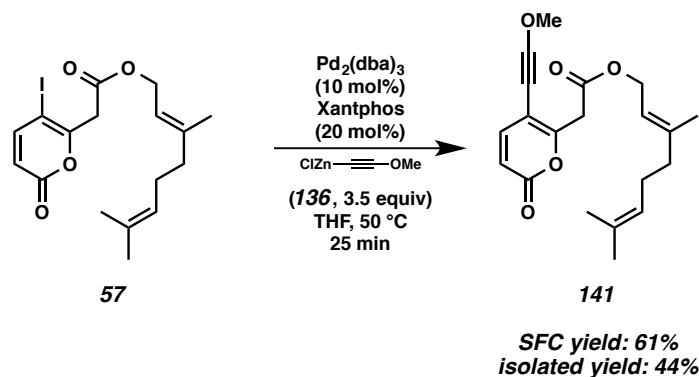


Methoxyethynyl zinc chloride (136). In a nitrogen glovebox, to a 0 °C solution of HNEt₂ (807 μL, 7.8 mmol) in THF (4.25 mL) was added a 2.5 M solution of *n*-BuLi in hexanes (2.72 mL, 6.8 mmol). The reaction was stirred for 25 min at 0 °C at which point 1,1-dimethoxy-2-chloroacetaldehyde (**60**) was added (228 μL, 2.0 mmol). The reaction was stirred at 0 °C and the formation of white precipitate was observed. After 2 h of stirring at 0 °C, anhydrous zinc chloride was added (300 mg, 2.2 mmol), and the reaction was stirred for another 15 min at 0 °C or until all the zinc chloride had dissolved. The resulting 0.25 M solution of methoxyethynyl zinc chloride (**136**) in THF was kept at 0 °C, in the glovebox, and used, as is, within hours of its generation.



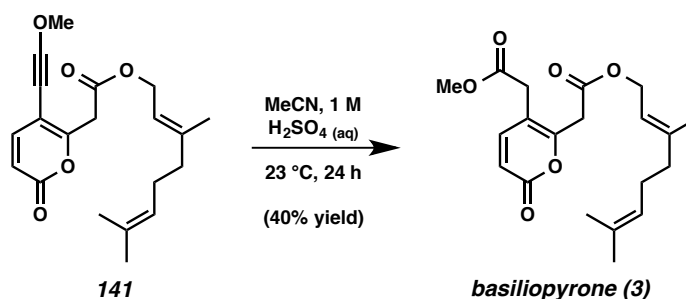
Methyl 2-(cyclohex-1-en-1-yl)acetate (139). General Procedure: In a nitrogen filled glovebox were combined Pd₂(dba)₃ (1.4 mg, 1.5 μmol), Xantphos (2.6 mg, 4.5 μmol), and THF (180 μL) in a glass vial. The reaction mixture was stirred for 30 min at 30 °C. Then a 1 M solution of known iodo-cyclohexene⁶ (**137**) in THF (30 μL, 0.030 mmol),

internal standard tridecane (6 μL , 0.025 mmol), and freshly made 0.05 M methoxyethynyl zinc chloride (**136**) solution (90 μL , 0.045 mmol) were added sequentially and the solution was stirred at 30 $^{\circ}\text{C}$. Aliquots (5 μL) were taken from the reaction solution at 15 min, 1 h, 2.5 h, and 4.5 h. Aliquots were diluted with Et_2O , pushed through a short pad of silica, and then injected on GC for analysis. Yields of methyl ester **139** and consumption of vinyl iodide **137** were then quantified. All spectral data for **139** match the literature.⁹



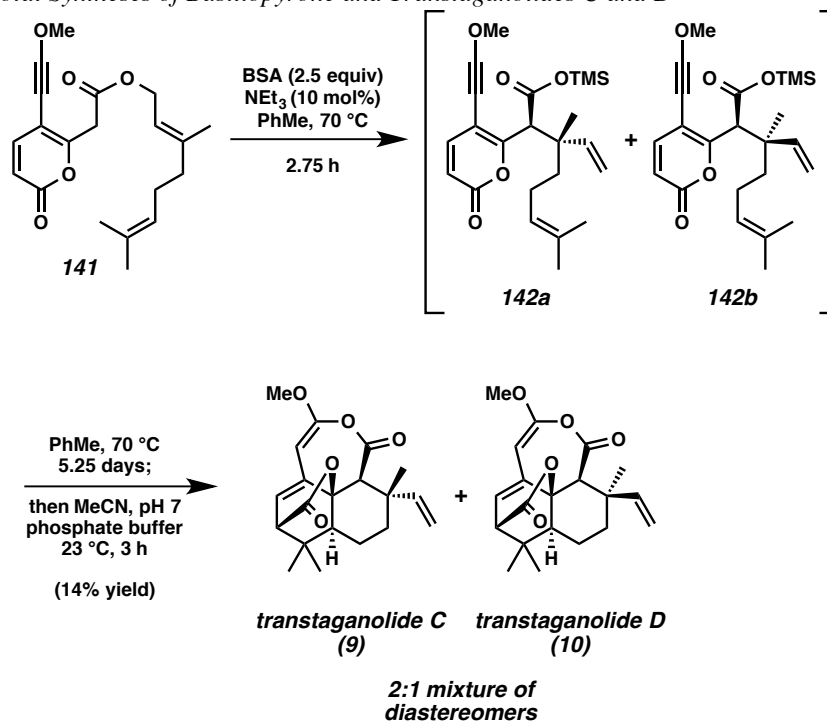
(E)-3,7-dimethylocta-2,6-dien-1-yl 2-(5-(methoxyethynyl)-2-oxo-2H-pyran-6-yl)acetate (141). In a nitrogen filled glovebox, a solution of $\text{Pd}_2(\text{dba})_3$ (18.8 mg, 0.0205 mmol) and Xantphos (23.8 mg, 0.0411 mmol) in THF (900 μL) was stirred at 40 $^{\circ}\text{C}$ for 25 min. Following the catalyst pre-stir, **57** (85.6 mg, 0.206 mmol) was added as a solution in THF (350 μL) with internal standard diphenylether (37.1 mg, 0.218 mmol). This was subsequently followed by the addition of freshly generated 0.25 M solution of methoxyethynyl zinc chloride (**136**) (2.9 mL, 0.719 mmol). The resulting 0.05 M reaction solution was heated to 50 $^{\circ}\text{C}$ and stirred for 25 min. The reaction mixture was then immediately removed from heat, diluted with 0 $^{\circ}\text{C}$ THF (12 mL), removed from the

glovebox, and flushed through a short pad of silica, eluting with a 30% solution of Et₂O in hexanes (150 mL). A small aliquot was then shot on SFC for analysis. Solvent was then removed by rotary evaporation and purified by column chromatography (EtOAc in a 50% solution of CH₂Cl₂ in hexanes 1%→2% on silica) to give 31 mg (44% isolated yield, 61% SFC yield) of **141** as a reddish, yellow oil; ¹H NMR (500 MHz, CDCl₃) δ 7.23 (d, *J* = 9.6 Hz, 1H), 6.20 (d, *J* = 9.6 Hz, 1H), 5.32 (tq, *J* = 7.1, 1.3 Hz, 1H), 5.08–5.04 (m, 1H), 4.65 (d, *J* = 7.2 Hz, 2H), 3.96 (s, 3H), 3.71 (s, 2H), 2.13–1.98 (m, 4H), 1.69 (s, 3H), 1.67 (s, 3H), 1.59 (s, 3H); ¹³C NMR (125 MHz, CDCl₃) δ 167.6, 160.8, 159.9, 146.8, 143.2, 132.0, 123.8, 117.8, 114.5, 104.4, 103.5, 66.4, 62.6, 39.6, 38.8, 31.8, 26.4, 25.8, 17.8, 16.6; FTIR (Neat Film NaCl) 2926, 2856, 2271, 1742, 1634, 1548, 1446, 1418, 1377, 1347, 1318, 1294, 1238, 1208, 1167, 1134, 1064, 1040, 969, 895, 870, 826 cm⁻¹; HRMS (Multimode-ESI/APCI) *m/z* calc'd for C₂₀H₂₅O₅ [M+H]⁺: 345.1697, found 345.1701.



Basiliopyrone (3). To a 23 °C solution of **141** (19 mg, 0.055 mmol) in MeCN (2 mL) was added a 1M solution of H₂SO₄ in water (500 μL). The reaction mixture was then stirred at 23 °C for 24 h. After the reaction had gone to completion, the mixture was slowly quenched with a saturated solution of NaHCO₃ (5 mL), such that the reaction mixture was no longer acidic. The solution was then extracted with EtOAc (4x 8 mL).

The organics were combined and sequentially washed with saturated NaHCO₃ solution (25 mL), saturated brine solution (25 mL), and then once again with saturated NaHCO₃ solution (25 mL), and saturated brine solution (25 mL). The organics were then dried over Na₂SO₄ and solvent was removed by rotary evaporation. Purification by column chromatography (EtOAc in hexanes 10%→25% on silica) yielded 8.1 mg (40% yield) of basiliopyrone (**3**) as a pale yellow oil. The spectroscopic data obtained from synthetic **3** match those published from natural sources; ¹H NMR (300 MHz, CDCl₃) δ 7.27 (d, *J* = 9.9 Hz, 1H), 6.27 (d, *J* = 9.5 Hz, 1H), 5.31 (tq, *J* = 7.2, 1.3 Hz, 1H), 5.10–5.04 (m, 1H), 4.64 (d, *J* = 7.2 Hz, 2H), 3.71 (s, 3H), 3.59 (s, 2H), 3.35 (s, 2H), 2.16–1.98 (m, 4H), 1.69 (s, 3H), 1.68 (s, 3H), 1.60 (s, 3H); ¹³C NMR (125 MHz, CDCl₃) δ 170.3, 167.5, 161.3, 155.8, 146.4, 143.4, 132.0, 123.9, 117.8, 115.3, 111.1, 62.9, 52.5, 39.7, 37.7, 34.9, 26.5, 25.8, 17.8, 16.7; FTIR (Neat Film NaCl) 2954, 2924, 2857, 1738, 1650, 1557, 1437, 1378, 1347, 1302, 1241, 1166, 1103, 1070, 975, 951, 872, 829 cm⁻¹; HRMS (Multimode-ESI/APCI) *m/z* calc'd for C₂₀H₂₆O₆ [M+H]⁺: 363.1802, found 363.1792.



Transtaganolides C (9) and D (10). To assure absolute purity of **141** (10 mg, 0.029 mmol), directly following its isolation, the substrate (**141**) was submitted to ¹H NMR in C₆D₆ and upon confirmation of its purity, the solvent was pumped off in the anti-chamber of a nitrogen filled glove box. This limited the possibility of substrate **141** decomposition as well as removed any deleterious, residual water. While the NMR solvent was removed in the anti-chamber, in the nitrogen filled glove box, the reaction glassware was silylated by the addition of BSA (20 μL), triethylamine (0.41 μL), and PhMe (5 mL). This solution was heated to 70 °C and stirred for 30 min. The solution was then cooled to ambient temperature and then discarded. The reaction vessel was then rinsed with PhMe (3 x 1 mL). Once all C₆D₆ was removed from the substrate **141**, **141** (10 mg, 0.029 mmol) was transferred to the previously silylated reaction vessel with PhMe (600 μL, 0.05M). To this solution was then added BSA (17.8 μL, 0.073 mmol) and triethylamine (0.041 μL, 0.0029 mmol). The reaction solution was heated to 70 °C and stirred for 2.75

h, at which point the Ireland–Claisen rearrangement had gone to completion. The reaction was then cooled to ambient temperature and diluted with PhMe (9.2 mL, 0.003M) that had been doped with excess BSA (12.25 μ L, PhMe:BSA = 1 mL:1.25 μ L). The reaction mixture was then reheated to 70 °C and stirred for 5 d and 6 h. The reaction mixture was cooled to ambient temperature and removed from the nitrogen filled glovebox. The solution was concentrated by rotary evaporation and to the crude reaction residue was added MeCN (8 mL) and pH 7 phosphate buffer (100 μ L). This solution was stirred at 23 °C for 3 h to allow for silyl cleavage and cyclization to the desired natural products (**9** and **10**). MeCN was then removed by passing a stream of air over the solution (rotary evaporation could not be accomplished without bumping the crude reaction mixture), and the remaining aqueous solution was further diluted with water (800 μ L) and saturated brine (200 μ L). The aqueous solution was then extracted with EtOAc (5 x 1 mL). The organics were pooled, dried over Na₂SO₄, and then concentrated by rotary evaporation. The crude oil was purified by normal phase HPLC (30% EtOAc in hexanes) to yield 0.90 mg (9% yield) of transtaganolide C (**9**) and 0.46 mg (5% yield) of transtaganolide D (**10**). The spectroscopic data obtained from synthetic **9** and **10** match those published from natural sources.

3.8 NOTES AND REFERENCES

Note: Portions of this chapter have been published, see: Gordon, J. R.; Nelson, H. M.; Virgil, S. C.; Stoltz, B. M. *J. Org. Chem.* **2014**, Article ASAP. doi: 10.1021/jo501924u.

- (1) (a) Nelson, H. M.; Murakami, K.; Virgil, S. C.; Stoltz, B. M. *Angew. Chem. Int. Ed.* **2011**, *50*, 3688–3691; (b) Nelson, H. M.; Gordon, J. R.; Virgil, S. C.; Stoltz, B. M. *Angew. Chem. Int. Ed.* **2013**, *52*, 6699–6703; (c) Gordon, J. R.; Nelson, H. M.; Virgil, S. C.; Stoltz, B. M. *J. Org. Chem.* **2014**, Article ASAP. doi: 10.1021/jo501924u.
- (2) (a) Marshall, J. A. in *Organometallics in Synthesis: A Manual* (Ed.: M. Schlosser) Wiley, Chichester, **2002**, 457; (b) Sakamoto, T.; Yasuhara, A.; Kondo, Y.; Yamanaka, H. *Synlett* **1992**, 502; (c) Sakamoto, T.; Yasuhara, A.; Kondo, Y.; Yamanaka, H. *Chem. Pharm. Bull.* **1994**, *42*, 2032–2035.
- (3) Löffler, A.; Himbert, G. *Synthesis* **1992**, 495–498.
- (4) Raucher, S.; Bray, B. L. *J. Org. Chem.* **1987**, *52*, 2332–2333.
- (5) Because of the instability of the methoxyethynyl zinc chloride (**136**), the organozinc reagent could not be characterized, and the solution was used assuming a 100% theoretical yield of formation.
- (6) Kropp, P. J.; McNeely, S. A.; Davis, R. D. *J. Am. Chem. Soc.* **1983**, *105*, 6907–6915.
- (7) Van Leeuwen, P. W. N. M.; Kamer, P. C. J.; Reek, J. N. H.; Dierkes, P. *Chem. Rev.* **2000**, *100*, 2741–2769.

- (8) Van Leeuwen, P. W. N. M.; Zuideveld, M. A.; Swennenhuis, B. H. G.; Freixa, Z.; Kamer, P. C. J.; Goubitz, K.; Fraanje, J.; Lutz, M.; Spek, A. L. *J. Am. Chem. Soc.* **2003**, *125*, 5523–5539.
- (9) Kapferer, T.; Brückner, R. *Eur. J. Org. Chem.* **2006**, 2119–2133.

APPENDIX 8

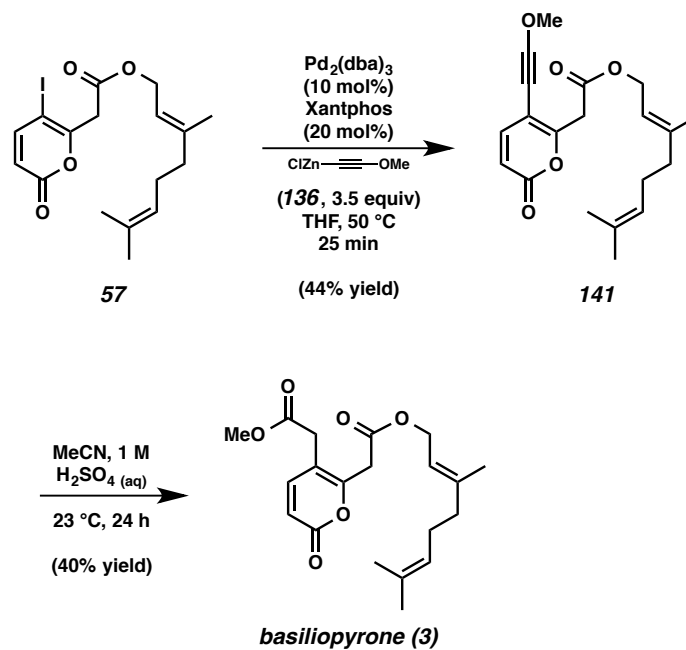
Synthetic Summary for Protecting-Group-Free Total Syntheses

Of Basiliopyrone and Transtaganolides C and D:

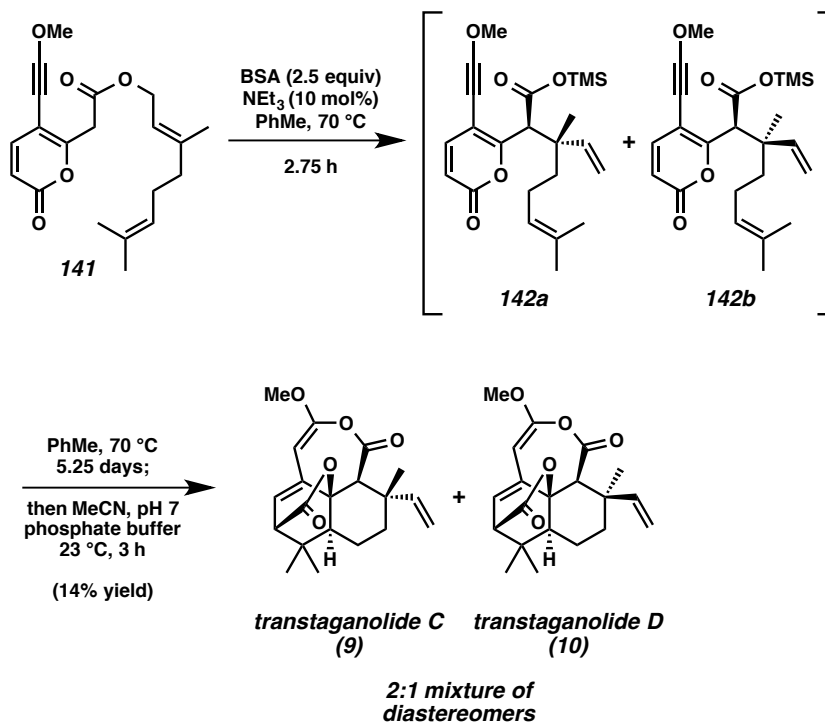
Relevant to Chapter 3

A8.1 SYNTHETIC SUMMARY FOR BASILIOPYRONE AND TRANSTAGANOLIDES C AND D

Scheme 8.1.1. Protecting-group-free synthesis of basiliopyrone (**3**).



Scheme 8.1.2. Protecting-group-free syntheses of transtaganolides C and D (9–10).

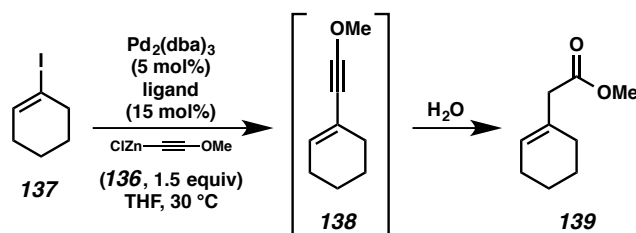


APPENDIX 9

Gas Chromatography and Supercritical Fluid Chromatography

Data: Relevant to Chapter 3

A9.1 GAS CHROMATOGRAPHY DATA FOR ORGANOZINC CROSS- COUPLING OPTIMIZATION



Yields of methyl ester **139**¹ and consumption of vinyl iodide **137**² were quantified using the calibration curves (Figure 9.1.1A and B), which graph the area ratio of gas chromatography (GC) peaks as a function of the molar ratio of either the methyl ester **139** and the tridecane internal standard or substrate **137** and the tridecane internal standard. This data was collected from several individual GC runs depicted in Table 9.1.1.

Figure 9.1.1. A) Calibration curve used to determine cross-coupling yields comparing methyl ester **139** and tridecane internal standard. B) Calibration curve used to determine cross-coupling substrate consumption by comparing vinyl iodide **137** and tridecane internal standard.

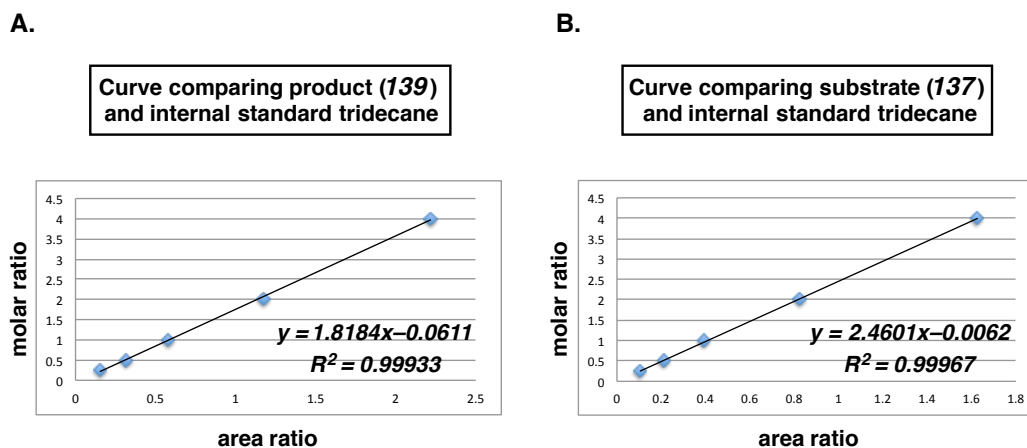
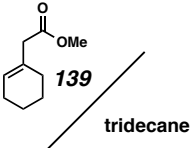
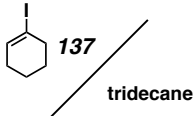
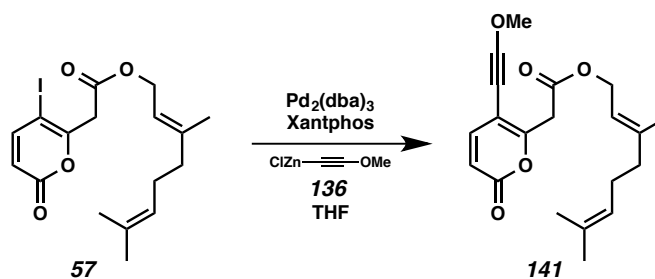


Table 9.1.1. A) The molar ratio of product **139** and tridecane with the associated peak area ratio obtained from GC analysis. B) The molar ratio of substrate **137** and tridecane with the associated peak area ratio obtained from GC analysis.

A.			B.		
					
entry	molar ratio	area ratio	entry	molar ratio	area ratio
1	4	2.217	1	4	1.626
2	2	1.169	2	2	0.8269
3	1	0.5758	3	1	0.3913
4	0.5	0.3133	4	0.5	0.2134
5	0.25	0.1547	5	0.25	0.1055

A9.2 SUPERCritical FLUID CHROMATOGRAPHY DATA FOR ORGANOZINC CROSS-COUPLING OPTIMIZATION



Yields of eneyne **141** were quantified using the calibration curves (Figure 9.2.1), which graph the area ratio of supercritical fluid chromatography (SFC) peaks as a function of the molar ratio of eneyne **141** and the diphenylether internal standard. This data was collected from several individual SFC runs depicted in Table 9.2.1.

Figure 9.2.1. Calibration curve used to determine cross-coupling yields comparing eneyne **141** and diphenylether internal standard.

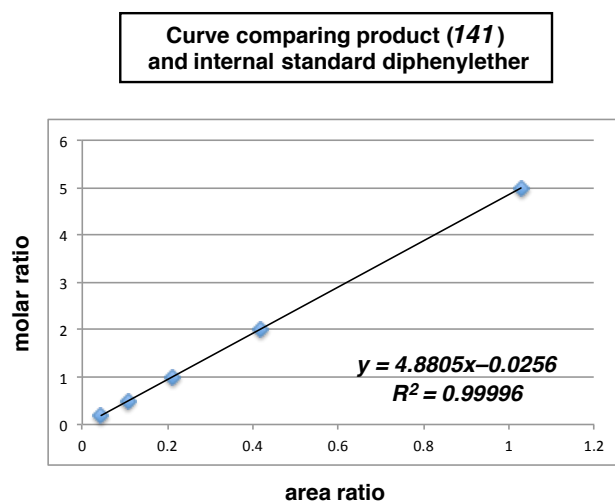
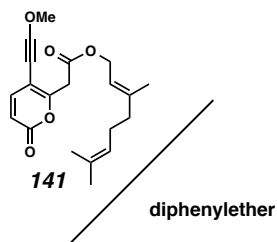


Table 9.2.1. The molar ratio of product **141** and diphenylether internal standard with the associated peak area ratio obtained from SFC analysis.



entry	molar ratio	area ratio
1	5	1.028
2	2	0.4189
3	1	0.2117
4	0.5	0.1059
5	0.2	0.04419

A9.3 NOTES AND REFERENCES

- (1) Methyl ester **139** was synthesized for GC studies using known methods: Kapferer, T.; Brückner, R. *Eur. J. Org. Chem.* **2006**, 2119–2133.
- (2) Iodo-cyclohexene (**137**) synthesized for GC studies using known methods: Kropp, P. J.; McNeely, S. A.; Davis, R. D. *J. Am. Chem. Soc.* **1983**, *105*, 6907–6915.

APPENDIX 10

Spectra Relevant to Chapter 3:

Negishi Cross-Coupling of Zinc Methoxyacetylides and Protecting-

Group-Free Total Syntheses of Basiliopyrone

And Transtaganolides C and D

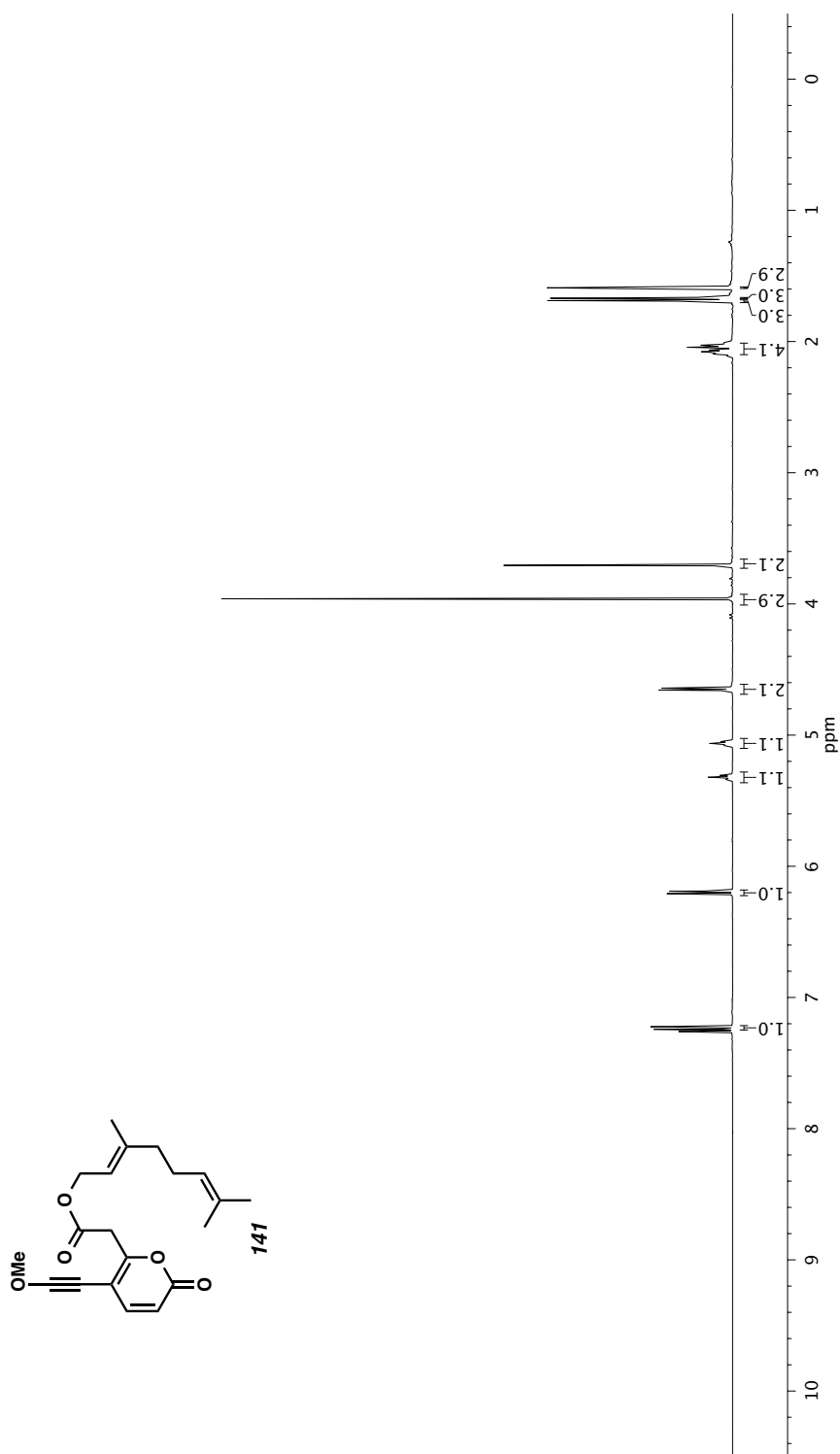


Figure A10.1.1 ¹H NMR (500 MHz, CDCl₃) of compound **141**.

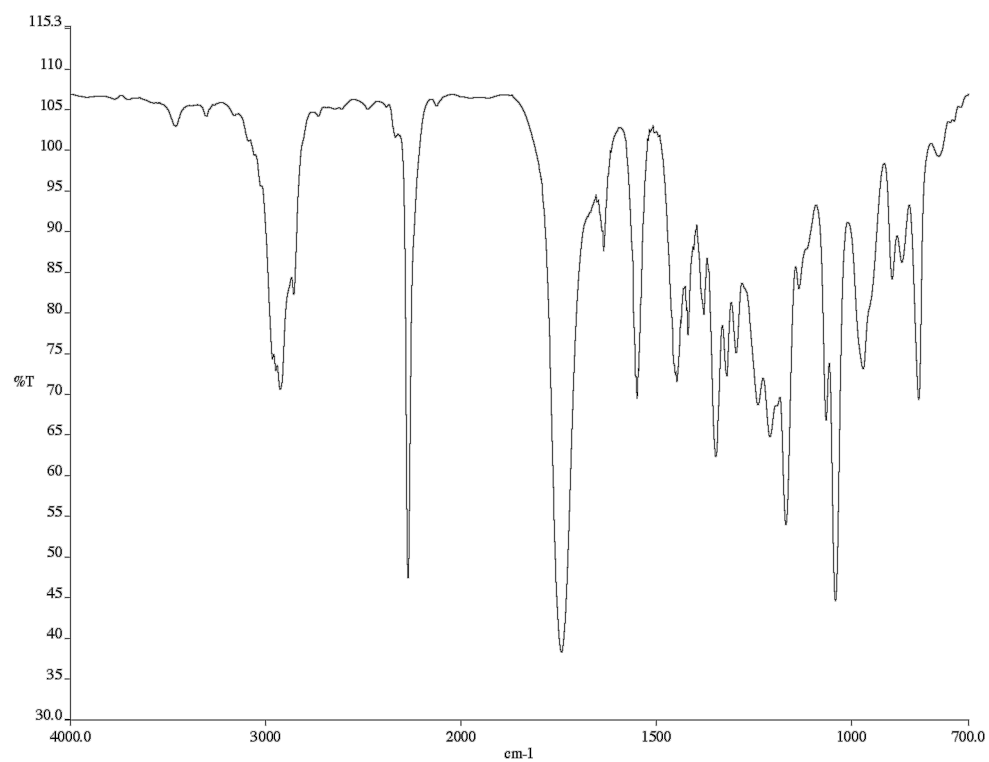


Figure A10.1.2 infrared spectrum (Thin Film, NaCl) of compound **141**.

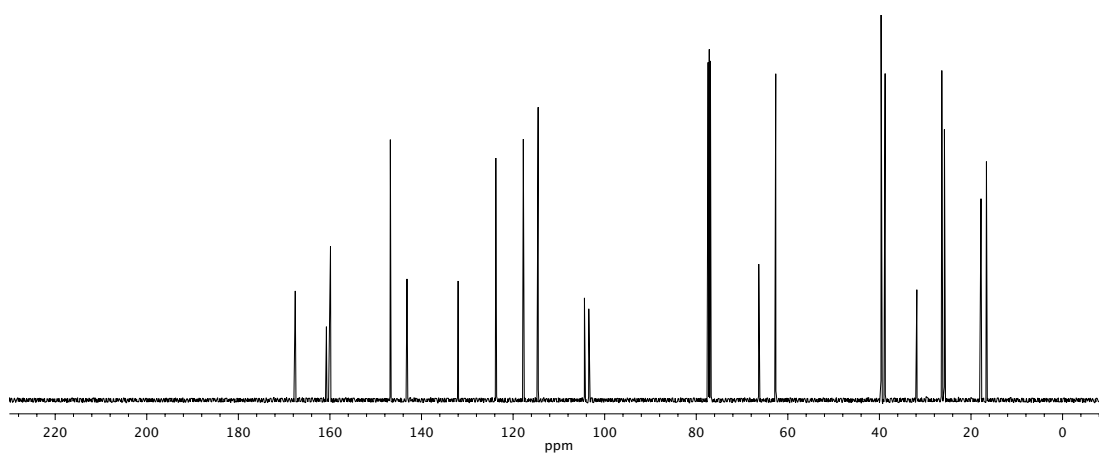


Figure A10.1.3 ¹³C NMR (125 MHz, CDCl₃) of compound **141**.

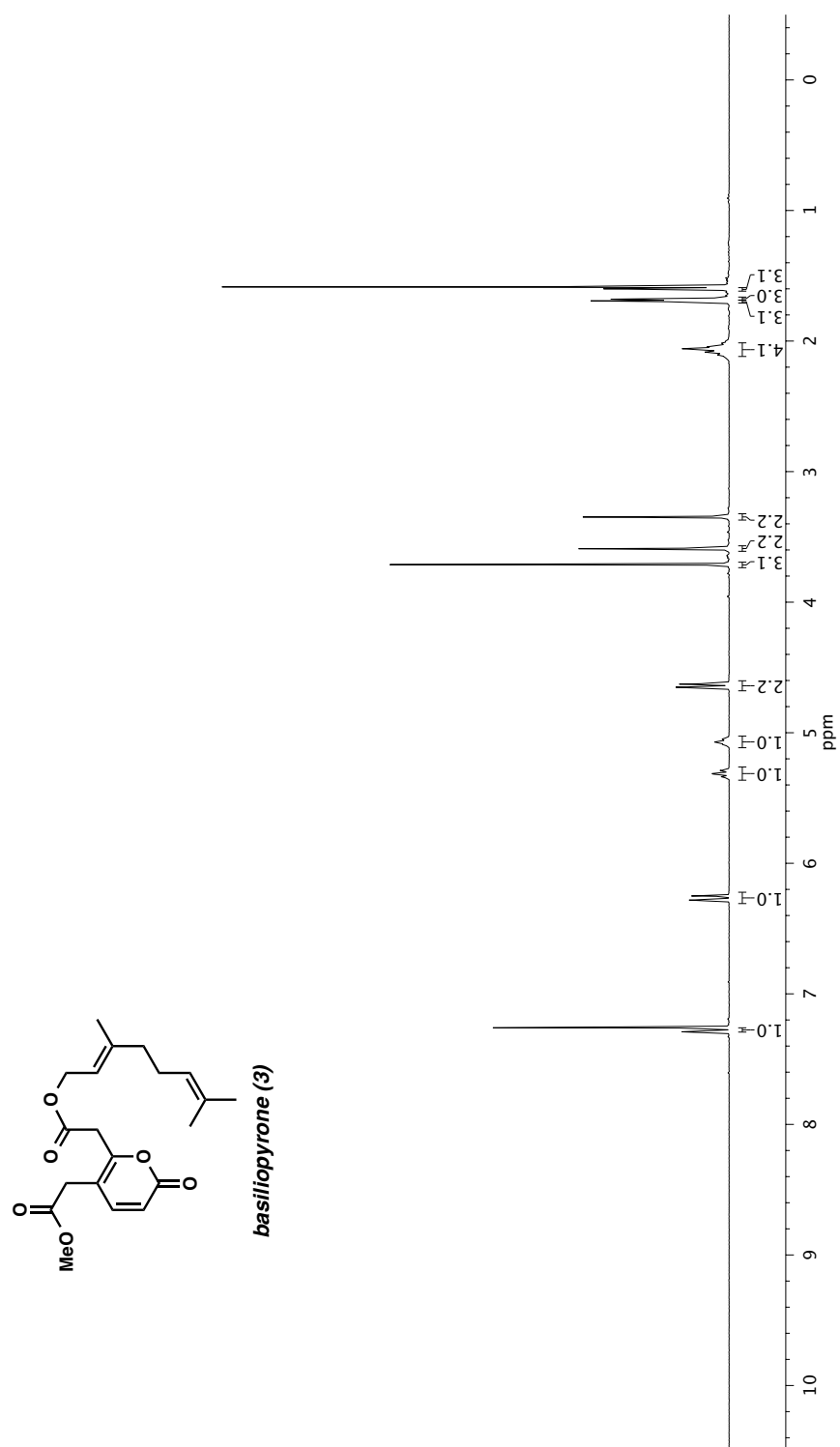


Figure A10.2.1 ¹H NMR (300 MHz, CDCl₃) of basilipyronone (3).

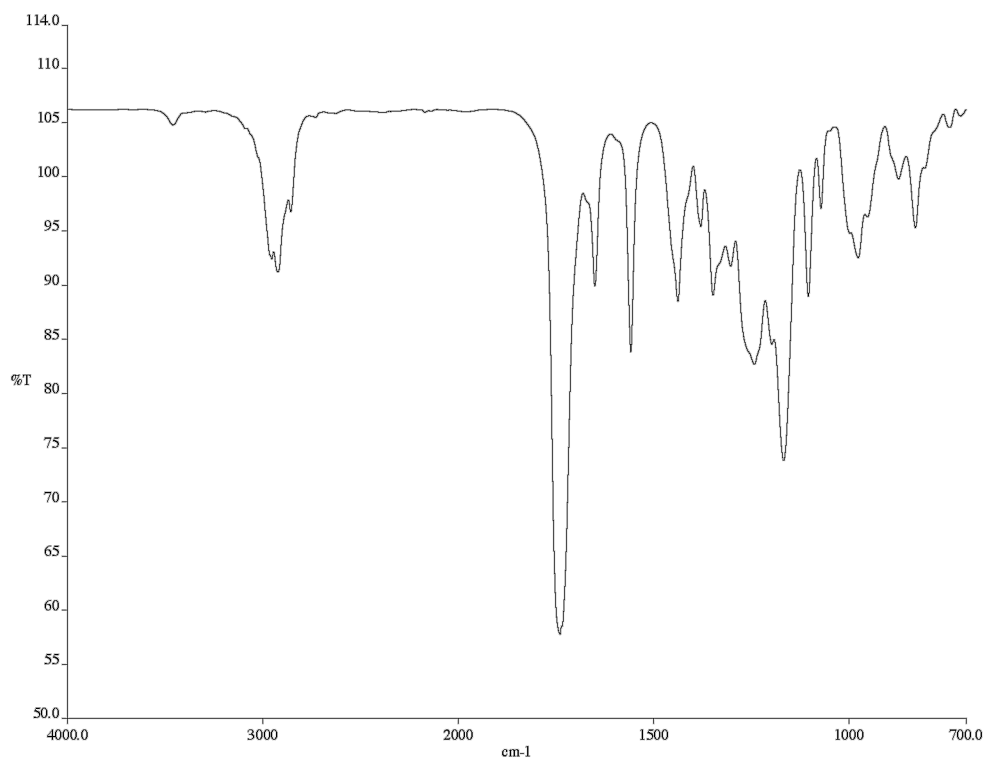


Figure A10.2.2 infrared spectrum (Thin Film, NaCl) of basiliopyrone (**3**).

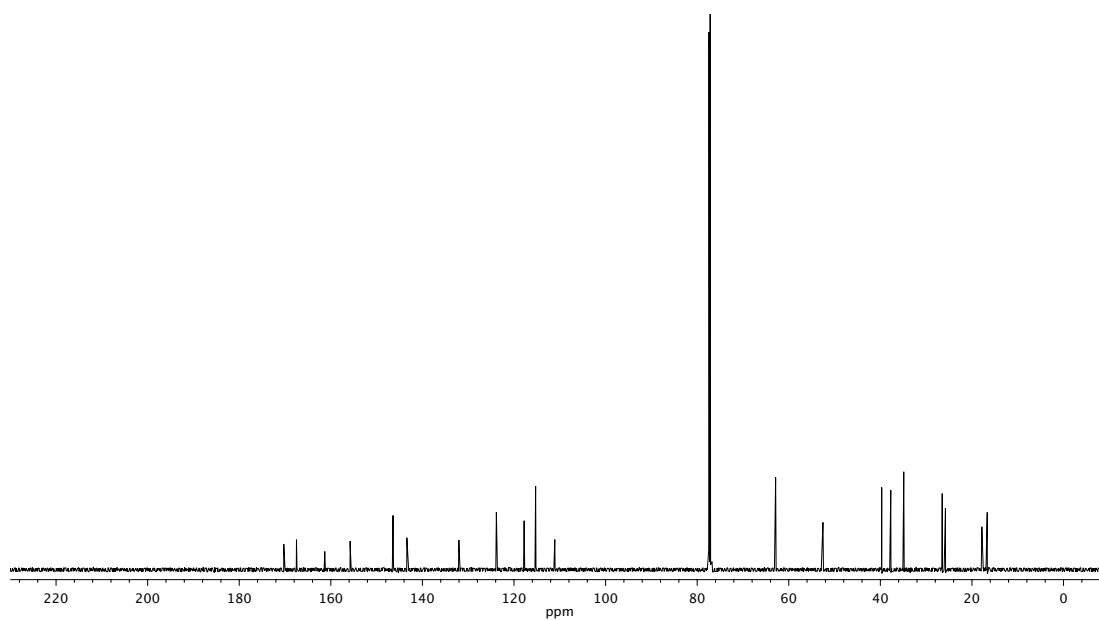


Figure A10.2.3 ^{13}C NMR (125 MHz, CDCl_3) of basiliopyrone (**3**).

COMPREHENSIVE BIBLIOGRAPHY

Afarinkia, K.; Bearpark, M. J.; Ndibwami, A. *J. Org. Chem.* **2005**, *70*, 1122–1133.

Appendino, G.; Prosperini, S.; Valdivia, C.; Ballero, M.; Colombano, G.; Billington, R. A.; Genazzani, A. A.; Sterner, O. *J. Nat. Prod.* **2005**, *68*, 1213–1217.

Batista, J. M.; López, S. N.; Da Silva Mota, J.; Vanzolini, K. L.; Cass, Q. B.; Rinaldo, D.; Vilegas, W.; Da Silva Bolzani, V.; Kato, M. J.; Furlan, M. *Chirality* **2009**, *21*, 799–801.

Christensen, S. B.; Andersen, A.; Smitt, U. W. *Prog. Chem. Org. Nat. Prod.* **1997**, *71*, 130–167.

Christensen, S. B.; Larsen, I. K.; Rasmussen, U.; Christophersen, C. *J. Org. Chem.* **1982**, *47*, 649–652.

Christensen, S. B.; Rasmussen, U. *Tetrahedron Lett.* **1980**, *21*, 3829–3830.

Corey, E. J.; Lee, D. H. *J. Am. Chem. Soc.* **1991**, *113*, 4026–4028.

Fillion, E.; Beingessner, R. L. *J. Org. Chem.* **2003**, *68*, 9485–9488.

Gordon, J.; Hamilton, C.; Hooper, A. M.; Ibbotson, H. C.; Kurosawa, S.; Mori, K.; Muto, S.; Pickett, J. A. *Chem. Comm.* **1999**, 2335–2336.

Gordon, J. R.; Nelson, H. M.; Virgil, S. C.; Stoltz, B. M. *J. Org. Chem.* **2014**, Article ASAP. doi: 10.1021/jo501924u.

Gul, S.; Schoenebeck, F.; Aviyente, V.; Houk, K. N. *J. Org. Chem.* **2010**, *75*, 2115–2118.

Gunes, H. S. *J. Fac. Pharm. Gazi.* **2001**, *18*, 35–41.

Imamura, Y.; Takikawa, H.; Mori, K. *Tetrahedron Lett.* **2002**, *43*, 5743–5746.

Ireland, R. E.; Varney, M. D. *J. Am. Chem. Soc.* **1984**, *106*, 3668–3670.

Ireland, R. E.; Wipf, P.; Xiang, J. N. *J. Org. Chem.* **1991**, *56*, 3572–3582.

Kapferer, T.; Brückner, R. *Eur. J. Org. Chem.* **2006**, 2119–2133.

Kazmaier, U.; Krebs, A. *Angew. Chem. Int. Ed.* **1995**, *34*, 2012–2014.

Kozytska, M. V.; Dudley, G. B. *Tetrahedron Lett.* **2008**, *49*, 2899–2901.

Kropp, P. J.; McNeely, S. A.; Davis, R. D. *J. Am. Chem. Soc.* **1983**, *105*, 6907–6915.

Larsen, P. K.; Sandberg, F. *Acta Chem. Scand.* **1970**, *24*, 1113–1114.

Larsson, R.; Sterner, O.; Johansson, M. *Org. Lett.* **2009**, *11*, 657–660.

Löffler, A.; Himbert, G. *Synthesis* **1992**, 495–498.

Marshall, J. A. in *Organometallics in Synthesis: A Manual* (Ed.: M. Schlosser) Wiley, Chichester, **2002**, 457.

Min, L.; Zhang, Y.; Liang, X.; Huang, J.; Bao, W.; Lee, C.-S. *Angew. Chem. Int. Ed.* **2014**, Article ASAP. doi: 10.1002/anie.201405770.

Navarrete, C.; Sancho, R.; Caballero, F. J.; Pollastro, F.; Fiebich, B. L.; Sterner, O.;

Appendino, G.; Muñoz, E. *J. Pharmacol. Exp. Ther.* **2006**, *319*, 422–430.

Nelson, H. M. A Unified Synthetic Approach to the Transtaganolide and Basiliolide

Natural Products. Ph.D. Dissertation, California Institute of Technology,

Pasadena, CA, 2013.

Nelson, H. M.; Gordon, J. R.; Virgil, S. C.; Stoltz, B. M. *Angew. Chem. Int. Ed.* **2013**,

52, 6699–6703

Nelson, H. M.; Murakami, K.; Virgil, S. C.; Stoltz, B. M. *Angew. Chem. Int. Ed.* **2011**,

50, 3688–3691.

Nelson, H. M.; Stoltz, B. M. *Org. Lett.* **2008**, *10*, 25–28.

Nelson, H. M.; Stoltz, B. M. *Tetrahedron Lett.* **2009**, *50*, 1699–1701.

Posner, G. H.; Dai, H.; Afarinkia, K.; Murthy, N. N.; Guyton, K. Z.; Kensler, T. W. *J.*

Org. Chem. **1993**, *58*, 7209–7215.

Posner, G. H.; Nelson, T. D.; Kinter, C. M.; Afarinkia, K. *Tetrahedron Lett.* **1991**, *32*,

5295–5298.

Rasmussen, U.; Christensen, S. B.; Sandberg, F. *Planta Med.* **1981**, *43*, 336–341.

Raucher, S.; Bray, B. L. *J. Org. Chem.* **1987**, *52*, 2332–2333.

- Rubal, J. J.; Moreno-Dorado, F. J.; Guerra, F. M.; Jorge, Z. D.; Saouf, A.; Akssira, M.; Mellouki, F.; Romero-Garrido, R.; Massanet, G. M. *Phytochemistry* **2007**, *68*, 2480–2486.
- Sakamoto, T.; Yasuhara, A.; Kondo, Y.; Yamanaka, H. *Chem. Pharm. Bull.* **1994**, *42*, 2032–2035.
- Sakamoto, T.; Yasuhara, A.; Kondo, Y.; Yamanaka, H. *Synlett* **1992**, 502.
- Saouf, A.; Guerra, F. M.; Rubal, J. J.; Moreno-Dorado, F. J.; Akssira, M.; Mellouki, F.; López, M.; Pujadas, A. J.; Jorge, Z. D.; Massanet, G. M. *Org. Lett.* **2005**, *7*, 881–884.
- Shibuya, H.; Ohashi, K.; Narita, N.; Ishida, T.; Kitagawa, I. *Chem. Pharm. Bull.* **1994**, *42*, 293–299.
- Snyder, S. A.; Treitler, D. S. *Angew. Chem. Int. Ed.* **2009**, *48*, 7899–7903.
- Sogo, S. G.; Widlanski, T. S.; Hoare, J. H.; Grimshaw, C. E.; Berchtold, G. A.; Knowles, J. R. *J. Am. Chem. Soc.* **1984**, *106*, 2701–2703.
- Still, W. C.; Gennari, C. *Tetrahedron Lett.* **1983**, *24*, 4405–4408.
- Toyoshima, C.; Nomura, H. *Nature* **2002**, *418*, 605–611.
- Van Leeuwen, P. W. N. M.; Kamer, P. C. J.; Reek, J. N. H.; Dierkes, P. *Chem. Rev.* **2000**, *100*, 2741–2769.

Van Leeuwen, P. W. N. M.; Zuideveld, M. A.; Swennenhuis, B. H. G.; Freixa, Z.;

Kamer, P. C. J.; Goubitz, K.; Fraanje, J.; Lutz, M.; Spek, A. L. *J. Am. Chem. Soc.*

2003, *125*, 5523–5539.

Zeng, W.; Fröhlich, R.; Hoppe, D. *Tetrahedron* **2005**, *61*, 3281–3287.

Zhou, X.; Wu, W.; Liu, X.; Lee, C.-S. *Org. Lett.* **2008**, *10*, 5525–5528.

INDEX

I

[5+2] annulation9, 13, 18, 66, 68, 78, 235, 241, 249

7

7-*O*-geranylscooletin2, 4, 84

A

ABD.....6, 7, 8, 9, 10, 12, 20, 235

ABDE6

acetalization68, 78

acetate1, 25, 26, 72, 77, 99, 252, 253

acetyl.....249

acetylene9, 13

acetylide.....13, 238, 241, 242

achiral66, 248

acid10, 11, 13, 14, 19, 26, 69, 72, 74, 75, 76, 78, 89, 101, 107, 109, 116, 119, 247

acylation17

alcohol7, 11, 19, 24, 25, 69, 71, 72, 73, 75, 77, 99, 100, 101, 104, 106, 107, 109, 118, 119

aldehyde.....19, 23, 68, 71, 73, 75, 76, 97, 113, 116, 117, 123

aldol4

alkoxy241

alkoxyacetylide.....238

alkylation7

alkynyl241, 248, 249

allyl17, 24, 25, 26, 88, 115

allylic19, 80, 81

amide13, 73, 74, 105, 106, 238

anhydride4, 25, 99, 114

aryl.....238

asymmetric68, 69, 131

asymmetrically67, 75

B

basiliolide	1, 2, 3, 6, 7, 8, 9, 10, 11, 14, 15, 16, 17, 18, 20, 21, 30, 31, 41, 42, 67, 235, 237
basiliopyrone	2, 5, 6, 80, 83, 84, 85, 247, 248, 249, 255
bicycle.....	3, 5
bidentate	238, 241
BINAP	239
bioactivity	1, 6
biomimetic	6, 7
biosynthesis	5, 6, 84, 85
biosynthetic.....	3, 4, 5, 6, 67, 80, 81, 83, 248
bipyridine.....	239
bite angle	241
bromination.....	7
BSA	12, 27, 77, 91, 102, 108, 110, 120, 256

C

carbamate.....	69, 88
carbon dioxide	3
cascade.....	12, 13, 14, 18, 20, 66, 68, 69, 71, 73, 74, 77, 82, 83, 85, 235, 243, 248, 249
catalyst	75, 236, 241, 244, 245, 246, 253
catalytic.....	12, 77, 243, 249
catalyzed	8, 238, 244, 247, 248
cation	3
chemoselective	78
chiral	69, 71, 82, 84, 85, 90
chloride	13, 69, 105, 238, 240, 241, 242, 245, 246, 247, 252, 253, 258
C-ring.....	6, 9, 11, 13, 66, 235, 238
cross-couple	238, 239, 244, 249
cross-coupling.....	11, 13, 14, 236, 238, 239, 240, 241, 242, 244, 245, 246, 247, 249, 264, 266
crystal	2, 82, 85, 152
cyclization.....	3, 11, 13, 14, 15, 66, 71, 81, 257
cycloaddition	5, 6, 7, 8, 10, 12, 13, 17, 19, 235, 248
cyclopropanation	15, 16
cyclopropane.....	16

D

DCC coupling	11, 14, 19
deprotection	72, 74, 77, 103, 118
derivative	10, 13, 14, 69, 71, 76, 85, 89
diastereomeric	69, 77, 81, 83, 91, 93
diastereomers	12, 14, 16, 17, 19, 23, 28, 29, 75, 77, 80, 94, 102, 111, 114, 116, 120, 123, 124, 129, 248
diastereoselective	15, 16, 19, 80
diastereoselectivity	19, 72, 74
Diels–Alder	5, 6, 7, 8, 10, 11, 12, 13, 17, 19, 66, 74, 80, 81, 83, 85, 108, 235, 248
diphosphine	239
dppb	239, 241, 242
dpp-benzene	239
dppe	239
dppf	239, 241, 242
dppp	239
D-ring	67

E

enal	71
enantioenriched	66, 68, 69, 76, 77, 80, 85, 89
enantiomer	81, 152
enantiomeric	80, 89, 152
enantioselective	67, 76, 78, 80, 84
enantiospecific	68
ene-yne	11, 241, 244, 247, 265, 266
enoate	7, 19, 23, 24, 72, 73, 75, 77, 97, 98, 105, 108
epi-basiliolide	14, 15, 18, 20, 21, 30, 235, 237
epoxide	76, 84, 115, 116
ester	11, 14, 16, 17, 19, 26, 27, 29, 30, 68, 69, 74, 76, 78, 80, 81, 82, 85, 89, 91, 94, 101, 102, 109, 110, 112, 119, 120, 122, 124, 126, 129, 131, 236, 238, 244, 247, 248, 249, 253, 264, 267
ether	67
ethoxyacetylde	13

G

geraniol	10, 11, 14, 69, 71, 76, 81, 85, 88, 89
----------------	--

H

H ₂ PHOX	239
heteroaromatic	244
Horner–Wadsworth–Emmons	72, 77
hydration	5, 71, 238, 244, 248
hydride	7, 73, 75, 112, 113, 122
hypothesis	4, 6, 67, 80, 241

I

ICR/DA.....	12, 13, 14, 18, 20, 66, 68, 69, 71, 73, 74, 77, 82, 89, 91, 102, 111, 120, 235, 243, 248
intramolecular	7, 8, 10, 16, 17, 66
iodide	13, 238, 241, 242, 253, 264
iodine	16
iodo-cyclohexene.....	238, 240, 241, 242, 243, 267
Ireland–Claisen.....	6, 10, 11, 12, 13, 15, 19, 66, 69, 74, 80, 81, 83, 84, 85, 108, 235, 248, 257
isomerization	17

K

ketene-acetal	9, 81, 235
---------------------	------------

L

lactal	17
lactone.....	7, 67
lactonization	3, 11
ligand	238, 241, 242
lithium.....	13, 238

M

metabolite	2, 4, 6, 83, 84
methoxy	9, 13, 248, 249
methoxyacetylde.....	13, 14, 19, 241, 244, 246, 249
methoxyethyl	95, 238, 240, 241, 242, 245, 246, 247, 252, 253, 258
methyl	75, 82, 112, 122, 238, 253, 264
methylation	4, 17
monocyclic	3, 66, 68, 248

N

Negishi.....235, 247, 249

O

olefin.....3, 17

olefination.....7, 17

organostannane.....236, 240

organotin.....249

organozinc.....238, 241, 244, 245, 246, 258

oxabicyclo[2.2.2]octene.....6, 67

oxidation.....3, 5, 8, 11, 17, 68, 73, 84

oxidative cleavage.....17, 76

oxidize.....71, 72, 73

oxy-acetylide.....236

P

palladium.....13, 14, 17, 19, 236, 238, 239, 241, 243, 244, 247, 249

pentacyclic.....67

polymerization.....240, 241, 242

protecting group.....19, 25, 72, 74

protection.....13, 72, 78

pyrone..6, 7, 8, 10, 11, 12, 14, 17, 19, 26, 27, 66, 68, 69, 72, 73, 74, 77, 80, 82, 83, 85, 89, 91, 101, 102, 107, 108, 110, 119, 120, 243, 244, 245, 246, 247, 248, 249

pyrophosphate.....3

Q

quaternary.....6, 7, 9, 10, 12, 15, 16, 17, 20, 248

R

racemate.....67

racemic.....80

rearrangement.....5, 6, 10, 12, 15, 19, 66, 74, 80, 81, 83, 84, 257

reduction.....7, 19, 69, 72, 73, 75, 78, 112, 113, 122, 123

retrosynthetic analysis.....9, 13, 68, 69, 243

S

saponification	16
SERCA-ATPase	1, 2
sigmatropic	5
silane	69, 82, 88, 91, 93, 120, 122
silyl	14, 19, 25, 29, 30, 69, 236, 257
Sonagashira	11
sparteine	69, 81, 88
stannane	13, 30, 70, 95, 126, 236, 249
stannyl	13, 14, 19, 236
stereocenter	9, 10, 248
stereochemistry	6, 71, 80, 81, 82, 83, 84, 85
stereocontrol	68, 80
Still–Gennari	71, 76
stoichiometric	236, 241, 243
substoichiometric	239, 241
super-stoichiometric	236

T

tautomerism	71
tetracycle	6, 68, 78, 235
tetracyclic	3, 68, 73, 74, 75, 76
<i>Thapsia</i>	1, 2, 3
thapsigargin	1, 2, 43, 44, 45
tin	13
total synthesis	7, 12, 18, 66, 67, 70, 76, 79, 235, 242, 247
translactonization	68, 75, 78
translactonized	72, 104
transtaganolide	1, 2, 3, 4, 5, 6, 7, 8, 9, 10, 11, 12, 13, 14, 20, 21, 43, 44, 45, 66, 68, 69, 70, 71, 72, 73, 74, 75, 76, 77, 78, 79, 80, 83, 84, 85, 95, 96, 97, 126, 127, 128, 144, 145, 146, 147, 148, 149, 150, 151, 235, 237, 242, 247, 248, 249, 257
tricycle	3, 6, 7, 9, 11, 12, 13, 14, 17, 19, 28, 68, 69, 72, 75, 77, 93, 103, 104, 108, 235, 236, 243
tricyclic	7, 8, 9, 10, 12, 20, 28, 66, 71, 77, 112, 113, 235, 242
triethylamine	12, 27, 77, 91, 102, 108, 110, 120, 256

V

vinyl69, 93, 122, 238, 242, 253, 264

W

water3, 14, 31, 95, 105, 109, 113, 116, 118, 123, 126, 248, 254, 256

Weinreb73, 74, 105, 106

Wittig7, 17

X

Xantphos241, 242, 243, 246, 249, 252, 253

Y

ylide19, 23

Z

zinc13, 238, 240, 241, 242, 245, 246, 247, 252, 253, 258

ABOUT THE AUTHOR

Jonny R. Gordon was born on June 15, 1984 in Los Angeles, CA to David Gordon and Donna Schwarzbach. Jonny spent the majority of his childhood participating in a variety of athletics, such as baseball, basketball, and volleyball, where he was often accompanied by his older sister Courtney. Academically, he always enjoyed math and science, a trait shared by his mother, Donna, which they most likely inherited from Donna's father, Jonny's grandfather, Jerome Schwarzbach, a once well established aeronautical engineer. In high school, Jonny developed a deep love of chemistry under the guidance of his prized mentor Dr. Garrett Biehle. Jonny graduated from the Oakwood School in 2003, and went on to pursue his undergraduate degree at Brown University.

While attending Brown University, Jonny continued to study the sciences, primarily organic chemistry, as well as find time to play for the Brown club volleyball team that notably finished second in all Eastern United States in 2004. In his senior year, Jonny worked in the laboratory of Professor Jason K. Sello, where he studied Lewis acid catalyzed Ugi reactions as well as got his first taste of total synthesis as he looked to develop a synthetic route to Indolmycin. Jonny graduated with an ScB in chemistry from Brown University in 2008.

After obtaining his undergraduate degree in 2008, Jonny moved back home to Los Angeles to pursue his graduate studies under the supervision of Professor Brian M. Stoltz at Caltech. In the fall of 2014, he earned his Ph.D. in Chemistry for his contribution to the total syntheses of the transtaganolide and basiliolide natural products.